

The diatom *Phaeodactylum tricornutum* as a sustainable microalgal cell factory: towards a biorefinery approach

Thomas Butler (MRes)



The
University
Of
Sheffield.

Thesis

Thesis submitted for the degree of Doctor of Philosophy
to The University of Sheffield, Sheffield, U.K.
Department of Chemical and Biological Engineering

March 2021

Thesis committee

Supervisor:

Dr Seetharaman Vaidyanathan

Senior Lecturer in Chemical and Biological Engineering

The University of Sheffield

Co - Supervisor:

Dr Jagroop Pandhal

Senior Lecturer in Chemical and Biological Engineering

The University of Sheffield

Submitted: March 2021

Thomas O. Butler

The diatom *Phaeodactylum tricornutum* as a sustainable microalgal cell factory:
towards a biorefinery approach

PhD Thesis, The University of Sheffield, Sheffield (2021)

To my English and Portuguese family and to Bárbara

“It always seems impossible until it’s done”

Nelson Mandela

Abstract

Microalgae offer a means of fixing atmospheric CO₂, thus providing realistic reductions in carbon emissions and producing valuable compounds and chemical precursors of high value. *Phaeodactylum tricornutum* is a well characterised model diatom and has been exploited commercially for single products; the nutraceuticals eicosapentaenoic acid (EPA) (omega-3 fatty acid for maintaining cardiovascular health), fucoxanthin (pigment for weight loss, antioxidant, and anticancer compound), and as a live feed additive for aquaculture. Natural pathways exist for the production of EPA and fucoxanthin in *P. tricornutum* but biomass and product yields are low. The aim of this thesis was to utilise a biorefinery approach with the model diatom, *P. tricornutum* CCAP 1055/1, for the production of multiple products of interest; particularly fucoxanthin, EPA, and protein using non-GMO methods, to enable economic viability. In this thesis, the concept of *P. tricornutum* as a cell factory and biorefinery chassis along with the challenges to overcome have been discussed.

A cost-effective powdered media formulation (JWP) was revealed to involve low preparation time and outperformed conventional liquid f/2 medium. JWP resulted in a higher biomass productivity and fucoxanthin, EPA, and protein yield. JWP was subsequently used for cultivation of *P. tricornutum* indoors and outdoors (8-18°C) in a prototype airlift photobioreactor (PhycoLift) using a repeated fed-batch approach. Indoor cultivation resulted in a higher biomass and fucoxanthin yield (with a higher average protein, chlorophyll *a*, and fucoxanthin content). Outdoor cultivation resulted in a higher protein, carbohydrate, total fatty acid (TFA), and EPA productivity (with a higher TFA, EPA, and carbohydrate content). EPA content was found to be inversely correlated with temperature. Commensal bacteria (*Marinobacter* sp. and *Halomonas* sp.) were isolated from the cultures and identified. The total bacteria count showed a sinusoidal growth profile, and it was apparent that *Halomonas* predominated at low algae densities, but at higher algae densities there was a community shift to *Marinobacter*. EPA secretion into the extracellular matrix has been hypothesised as a bacterial control agent, but this was not observed in the present study.

A high throughput flask screening approach was used to optimise product yields, particularly fucoxanthin and EPA using f/2 medium as a baseline. A culture medium

consisting of nitrate and phosphate at 4.41 mM and 0.18 mM (5-fold those employed in the traditional f/2 medium), salinity at 33 ‰, 2 % CO₂ (v/v in air), and a transition to mixotrophy using glycerol (0.01 M) were found to result in increased biomass (0.20 g L⁻¹ d⁻¹), fucoxanthin (1.78 mg L⁻¹ d⁻¹), EPA (7.54 mg L⁻¹ d⁻¹), and protein yields (15.65 mg L⁻¹ d⁻¹), up to ten-fold higher than the f/2 control medium.

Harvesting algae biomass from suspended cultures is a major bottleneck industrially and can account for up to 30 % of the production cost. A series of biobased flocculants were examined and a tannic acid-based derivative was found to flocculate the algal biomass effectively within 10 minutes, resulting in a high harvesting efficiency (>85 %), and a concentration factor ≥ 5.6 , with promising economic potential for wider usage (cost savings of >US \$61 ton⁻¹ biomass compared with chemical and other biobased flocculants).


Finally, three different *P. tricornutum* strains; CCAP 1055/1, UTEX 646 and a commercial strain - N017 (Necton, Portugal) were screened to determine the influence of strain on product yields cultivated in brackish seawater. It was identified that *P. tricornutum* UTEX 646 resulted in the highest biomass productivity and highest EPA, TFA, protein, and carbohydrate yield. Whereas, the *P. tricornutum* N017 strain had the highest fucoxanthin productivity. Warm white light emitting diodes (LEDs) resulted in a higher biomass productivity, fucoxanthin, and carbohydrate yield, but a lower EPA, TFA, and protein yield compared with red: blue LEDs (2.25:1). The bacterial community composition was found to be similar under white and red: blue LEDs. *Marinobacter* sp. was present in all strains and dominated at most stages of cultivation indicating a commensal relationship. *Halomonas* sp. was only present in *P. tricornutum* CCAP 1055/1 and the *P. tricornutum* N017 strain. *Algoriphagus* sp. was only present in *P. tricornutum* CCAP 1055/1 and was low in number. Comparatively, *Sphingorhabdus* and *Croceibacter* spp. were present in the commercial *P. tricornutum* N017 strain. The total bacterial count was observed to be lower under red: blue LEDs for all three strains over the cultivation period, which may reveal potential to reduce bacterial loading.

In summary, UK outdoor cultivation under cold conditions utilising a biorefinery approach has been demonstrated to be feasible with an airlift PBR (Phycolift), but further improvements are needed for economic viability; a commercially viable and environmentally

friendly solution to harvesting biomass using a biobased flocculant has been demonstrated; simple culture condition manipulation using a high-throughput standardised flask screening setup has been showcased to improve biomass, EPA, fucoxanthin, and protein yields; and commensal bacteria have been isolated and characterised. This thesis has real commercial application to rapidly screen treatments for elevating biomass and product yield, whilst decreasing the time taken for harvesting at reduced cost, for example, the production of fucoxanthin, and a depigmented by-product as an aquaculture additive.

Declaration

I hereby declare that this thesis is my own work and effort which was conducted at the University of Sheffield, U.K. This work has not been submitted anywhere for any other degree of qualification. Where other sources of information have been used, they have been acknowledged.

Signature:..... Date: 24/03/2020

Thomas O. Butler

This copy of the thesis has been submitted with the condition that anyone who consults it is understood to recognise that the copyright rests with its author. No quotation and information derived from this thesis may be published without prior written consent from the author or the University (as may be appropriate).

Acknowledgements

I would like to express enormous gratitude to my supervisor, Dr Seetharaman Vaidyanathan (Raman), for allowing me to embark upon this challenging journey to become an independent scientist. I would like to thank him for always being approachable whatever the time of day, and for guiding and supporting me throughout my research. I am also thankful to my former colleague and current good friend Dr Rahul Kapoore who really motivated me to explore areas outside my comfort zone, it has been a pleasure to write grants, papers, and work on projects together. I look forwards to visiting you in Swansea! Thanks to my second supervisor, Dr Jagroop Pandhal (Jags) for being there as a great sounding board. A special thanks to Dr Joy Mukherjee who took time to teach me how to use the FTIR, the SEM, and for our general discussions about science, a truly modest and inspiring scientist. I'm so pleased you are now teaching in the Diamond. I hope we can all work together in the future again. Dr Caroline Evans, I enjoyed your proteomic lectures and though we haven't had chance to work together I look forward to working with you in the future.

Thanks to all the algae postdoc and PhD cohort, past and present who I have enjoyed working with. A hugely passionate group of individuals who are committed to shaping a sustainable future (mostly doctors now - Gloria Padmaperuma, Tom Burns, Josie McQuillan, Hannah Leflay, Faqih Shuhaili, Maria Heute-Ortega, Muhammad Hashim, Deepak Sethi, Nella Rocuzzo, Isabel Narez). Thanks to Nella for allowing me to work with her to help bring her infochemical work to fruition, it's amazing what 4 years work can achieve! A special thanks goes to all the MSc and Meng students I mentored (Charlotte Pheasey, Victor Gonzalez, Omar Corona, Harry Doyle, Miriam Dansasuk, Ahmad Abdullah, Hayden Ormshaw, Karen Acurio, and Jules Harvey). I know you have all followed your dreams and you have helped me follow mine.

Thanks to the technicians (James Grinham and Duncan Schofield), electricians (Oz, Usman, Glynn Reynolds, and Mark McIntosh), and the cleaners, without them very little would be working in CBE. It was a pleasure running the Half Marathon in Nottingham with James Grinham, James Baker, Giulia Lambiase, Yash Patel, Bilal Khorsheed, Will and Will (Morgan-Evans and Kerry), to raise money and awareness for the mental health charity MIND.

I would like to thank everybody in the CBE department and through the University for maintaining a great social life during the PhD, adventures in Wales, swimming team socials (especially Aldo Gutierrez and Josh Adjodha), nights out (especially Cubana, The Red Deer, Dempseys with the Friday night crew; Oscar, Josh, Kit, José, Josie, Kacper, Jon, Justin, John, Elyane, Romain, Stefan, Annabel, Mado, Alex, the list goes on). I miss you all and can't wait for our next reunion! It was a pleasure understanding the importance of everybody's PhD in society; whether that be granulation, bacteria, yeast, mammalian cells, battery storage, wastewater treatment, everyone plays a role to make the world a better place. A special shout out to Lucy and Oscar - for giving me a home to collect the last bits of data analysis when I was living in the Netherlands. You will always be true friends. Likewise, Eike, thanks for always being there, through our Marine Biology Bachelors together and our amazing trips to Germany, The UK, Sri Lanka and Bermuda. We'll always be friends through life. You still got your Dr title before me! I look forward to diving with you soon buddy!

Thanks to the Varicon Aqua team; Joe, Marco, Ned, Rita, Alex, and Ignis. You guys taught me the engineering skills I know. Thanks for the opportunity Joe, and it was a pleasure working with you all. Thanks also Joe for the trusty BMW company car so I could make it to the site, it only broke down a few times...

A special thanks to Prof. Maria Barbosa for allowing me to conduct a short Guest PhD at Wageningen University to be reunited with my love, Bárbara. It was a pleasure working on the Magnificent Project and working in AlgaePARC cultivating algae outdoors in the Green Wall Panels. Marta and August, it was a pleasure working with you. Thanks everybody in the Bioprocess Engineering Department (BPE) for welcoming me and accepting me as one of your own; Wendy, Renske, Pieter, Christian, Snezana, Fred, Rick, Narcis, Fabian to name but a few. Thanks to Necton, especially João Navalho for allowing me to test their strain. Thanks, Timon, for introducing me to Marieke at Synalgae.

Thanks to Lgem/Synalgae for their patience whilst I wrote my thesis; Jan, Marieke, Jeroen, Eugène, Sander, Bas, Ruud, it's a pleasure to work with you all and to bring the knowledge I have learned to the company.

It is at the end of this journey that I must go to the beginning. Thanks to Dr Jonathan Rand for first inspiring me to conduct a PhD, it was great working with you at ECOSYL

Products Ltd. Thanks to Dr Gary Caldwell at Newcastle University for inspiring me with how algae could change the world. Thank you to the Algaecytes team (Dr John Dodd, Naz Bashir, Dr George Taylor, John MacDonald and Georgina Andrews), the SAMS team (Prof John Day, Dr Carole Shellcock, Naomi Thomas, Elaine Mitchell, Mair Clark, Christine Campbell and Joanne Field) and the Algenuity team (Dr Andrew Spicer, Dr Henry Taunt, Gavin Lowe, Gino Schiano Di Visconte) for all the laughs and teaching me a lot of what I know. The algae world is small and our paths will cross!

I would like to thank my family (British and Portuguese) and girlfriend most of all, for their support, their laughs, their motivation, and for putting up with my talks of how microalgae are going to change the world. Mum and Dad, I am so grateful for all your support through my life, allowing me to chase my dreams, forging my own path. I know you will both always be there for me. I really hope after reading this thesis my sister, Dr Kim Butler (she got her medical degree well before I even submitted my PhD) will understand why I have embarked upon a career in microalgae since 2014. Bárbara thank you for being my everything. Without you, this thesis would not have been submitted. I love you with all my heart and all the blood in my veins. I can't wait to start our next projects, whatever happens next, I know it involves you. Family and friends are everything and are what life is all about. It is to my family and Bárbara that I dedicate this thesis.

Table of Contents

| | |
|--|-----------|
| ABSTRACT | 6 |
| DECLARATION | 10 |
| ACKNOWLEDGEMENTS | 12 |
| CHAPTER 1: GENERAL INTRODUCTION | 22 |
| 1.1. MICROALGAE AS A SUSTAINABLE BIOBASED FEEDSTOCK | 22 |
| 1.2. THE MARINE DIATOM - <i>PHAEODACTYLUM TRICORNUTUM</i> | 23 |
| 1.3. CHALLENGES IN IMPLEMENTING <i>P. TRICORNUTUM</i> AS A CELL FACTORY | 25 |
| 1.3.1. UPSTREAM – PROCESS OPTIMISATION | 26 |
| 1.3.2. DOWNSTREAM | 26 |
| 1.4. GOAL OF THE THESIS | 27 |
| 1.5. OUTLINE OF THE THESIS | 28 |
| CHAPTER 2: <i>PHAEODACTYLUM TRICORNUTUM</i>: A DIATOM CELL FACTORY | 31 |
| 2.1. ABSTRACT | 32 |
| 2.2. MICROALGAE CHASSIS IN THE BIOBASED ECONOMY | 33 |
| 2.3. <i>P. TRICORNUTUM</i> – A WELL-STUDIED DIATOM | 34 |
| 2.4. CULTIVATION OF <i>P. TRICORNUTUM</i> | 35 |
| 2.5. UPSTREAM DEVELOPMENTS | 37 |
| 2.6. DOWNSTREAM CONSIDERATIONS AND CHALLENGES | 41 |
| 2.7. TOWARDS A DIATOM BIOREFINERY | 43 |
| 2.8. CONCLUDING REMARKS | 45 |
| CHAPTER 3: TOWARDS A <i>PHAEODACTYLUM TRICORNUTUM</i> BIOREFINERY IN AN OUTDOOR UK ENVIRONMENT (8-18°C) | 58 |

| | |
|---|-----------|
| 3.1. ABSTRACT | 59 |
| 3.2. INTRODUCTION | 60 |
| 3.3. MATERIALS AND METHODS | 63 |
| 3.3.1 <i>PHAEODACTYLUM TRICORNUTUM</i> CULTURE AND ROUTINE MAINTENANCE | 63 |
| 3.3.2 <i>PHAEODACTYLUM TRICORNUTUM</i> FLASK SCREENING AND EXPERIMENTAL APPROACH | 64 |
| 3.3.3. HYDROPONICS AND POWDERED MEDIA SCREENING | 64 |
| 3.3.4. INDOOR/OUTDOOR CULTIVATION IN A PROTOTYPE AIRLIFT PHOTOBIOREACTOR | 66 |
| 3.3.5. GROWTH AND FATTY ACID PROFILES OF ISOLATED COMMENSAL BACTERIA | 69 |
| 3.3.6. ANALYTICAL METHODS | 69 |
| 3.4. RESULTS AND DISCUSSION | 73 |
| 3.4.1. EVALUATION OF POWDERED CELL-HI RANGE COMPARED WITH FLORAMICROBLOOM AND STANDARD F/2 UNDER NON-STERILE CONDITIONS | 73 |
| 3.4.2. GROWTH AND BIOCHEMICAL COMPOSITION | 73 |
| 3.4.3. PERFORMANCE OF POWDERED AND HYDROPONICS MEDIA: COST, BIOMASS PRODUCTIVITY AND PRODUCT YIELDS | 75 |
| 3.4.4. COMMENSAL BACTERIAL ISOLATION, IDENTIFICATION AND ENUMERATION | 76 |
| 3.4.5. NITRATE AND PHOSPHATE UPTAKE | 80 |
| 3.5. CONCLUSION | 97 |

CHAPTER 4: PHAEODACTYLUM TRICORNUTUM – CULTURE CONDITION MANIPULATION TOWARDS BIOREFINERY CHASSIS DEVELOPMENT **100**

| | |
|--|------------|
| 4.1. ABSTRACT | 101 |
| 4.2. INTRODUCTION | 102 |
| 4.3. MATERIALS AND METHODS | 104 |
| 4.3.1. <i>PHAEODACTYLUM TRICORNUTUM</i> CULTURE AND ROUTINE MAINTENANCE | 104 |
| 4.3.2. <i>P. TRICORNUTUM</i> GROWTH IN ALGEM [®] FOR INITIAL GROWTH OPTIMISATION | 105 |
| 4.3.3. EXPERIMENTAL CULTURE SETUP FOR HIGH THROUGHPUT FLASK SCREENING SETUP | 105 |
| 4.3.4. EFFECT OF MODIFIED F/2 MEDIUM ON BIOCHEMICAL COMPOSITION | 106 |
| 4.3.5. EFFECT OF SALINITY ON BIOCHEMICAL COMPOSITION | 106 |
| 4.3.6. EFFECT OF CARBON SOURCE ON BIOCHEMICAL COMPOSITION; BICARBONATE, CO ₂ AND GLYCEROL | 107 |

| | |
|--|------------|
| 4.3.7. ANALYTICAL METHODS | 107 |
| 4.3.8. STATISTICAL ANALYSIS | 110 |
| 4.4. RESULTS AND DISCUSSION | 110 |
| 4.4.1. PRE-OPTIMISATION FOR GROWTH: EFFECT OF TEMPERATURE AND LIGHTING REGIME ON GROWTH OF <i>P. TRICORNUTUM</i> | 110 |
| 4.4.2. EFFECT OF F/2 MODIFICATION ON BIOCHEMICAL COMPOSITION: INCREASING NITRATE AND PHOSPHATE CONCENTRATION | 112 |
| 4.4.3. EFFECT OF F/2 MODIFICATION ON NUTRIENT UPTAKE RATE | 116 |
| 4.4.4. EFFECT OF SALINITY ON BIOCHEMICAL COMPOSITION | 118 |
| 4.4.5. EFFECT OF CARBON ON BIOCHEMICAL COMPOSITION | 122 |
| 4.4.6. EFFECT OF BICARBONATE ON BIOCHEMICAL COMPOSITION | 122 |
| 4.4.7. EFFECT OF CO ₂ CONCENTRATION ON BIOCHEMICAL COMPOSITION | 124 |
| 4.4.8. EFFECT OF GLYCEROL AND 2 % CO ₂ ON BIOCHEMICAL COMPOSITION | 126 |
| 4.5. CONCLUSION | 129 |

CHAPTER 5: THE TRANSITION AWAY FROM CHEMICAL FLOCCULANTS: COMMERCIALY VIABLE

HARVESTING OF *PHAEODACTYLUM TRICORNUTUM* **132**

| | |
|---|------------|
| 5.1. ABSTRACT | 133 |
| 5.2. INTRODUCTION | 134 |
| 5.3. MATERIALS AND METHODS | 135 |
| 5.3.1 <i>PHAEODACTYLUM TRICORNUTUM</i> CULTURE AND GROWTH CONDITIONS | 135 |
| 5.3.2 INORGANIC AND BIOBASED FLOCCULANTS | 136 |
| 5.3.3. HARVESTING EXPERIMENTAL SETUP | 137 |
| 5.3.4. FLOCCULATION AND SEDIMENTATION EXPERIMENTS | 139 |
| 5.3.5. EFFECT OF FLOCCULANT DOSAGE, FLOCCULATION TIME, FLOCCULATION TEMPERATURE, AND BIOMASS CONCENTRATION ON FLOCCULATION EFFICIENCY | 139 |
| 5.3.6. EFFECT OF FLOCCULANTS ON FATTY ACID METHYL ESTER (FAME) COMPOSITION USING A WET PROCESSING METHOD | 140 |
| 5.3.7. FTIR ANALYSIS OF TANFLOC 6025 AND 8025 | 141 |
| 5.4. RESULTS AND DISCUSSION | 141 |

| | |
|--|------------|
| 5.4.1. AUTOFLOCCULATION AND ALKALINE FLOCCULATION | 141 |
| 5.4.2 BIO-BASED FLOCCULATION | 143 |
| 5.4.3. EFFECT OF LOWERING TANFLOC DOSAGE AND FLOCCULATION TIME | 148 |
| 5.4.4. SURFACE FUNCTIONAL GROUPS OF TANFLOC | 150 |
| 5.4.5. EFFECT OF TEMPERATURE AND BIOMASS CONCENTRATION ON FLOCCULATION WITH TANFLOC 8025 | 152 |
| 5.4.6. COST ANALYSIS OF TANFLOC 8025 COMPARED WITH OTHER COMMERCIALY VIABLE FLOCCULANTS | 154 |
| 5.5. CONCLUSION | 155 |

CHAPTER 6: EVALUATING THE BIOREFINERY POTENTIAL OF THREE *PHAEODACTYLUM*

TRICORNUTUM STRAINS **157**

| | |
|---|------------|
| 6.1. ABSTRACT | 158 |
| 6.2. INTRODUCTION | 159 |
| 6.3. MATERIALS AND METHODS | 161 |
| 6.3.1. <i>PHAEODACTYLUM TRICORNUTUM</i> STOCK CULTURE AND ROUTINE MAINTENANCE | 161 |
| 6.3.2. EXPERIMENTAL CULTURES | 162 |
| 6.3.3. BIOMASS SAMPLING | 162 |
| 6.3.4. DRY WEIGHT DETERMINATION | 163 |
| 6.3.5. QUANTUM YIELD | 163 |
| 6.3.6. BACTERIA ISOLATION AND ENUMERATION | 164 |
| 6.3.7. BACTERIA DNA-AMPLIFICATION, SEQUENCING, AND IDENTIFICATION | 164 |
| 6.3.8. <i>P. TRICORNUTUM</i> DNA-AMPLIFICATION, SEQUENCING, AND IDENTIFICATION | 164 |
| 6.3.9. FATTY ACID ETHYL ESTER (FAEE) DETERMINATION | 165 |
| 6.3.10. COMBINED EXTRACTION OF CARBOHYDRATE, PIGMENT AND PROTEIN | 165 |
| 6.3.11. PIGMENT ANALYSIS BY HPLC – CHLOROPHYLL A AND FUcoxANTHIN | 165 |
| 6.3.12. ELEMENTAL COMPOSITION | 166 |
| 6.3.13. STATISTICAL ANALYSIS | 166 |
| 6.4. RESULTS AND DISCUSSION | 167 |
| 6.4.1. STRAIN DIFFERENCES IN GROWTH AND BIOCHEMICAL COMPOSITION UNDER WARM WHITE LIGHT | 167 |
| 6.4.2. EFFECT OF RED: BLUE LEDs ON GROWTH AND BIOCHEMICAL COMPOSITION OF <i>P. TRICORNUTUM</i> CCAP 1055/1, UTEX 646 AND NECTON | 169 |

| | |
|---|------------|
| 6.4.3. EFFECT OF WARM WHITE AND RED: BLUE LEDs ON PRODUCTIVITIES IN <i>P. TRICORNUTUM</i> UTEX 646 AND N017 | 174 |
| 6.3.4. EFFECT OF LIGHTING ARRANGEMENT ON COMMENSAL BACTERIA POPULATION | 175 |
| 6.5. CONCLUSION | 177 |

CHAPTER 7: GENERAL DISCUSSION: *PHAEODACTYLUM TRICORNUTUM*: AN EMERGING CELL FACTORY FOR BOTH FUCOXANTHIN PRODUCTION AND AQUACULTURE FEED (AQUAFEED)

SUPPLEMENTATION 179

| | |
|--|------------|
| 7.1 MICROALGAE AS A GLOBAL SOLUTION TO WORLD ISSUES | 179 |
| 7.2 THE DIATOM <i>PHAEODACTYLUM TRICORNUTUM</i> AS AN EMERGING CELL FACTORY: PRODUCTS OF INTEREST (FUCOXANTHIN AND EICOSAPENTAENOIC ACID) | 180 |
| 7.3 THE DIATOM <i>PHAEODACTYLUM TRICORNUTUM</i> AS AN EMERGING CELL FACTORY: BOTTLENECKS TO COMMERCIALISATION | 182 |
| 7.4 <i>PHAEODACTYLUM TRICORNUTUM</i>: INDOOR VS OUTDOOR UK CULTIVATION AT COLD TEMPERATURES AND LOW LIGHT | 187 |
| 7.5 CULTURE CONDITION MANIPULATION FOR INCREASED PRODUCT YIELDS | 188 |
| 7.6 THE TRANSITION AWAY FROM CHEMICAL FLOCCULANTS: COMMERCIALY VIABLE HARVESTING OF <i>P. TRICORNUTUM</i> | 188 |
| 7.7 STRAIN SCREENING AND POTENTIAL OF WHITE AND RED: BLUE LEDs | 190 |
| 7.8 MAIN CONCLUSION | 191 |
| 7.9 FUTURE OUTLOOK | 192 |
| 7.9.1 UPSTREAM DEVELOPMENTS | 192 |
| 7.9.2 DEVELOPMENT OF WET SEQUENTIAL EXTRACTION METHODS TO BYPASS DRYING AND PRODUCT FORMULATION | 195 |
| 7.9.3 HIGH COST OF DRYING | 195 |
| 7.9.4 EXTRACTION FROM DRY MATERIAL | 196 |
| 7.9.5 WET EXTRACTION | 196 |
| 7.9.6 FUCOXANTHIN ENCAPSULATION | 197 |
| 7.9.7 AQUAFEED FORMULATION | 198 |

| | |
|---|------------|
| 7.9.8 COST EFFECTIVE PRODUCTION OF <i>P. TRICORNUTUM</i> FOR BOTH FUCOXANTHIN AND DEPIGMENTED MICROALGAL BIOMASS FOR AQUACULTURE FEED | 199 |
| APPENDIX A | 201 |
| SUPPLEMENTARY FILES | 201 |
| APPENDIX B | 221 |
| SUPPLEMENTARY FILES | 221 |
| APPENDIX C | 234 |
| SUPPLEMENTARY FILES | 234 |
| APPENDIX C1. IONIC COMPOSITION OF MODIFIED F/2 AND INSTANT OCEAN | 234 |
| APPENDIX C2. ALKALINE FLOCCULATION | 235 |
| APPENDIX C3. TESTING THE EFFECT OF THE HARVESTING PROTOCOL ON CELL VIABILITY | 236 |
| APPENDIX C4. TESTING THE EFFECT OF THE HARVESTING PROTOCOL ON PRODUCT ACCUMULATION | 238 |
| APPENDIX D | 243 |
| SUPPLEMENTARY FILES | 243 |
| BIBLIOGRAPHY | 254 |
| ABOUT THE AUTHOR | 280 |
| LIST OF PUBLICATIONS | 281 |

Chapter 1: General introduction

1.1. Microalgae as a sustainable biobased feedstock

To transition from a petro-based to a biobased economy requires the capacity to produce both high-value low-volume (e.g. speciality pigments and recombinant antibodies), as well as low-value high volume products (omega-3 fatty acids, biofuels, bioplastics, whole cell biomass for food/feed). Recent trends have highlighted the potential for developing microalgae-based cell factories, to establish environmentally sustainable manufacturing solutions. Microalgae are photosynthetic organisms that possess the machinery to produce high-value phytochemicals, and have the capacity to utilise carbon dioxide as a feedstock, and remediate wastewater components such as nitrate, phosphate and pharmaceutical contaminants (Xiong et al., 2018). Compared to plant cells, microalgae can be relatively quick to grow (several hours to a day for a single doubling), and can be harvested daily, offering a more economically viable processing alternative. Their ability to grow in a multitude of niches including marginal land, desert land, brackish water or the open ocean, prevents soil degradation and reduces freshwater consumption compared with traditional crops.

Industrial scale cultivation for commercial manufacturing has largely been focussed on harnessing the natural capabilities of selected species for single products, such as β -carotene from *Dunaliella salina*, phycocyanin from *Arthrospira* spp., and astaxanthin from *Haematococcus pluvialis*. Alternatively, other industries have utilised the whole biomass as a live feed for aquaculture hatcheries but the production process is not profitable. The five most important microalgae in terms of annual biomass production (>29 tonnes per annum valued at >US \$650 million) are *Spirulina* (*Arthrospira*), *Chlorella*, *Dunaliella*, *Haematococcus* and *Nannochloropsis* with biomass values of US \$13-120 kg⁻¹ (Olaizola and Grewe, 2019). The reference cost price for a 25 m² system of microalgae biomass in aquaculture hatcheries (on a dry matter content) is €290 kg⁻¹ and €329 kg⁻¹ for tubular photobioreactors under artificial light and a greenhouse, respectively (Oostlander et al., 2020),

but dewatering (i.e. centrifugation or membrane filtration) and drying (e.g. spray drying) was not taken into account in this cost assessment, revealing that the cost of production is likely an underestimate. To date the production of bulk commodities from microalgae is not economically viable but it has been shown that large-scale cultivation in the south of Spain is around 3.4 euros kg⁻¹ dry weight (flat-panel photobioreactors at 100 ha scale) with downstream processing costs of 0.9-1.1 euros kg⁻¹ DW (resultant revenue of 0.3-2 euros kg DW⁻¹) demonstrating that significant steps need to be taken before production of bulk commodities from microalgae is economically viable, especially in small-scale operations (<5 hectares). Adopting a biorefinery approach with microalgae has yet to be commercially validated. In a biorefinery approach multiple products of interest are produced from biomass to add value to the process compared to a conventional single product approach. Whilst several microalgae are at various stages of development as cell factories, there is a growing body of knowledge on the pennate diatom, *Phaeodactylum tricornerutum* (*P. tricornerutum*), and its development as a microalgae cell chassis.

1.2. The marine diatom - *Phaeodactylum tricornerutum*

Phaeodactylum tricornerutum is a model diatom found in marine ecosystems which is cultivated industrially for high value products; fucoxanthin (AlgaTechnologies, Israel) and eicosapentaenoic acid (EPA) (Simris, Sweden). *P. tricornerutum* is a potential biorefinery chassis which can be exploited for a range of natural products with market potential including high value products such as nutraceuticals (fucoxanthin) and lower value products (EPA, protein, and chrysolaminarin) for animal and aquaculture feed, via sequential extraction (Butler et al., 2020). *P. tricornerutum* also has potential for docosahexaenoic acid, biodiesel, and genetically engineered products (recombinant antibodies and bioplastics) (Butler et al., 2020). It is a commercially viable species, and is cultivated industrially by at least eight companies in Europe (eicosapentaenoic acid, whole cell biomass for aquafeed, and extracts for cosmetics) with an estimated annual production of four tonnes of dry biomass (Araújo and García-tasende, 2021).

In diatoms, fucoxanthin is one of the primary light harvesting pigments (along with chlorophyll *a* and *c* in the fucoxanthin-chlorophyll protein (FCP) complex in the chloroplast which traps light energy, plays an important role in non-photochemical quenching (NPQ), and offers photoprotection (Wang et al., 2018; Yang and Wei, 2020). *P. triornutum* typically exhibits a content between 1.0-2.6 % DW (Derwenskus et al., 2020a). Fucoxanthin has a range of health benefits (animal and human trials) including anti-inflammatory, anti-tumour, anti-obesity, antimalarial and anti-diabetes (Bae et al., 2020). In 2016, global fucoxanthin production was approximately 500 tons (primarily from macroalgae - brown seaweeds) and the market appeared to have grown at an annual rate of 5.3 % to 2021 (Gao et al., 2020). The selling price is estimated at US \$175 kg⁻¹ for biomass containing 1 % fucoxanthin (Leu & Boussiba, 2014) and US \$0.20-0.74 in capsular/softgel form (Timmermans, 2017; Wu et al., 2016). To date only one company (AlgaTechnologies, Israel) is producing fucoxanthin (FucoVital™) from *P. triornutum* profitably for liver health. Other examples of commercial fucoxanthin are from macroalgae e.g. Solaray Fucoxanthin Special Formula® and fūcoTHIN® from Garden of Life.

EPA is an essential omega-3 fatty acid for human nutrition with the recommended daily intake (RDI) of 250 mg each day (Ryckebosch et al., 2014). EPA is a precursor for signalling molecules such as eicosanoids and has defined benefits in cardiovascular health, cancer treatment, and for numerous mental health diseases (Deckelbaum & Torrejon, 2012; Oscarsson & Hurt-Camejo, 2017). EPA is currently mainly derived from fish oil (and to some extent krill oil) and to meet the RDI 0.8 g of fish oil must be consumed daily by humans, whereas for microalgae the daily intake would range from 1.3-12.5 g oil day⁻¹ (Ryckebosch et al., 2014). The market size for EPA is US \$300 million and the selling price is US \$200-500 kg⁻¹ (Alam et al., 2020). EPA is highly dependent on the strain, PBR system and cultivation conditions and can range from 3.1-5 % DW without using GMO methods (Derwenskus et al., 2020). Currently only Simris (Sweden) is producing a commercial EPA product from *P. triornutum*. However, other microalgae such as *Nannochloropsis* spp. are used for EPA algal oil products e.g. Vegan True®, Non-Fish Omega-3s from Source Naturals® and iWi®.

Chrysolaminarin is the carbohydrate stored in the vacuole that exhibits antitumour, antioxidant, and immunomodulatory capacities, but as yet has not been commercially

exploited (Yang et al., 2020). Examples of genetically engineered products include bioplastics and recombinant antibodies such as monoclonal antibodies against Hepatitis A and the Marburg virus (Hempel et al., 2017; Hempel and Maier, 2016). The bacterial (*Ralstonia eutropha*) poly-3-hydroxybutyrate (PHB) pathway has been introduced into *P. tricornutum* which resulted in 10.6 % DW PHB (forming granule-like structures in the cytosol) and has revealed the potential of *P. tricornutum* for biodegradable bioplastics to be used as part of the biobased economy to replace >140 million tons of plastic consumed worldwide (Hempel et al., 2011a).

P. tricornutum is perhaps the most well characterised diatom (Sethi et al., 2020). Overall, *P. tricornutum* could be an important microalgae candidate as a diatom cell factory attributable to its biochemical composition (fucoxanthin, EPA, essential amino acids and minerals), robust growth in mass culture systems, tolerance of low-light levels and high pH, the ability to grow without silicate (making media formulation simpler and more economical), and the well characterised genome and engineering tools available. In outdoor mass cultivation the typical profile of *P. tricornutum* is 26 % carbohydrate, 0.5 % carotenoids, 2 % chlorophyll, 36 % protein and 18 % lipid (Reboloso-Fuentes et al., 2001) but this depends on the strain used and the cultivation conditions. Before *P. tricornutum* can become a commercial reality as a biorefinery chassis for high-value (fucoxanthin) and bulk products (ingredients for aquaculture/animal feed, functional food for humans, bioplastics and biofuels), both upstream and downstream developments need to be made for commercial development.

1.3. Challenges in implementing *P. tricornutum* as a cell factory

Through minimising the costs of production of the entire process (upstream and downstream), the feasibility of *P. tricornutum* as a biorefinery organism for fucoxanthin and aquaculture feed could become commercially viable by 2025. Novel downstream processing methods should incorporate a wet process (omitting the drying step) for a reduction in costs and require methods that are easily scalable with lower capital and operating costs. Currently

the cost of harvesting is up to 30 % of the total cost of production (Van Haver and Nayar, 2017). Mild wet extraction techniques (to avoid drying) are required that do not result in damage to the products; particularly proteins which are vulnerable to denaturation and carotenoids which can easily be degraded and change their stereochemistry.

1.3.1. Upstream – process optimisation

Currently the biomass productivity and product yields of *P. tricornutum* are low compared with other cell chassis' such as bacteria and yeast. Current photoautotrophic biomass productivity levels are lower by two orders of magnitude and need to be improved to compete with heterotrophic cell chassis. An emphasis on process conditions such as media optimisation, temperature and light, have been investigated to improve product yields such as EPA and fucoxanthin, but utilising a single product approach. For the purpose of this thesis, the importance of macronutrients (nitrate and phosphate), salinity, and carbon source (bicarbonate, CO₂ and glycerol) on biomass productivity and product yields will be emphasised exploring a biorefinery approach. Indoor and outdoor cultivation will be compared in an airlift PBR for determining the feasibility of a biorefinery (fucoxanthin, EPA, protein and carbohydrate) using a fed-batch approach.

1.3.2. Downstream

Biomass harvesting can represent up to 30 % of the microalgal production cost in suspended cultures. Centrifugation is adopted in the microalgal industry for high value products but is not economically viable for bulk ingredients. Comparatively, flocculation appears to be an inexpensive and effective method for harvesting *P. tricornutum*. However, current flocculation methods are either toxic (e.g., aluminium as a chemical flocculant) or expensive (chitosan). This work aimed at understanding the following questions. Can auto-flocculation be induced without adding chemicals? Alternatively, could bio-flocculation present a different, sustainable approach? It would then be interesting to adopt a wet approach for the sequential extraction of several products of interest.

1.4. Goal of the thesis

In this thesis, the aim was to understand how to increase biomass and product yields for the development of a biorefinery process using *P. tricornutum* CCAP 1055/1 for multiple products; primarily fucoxanthin (as a weight loss supplement), and biomass rich in EPA, protein and carbohydrate for aquafeed. Both upstream (low biomass and product yields) and downstream challenges (low-cost harvesting) are addressed to reduce the cost of production (Figure 1.1).

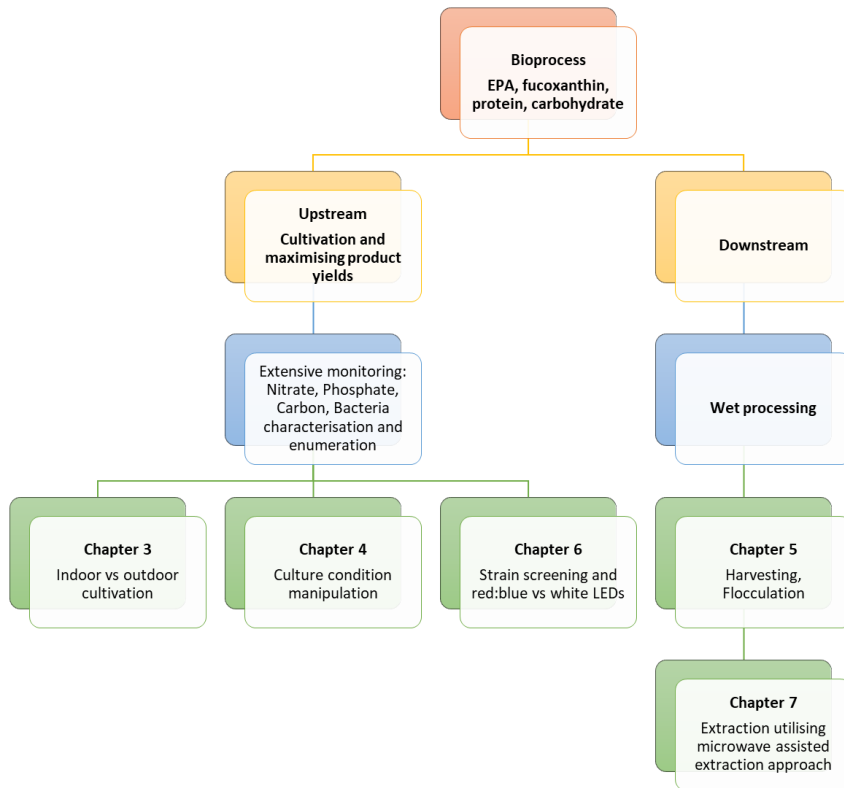
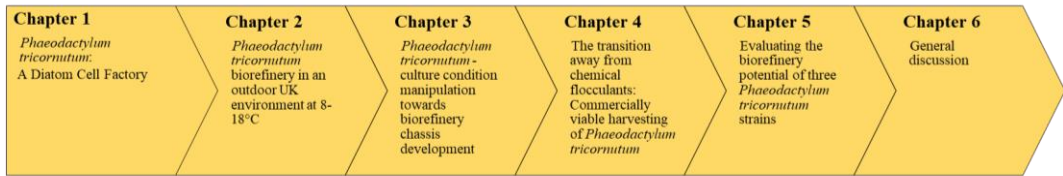


Figure 1.1 - Bottlenecks to overcome for the exploitation of *P. tricornutum* for multiple products utilising a biorefinery approach.

1.5. Outline of the thesis

The thesis will be outlined as below:



The concept of *P. tricornerutum* as a diatom cell factory and the challenges to overcome for a commercial biorefinery will be discussed in **chapter 1**. In **chapter 2** a commercially viable and time saving hydroponics fertiliser mix and powdered media formulations from Varicon Aqua Solutions will be compared with conventional f/2 medium for increased biomass, EPA, fucoxanthin, and protein yields. *P. tricornerutum* was cultivated indoors, and outdoors under cold conditions and low light in the UK using an airlift PBR (PhycoLift) in a repeated fed-batch operation. The objectives were to observe differences in the biochemical composition and determine if there is a relationship between light/temperature and biochemical composition. Commensal bacteria in both indoor and outdoor settings were identified and monitored over the fed-batch cultivation period. In **chapter 3** limitations in conventional f/2 medium will be discussed and an alternative media formulation will be proposed. Further work was conducted on elevating product yields through cultivation condition manipulation. In **chapter 4** the high cost of harvesting will be reviewed and alternative biobased, environmentally friendly flocculants will be evaluated (harvesting efficiency, concentration factor, time, scalability, and economic viability) against traditional chemical flocculants. In **chapter 5** a strain screening investigation will be discussed to determine the importance of strain selection on biomass productivity and product yields. Red/blue light emitting diode (LED) lighting (as an alternative to warm white LEDs) was evaluated for improving biomass and product yields and for observing the effect on the commensal bacterial population. **Chapter 6** is a general discussion which provides an outlook of the proposed upstream and downstream improvements to *P. tricornerutum* cultivation and

processing for industrial application. Future bottlenecks to overcome and the steps required for reducing the cost of production are discussed to achieve the aim of developing an economically viable biorefinery production platform utilising *P. tricornutum* for multiple products and applications.

Chapter 2: *Phaeodactylum tricornutum*: a diatom cell factory

This chapter is published as:

Butler, T., Kapoore, R.V. and Vaidyanathan, S., 2020. *Phaeodactylum tricornutum*: a diatom cell factory. *Trends in biotechnology*, 38(6), pp.606-622.

2.1. Abstract

A switch from a petro-based to a bio-based economy requires the capacity to produce both high-value low-volume, as well as low-value high volume products. Recent trends point to the case for developing microalgae based microbial cell factories, with the objective of establishing environmentally sustainable manufacturing solutions. Diatoms display rich diversity and potential in this regard. Here, we focus on *Phaeodactylum tricorutum*, a pennate diatom commonly found in marine ecosystems and discuss recent trends in developing the chassis for a suite of natural and genetically engineered products. Both upstream and downstream developments are reviewed for the commercial development of *P. tricorutum* as a cell factory for multiple products of interest.

Keywords: Microbial chassis, biorefinery, EPA, fucoxanthin, biodiesel

2.2. Microalgae chassis in the biobased economy

The growing world population is constantly placing increasing demands on available resources that need to be utilised in innovative and environmentally sustainable ways for providing us with food security, energy, and chemicals (Abel et al., 2016). A transition to the **bio-based economy** (see **Glossary**) from an environmentally unsustainable petroleum-based economy will require capacity to incorporate low-value, high volume productions, in addition to high-value low volume manufacturing, and remains a techno-economic challenge. Nevertheless, there is an increasing desire to create microbial cell factories that can address this capability. Microbial cell factory hosts have predominantly been proposed for high-value products, such as the production of recombinant vaccines and therapeutics for the prevention and treatment of diseases. *Escherichia coli* has often remained the choice for development as a microbial **cell chassis**, but eukaryotic platforms, such as *Saccharomyces cerevisiae* (Jouhten et al., 2016), Chinese hamster ovary (CHO) cell lines (Brown et al., 2019), and plants (Park and Wi, 2016) are also well developed. However, with the ever-increasing need to provide environmentally sustainable solutions to manufacturing that are also economically viable for a multitude of products including low-value high-volume products, alternative platforms with diverse capabilities are required. In this regard, microalgae offer alternative promise.

Microalgae are photosynthetic organisms that possess the machinery to produce high-value phytochemicals, and have the capacity to utilise carbon dioxide as a feedstock, potentially enabling economic and environmentally sustainable manufacturing solutions. Compared to plant cells, they can be relatively quick to grow (doubling times in hours typically, and biomass productivities in days as opposed to months or years for plants), can be grown on non-arable land with potential for reclamation of nutrients from waste resources (wastewaters and waste CO₂ sources), offering higher process turnover and economically viable processing alternatives. Their ability to grow in a multitude of niches including marginal land, desert land, brackish water or the open ocean, not only offers effective resource utilisation, but also indicates an adaptive lifestyle with a diversity of metabolic capabilities that could be tapped into. Industrial scale cultivations for commercial manufacturing have largely focussed on harnessing the natural capabilities of selected species, such as β -carotene

from *Dunaliella salina*, phycocyanin from *Arthrospira* spp., and astaxanthin from *Haematococcus pluvialis*. However, this trend is slowly changing. The genomes of >40 microalgae species are now publically accessible and more are in the pipeline, with an increasing array of tools being developed to engineer metabolic pathways towards development of cell factories that are tractable and functionally diverse. There is a growing body of knowledge on the biochemical makeup, metabolic pathways and functional capabilities of a handful of species. However, given the vast diversity of microalgae, they still remain a largely untapped resource.

Much of our knowledge on microalgae metabolism and tools development in a manufacturing context, in the recent years, has been driven by the need to develop microalgae for biofuel production. Current consensus points towards a **biorefinery** concept in manufacturing, with multiple product streams ('t Lam et al., 2017; Gifuni et al., 2019; Markou and Nerantzis, 2013), especially for producing low-value high-volume products. Alternative product streams for productions from the same microalgae chassis will be needed. In addition to harnessing the natural product spectrum from microalgae that include bioactives with nutraceutical and cosmeceutical properties, there is also a drive to develop engineered microalgae towards therapeutic protein production (Hempel et al., 2017; Specht and Mayfield, 2014), bioplastic precursors (Hempel et al., 2011a) and plant terpenoids (Adamo et al., 2019). Moving forward, the challenge is in developing microalgae chassis to accommodate the biorefinery concept, for economically viable propositions that can harness potential environmental sustainability offered by using a microalgae chassis for biomanufacturing. Whilst several microalgae are at various stages of development as cell factories (Box 1), there is a growing body of knowledge on the pennate diatom, *Phaedactylum tricornutum*, and its development as a microalgae cell factory, which we discuss here.

2.3. *P. tricornutum* – a well-studied diatom

P. tricornutum is a model diatom (Box 2) that exhibits a complex sexual life cycle and is perhaps the most characterised of all diatoms so far. It is a robust laboratory species and can

be grown in a range of culture media. It is known to accumulate a spectrum of marketable products, and is a commercially viable species for large-scale cultivation (Table 1). Its potential for being a suitable chassis can be attributed to its ability to grow in seawater, a tailored molecular toolbox, and the ability for multiple products of interest to be extracted sequentially (Remmers et al., 2018; W. Zhang et al., 2018). In outdoor mass culture systems, it has been shown to dominate and outcompete other microalgae species with a tolerance for high pH and an ability to grow under low light (Remmers et al., 2017; Spilling et al., 2013).

P. tricornutum has unique biology amongst diatoms (Box 3). **Gene knockout tools** have been developed (Serif et al., 2017; Weyman et al., 2015) and the genome can now be edited by CRISPR/Cas-9 for gene-targeted mutations (Nymark et al., 2016b; Slattery et al., 2018; Stukenberg et al., 2018). Advances in genetic knowledge of *P. tricornutum* has contributed to its development as a chassis for the production of non-native components, including polyhydroxybutyrates (PHBs) for bioplastics (Hempel et al., 2011a), monoclonal antibodies (Hempel et al., 2017) and plant triterpenoids, which are not endogenous to the organism (Adamo et al., 2019) and levels of DHA which are low in native strains have been elevated (Hamilton et al., 2015).

The biochemical characteristics, robust growth in mass culture systems, tolerance of low-light levels and high pH, and the well characterised genome and engineering tools available suggest *P. tricornutum* could be an important microalgae candidate as a diatom cell factory. For this platform organism to produce products of interest on a commercial scale, process optimisations based on developments upstream and downstream are essential.

2.4. Cultivation of *P. tricornutum*

Both indoor and outdoor settings in photobioreactors (PBRs) (tubular, column, flat-panel, and proprietary types) and open (raceway) ponds have been used to cultivate *P. tricornutum*, with varying product yields and productivities (Table 1). Flat-panel PBR configurations have shown improved biomass, EPA and fucoxanthin productivities, attributable to low shear stress and effective illumination (Guler et al., 2019). High energy requirement for temperature maintenance (Tredici et al., 2015) and temperature dependent loss

of biomass to photorespiration (Meiser et al., 2004) are challenges to address with the use of PBRs. Light is a major influencing factor in product accumulations. Current photosynthetic productivity in microalgae, in general, is lower than theoretically attainable levels in the **photoautotrophic** mode (Remmers et al., 2018). Light intensity (Heydarizadeh et al., 2017), wavelength (Jungandreas et al., 2014) and photoperiod (Sirisuk et al., 2018) are all known to have an influence on *P. tricornutum* metabolism and in turn affect productivities. In terms of product accumulations, low light intensities appear to favour the accumulation of fucoxanthin (Gómez-Loredo et al., 2016; McClure et al., 2018) and EPA (Acién Fernández et al., 2000), whilst higher light intensities appear to favour accumulation of storage components, chrysolaminarin (Wagner et al., 2016), and triacylglycerides (TAGs) (Huete-Ortega et al., 2018), with degradation of synthesised chrysolaminarin in the dark (Wagner et al., 2016), under N-limitation. However, under nutrient rich conditions, TAG and EPA contents were found to be independent of the applied light intensity (Remmers et al., 2017).

P. tricornutum is a successful photoautotroph but is also capable of **mixotrophic** growth on glucose, acetate, fructose and glycerol. Based on various reports, glycerol appears to be the most suitable organic carbon source for mixotrophic growth, resulting in the highest biomass and EPA productivities to date (Table 1), but it has not been explored for other products of interest. **Mixotrophy** with glycerol mimics typical responses with nitrogen limitation resulting in increases in triacylglycerides but there are also resultant increases in biomass without loss of photosynthetic capacity of the cell (Villanova et al., 2017).

Nitrogen and phosphorus limitations have been successfully used to alter product accumulations in *P. tricornutum* (Abida et al., 2015; Alipanah et al., 2018, 2015; Brembu et al., 2017; Huete-Ortega et al., 2018), and silicon is known to be a non-obligatory requirement for growth of the organism, although it may have a positive influence on some growth processes as found under low temperature and green light (Zhao et al., 2014), so can also be used to alter product accumulation (Brembu et al., 2017). Whilst nitrate is a commonly examined nitrogen substrate, a switch to ammonium can lead to increased lipid productivity (Huete-Ortega et al., 2018), and encouraging environmental benefits could be attained by switching to urea, or ammonium nitrate (Pérez-López et al., 2014), in large scale cultivations.

It is anticipated that developments in PBR configuration, lighting, media formulation, carbon assimilation/utilisation, in combination with bioprospecting can result in significantly increased biomass and product yields. However, to elevate intrinsic yields, upstream developments through the manipulation of product pathways may be required.

2.5. Upstream developments

Toolkits for a tractable chassis

Domestication of microalgae is often hindered by the absence of controllable sexual cycles that would allow combining desirable traits and the removal of unwanted alleles. To date, in microalgae, the genetic toolkits developed for *P. tricornutum* is one of the most advanced, and both nuclear (Kira et al., 2016) and chloroplast (Xie et al., 2014) transformations have been achieved. Identifying endogenous promoters, well mapped plasmids, antibiotics-free **selection markers** and successful modes of DNA delivery will not only enable developing an appropriate understanding of the chassis but also a tractable chassis fit for purpose. For the effective expression of recombinant proteins adapting DNA sequences to host specific codon usage whilst avoiding weakly translated codons is beneficial for protein translation, but as *P. tricornutum* possesses a typical GC-content of 48 %, this might be less critical and foreign genes and enzymes can be expressed without codon optimisation (Hempel and Maier, 2016; Yan et al., 2016).

The pPhaT-1 plasmid has been the most frequently used vector and contains the *sh-ble* gene that confers resistance to antibiotics zeocin and phleomycin (Jeon et al., 2017). Alternatively, the pPhAP1 vector with an alkaline phosphatase promoter has been shown to be effective with enhanced green fluorescent protein (EGFP) expression at 9.3-10.5 times greater than other diatom vectors showcasing the potential of the vector in obtaining high yields of recombinant protein (Lin et al., 2017). In terms of promoters, the light regulated *fcpA* (LHCF1) and *fcpB* (LHCF2) promoters are the most frequently used but they are constrained by being light dependent and inactive in the dark (Nymark et al., 2013). A nitrate reductase (NR) promoter has been used in *P. tricornutum*, that is reportedly better than LHCF1 in green

fluorescent protein (GFP) expression (Chu et al., 2016). The NR promoter inhibits transcription in ammonium, but this has been reported to be 'leaky' (Chu et al., 2016). Alternatively, EF2 that encodes elongation factor 2 is a possible new constitutive promoter with higher expression than LHCF2 that is not significantly affected by light (Seo et al., 2015). Other endogenous promoters that have been shown to have good performance characteristics include the alkaline phosphatase promoter (Lin et al., 2017) and glutamine synthetase promoter (Erdene-Ochir et al., 2016). In addition, potential promoter regions identified from diatom-infecting-viruses (DIVs) have also been shown to function effectively (Kadono et al., 2015). Constitutive promoters to express multiple target genes have also been recently demonstrated (Erdene-Ochir et al., 2016; Kadono et al., 2015; Seo et al., 2015). Introns can also be included in the expression cassette that contain transcriptional enhancers or sequences conferring enhanced mRNA stability or enhanced mRNA turnover.

The availability of bacterial conjugation (Karas et al., 2015; Slattery et al., 2018) for economic genetic transformations provides a viable solution to the more expensive alternatives of biolistics and electroporation. In bacterial conjugation, DNA is replicated stably within the nucleus as an episome. This presents an opportunity for artificial chromosome transfer into diatoms and could result in a one-step transfer of whole metabolic pathways, as has been shown for vanillin biosynthesis (Slattery et al., 2018), where a plasmid encoding eight genes involved in vanillin biosynthesis has been shown to be successfully propagated in *P. tricornutum* over four months with no evidence of rearrangements.

Genome editing tools offer a breakthrough in targeted mutagenesis for the development of *P. tricornutum* as a cell factory, given that the organism is diploid and sexual reproduction cannot be controlled in the laboratory, limiting random mutagenesis as a useful tool for trait improvements. From an industrial perspective, genome editing is not yet subject to regulatory approval as the mutants are not stated as genetically modified (GM) (Podevin et al., 2013), and more importantly the changes introduced are believed to be more tractable. Meganucleases (Daboussi et al., 2014), TALENS (Serif et al., 2017; Weyman et al., 2015), and CRISPR/Cas9 with an optimised Cas9 (Nymark et al., 2016a; Slattery et al., 2018; Stukenberg et al., 2018) have all been shown to work in *P. tricornutum* for targeted genetic

engineering and the generation of stable knockouts. Using these techniques can result in marker free transgenic types.

Using a non-genetically modified organism approach, **adaptive laboratory evolution** has been shown to result in a two-fold increase in growth and fucoxanthin content in semi-continuous cultivation over only 11 generations with red and blue light (Yi et al., 2015). Adaptations to elevated carbon dioxide levels over nearly 2000 generations (Li et al., 2017a) have shown to evolve lower mitochondrial respiration.

Genome scale metabolic models (GSM) have been developed for *P. tricornutum* (Levering et al., 2016). Further developments in pathway elucidation can result in developments using a top down or bottom-up approach for elevating products of interest and synthesising heterologous compounds.

Improved knowledge of product biosynthetic pathways and their regulation

By far the most widely investigated process, driven by the need to develop alternative renewable strategies for meeting our energy demands, is the accumulation of storage neutral lipids (triacylglycerols - TAGs), which can be converted to biodiesel. Nitrogen depletion is the most widely employed strategy to induce TAG accumulation in microalgae, and this is no different in *P. tricornutum* (Longworth et al., 2016; Remmers et al., 2017; Shemesh et al., 2016). Briefly, *de novo* fatty acid synthesis occurs in the plastid, followed by two known routes to TAG synthesis: (a) acyl lipid assembly in the endoplasmic reticulum (Kennedy pathway) and (b) the acyl-CoA independent pathway involving phospholipid:diacylglycerol acyl transferase (PDAT) which involves the chloroplast membrane lipids (Figure 1).

More recently, the role of Methylcrotonyl-CoA Carboxylase (Ge et al., 2014), phosphoenolpyruvate carboxykinase (PEPCK) (Yang et al., 2016), Diacylglycerol Acyltransferase (DGAT) (Dinamarca et al., 2017), 1-Acylglycerol-3-Phosphate O-Acyltransferase 1 (AGPAT1) (Balamurugan et al., 2017), and Malic enzyme (ME) (Zhu et al., 2018) have all been implicated in TAG synthesis in *P. tricornutum*, in addition to the identification of lipases (Barka et al., 2016), which play a role in TAG degradation and reallocation of fatty acids to maintain lipid homeostasis in the plastids (Figure 1). TAG accumulation involves remodeling of intermediate metabolism, especially reactions in the

tricarboxylic acid (TCA) and the urea cycles (Levitan et al., 2015), and restructuring of carbon metabolism through down regulation of the Calvin cycle, chrysolaminarin biosynthesis and up-regulation of the TCA cycle, and pyruvate metabolism to reroute the carbon to lipids (Alipanah et al., 2015; Bai et al., 2016; Longworth et al., 2016). This has also been linked to cell cycle arrest (Kim et al., 2017). With regards to EPA, the involvement of elongases and desaturases in EPA synthesis has been demonstrated, both through homologous and heterologous expression (Dolch and Maréchal, 2015; Hamilton et al., 2016). For fucoxanthin synthesis, phytoene synthase (psy) regulation has been shown to be involved (Kadono et al., 2015). The metabolic pathways and regulatory nodes for chrysolaminarin synthesis are not yet as well investigated. Two potential 1,6-beta transglycolases involved in the branching of 1,3 beta glucan chains have been characterised and found to be associated with the vacuole, suggesting branching of chrysolaminarin may occur in these organelles (Huang et al., 2016). It appears that the carbohydrate storage in the vacuoles is intertwined with carbohydrate metabolism, photosynthetic homeostasis and plastid morphology (Huang et al., 2018). UDP-glucose pyrophosphorylase (UGPase) has been identified as a rate limiting enzyme that might play an important role in chrysolaminarin biosynthesis (Zhu et al., 2016).

Carbon capture and photosynthesis in P. tricornutum

Photoautotrophic growth is a key advantage of this microbial chassis and an understanding of carbon capture and photosynthesis is essential in developing the chassis. Compared to plant systems, the understanding of this aspect is still fragmentary, but recent developments are encouraging. *P. tricornutum* is known to take up bicarbonate, a ‘chloroplast pump’ acting as the primary active transporter (Hopkinson et al., 2016a). Several carbonic anhydrases (CAs) have been identified in *P. tricornutum* that participate in the carbon capture mechanisms to maintain sufficient partial pressure in the **pyrenoid** for CO₂ fixation by Rubisco. *P. tricornutum* appears to lack both and cytoplasmatic CAs and CAs (Hopkinson et al., 2016a). However, recently a theta-type CA localised in the thylakoid lumen with essential roles in photosynthesis and growth of the organism has been reported (Kikutani et al., 2016). CCM mechanisms in diatoms appear to be diverse between species (Young and Hopkinson,

2017). Plasma membrane type aquaporins are known to function in CO₂/NH₃ transport and provide photoprotection (Matsui et al., 2018).

Photosynthetic efficiencies in diatoms, although higher than in plants, can still be improved with appropriate knowledge of light harvesting and utilisation in diatoms. There is still substantial scope in bridging the gap between currently achievable and theoretical conversion yields (Remmers et al., 2018). The fucoxanthin-chlorophyll proteins (FCPs) are the most characterised light harvesting complexes in diatoms. In *P. tricornutum*, FCPs associated with both the photosystems I and II have been characterised (Gundermann and Buchel, 2014). Although there are similarities with plant systems, there are also differences in pigmentation (Gundermann and Buchel, 2014). The photosystems are segregated in subdomains, which minimise physical contact, as required for improved light utilisation, but are interconnected, ensuring fast equilibration of electron carriers for efficient optimal photosynthesis (Flori et al., 2017). More recently, the efficacy of light harvest and energy transfer in these systems is becoming clearer with the structural elucidation of the complex (Wang et al., 2019).

2.6. Downstream considerations and challenges

P. tricornutum cultivations are typically suspended cultures, requiring cell harvest and extraction stages, which represent a target for increasing the cost competitiveness of *P. tricornutum* as a cell factory. Downstream processing costs have a significant contribution to overall process costs (typically ranging between 20-60%) ('t Lam et al., 2019). Harvesting alone can contribute to 23% of the cultivation cost with raceway cultivations, but can be as low as 5-7% with photobioreactors, due to the potential for higher biomass concentrations (Ruiz et al., 2016).

The aim of harvesting is to concentrate the biomass by 10-300 fold (typically from 0.05-0.5% to 5-15% total solids) for subsequent drying/extraction or direct extraction of wet biomass in the shortest period to avoid spoilage, especially in warm climates (Vandamme et al., 2010). It is essential for the harvesting technique to be quick, have good harvesting

efficiency (>90%), inexpensive, leave behind little or no toxic residues, and not affect the quality of the biomass (’t Lam et al., 2017). Traditionally, centrifugation has been used for harvesting, and the apparatus include conventional cream separators, bucket centrifuges and super-centrifuges. Nevertheless, centrifugation is energy intensive and can account for 20-25 % of the cultivation costs (’t Lam et al., 2017).

A wide variety of harvesting methods have been suggested for *P. tricornutum* (Figure 2). Novel methods include the use of hydrocyclones, nanoparticles, ultrasonic harvesting, flotation, and tangential flow membrane filtration. However, the most well researched area for harvesting *P. tricornutum* have centered around flocculation with this method being scalable. Flocculants are well characterised and are effective through different modes; charge neutralisation (inorganic flocculants), sweeping, polymeric bridging (organic flocculants) and electrostatic patch mechanisms (Vandamme et al., 2013). Alternatively, autoflocculation can be effective in a narrow pH window (10-10.5) in the presence of magnesium with flocculation induced by the precipitation of brucite (magnesium hydroxide), which causes charge neutralisation and adsorption of hydroxide particles onto the cell wall of *P. tricornutum* (Formosa-Dague et al., 2018; Vandamme et al., 2015b). To date many flocculants have been tested (cationic, anionic and nonionic) but there has been an inconsistency with the setup design, flocculant concentrations used, the initial biomass density, optimal pH and the time required for optimal harvesting. Bioflocculation using closely associated bacteria within the culture, and the influence of extracellular proteins on the harvesting efficiency (Buhmann et al., 2016), are innovative, environmentally friendly and potentially cost-effective approaches that warrant further investigation.

The range of extraction techniques investigated in *P. tricornutum* is showcased in Figure 2 and comprises biochemical, mechanical and physical methods. The conventional scalable methods (e.g., bead milling for cell disruption followed by solvent extraction) are mainly constrained by economic and environmental drawbacks associated with the extraction and purification of bioactives, in conjunction with degradation issues (Kapoor et al., 2018). Modern green extraction techniques mitigate most concerns of traditional techniques and warrant further investigation. These green solutions include microwave assisted extraction (MAE), pulsed electric field (PEF), ultrasound assisted extraction (UAE), pressurized liquid

extraction (PLE), supercritical fluid extraction (SFE) and the use of enzymes and ionic liquids (Esquivel-Hernández et al., 2017). Ethanol has been suggested as a green solvent for the extraction of fucoxanthin and EPA from *P. tricornutum* biomass (Delbrut et al., 2018) that doesn't require a drying step when used as a water-miscible solvent in PLE (Derwenskus et al., 2019). Lipid extractions can also be enhanced with microwaves (MWs) or the application of deep eutectic solvents (DESs) for cell wall disruption, followed by supercritical CO₂ (scCO₂) and dimethyl carbonate (DMC) extractions. The fatty acid profiles from such extractions can be similar to the traditional Bligh and Dyer extraction method albeit with higher selectivity (Tommasi et al., 2017). More detailed knowledge is required from the cell walls of microalgae to facilitate successful cell disruption and extraction approaches. There is still a requirement to develop these environmentally friendly methods at pilot scale with an emphasis on MAE and PLE due to the wide spectrum of microalgal metabolites that can be extracted (Erdene-Ochir et al., 2016).

Whole cell formulations for end-use could be a cost-effective approach that would obviate the need for extraction steps and alleviate product stability/storage concerns. This is in particular useful in the delivery of bioactives in food/feed formulations, as has been demonstrated for effective delivery of omega-3 fatty acids in Salmon feed (Sørensen et al., 2016).

2.7. Towards a diatom biorefinery

The biorefinery principle is well defined but has very rarely been put into practice. t'Lam and colleagues (t Lam et al., 2017) evaluated that a multi-product biorefinery is not currently feasible with downstream processing accounting for 50-60 % of the process. Currently there is too much emphasis on inflated prices of microalgal products such as pigments as has been observed in the *H. pluvialis* derived astaxanthin industry. Inflated prices may work for fucoxanthin from *P. tricornutum*, which relies on clinical backing for the associated health claims. Few studies have fully addressed the options of sequentially extracting products from *P. tricornutum* biomass in an integrated biorefinery (Figure 2).

Sequential extraction of fucoxanthin, followed by EPA and chrysolaminarin, in turn has been suggested as a possibility (W. Zhang et al., 2018). However, the economic viability of this proposition is yet to be investigated.

The economic feasibility of a microalgae biorefinery has been argued for with production costs of €6-7/kg DW and a resulting revenue of €31/kg DW including cultivation and downstream processing. Production costs of €3-6/kg DW over the same scale can be achieved even with closed tubular PBRs (Matilde S.Chauton et al., 2015), but the electricity costs required for cultivation are high (62 % of the costs of cultivation in an indoor setting) (Pérez-López et al., 2014) and consequently there is a necessity to produce microalgal products in an outdoor setting. More careful integration of the downstream processing units could result in a cost-effective solution ('t Lam et al., 2017). Using bioflocculation in combination PEF for the 'milking' of *P. tricornutum* cells (Figure 2) through a wet processing method could result in the release of multiple products of interest without killing the cells, but this remains to be tested.

2.8. Concluding remarks

As showcased above, *P. tricornutum* has great potential as a microbial cell chassis for homologous and heterologous compounds. The high photosynthetic efficiency, a detailed understanding of product pathways, a well-developed suite of molecular tools, in conjunction with the ability to produce a spectrum of marketable products, all point to great promise for the future development of the chassis. *P. tricornutum* has been explored to produce single products at pilot scale, including TAGs for biodiesel and fatty acids of nutraceutical value (EPA and DHA), but products such as recombinant proteins and chysolaminarin are yet to see large scale trials. Fucoxanthin appears to be the only product that has been shown to be commercially viable currently, due to its high selling price, but as product supply increases, selling prices may fall as observed in the astaxanthin industry. There is also considerable potential for the development of more products of value using the chassis as demonstrated with heterologous compounds and scope for reallocation of carbon to maximize specific productivities. Nevertheless, long-term sustainable commercial productions from *P. tricornutum* will require development of a biorefinery approach to valorize cultivations with incorporation of multiple product streams. Despite the promise challenges remain that require attention. A primary challenge is in maximising biomass productivities, in a way to make the most of photoautotrophy and develop processes that are cost effective and competitive compared to other heterotrophic hosts. Learning to make the most of the photosynthetic capacity and increasing carbon uptake and routing to products of value are desirable. The developments in PBR technology, and innovative downstream processing options that drive down costs necessary to enable economical extraction of several products of interest that are also environmentally sustainable are needed within a biorefinery approach (see Outstanding questions).

Industrial cultivation of genetically engineered *P. tricornutum* will require secondary containment such as glass houses or polythene tunnels, antibiotic resistance needs to be replaced with other selection markers such as fluorescent proteins and legislation will have to be complied with in terms of genetically modified organisms especially as the regulations

surrounding CRISPR-Cas 9 are as yet bordering on uncharted waters in the EU. Nevertheless, the future for *P. tricornutum* as a microalgal cell chassis is certainly bright.

Acknowledgements

The authors are grateful to the UK BBSRC (BB/K020633/1; BB/L013789/1- (Phyconet) PHYCBIV-13; PHYCBIV-28) and EPSRC (EP/E036252/1 and DTA 1912024) for financial assistance, which enabled this work.

Glossary

Adaptive laboratory evolution: is a method employed to gain insights into the fundamentals of molecular evolution and adaptive changes that occurs in populations during long term selection under specific growth conditions. The organism is repeatedly cultured by exposure to pre-defined conditions to accelerate evolution in the laboratory.

Allele specific expression (also known as allelic bias): is one where one allele is expressed at levels higher than the other.

Bio-based economy: is where biological feedstock and/or bioprocesses are employed to derive products of value for economic gain, as sustainable solutions to the challenges we face (food, energy, chemicals, health, materials, and environmental protection).

Bio-refinery: is a process which aims to replace oil with biomass as a feedstock for fuel and chemical production through the integration of green chemistry and sustainable production. The aim is to produce multiple products from biomass to add value to the process (in a way akin to chemical refinery).

Cell chassis: can refer to a cell host or an organism with a genome that can be altered to maintain heterologous DNA parts for gene expression.

Downstream processing: refers to steps involved downstream of cultivation to recover products of interest, and can encompass cell harvest and the extraction of products of interest from natural sources followed by product purification or formulation.

Gene knockout tools: are tools used to make an organism's gene inoperative. These are usually developed to study gene function and to investigate the phenotype after gene loss.

Genome editing: targets precise sites within a genome by introducing double strand breaks into a specific guided site that is repaired resulting in a modest deletion of a few nucleotides of the native gene. Insertional activation is not required for mutations to be created through incorporation of a non-native gene encoding a selectable marker.

Gibson and Golden Gate assembly: are assembly methods used across the synthetic biology community which employ a 'one-pot/tube' method and do not rely on restriction sites. Gibson assembly involves long-overlap assembly (exonuclease for annealing fragments, polymerase for filling the gaps and DNA ligase for sealing the nicks in the assembled DNA) where multiple parts can be assembled (promoters, terminators and other short sequences).

Golden Gate is based on Type II S restriction endonucleases, which cleaves double-stranded DNA outside their recognition sites resulting in a short single-stranded overhang with Bsal restriction sites utilised for a simultaneous digestion and ligation preventing re-ligation.

Mixotrophy: a mode of cultivation where the culture utilises both carbon dioxide and organic carbon supplemented in the nutrient medium.

Photoautotroph: is an organism that can make energy from sunlight and carbon dioxide through photosynthesis to synthesise organic compounds for nutrition.

Pyrenoid: are sub-cellular compartments in the chloroplast of most algae and are associated with the carbon concentrating mechanism (augments photosynthetic productivity by increasing inorganic carbon).

Secondary endosymbiotic events: are events which occurred when a living cell engulfed another eukaryotic cell that had undertaken primary endosymbiosis resulting in a cell with a double phospholipid bilayer around the mitochondria and chloroplasts.

Selection markers: are sequences that are expressed for a specific set of traits that provide the transformed cells with different properties from untransformed cells. Selection markers affect the condition under which the transformed cell can grow such as, antibiotic resistant transformed cells growing in medium with antibiotics.

Transposon (also known as a jumping gene): is a DNA sequence that can alter its position within a genome, occasionally resulting in a reverse mutation, altering the cells genetics and genome size.

Table I: Alternative microalgae (genome sequenced) cell factories under development and their biotechnological potential

| Organism | Genome size (Mb) | Biotechnology potential | Opportunities | Challenges |
|--|--|---|--|--|
| <i>Chlamydomonas reinhardtii</i> CC-503 cw92 mt + | 120 (chloroplast and mitochondria sequenced) | Biofuels, recombinant proteins, model chassis | Fast growth (6–8 h doubling time); all three genomes completed and well annotated; easily transformable with inducible and constitutive promoters; cloning methods developed for insertion of multiple genes (Gibson and Golden Gate assembly); range of plasmids and strains (>300 and >2700, respectively); advanced genome editing (CRISPR/Cas9, ZFNs, TALENs); detailed omic studies/data | Low oil content; poor growth in open ponds, sensitive to solar irradiance; internal RNA silencing mechanism preventing gene expression, no standardized expression strain, poor expression of heterologous proteins, relatively few protein-coding genes from the genome have been fully functionally validated, number of transgenes to regulate expression is low, gene silencing reported; requirement for freshwater |
| <i>Chlorella vulgaris</i> C-27 | Only the chloroplast has been sequenced | Biodiesel, proteins, wastewater treatment | Rapidly consumes nitrate and phosphate; oil and starch accumulation (more in brackish water strains) | Most strains are freshwater; small cells are difficult to harvest, algaenan cell wall makes extraction difficult; the nuclear genome remains to be sequenced; difficulties noted in transforming cells even by biolistics |
| <i>Nannochloropsis oceanica</i> CCAP 211/48 (CCMP 1779) | 28.7 | Biodiesel, EPA, violaxanthin | Optimal techniques for homologous recombination have been developed, genetically tractable chassis, plasmid transformation through electroporation, advanced genome editing tools (CRISPR/Cas9) | Small cells are difficult to harvest, algaenan cell wall makes extraction difficult; vulnerable to contamination in large-scale culture |
| <i>Porphyridium purpurum</i> CCMP 1328 | 19.7 | PUFAs; EPA and APA; exopolysaccharides | A wide spectrum of products; exopolysaccharides secreted into the medium; successful transformation through biolistics | Not yet cultivated outdoors at a large scale; poor genome annotation |
| <i>Tetraselmis</i> sp. CCMP 881 | Only the chloroplast has been sequenced | Proteins, PUFAs, carbohydrates | Cultivated at scale without culture collapse in semi-continuous mode; easy to harvest (gravitational settlement) | The nuclear genome has not been sequenced, little or no annotation of chloroplast; transformation procedures not well studied |
| <i>Synechocystis</i> sp. PCC 6803 | 3.57 | Terpenoids, PHE, biomethane, phycocyanin | Molecular toolbox for genetic modifications has been developed, high-throughput system biology for genome-wide analysis (omic approaches); produces a diverse range of products; green light inducible lytic system for production of products of interest | Low product titers; biofilm fouling; high production cost; difficulties in outdoor cultivation and harvesting |
| <i>Scenedesmus obliquus</i> UTEX 393 | Only the chloroplast has been sequenced | Lutein, β -carotene, biodiesel, wastewater treatment | High lipid productivity, efficient nutrient assimilation; ability to alter morphology through agglomeration that improves resilience against grazers | Tools for genetic manipulation need development |
| <i>Hematococcus pluvialis</i> | Only the chloroplast has been sequenced | Astaxanthin, biodiesel, PUFAs | Detailed investigations on cultivation and elevating astaxanthin productivity; easy to harvest (gravitational settlement); detailed techno-economic assessments conducted; conventional mutagenesis well-established | Vulnerable to contamination; nuclear genome unsequenced; the chloroplast is the largest sequenced and is poorly annotated; high cost of production, vulnerable to photobleaching under high light; only been produced at large scale for astaxanthin, only the biosynthetic pathway of astaxanthin is well understood; thick walled-aplanospore makes product extractions difficult; genetic manipulation tools poorly developed; low biomass and product yields |
| <i>Dunaliella Salina</i> CCAP 19/18 | 300 (chloroplast and mitochondria sequenced) | β -Carotene, biodiesel | Extremophile (salt-tolerant); lack of cell wall makes it suitable for extractions; easily transformable; lower risk of contamination | Slow growing; shear-sensitive and difficult to harvest |
| <i>Athrospira platensis</i> YZ | 6.62 (still under completion) | Phycocyanin, protein, PUFAs, vitamins, minerals, bioethanol | Extremophile (high alkalinity); detailed cultivation studies and at scale; easy to harvest; phycocyanin is water-soluble and easy to extract | Genetic manipulation tools poorly developed; low biomass and product yields |

Text Box 2: Diatoms and their biotechnology potential

Diatoms are among the most successful and productive photoautotrophs in the marine environment, responsible for about 40% of primary productivity in the oceans and 20% of global CO₂ fixation, with biogeochemical transfer of important nutrients such as nitrogen, carbon and silicon (Bowler et al., 2010). They dominate the phytoplankton community in the oceans under nutrient replete conditions, rapidly growing and dividing, and have the ability to survive long periods of light and nutrient limitation (Benoiston et al., 2017). They have been shown to possess more competitive traits compared to other phytoplankton groups (Lima-Mendez et al., 2015). Diatom genomes harbor a combination of genes and metabolic pathways first thought to be exclusive to plants and animals. Diatoms have the urea cycle and the ability to generate chemical energy from the breakdown of lipids that were considered distinctive animal features, and also have evidence of a C₄ photosynthetic pathway that has previously been recorded only in plants. Their evolution can be traced to **secondary endosymbiotic events**, with red and green microalgae, in addition to exosymbiotic gene acquisitions (Benoiston et al., 2017; Brembu et al., 2017). This provides them with a gene pool with diverse metabolic potential. **Allele specific expression** is an additional feature that may permit further phenotypic plasticity and thus help diatoms to thrive in dynamic highly unstable environments (Tirichine et al., 2017). Sequenced diatoms (Table I) provide the foundations for understanding their cellular makeup, with their genomic and epigenomic characteristics indicating a high versatility and resilience for survival under demanding environments (Benoiston et al., 2017; Tirichine et al., 2017). Some of these traits also bear the potential for serving as robust production vehicles.

Table II (Text Box 2): Sequenced diatoms, developmental status and their biotechnological relevance.

| Species/strain | Structural Type | Genome size and composition | Genetic toolkits & biochemical knowledge | Biotechnological relevance |
|--------------------------------------|-----------------|---|---|--|
| <i>Phaeodactylum tricoratum</i> | Raphid pennate | 27.4 MB. 88 chromosomes. Transposable elements make up 6.4 % of the genome. | High frequency of targeted mutagenesis possible with meganucleases, TALENS, CRISPR-Cas9; nuclear and chloroplast transformations demonstrated; multiple plasmids can be co-transformed; Golden Gate Assembly possible for cloning multiple genes of interest; several constitutive and inducible promoters are known to function well; a wide range of reporters (LUC, GUS, GFP, YFP, CFP) have been shown to work; overexpression and gene silencing are well developed. (see this review) | Production of several endogenous and heterogenous biochemicals including TAGs for biodiesel, fucoxanthin, EPA, chrysolaminarin, sterols, recombinant proteins, vanillin, PHBs. |
| <i>CCAP 1055/1</i> | | | | |
| <i>Thalassiosira pseudonana</i> | Polar centric | 32.4 MB. 65 chromosomes. Transposable elements make up 1.9 % of the genome. | Transformation by biolistics and conjugation shown to work. Gene silencing and gene knock-outs established. Secretion of recombinant proteins shown. Multiple plasmids can be co-transformed. Golden Gate Assembly possible for cloning multiple genes of interest. Overexpression and gene silencing are developed. | Silica biomineralisation; model for understanding the mechanisms behind silicification and TAG accumulation. |
| <i>CCMP 1335</i> | | | | |
| <i>Thalassiosira oceanica</i> | Polar centric | 81.6 MB. 51 chromosomes. | Transformation by biolistics. High genomic plasticity as shown from horizontal gene transfer. | Highly tolerant to low iron levels, reaching near maximal growth, might be a good biological indicator for iron stress; model for iron uptake studies. |
| <i>CCMP 1005</i> | | | | |
| <i>Fragilariopsis cylindrus</i> | Raphid pennate | 61.1 MB. | No known methods of transformations published. | Adaptations to polar conditions and survival in sea ice; antifreeze proteins. |
| <i>CCMP 1102</i> | | | | |
| <i>Pseudo-nitzschia multiseries</i> | Raphid pennate | 281.7 MB. | No known methods of transformations published. | Produces domoic acid, analogue for glutamic acid which causes Amnesic Shellfish Poisoning (ASP). |
| <i>CLN-47</i> | | | | |
| <i>Pseudo-nitzschia multistriata</i> | Raphid pennate | 59 MB. | Biolistics transformation, h4 (constitutive) promoter, <i>sh-ble</i> gene for resistance to antibiotic zeocin. Meiotic toolkit with 42 potential genes involved in meiosis. | Domoic acid production. Ability to reproduce sexually for classical loss of function screens and different combinations of double transformants. |
| <i>B856</i> | | | | |
| <i>Pseudo-nitzschia australis</i> | Raphid pennate | | No known methods of transformations published. | Contaminated genome with bacterial sequences-potential obligate symbiotic relationship; produces Isodomoic acid, unusual amnesic shellfish poisoning toxin. |
| <i>HAB 200</i> | | | | |
| <i>Seminavis robusta</i> | Pennate | Only the chloroplast has been sequenced | Meiotic toolkit with 42 potential genes involved in meiosis; the mating system is heterothallic so sex can be controlled reliably as sexual reproduction cannot begin until compatible clones are mixed, best success in mating and F1 development of the diatoms. | Sexual crosses can be made routinely, offering the potential for forwards genetics. |
| <i>D6</i> | | | | |
| <i>Fistulifera</i> sp. | Raphid pennate | Chloroplast sequenced | Biolistics; endogenous and heterogenous promoters. | High concentrations of EPA; high biomass productivity. |
| <i>JPCC DA058</i> | | | | |
| <i>Odontella sinensis</i> | Polar centric | Chloroplast sequenced | No known methods of transformations published. | Brevetoxin interactions at the cellular and subcellular level. |

Text Box 3: Biology of *P. tricornutum*

P. tricornutum is a marine species including brackish water strains (Figure I), such as CCAP 1052/6 (UTEX 646) and CCAP 1052/1B (UTEX 640), but only CCAP 1052/1B has been reported to grow in freshwater (Yongmanitchai and Ward, 1991). To date UTEX 640 has been the workhorse for high biomass and EPA productivities, CCAP 1055/1 for genetically engineered products of interest and UTEX 646 for monoclonal antibodies (Table 1). Strain UTEX 640 has the highest natural EPA content of 5.14 % DW (Derwenskus et al., 2019) but a genetically engineered CCAP 1055/1 has an EPA content of 8.54 % DW (Wang et al., 2017). For the commonly used strains for maximizing lipid productivities it has been identified that UTEX 640 is better than UTEX 646 in terms of biomass and lipid productivities (Rodolfi et al., 2017). Bioprospecting can lead to the isolation of strains with biotechnological significance, for example, three new strains (M26, M28, and M29) were isolated from two fjords in Norway and M28 had a high TFA content of 42.9 % DW (Steinrücken et al., 2018). Strain M21 was of particular interest because it had a high growth rate at 10°C and a high EPA content which increased in the stationary phase to 4.6 % DW (Steinrücken et al., 2017).

The great adaptability of *P. tricornutum* has been attributed to its pleiomorphism (four different morphotypes known - oval, fusiform, triradiate, and cruciform, and the predominating morphotype appears strain specific) (De Martino et al., 2007; Ovide et al., 2018; Steinrücken et al., 2018). Most *P. tricornutum* strains predominate as fusiforms but some strains have been found to predominate as oval forms (CCAP 1052/1B and CCAP 1055/5) and some as triradiates (CCAP 1055/7) (De Martino et al., 2007). From a biotechnological point of view the fusiform morphotype appears most commercially relevant due to its growth rate (~1.4 times higher than comparable oval cells) (De Martino et al., 2007) and a greater antibacterial activity (twice as much as the ovals) attributable to the EPA, hexadecatrienoic acid, and palmitoleic acid content (Desbois et al., 2010).

The main polysaccharide in the fusiform cell morphotype is a sulphated glucuronomannan that has been suggested to play a role in cell-wall biogenesis and the frustule architecture (Le Costaouec et al., 2017). It has been found that the carbohydrate composition differs between morphotypes but the structure of glucuronomannan appears conserved in

fusiform and oval morphotypes (Willis et al., 2013). This might have biotechnological implications with respect to product extractions.

P. tricornutum has a small genome of 27 Mbs that nevertheless encodes a plethora of genes, around 12,000, with 26 % of the genes being species-specific (Rastogi et al., 2018; Velmurugan and Deka, 2018). It has been found to contain class I retrotransposons and a few class II transposons, which appear to be modulated by different stressors, such as nitrogen depletion (Hermann et al., 2014; Rogato et al., 2014; Veluchamy et al., 2015). The **transposons** contribute to 6.4 % of the genome (Hermann et al., 2014; Ovide et al., 2018), which offers potential for creating or reversing mutations in the cells for biotechnological exploitation. It is less silicified among diatoms and the requirement for silicon is not obligatory. This not only favours large-scale cultivations, but also enables ease of introducing DNA into the cell. It is now routine to express multiple transgenes in *P. tricornutum* through the **Gibson and Golden Gate assembly** (Adamo et al., 2018; Weyman et al., 2015).

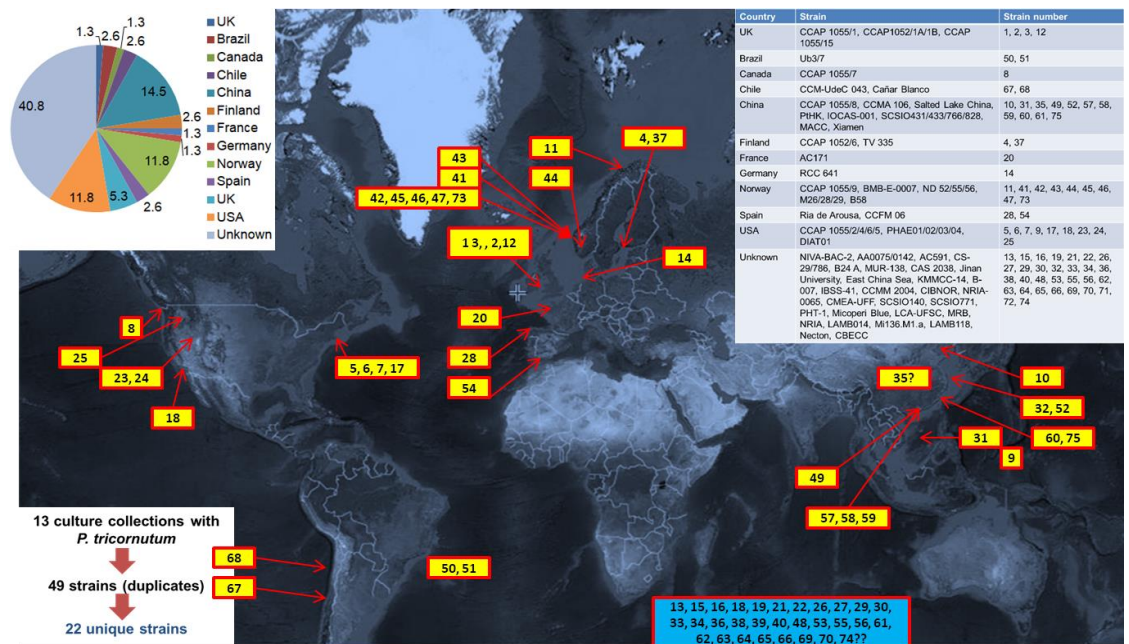


Figure I: Global distribution of *P. tricornutum* strains, showcasing 75 isolates reported in the literature (including synonymous ones). These include 22 unique strains held in 13 culture collections. A high proportion of these is of unknown origin (40.8 %).

Table 1: Products derived from *P. tricornutum* cultivation. Details given are for the most advanced productions scales reported in the literature. PBR - photobioreactor; (R) - recombinant strain; TSP - total soluble protein.

| Product class | Product | Strain | Product yield/productivity reported | Functional end-use | Operational conditions | Ref. | |
|-----------------------------------|--|----------------------------|-------------------------------------|--|---|----------------------------------|---------------------|
| Lipids | EPA | UTEX 640 | 3% DW; ~60 mg/L/d | Nutraceutical, cardiovascular health, precursor for prostaglandin-3, thromboxane-3 and leukotriene-5 eicosanoids | Outdoor chemostat split-cylinder airlift PBR (50-60L), Almeria, Spain, photoautotrophic/mixotrophic with glycerol | (Fernández Sevilla et al., 2004) | |
| | DHA | CCAP 1055/1 (R) - Pt_EI05 | 0.64% DW | Nutraceutical, primary structural component of the human brain, cerebral cortex, skin and retina | Indoor horizontal fence PBR (550 L), photoautotrophic | (Hamilton et al., 2015) | |
| | | CCAP 1055/1 (R) - Pt_EI05 | 0.26 % DW | | Indoor raceway (1250 L), photoautotrophic | | |
| | | | CCAP 1055/1 (R) - Pt_MCAT_PtD5b | 0.92 % DW | | Indoor flasks, photoautotrophic | (Wang et al., 2017) |
| | ARA | | CCAP 1055/1 (R) - Pt_MCAT_PtD5b | 1.89 % DW | Nutraceutical, prostaglandin precursor | Indoor flasks, photoautotrophic | (Wang et al., 2017) |
| TAG | | UTEX 640 | 58.5 mg/L/d, 45 % DW | Biodiesel | Green Wall Panel III (≤40 L), outdoor, photoautotrophic | (Rodolfi et al., 2017) | |
| Carbohydrates | Brassicosterol | CCAP 1055/1 (R) - LjLUS-25 | | Decreased risk of coronary heart disease, anti-inflammatory activities | Lab PBR (≤1L), photoautotrophic | (Adamo et al., 2019) | |
| | Chrysolaminarin | CAS | 14% DW; 94 mg/L/d | Antioxidant | Indoor flat-plate PBR (50 L), photoautotrophic | (Baoyan et al., 2017) | |
| Terpenoids | Fucoxanthin | CAS | 0.7% DW; 4.7 mg/L/d | Antioxidant, anti-obesity, anticancer, anti-inflammatory | Indoor flat-plate PBR (50 L), photoautotrophic | (Baoyan et al., 2017) | |
| | Lupeol | CCAP 1055/1 (R) - LjLUS-25 | 0.01% DW | Antiprotozoal, antimicrobial, antitumour, chemopreventative | Lab Algem PBR (≤1L), photoautotrophic | (Adamo et al., 2019) | |
| | | CCAP 1055/1 (R) - AtLUS-6 | 0.0013% DW | | Indoor horizontal fence PBR (550 L), photoautotrophic | (Adamo et al., 2019) | |
| | Betulin | CCAP 1055/1 (R) - LjLUS-25 | Detectable levels | Antitumour | Lab Algem PBR (≤1L), photoautotrophic | (Adamo et al., 2019) | |
| Heterologous compounds & Proteins | Polyhydroxybutyrate (PHB) | CCAP 1055/1 (R) | 10.6% DW | Bioplastics | Indoor flasks (≤1L), photoautotrophic | (Hempel et al., 2011a) | |
| | Human IgGαHBsAg. Ab against Hepatitis B virus surface protein | UTEX 646 (R) | 0.0021% DW; 8.7% TSP | Monoclonal antibody | Indoor flasks (≤1L), photoautotrophic | (Hempel et al., 2011b) | |
| | IgG1/kappa Ab CL4mAb. Hepatitis B Virus surface protein without the ER retention signal (DDEL) at the C-terminus of both antibody chains | UTEX 646 (R) | 2.5 mg/L (secreted) | Monoclonal antibody | Indoor flasks (≤1L), photoautotrophic | (Hempel and Maier, 2012) | |
| | Monoclonal IgG antibodies against the nucleoprotein of Marburg virus (close relative of Ebola virus) | UTEX 646 (R) | 2 mg/L (secreted) | Monoclonal antibody | Indoor flasks (≤1L), photoautotrophic | (Hempel et al., 2017) | |
| Whole cell | Biomass | UTEX 640 | 25.4 g/L, 1.7 g/L/d | Aquaculture/animal feed | Outdoor split-cylinder airlift PBR (60 L), mixotrophic (0.1 M glycerol) | (Fernández Sevilla et al., 2004) | |

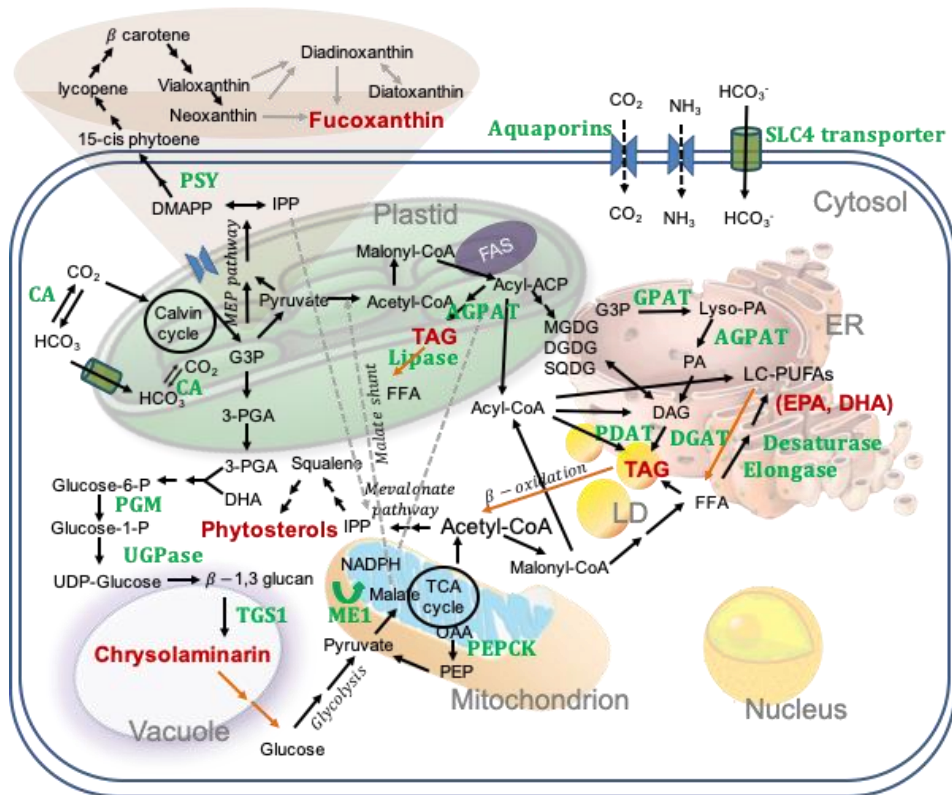
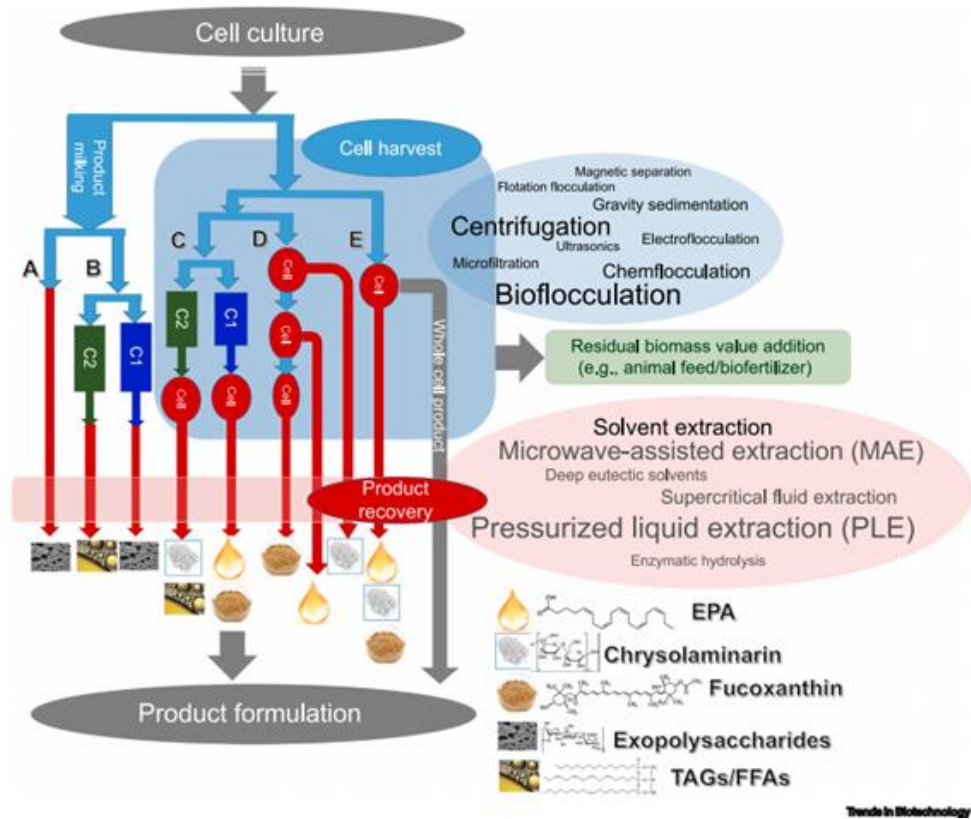


Figure 1: Biochemical knowledge of synthesis and accumulation of key products (in red font) within key organelles in *P. tricornutum*, resulting from investigations in recent years. Relevant enzymes or proteins are in green font. Black arrows indicate synthesis routes and red arrows indicate degradation routes. Grey arrows indicate hypothesized routes. Dotted arrows indicate transfer between organelles; DMAP – Dimethylalyl diphosphate; IPP – Isopentyl diphosphate; G3P – Glyceraldehyde-3-phosphate; 3-PGA- 3-phosphoglycerate; FFA – Free fatty acid; PEP – Phosphoenol pyruvate; OAA – Oxaloacetate; MGDG – Monogalactosyl diacylglycerol; DGDG – Digalactosyl diacylglycerol; SQDG – Sulphoquinovosyl diacylglycerol; PA - ; DAG – diacylglycerol; TAG - triacylglycerol; GPAT - Glycerol-3-phosphate acyltransferase; AGPAT -1-acyl-glycerol-3-phosphate acyltransferase; ; PDAT – Phospholipid diacylglycerol acyltransferase; DGAT – Diacylglycerol acyltransferase; TGS1 – 1,6-β-transglycosylase; PGM - Phosphoglucomutase; UGPase – UDP glucose pyrophosphorylase; ME1 – Malic enzyme 1; PEPCK – Phosphoenolpyruvate carboxykinase; PSY – Phytoene synthase; CA – carbonic anhydrase.



Trends in Biotechnology

Figure 2 - Options for the development of a biorefinery approach with *P. tricornutum* cultivations. (A) Simultaneous harvest of products; (B) Sequential extraction of products temporally separated; (C) Alternating product centered operation (C1 and C2 are different operational conditions); (D) Direct sequential milking of products from culture; (E) Alternating product centered operations (C1 and C2 are different operational conditions), followed by direct milking of products. A, B and C involve cell harvesting (W. Zhang et al., 2018), whilst D and E do not involve separation of cells from the culture. Products a, b, and c could be Fucoxanthin, EPA, and Chrysolaminarin, respectively, and C1 and C2 could be N replete, low light conditions and N deplete, high light conditions, respectively, as an example. The key downstream processing stages of cell harvest and product recovery (extractions) from the cells that have been explored for *P. tricornutum* are highlighted at the top. Size of the options indicates relative effectiveness considering factors including, performance, suitability to commercial application, cost effectiveness, toxicity, etc. Green extraction techniques are highlighted in green.

Chapter 3: Towards a *Phaeodactylum tricornutum* biorefinery in an outdoor UK environment (8-18°C)

This chapter is being prepared for publication:

Thomas O. Butler^{1*}, Gloria Padmaperuma¹, Alessandro M. Lizzul², and Seetharaman Vaidyanathan¹

¹Department of Chemical and Biological Engineering, The University of Sheffield, Sheffield, S1 3JD, UK; S.vaidyanathan@sheffield.ac.uk (S.V.)

²Varicon Aqua Solutions Ltd., Ball Mill Top Business Park, Unit 12, Hallow, WR2 6PD, UK

Highlights

- Cultivation with Cell-Hi JWP resulted in an increase in biomass, fucoxanthin, EPA, and protein yield
- UK outdoor winter cultivation was possible at 8-18°C in the Phyco-Lift airlift photobioreactor
- An inverse correlation between temperature and EPA was observed
- Commensal bacteria followed a sinusoidal growth profile in microalgal cultures
- *Halomonas* appeared to dominate at lower algal biomass densities and *Marinobacter* dominated in late growth stages

3.1. Abstract

P. tricornutum is a model diatom and a potential biorefinery chassis which can be exploited for a range of natural products for the nutraceutical market (fucoxanthin and eicosapentaenoic acid - EPA) and aquaculture feed (protein, fatty acids and carbohydrate). There is a necessity to improve growth rates and reduce costs in microalgae cultures for commercial realisation of a biorefinery chassis. A media screening was conducted to explore the potential of cost-effective cultivation media; a series of commercial powdered media (Cell-Hi F2P, JWP and WP) and a hydroponics medium (FloraMicroBloom) were compared against f/2 medium. The commercial powdered medium, Cell-Hi JWP, was identified as the optimal formulation for growth, fucoxanthin, EPA, and protein. Cultivation outdoors in the UK during September and October (8-18°C) was investigated to observe how the biochemical composition differed from cultivation indoors under controlled temperature and lighting. Chlorophyll *a* content was positively correlated with fucoxanthin and EPA content and temperature appeared inversely correlated with EPA content. During the reactor operation, the culture remained unialgal but commensal bacterial counts revealed a sinusoidal growth profile. A change in the bacterial community composition from *Halomonas* to *Marinobacter* dominance was observed. Biofilm formation was observed in areas of the reactor with low flow zones which was shown to consist of the *P. tricornutum* oval morphotype and bacteria which adhered to the cells. Fatty acid analysis appeared to show that *P. tricornutum* was the dominating species in the biofilm. The results reported here showcase the potential of outdoor cultivation during cold conditions and associated challenges, but artificial supplementation of light may be required to further increase biomass productivity and product yields during the dark period.

Keywords: microalgae; *Phaeodactylum*, outdoor cultivation, air-lift, bubble column, biorefinery

3.2. Introduction

P. tricornutum is a model diatom and a potential biorefinery chassis which can be exploited for a range of natural products including high value (fucoxanthin) and lower value products for animal feed and aquaculture (protein, fatty acids and carbohydrate) which can be extracted sequentially (Butler et al., 2020). It is a commercially viable species and is cultivated by at least eight companies in Europe with an estimated annual production of four tonnes of dry biomass (Araújo and García-tasende, 2021). *P. tricornutum* dominates and outcompetes other microalgal species and is able to tolerate high pH and grow under low light (Butler et al., 2020). It is robust at laboratory, pilot, and demonstration scale, and can be cultivated in a range of cultivation media (Walnes, f/2 and COMBO), enriched seawater and fertiliser media without the requirement for silica (Branco-Vieira et al., 2020; Lebeau and Robert, 2003; Sethi et al., 2020).

High productivities of microalgal cells require the formulation of suitable culture media and standard media typically result in low productivities. A typical standard culture medium contains macronutrients (nitrogen, phosphorous, potassium, calcium, magnesium and sulphur), micronutrients (iron, manganese, molybdenum, zinc, boron, copper and cobalt), vitamins (cyanocobalamin, thiamine and biotin) and can contain a source of inorganic carbon (i.e. bicarbonate). The medium is typically formulated to provide the cells with a suitable pH, osmolarity, and the nutrients essential for cell survival and growth. The development of a standardised, optimal cell medium is of paramount importance because deviations can result in alterations in cell growth and product formation. The preparation of cell culture media is typically complex, expensive (labour, sterilisation, water purification, chemical storage), requires refrigeration, and is time consuming. The large number of process steps and the components in media formulation can lead to reduced efficiency and increased costs in conjunction with the potential introduction of variability which can impact the growth of the cells. Care has to be taken to add components in a particular order to enable dissolution and avoid precipitation (de Carvalho et al., 2019).

Media components can be replaced by more economical alternative sources (such as fertilisers) and can result in a higher biomass productivity and biochemical composition (protein and fatty acids) (Colusse et al., 2020). Due to low microalgal productivities and a

high medium cost (US \$2.6-8.3 per m³) the cost of production for microalgae is high with nitrate and phosphate represent 83 and 31% of the medium cost respectively (Colusse et al., 2019). When formulating a low-cost medium, it should not only reduce cost, but also decrease preparation time, simplify the workflow, and reduce the complexity of the media preparation, all of which are important in a commercial setting. There is a requirement for a dry media powder formulation which ensures a standardised product which does not vary from batch to batch and does not affect cell growth or composition.

Powdered media are a good solution since they require less storage space (stored as a concentrated powder or stock and stored for shorter periods of time), is easier to ship and remains stable over longer periods of time compared with liquid media (Kern, 1994). Dry powdered media have traditionally been manufactured using ball-milling technology and the constituents are simultaneously crushed and mixed under controlled temperatures and humidity whilst avoiding contaminating dust (Jayme et al., 2002). To date Cell-Hi F2P has been used in at least 24 studies for cultivation of microalgae in the published literature with concentrations ranging from 0.1 to 0.5 g L⁻¹ (Appendix A). Cell-Hi WP has been used in at least 8 publications with a concentration ranging from 0.1 to 0.67 g L⁻¹ (Appendix A). One recently optimised media by Varicon Aqua Solutions Ltd. (JWP) has not been published for microalgal cultivation and to date no study has evaluated the performance of these media formulations with standardised liquid media commonly used for microalgae in terms of growth and biochemical analysis. It has been found that media can have a dramatic effect on the growth and biochemical composition of microalgae (Butler et al., 2017; Praba et al., 2016) and this warrants investigation.

P. tricornutum can be cultivated indoors and outdoors in a range of photobioreactors (PBRs) (including tubular, flat-plate, and column) and open (raceway) ponds with biomass and product yields described in Butler et al. (2020). The biomass productivity of *P. tricornutum* has been reported to range from 0.025-1.7g L⁻¹ d⁻¹ (Fernandez et al., 1998; Veronesia et al., 2015). To date the highest biomass concentration (25.4 g L⁻¹), productivity (1.7 g L⁻¹ d⁻¹) and EPA productivity (56 mg L⁻¹ d⁻¹) were obtained in an outdoor split-cylinder airlift PBR (60 L) in Almeria, Spain using mixotrophic cultivation with 0.1 M glycerol using *P. tricornutum* UTEX 640 (Fernández Sevilla et al., 2004). Comparatively, the highest oil

(TAG) yield ($58.5 \text{ mg L}^{-1} \text{ d}^{-1}$) in the same strain was attained in flat panel PBRs (Green Wall Panel III) using photoautotrophic conditions (up to 45 % TAG DW) (Rodolfi et al., 2017). The highest fucoxanthin productivity ($4.7 \text{ mg L}^{-1} \text{ d}^{-1}$) was also obtained in a flat-plate system using photoautotrophic conditions (Baoyan et al., 2017). Flat panel configurations are optimal for biomass, EPA, and fucoxanthin productivities attributable to their low shear stress and effective illumination (Guler et al., 2019), but they are constrained by high rates of biofouling and their difficulty to clean (Lizzul, 2016). To date the majority of studies on outdoor productivity have been performed in temperate countries such as Spain and Italy, with high irradiances for high growth. Only limited studies are available from higher latitudes where microalgae are grown in cold climates with lower irradiances and photoperiods (Steinrücken et al., 2018).

PBRs result in higher productivities and more hygienic processes than raceway cultivation and can provide (to some degree) a physical barrier against contamination and grazers (Chiaramonti et al., 2013) but they are cost prohibitive for most microalgal production facilities. Currently the cost of microalgal production is 9-10 euros kg^{-1} DW (low labour cost countries) in PBRs compared with 0.4-1.8 euros kg^{-1} in open raceway systems (Banerjee and Ramaswamy, 2017; Slade and Bauen, 2013). Comparatively the cost of production in aquaculture hatcheries is 329 euros kg^{-1} (25 m^2 scale) in a greenhouse setting and decreases to 43 euros kg^{-1} through the use of artificial illumination at 1500 m^2 scale (Oostlander et al., 2020). Challenges to overcome with PBRs are reactor design for ensuring high volumetric/areal productivities, high yield on light, low shear but minimal fouling, low pumping costs, avoidance of high energy requirement for temperature maintenance and a requirement to minimise biomass losses due to photorespiration (Meiser et al., 2004; Tredici et al., 2015).

The typical biomass composition of *P. tricornutum* wild type as dry weight is 12.73-57 % lipid (Rodolfi et al., 2009) with 7-42 % DW as total fatty acids (TFAs) (Breuer et al., 2012; Reboloso-Fuentes et al., 2001), 27-51 % protein, 17-26 % carbohydrate, 2.04 % chlorophyll (~75 % chlorophyll *a* and 25 % chlorophyll *c*), 0.24 % carotenoids, 15.9 % ash and 0.25 % neutral detergent fibre (Di Lena et al., 2020; KaiXian and Borowitzka, 1993; Reboloso-Fuentes et al., 2001). Mineral elements make up 7.35 % DW with calcium,

potassium and sodium encompassing 69 % (Reboloso-Fuentes et al., 2001). Low light appears to favour the accumulation of fucoxanthin and EPA (Ación Fernández et al., 2000; Gómez-Loredo et al., 2016; McClure et al., 2018), whereas higher light intensities favour storage compounds (carbohydrate and TAG) with the degradation of the carbohydrate chrysolaminarin in the dark under N-limitation (Huete-Ortega et al., 2018; Wagner et al., 2016). However, to date, limited studies exist on showing how the biochemical composition varies indoors and outdoors over time in PBRs.

The first aim of this paper was to determine the optimal cost-effective medium for obtaining high biomass and product (fucoxanthin, EPA, protein, carbohydrate and TFA) yields utilising a biorefinery approach for the model strain *P. tricornutum* CCAP 1055/1. The next step was to cultivate *P. tricornutum* CCAP 1055/1 indoors (under controlled lighting and temperature) and outdoors (under low light and temperatures with high variability; 8-18°C) in a prototype airlift photobioreactor to look at the effect on biochemical composition to evaluate the potential of a biorefinery. The effect of cultivation time, light and, temperature on biochemical composition was investigated. The commensal bacterial population was monitored and compared in the airlift PBR indoors and outdoors.

3.3. Materials and methods

3.3.1 *Phaeodactylum tricornutum* culture and routine maintenance

P. tricornutum CCAP 1055/1 stock cultures were routinely maintained by the transfer of a 10% (v/v) inoculum into a 1 L Erlenmeyer flask, containing 800 mL f/2 medium (0.882 mM phosphate and 0.036 mM phosphate) (Guillard, 1975), using 33 g L⁻¹ Instant Ocean (Aquarium Systems, UK) (S5.1. Ionic composition of modified f/2 and Instant Ocean. The stock culture was incubated at continuous irradiance with white lights ca. 150 μmol photons m⁻² s⁻¹ surface irradiance (2700 k Hansa ECO Star silver lamps), at 21 °C (± 1 °C). The stock culture was sparged with air at 1 lpm (1.25 vvm) (using a ACO-9620, Hailea pump) through a 0.22 μm air filter.

3.3.2 *Phaeodactylum tricornutum* flask screening and experimental approach

Stock cultures were harvested during late-log, centrifuged at 4000 rpm for 10 mins (3500 g), washed with 20 mL phosphate buffered saline and re-suspended in 250 ml Erlenmeyer flasks for experimental flask screening. The experimental cultures were incubated at 21°C (Series 4, LMS incubator, UK) and agitated at 120 rpm using a Stuart reciprocating table shaker (SSL2, UK) under continuous light at $142 \pm 33 \mu\text{mol photons m}^{-2} \text{s}^{-1}$ for the Cell-Hi medium screening (provided by 2700 k Hansa ECO Star silver lamps) for 7 d. The initial inoculum density was an optical density of 750 nm (OD750) = 0.12 (equivalent to ca. $1 \times 10^6 \text{ cells mL}^{-1}$, $0.02 \text{ g L}^{-1} \text{ DW}$) and growth was monitored daily by measuring cell count and biomass concentration (determined by dry weight).

3.3.3. Hydroponics and powdered media screening

Cell-Hi powdered (Varicon Aqua Solutions Ltd.) stock solutions ($1 \text{ kg } 10 \text{ L}^{-1}$ for Cell-HI F2P, $1.5 \text{ kg } 10 \text{ L}^{-1}$ for WP, and $1 \text{ kg } 20 \text{ L}^{-1}$ for Cell-HI JWP) (Appendix A) were prepared by thoroughly mixing at room temperature (20°C) with a magnetic stirrer (N2400-2000 Starlab, UK) until the product dissolved. The final concentrations of Cell-Hi F2P, WP and JWP were 0.1, 0.15, and 0.1 g L^{-1} respectively as recommended by the manufacturers (Appendix A, Table S3.5). An optimised FloraSeries Hydroponic fertiliser (GHE, Fleurance, France) (Appendix A); 1 mL L^{-1} FloraMicro (M) and 1 mL L^{-1} FloraBloom (B) (M2B1) was also tested for comparison (Table 3.1 - Media composition of f/2, FloraMicroBloom (M2B1), and Powdered Cell-Hi range from Varicon Aqua Solutions Ltd.).

Each culture was pre-acclimated to the respective medium for one week before experimentation (preliminary experimentation) in 250 mL flasks with a liquid volume of 150 mL under the conditions described above (3.3.2). Preliminary experimentation revealed that there was no effect of replacing deionised water with tap water on growth or biochemical composition (data not shown) and therefore tap water was used. Media was added to the 250 mL flasks with 150 mL media under non-sterile conditions (no autoclaving or filter sterilisation) and compared to the control (f/2 filter sterilised).

Microalgal cultures were harvested by centrifugation (4000 rpm, 10 mins), the pellets washed with 0.01 M phosphate buffered saline (PBS) and transferred to a 2 mL Eppendorf safe-lock tube, centrifuged (13,000 rpm, 5 mins) and stored at -20°C.

Table 3.1 - Media composition of f/2, FloraMicroBloom (M2B1), and Powdered Cell-Hi range from Varicon Aqua Solutions Ltd.

| | mM | f/2 | M2B1 | F2P | JWP | WP | Instant Ocean Seawater |
|------------------------------|--------------------|-------|-------|--------|-------|--------|------------------------|
| Total N | | 0.88 | 7.14 | 0.99 | 0.64 | 1.02 | - |
| Phosphate | | 0.04 | 0.35 | 0.04 | 0.02 | 0.02 | - |
| Sodium | | 0.93 | - | 1.03 | 0.08 | 0.08 | 430.24 |
| Potassium | | - | 0.70 | 0.10 | 0.06 | - | 13.25 |
| Magnesium | | - | 1.23 | - | 92.22 | - | 49.86 |
| Sulphur | | 0.12 | 1.56 | 0.46 | 9.23 | - | 25.15 |
| Calcium | | - | 3.49 | - | 46.50 | - | 9.16 |
| Bicarbonate | | - | - | - | - | - | 3.00 |
| | µM | f/2 | M2B1 | F2P | JWP | WP | Instant Ocean Seawater |
| Copper | | 0.04 | 3.15 | 0.05 | - | 0.10 | - |
| Cobalt | | 0.08 | - | 0.09 | - | 0.09 | - |
| Iron | | 11.65 | 42.98 | 14.32 | 3.26 | 6.02 | - |
| Manganese | | 0.91 | 14.56 | 1.09 | 8.40 | 2.23 | - |
| Molybdenum | | 0.02 | 0.83 | 0.03 | 2.28 | 0.05 | - |
| Zinc | | 0.08 | 4.59 | 0.10 | - | 0.20 | - |
| Boron | | - | 18.50 | - | 13.50 | 429.90 | - |
| | mg L ⁻¹ | f/2 | M2B1 | F2P | JWP | WP | Instant Ocean Seawater |
| Vitamin B12 (cyanocobalamin) | | 0.03 | 0.03 | 0.57 | 8.98 | 0.30 | - |
| Vitamin B1 (Thiamine HCl) | | 0.10 | 0.10 | 113.26 | 9.97 | 29.40 | - |
| Vitamin H (Biotin) | | 0.03 | 0.03 | 0.57 | 1.99 | 0.60 | - |
| N/P ratio | | 24.50 | 20.40 | 24.75 | 33.68 | 53.68 | - |
| NPK ratio | | - | - | 9 2 2 | 4 1 7 | 14 1 3 | - |

3.3.4. Indoor/outdoor cultivation in a prototype airlift photobioreactor

A proprietary demonstration scale 10 L airlift glass tubular photobioreactor (ALR) PhycoLift (8 L working volume) similar to that described by Lizzul (2016) was supplied by Varicon Aqua Solutions Ltd. (details in Appendix A) and setup at the University of Sheffield for outdoor cultivation in a greenhouse without temperature control and utilising only natural sunlight (Figure 3.1). For the indoor trial the PBR was illuminated with light emitting diode

A culture pre-acclimated to JWP as described in 3.3.2 and 3.3.3. was used to inoculate a 5 L Duran bottle, containing 4 L of JWP Cell-Hi range (0.4 g L^{-1}) at an inoculation of 10% (v/v). The culture was aerated at 3 lpm (0.7 vvm) (filtered air $0.22 \text{ }\mu\text{m}$), and maintained at $22 \pm 1^\circ\text{C}$ with a continuous irradiance of ca. $250 \text{ }\mu\text{mol photons m}^{-2} \text{ s}^{-1}$. Cells from the 5 L Duran bottle were harvested during late-log, centrifuged, washed as above and inoculated at 0.1 g L^{-1} (ca. $5 \times 10^6 \text{ cells mL}^{-1}$) for a one-week acclimation period to the indoor and outdoor setting and then the repeated fed-batch experiment was conducted.

To avoid nitrate and phosphate limitation Cell-Hi JWP (0.4 g L^{-1}) was added at two time points: day 0 and after 7 d to avoid nutrient limitation. On day 15, the reactor volume was harvested to a biomass concentration of $\sim 0.1 \text{ g L}^{-1}$ and supplied with fresh JWP medium. Before the harvest, 6 mm diameter silicon BioBeads (Varicon Aqua, UK) were added to remove the fouling in low flow areas and collected using a sieve.

Light impinging on the reactor surface was monitored using a digital lux meter MM-LM01 (Max Measure, UK) and logged every 5 mins (LuxMeter Communication Tool). The daily total irradiance ($\text{mol photons m}^{-2} \text{ d}^{-1}$) was obtained from the sum of the recorded light intensity ($\mu\text{mol photons m}^{-2} \text{ s}^{-1}$) recorded daily. pH was monitored every 30 mins using a NeuLog pH logger sensor (Westlab, US) and logged on a laptop through NeuLogTM software. The PBR temperature was monitored every 30 mins using an RC-4 temperature logger (Ellitech, UK).

A sample was taken daily at the same time (11 am) for OD, cell count, DW, dissolved inorganic nitrate (DIN) and dissolved inorganic phosphate (DIP). Samples for bacterial enumeration (1 mL) and dissolved inorganic carbon (DIC) (5 mL) were taken every other day (5 mL). Samples for biochemical composition determination (5 mL triplicate aliquots) were taken every 2 days for the indoor and outdoor system and lyophilized. The supernatant of the culture obtained after centrifugation was filtered through a $0.22 \text{ }\mu\text{m}$ filter (Sartorius, UK), frozen at -20°C and lyophilized for extracellular fatty acid analysis.

3.3.5. Growth and fatty acid profiles of isolated commensal bacteria

Growth (OD_{600}) experiments with bacterial strains in monocultures were performed in TC-Treated 24-well microplates (Corning® Costar) with a ‘modified marine broth’; f/2 medium, 33 g L⁻¹ Instant Ocean, 5 g L⁻¹ peptone (Sigma, UK), 1 g L⁻¹ yeast extract (Sigma, UK). Initially a single colony forming unit (CFU) was placed into 6 mL of modified marine broth in 15 mL Falcon tubes and cultivated for 24 h in an Innova incubator (150 rpm) at 37°C, this was repeated in triplicate. Three millilitres of modified marine broth were added to the microplate and the bacteria monocultures were inoculated at $OD_{600} \sim 0.1$. A blank (f/2 marine broth) was used to confirm there was no contamination between wells. The isolates were cultivated for 5 d (kinetic cycles = 121) using a Tecan machine with culture settings as follows: 22-26°C, shake duration 1000 s, kinetic interval 1600 s.

For fatty acid analysis of the bacteria, 5 mL of culture from the 15 mL Falcon tube was also analysed using direct transesterification of the frozen (-20°C) wet biomass (3.3.6.4). In addition, a bacterial biofilm and the *P. tricorutum* culture obtained from the outside PBR run 2 after 15 d were analysed to determine the fatty acid profiles.

3.3.6. Analytical methods

3.3.6.1. Biomass sampling and determination of microalgal cell growth

Microalgae cell concentration were determined using an Advanced Neubauer haemocytometer (BS-748, Hawksley) and a microscope (BX51, Olympus). The cells were counted using Image J software (Labno, University of Chicago): <https://www.unige.ch/medecine/bioimaging/files/3714/1208/5964/CellCounting.pdf>. The maximum growth rate (μ) was calculated according to Butler et al. (2018) but as a function of each day. Dry weight was performed by centrifugation at (4000 rpm, 10 mins) of 5 mL of samples, washed with 20 mL of 0.01 M phosphate buffered saline (PBS) to remove any adhering medium etc. transferred to a 2 mL Eppendorf safe-lock tube, centrifuged at (13,000 rpm, 5 mins) (12,500 g) and stored at -20°C. The samples were then lyophilised (CoolSafe freeze dryer, Labogene, Denmark) and weighted using a 5 d.p. balance (Sartorius, UK) for subsequent data analysis

(chlorophyll *a*, protein, carbohydrate, and FAMES), approximately 2 mg of dried microalgal sample was used.

3.3.6.2. Determination of dissolved inorganic nitrogen (DIN), dissolved inorganic phosphate (DIP) and dissolved inorganic carbon (DIC) from the supernatant

Dissolved inorganic nitrogen (DIN) in the media was determined at OD₂₂₀ nm as described in Collos et al. (1999). Dissolved Inorganic Phosphate (DIP) in the media was determined following the method of Strickland and Parsons (1968) and the OD₈₈₅ nm reading was taken after 15 mins (longer times did not result in significantly different values, data not shown). Dissolved inorganic carbon (DIC) was calculated using the back-titration procedure described by Chen et al. (2016). Detailed descriptions of these methods are found in Appendix A.

*3.3.6.3. Biochemical composition (chlorophyll *a*, protein, carbohydrate)*

Combined extraction of chlorophyll *a*, carbohydrate, and protein was carried out according to Chen and Vaidyanathan (2013) with slight modification (Appendix A) using approximately 2 mg of lyophilised biomass.

3.3.6.4. Fatty acid analysis and EPA determination using direct transesterification

A modified version of Kapoore et al. (2019) was used for fatty acid methyl ester (FAME) direct transesterification using direct transesterification on the dry biomass with methanolic-HCl (7%) replacing BF₃ as the acid catalyst (Appendix A).

3.3.6.5. Fucoxanthin analysis

Fucoxanthin content was determined with a slightly modified spectrophotometric method by Wang et al. (2018) after washing 5 mL of pelleted culture with deionised water and extraction with 5 mL 100 % ethanol .

3.3.6.6. Bacterial isolation, identification and enumeration

Commensal bacteria from the Cell-Hi media screen experimental cultures, and the indoor/outdoor PBRs were isolated by streaking out to form single colonies on a 'modified marine agar medium' with the growth medium supplemented with 33 g L⁻¹ Instant Ocean, 5 g L⁻¹ peptone (Sigma, UK), 1 g L⁻¹ yeast extract (Sigma, UK) and 15 g L⁻¹ agar.

Genomic DNA was extracted using colony PCR by using a sterile pipette tip to take a single colony and this was re-suspended in 100 µl sterile deionised water and heated at 98°C for 10 mins in a Thermal Cycler (Applied Biosystems, USA). Colony PCR 16S rRNA genes were amplified from the bacterial isolates using primer pair 27F (5'-AGAGTTTGATCMTGGCTCAG-3') (Lane et al., 1991) and 1492R (5'-GGTTACCTTGTTACGACTT-3') (Turner et al., 1999). All PCR reactions with a final volume of 50 µl contained: 28.5 µl deionised H₂O, 5 µl genomic template DNA, 10 µl 5 x Phusion HF buffer, 1 µl 10 mM dNTPs, 2.5 µl 10 µM of each primer, and 0.5 µl Phusion DNA polymerase (Phusion high-fidelity PCR kit, Thermo, UK). PCR was performed in a thermocycler (Applied Biosystems, USA) under the following conditions: initial denaturing step of 1 min at 98°C followed by 35 cycles of denaturing (98°C for 10 s), annealing (58°C or 56°C for 15 s), and elongation (72°C for 45 s). A final elongation step was performed at 72°C for 8 mins. Products for two replicate PCR amplifications with clear white bands (ca. 1.5 kbp) were combined for each sample and purified using a QIAquick PCR purification kit (Qiagen Inc., CA). Products were sequenced using a BigDye® Terminator kit v3.1 (Applied Biosystems) and analysed using an ABI 3730 DNA sequencer (Applied Biosystems). The 16S rDNA sequences were compared against the GenBank database using the NCBI Blast program.

From each treatment and time point 1 mL of culture was added to 9 mL of Maximum Recovery Diluent (MRD) (with 33 g L⁻¹ Instant Ocean, 1 g L⁻¹ peptone and 8.5 g L⁻¹ sodium chloride and adjusted to pH 7.0) and vortexed for 10 s. Serial 10-fold dilutions were made in triplicate of the homogenate in MRD. From each dilution, the pour plate technique was used, and an aliquot (0.1 mL) of appropriate dilution factor of the homogenate was plated out. The

plates were incubated aerobically at room temperature and counted after 3 days. Bacterial cell numbers were estimated by counting colony-forming units (CFU) and only reads between 30 and 300 CFU were used.

3.3.6.7. Scanning electron micrograph imaging of biofilm

The biofilm was spread evenly on a glass slide and allowed to dry in a laminar flow. Specimens were fixed in 3% Glutaraldehyde (G7776, Sigma Aldrich) in 0.1 M Sodium Phosphate overnight. Specimens were washed twice (0.1M phosphate buffer) with 10 min intervals at 4°C. The cells were post-fixed in a 1% aqueous osmium tetroxide solution for 1 hour at room temperature. The fixed cells were rinsed and dehydrated at room temperature through a graded series of ethanol: 75, 95, 100 and 100 % ethanol for 15 mins, followed by a final dehydration step with 100% ethanol for 15 mins. The samples were then lyophilized mounted on aluminium stubs, attached with Carbon Sticky Tabs, and coated with approximately 25 nm of gold in an Edwards S150B sputter coater. Fixed cells were examined using a JSM-6010LA InTouchScope™ Multiple Touch Scanning Electron Microscope (JEOL Ltd., Japan) at an accelerating voltage of 15Kv.

3.3.6.8. Statistical analysis

Each treatment was performed in triplicates and the mean and standard error of the dependent variables are presented in the results. Statistical analysis of the experimental data was conducted using SPSS statistical software (SPSS Statistics 26, IBM). The data was tested for normality using a Kolmogorov-Smirnov test and if these data were normally distributed ($P>0.05$) they were subsequently tested for equal variance using Levene's test. If variances were considered equal then a one-way ANOVA/MANOVA and a *post-hoc* Tukey's test was utilised to understand where the differences were. If samples were not normally distributed ($P<0.05$) then a Kruskal-Wallis and *post-hoc* Dunn's non-parametric comparison was undertaken to understand the changes. The statistical difference of each set of experiments was studied with the analysis of the *P* value. In addition, this value was used to select parameters that were significant.

3.4. Results and discussion

3.4.1. Evaluation of powdered Cell-Hi range compared with FloraMicroBloom and standard f/2 under non-sterile conditions

The aim was to evaluate the use of powdered media for the cultivation of *P. tricornutum* and its effect on growth and biochemical composition (primarily fucoxanthin, EPA and protein). The range of powdered media was compared: Varicon Cell-Hi, the optimised hydroponics medium formulation (M2B1) (Appendix A) compared with sterilised f/2 medium as the control.

3.4.2. Growth and biochemical composition

A maximum cell density (1.69×10^7 cells mL⁻¹) and biomass concentration (0.45 g L⁻¹ DW) was observed with Cell-Hi JWP which was higher when compared with the sterilised f/2 control medium (1.26×10^7 cells mL⁻¹, 0.34 g L⁻¹) and M2B1 (1.46×10^7 cells mL⁻¹, 0.35 g L⁻¹) but only the biomass concentration was significantly higher ($p < 0.01$) (Figure 3.2). The biomass concentration attained after 7 days with f/2 medium was similar to that obtained by Penhaul Smith et al. (2020) after 3 weeks using the same medium, but in the current study a higher light intensity and continuous light was applied which likely resulted in higher growth. Biochemical analysis was conducted after 7 days of cultivation to determine if the content and yield of fucoxanthin, EPA, and protein were higher in M2B1 compared with the Cell-Hi powdered range and if there was any effect on the chlorophyll *a* content.

The highest fucoxanthin (1.33 % DW), EPA (3.31 % DW), protein (46.38 % DW), TFA (9.61 % DW), and chlorophyll *a* content (1.62 % DW) was observed with JWP. The EPA content was 1.4-fold higher than the f/2 sterile control (2.34 % DW) and the fucoxanthin content was >1.6-fold higher than the f/2 sterile control. In comparison, 0.72 % DW fucoxanthin was obtained in the axenic *P. tricornutum* UTEX 646 and increased to 1.23 % DW with a commensal bacterium, cultivated under similar conditions using f/2, 20°C without CO₂ addition (Vuong et al., 2019).

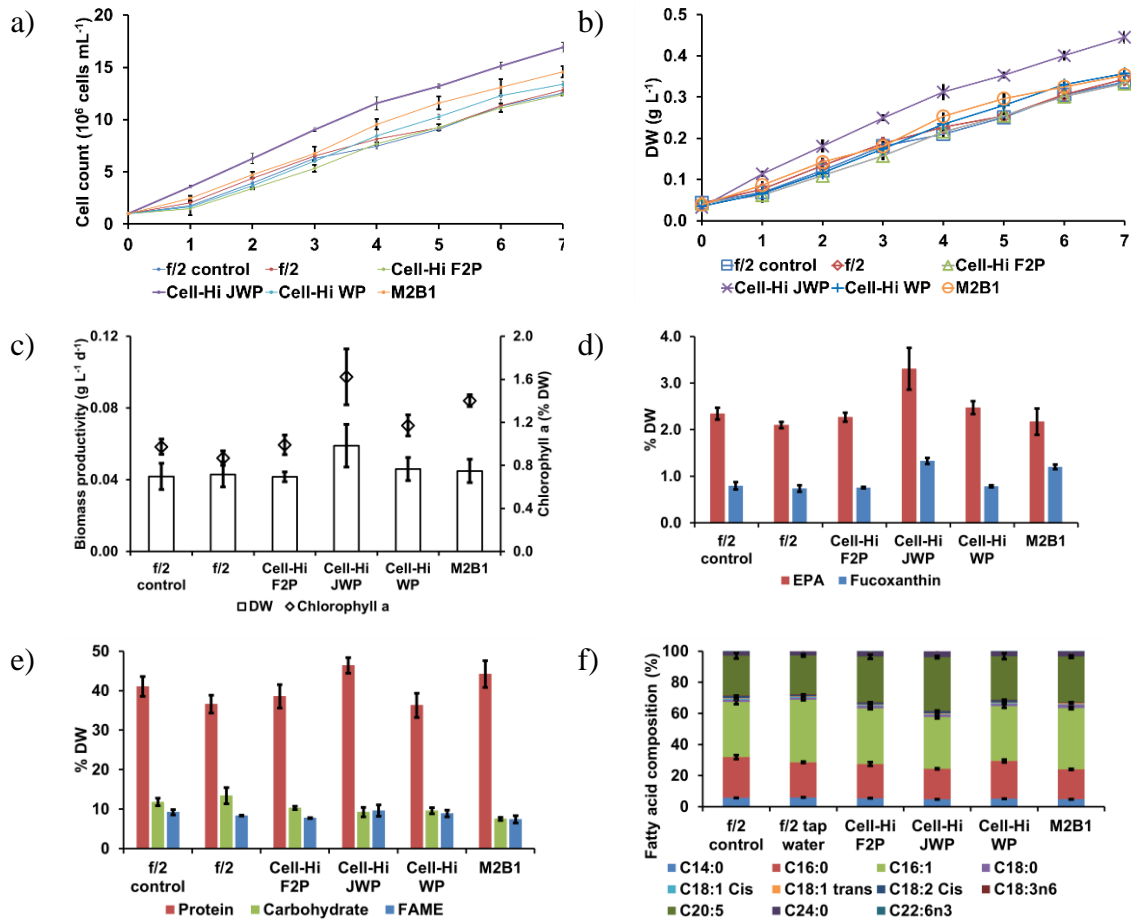


Figure 3.2 - Comparison of Varicon Cell-Hi range powders with f/2 control (sterile), f/2 (non-sterile) and optimal FloraMicroBloom formulation (M2B1): a) cell count, b) biomass concentration, c) biomass productivity and chlorophyll *a* content, d) Eicosapentaenoic acid (EPA) and fucoxanthin content, e) protein, carbohydrate and fatty acid methyl ester (FAME) content, f) fatty acid composition (%)

3.4.3. Performance of powdered and hydroponics media: cost, biomass productivity and product yields

In a commercial setting, agricultural fertilisers typically replace pure chemicals (Ación et al., 2012). When evaluating the cost of a medium two key factors need to be taken into account; the cost of the medium itself and the time taken for preparation. The commercial baseline medium (f/2) was found to be the most expensive (£966 per m³ including mixing and labour cost) but the benefit is that it only takes 1 h to prepare the media for microalgal cultivation saving time and operating expenditure (OPEX). Comparatively laboratory f/2 costs £53.89 per m³ and is considerably cheaper, but the trade-off is that several powders have to be weighed out and stock solutions have to be made (requiring up to four hours) increasing media preparation time. In addition, there is a risk of the stock solutions being contaminated by microorganisms such as fungi and a requirement for refrigeration space to store the solutions.

Varicon's Cell-HI powders were found to be more economical than the hydroponics medium (FloraMicroBloom) and laboratory media with Cell-Hi F2P being the most economical (£20.60 per m³) and > 2-fold cheaper than laboratory f/2 in terms of media cost alone when taking into account media preparation. Overall, due to the medium cost and biomass concentrations attained, the most economical medium for *P. tricornutum* was Cell-Hi JWP (£52.53 per kg dry biomass).

The highest fucoxanthin ($0.77 \pm 0.05 \text{ mg L}^{-1} \text{ d}^{-1}$), EPA ($1.91 \pm 0.23 \text{ mg L}^{-1} \text{ d}^{-1}$) and protein ($26.87 \pm 0.89 \text{ mg L}^{-1} \text{ d}^{-1}$) yields were obtained with JWP medium which were significantly higher than the other media ($p < 0.05$) (Table 3.). Interestingly, JWP has a lower nitrogen concentration than the other media but it is possible that that JWP performed better than the other media as it was higher in magnesium, sulphur, calcium, cyanocobalamin (vitamin B12) and biotin (vitamin H) (Table 3.1). It is also possible that as *P. tricornutum* cultivated with JWP resulted in a higher biomass concentration, there was a lower light per cell/gram of biomass, which could have resulted in an increase in fucoxanthin and EPA as these are both accumulated under low light (Butler et al., 2020). Since the interest was mainly on the production of high value products (fucoxanthin and EPA) and protein from *P. tricornutum*, it was thus decided that JWP was the optimal medium for scaling up.

Table 3.2 - Biomass, product yields, and economic analysis (March 2021) of media after 7 d cultivation comparing f/2, Cell-Hi powdered range and FloraMicroBloom hydroponics (M2B1)

| | f/2 | Cell-Hi F2P | Cell-Hi JWP | Cell-Hi WP | M2B1 |
|---|--------------|--------------|--------------|--------------|--------------|
| Biomass concentration (g L⁻¹) | | | | | |
| DW | 0.34 ± 0.01 | 0.33 ± 0.00 | 0.45 ± 0.01 | 0.36 ± 0.01 | 0.35 ± 0.01 |
| Biochemical yield (mg L⁻¹ d⁻¹) | | | | | |
| Chlorophyll <i>a</i> | 0.37 ± 0.02 | 0.41 ± 0.04 | 0.94 ± 0.14 | 0.54 ± 0.05 | 0.63 ± 0.01 |
| Protein | 15.69 ± 0.85 | 16.07 ± 1.22 | 26.87 ± 0.89 | 16.73 ± 1.58 | 20.07 ± 1.89 |
| Carbohydrate | 5.77 ± 1.01 | 4.29 ± 0.18 | 5.34 ± 0.56 | 4.43 ± 0.42 | 3.41 ± 0.24 |
| FAME | 3.58 ± 0.06 | 3.22 ± 0.04 | 5.53 ± 0.73 | 4.11 ± 0.46 | 3.36 ± 0.44 |
| EPA | 0.9 ± 0.03 | 0.94 ± 0.04 | 1.91 ± 0.23 | 1.14 ± 0.08 | 0.99 ± 0.13 |
| Fucoxanthin | 0.32 ± 0.04 | 0.31 ± 0.01 | 0.77 ± 0.05 | 0.36 ± 0.02 | 0.54 ± 0.01 |
| Medium cost | | | | | |
| Cost per m ³ | 5.80 | 2.56 | 5.38 | 4.44 | 26.67 |
| Medium preparation cost | | | | | |
| Cost per m ³ (media/mixing/labour) | 53.89 | 20.60 | 23.42 | 22.48 | 38.78 |
| Cost per kg microalga biomass (DW) | 156.70 | 61.80 | 52.53 | 62.88 | 109.53 |

*Commercial f/2 (Sigma Aldrich) costs £954 per m³ and £966 per m³ when mixing and labour is taken into account

Hydroponics media cost based on purchasing 5 L quantity from:

https://www.amazon.co.uk/s?k=flora+microbloom&ref=nb_sb_noss (Accessed 20/03/2021)

3.4.4. Commensal bacterial isolation, identification and enumeration

At industrial scale, axenic conditions are nearly impossible to attain, especially in open culture systems (Croft et al., 2005; Kazamia et al., 2012). Microalgae and bacteria are known to cohabit and interact in aquatic environments (Yao et al., 2019). Microalgae live closely associated with heterotrophic bacteria which may utilise secreted microalgal-derived organic substances such as extra polymeric substances (EPS) as a carbon source (Buhmann et al., 2016). From this mutualistic relationship, bacteria can also promote microalgal growth by reducing dissolved oxygen concentration and consuming organic material secreted by microalgae (Han et al., 2016). Macro- and micronutrients have an essential role in the interactions between the two organisms and it has been revealed that vitamins, iron and

carbon-containing compounds are usually exchanged between them (Helliwell et al., 2011; Vuong et al., 2019).

It was decided to identify and quantify the commensal bacteria population in a series of minimal media (f/2, Cell-Hi range and M2B1) without organic carbon addition in non-sterile and sterile conditions to compare the bacteria composition compared with *P. tricornutum* growth. Three bacterial species were identified with *Marinobacter* sp. and *Halomonas* sp. detected in all media but *Algoriphagus* sp. was only detected in f/2 (both sterile and non-sterile) and Cell-Hi F2P. After 7 d of cultivation in each medium, the highest bacterial content was observed in *P. tricornutum* cultivated with M2B1 (1.52×10^5 cells mL⁻¹) and the lowest content was observed with Cell-Hi F2P (2.67×10^4 cells mL⁻¹) which was significantly lower (Figure 3.3) and it is possible that there was more carbohydrate excreted as a substrate in M2B1. Carbohydrates leaked into the medium by the microalgae are known to provide the carbon source for the commensal bacteria to grow (Han et al., 2016). The bacteria count could also have been higher in M2B1 because there was more total nitrogen available in the media and some bacteria have been found to take up dissolved inorganic and organic nitrogen and bacteria can account for 38 % of total ammonium uptake (Veuger et al., 2005). Interestingly, over the 7 d cultivation period there was a decrease in the total bacterial count in all media compositions and the community composition changed (Figure 3.3). On day 1, *Halomonas* sp. was dominant (>94 %) in all media compositions but on day 4 the composition decreased to <79 % and on day 7 to <50 %, with a subsequent increase in *Marinobacter* sp. *Algoriphagus* sp. was only observed in f/2 and F2P Cell-Hi throughout the cultivation period but was <2 % of the bacterial composition. It must be noted that other non-cultivable bacteria are likely to be present and the modified marine agar medium only provides a ‘snapshot’ of the bacteria present.

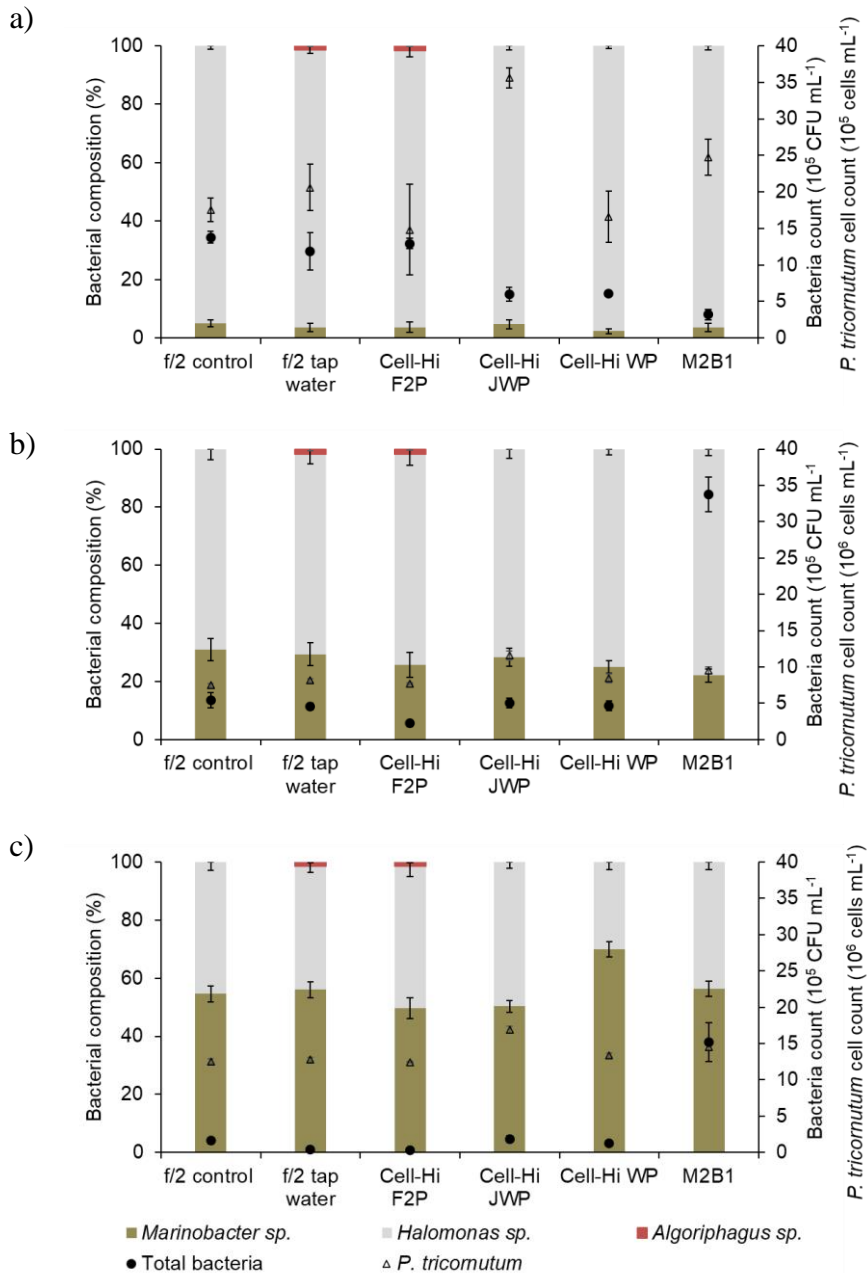


Figure 3.3 – Commensal bacterial composition over a 7 d cultivation period; a) after 1 d, b) after 4 d and c) after 7 d of algal cultivation.

In the literature, marine agar has commonly been used to isolate marine bacteria from *P. tricorutum* (Soto et al., 2005; Vuong et al., 2019; Chorazyczewski et al., 2021). For bacteria identification from microalgae (including *P. tricorutum*), typically 16 S sequencing

is used (Moejes et al., 2017; Vuong et al., 2019), but recently advanced techniques such as nanopore sequencing (MinION) (<https://earthmicrobiome.org/>), Illumina sequencing, and metagenome-based analyses (including marker genes) have been explored for bacteria identification (Krohn-Molt et al., 2017; Moejes et al., 2017; Shi et al., 2018; Kimbrel et al., 2019) and these should be adopted for *P. tricornutum* cultures to determine the community composition.

P. tricornutum has been found associated with commensal bacterial isolates which appear to be strain dependent. The Rhodobacteraceae were found to be dominant in the *P. tricornutum* mesocosms in one study (Kimbrel et al., 2019), but the Proteobacteria were found to be the most abundant bacteria (>95 %) isolated from *P. tricornutum* MASCC, Yellow Sea, China where 58 known species were found using 16 S barcoding using the V4 region and Illumina HiSeq sequencing (Shi et al., 2018). Comparatively, Proteobacteria, Bacteroidetes, Actinobacteria, and Firmicutes were found to be associated with *P. tricornutum* CCAP 1052/1B (Moejes et al., 2017). *Muricauda*, *Algoriphagus*, *Devosia*, *Marinobacter* and *Alcanivorax* spp. have been isolated from strain ‘Flour Bluff’ (Chorazyczewski et al., 2021). Comparatively, *Stappia* sp., *Halomonas* sp., *Rhizobium* sp., *Microbacteria* sp., and *Isomarina* sp. have been isolated from *P. tricornutum* UTEX 646 cultures, with *Stappia* sp. observed to be the most abundant (Vuong et al., 2019). *Micrococcus* sp. and *Alteromonas* sp. have been isolated from an unknown strain of *P. tricornutum* (Le Chevanton et al., 2013). Two novel bacterial species (*Mameliella phaeodactyli* and *Phaodactylibacter xiamenensis*) have been isolated from a *P. tricornutum* strain isolated from Xiamen, China (Chen et al., 2019).

Bacteria and *P. tricornutum* have been observed to show a mutualistic relationship where the bacteria secrete ammonium (e.g. from methylamine), vitamins, and growth-promoting factors, and may play a role in regulating nitrogen metabolism enabling the diatom to grow, whilst *P. tricornutum* secretes organic material such as free amino acids for the bacteria to grow (Shi et al., 2018; Suleiman et al., 2016; van Tol, 2019).

Some bacteria such as *Halomonas* sp., *Rhizobium* sp., *Microbacteria* sp., and *Idomarina* sp. have no effect on the growth of *P. tricornutum* (Vuong et al., 2019). Whereas, *Alteromonas* isolated from *P. tricornutum* has shown enhanced biomass accumulation in other microalgae (Le Chevanton et al., 2013). *Stappia* sp. K01 (intact cells) and *Arenibacter* spp.

isolated from *P. tricornutum* result in a higher algal growth rate, and *Stappia* sp. K01 also results in a higher chlorophyll and fucoxanthin content (Johansson et al., 2019; Vuong et al., 2019). *Marinobacter* sp. has been found to result in an increase in biomass concentration and lipid content (Chorazyczewski et al., 2021). *Marinobacter* FL06 was found to induce flocculation in *P. tricornutum* and it has been theorised that chemotaxis is involved (Lei et al., 2018). On the other hand, *Micrococcus* sp. has been shown to have algicidal behaviour in some microalgae (Le Chevanton et al., 2013), and *Algoriphagus* sp. and *Muricauda* sp. resulted in decreases in biomass concentration and lipid content in *P. tricornutum* (Chorazyczewski et al., 2021). Furthermore, *Kordia algicida* can release a protease which lyses *P. tricornutum* (Cao et al., 2019). *Labrenzia* sp. KD531 has also been observed to lyse *P. tricornutum* cells (Chen et al., 2017).

P. tricornutum has been observed to secrete allelopathic chemicals and further work should be conducted on microalgal-bacterial interactions determining the metabolites involved through metabolomics.

3.4.5. Nitrate and phosphate uptake

The nitrate and phosphate content in the medium was analysed throughout the cultivation, and the uptake rates were calculated to determine if nitrate and phosphate uptake could be correlated to each other and with higher microalgal cell growth.

It did not appear that nitrate and phosphate uptake rate were correlated with growth (*P. tricornutum* cultivated in JWP had the highest growth rate, but a low nitrate and phosphate uptake rate). Nitrate and phosphate uptake also did not appear to be correlated to each other. However, it was interesting to observe that nitrate uptake was higher in all cultures than phosphate (up to 19-fold increase).

After the 7 d cultivation period, nitrate was limiting ($<90 \mu\text{M}$) in all media, with the exception of M2B1 ($253 \mu\text{M}$ remaining) (Figure 3.4, a). The highest DIN cellular uptake ($352 \mu\text{M pM cell}^{-1} \text{ d}^{-1}$) and biomass uptake rate ($9.48 \text{ mM g}^{-1} \text{ DW}$) were observed in f/2 medium after the first day, but this was not statistically higher than when *P. tricornutum* was cultivated in F2P. The highest average uptake rate ($3.80 \text{ mM g}^{-1} \text{ DW}$) was observed in f/2 cultures which

were significantly higher than in Cell-Hi WP, JWP and M2B1 ($p < 0.05$). The nitrate uptake rate in the f/2 formulations was significantly higher than in Cell-Hi JWP and WP ($p < 0.05$). However, it is unknown why this was the case. Sodium at > 2.6 mM facilitates nitrate uptake but the sodium content was similar in all media (~ 443 mM) so this is unlikely to have contributed (Rees et al., 1980) (Appendix A).

During the 7 d cultivation period phosphate was depleted from the medium after 1 d in sterile f/2, non-sterile f/2 and Cell-Hi F2P, after 2 d in Cell-Hi-WP cultures, and after 3 d in JWP, but was not depleted in M2B1 (54 μ M available) (Figure 3.4, e). The highest DIP cellular uptake (56 μ M pM cell⁻¹ d⁻¹), biomass uptake rate (2.99 mM g⁻¹ DW) and average uptake rate (0.90 mM g⁻¹ DW) were observed in M2B1 medium after the first day. The uptake rate per gram dry biomass was significantly higher ($p < 0.05$). As phosphate was depleted from the medium in all treatments (except M2B1) it is possible that *P. tricornutum* was phosphate starved which could have accounted for the higher carbohydrate and TFA content compared with cultivation in the M2B1 medium (Figure 3). Adaptation to phosphorous starvation is complex and often polyphosphate is utilised, followed by phospholipids (Abida et al., 2015). During limited availability of DIP, microalgae can access organically bound phosphorus through the secretion of alkaline phosphatases and 5'-nucleotidases construction of extracellular phospholipids, proteins and nucleic acids (Buhmann et al., 2016). 5'-nucleotidase activity has been detected at the *P. tricornutum* plasma membrane and alkaline phosphatase activity at the cell walls and as an extracellular component (Buhmann et al., 2016; Flynn et al., 1986). Alkaline phosphatase is 40-60 % more abundant in axenic cultures of CCAP 1055/1 and it has been believed that bacteria could contribute to phosphorous acquisition (Buhmann et al., 2016).

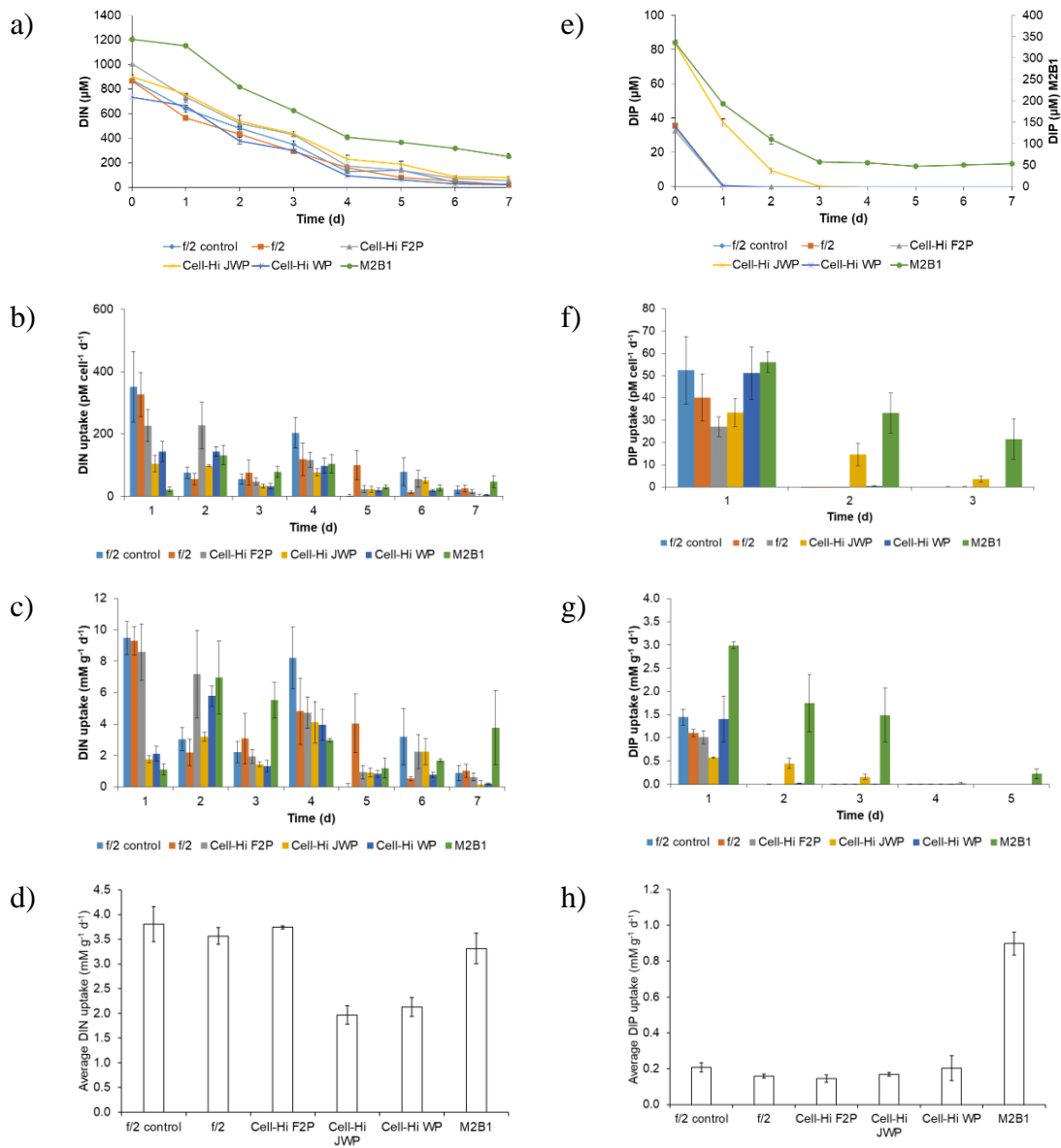


Figure 3.4 – Nitrate uptake; a) dissolved inorganic nitrate (DIN) in the medium, b) DIN uptake per cell, c-d) DIN uptake per gram biomass, and phosphate uptake; e) dissolved inorganic phosphate (DIP) in the medium, f) DIP uptake per cell and g-h) DIP uptake per gram biomass

As JWP was a cost effective medium and resulted in the highest biomass concentration and yield of fucoxanthin, EPA, and protein, and a relatively low bacteria content it was further investigated for comparing growth and biochemical composition in an indoor and outdoor prototype airlift PBR.

3.4.2. *Indoor and outdoor cultivation in a prototype airlift PBR; a fed-batch approach*

3.4.2.1. *PBR setup and environmental conditions*

The aim was to evaluate the performance of *P. tricornutum* towards a biorefinery chassis comparing indoor and outdoor cultivation. Details about the reactor configuration can be found in Appendix A. During the one-month cultivation there was no relationship observed between irradiance and temperature (Appendix A). This was surprising as irradiance and temperature were strongly correlated in Bergen, Norway (Steinrücken et al., 2018). The minimum temperature observed during run 1 in September was 8°C, the maximum was 18°C and the average was 13°C (Table 3.2). Comparatively for run 2 in late-September and October the minimum temperature observed was 8°C, the maximum was 19°C and the average was 12°C (Table 3.2). The culture temperature varied significantly during the day (14-21°C) and night (as low as 1°C to 14°C). The greatest fluctuations during 24 h were between 10°C at night and 21°C during the day.

The average photoperiod in run 1 in September was 12 h with an average daylight intensity of 118 $\mu\text{mol photons m}^{-2} \text{s}^{-1}$ impinging upon the surface of the reactor (Table 3.2). The maximum daylight impinging upon the reactor was 221 $\mu\text{mol photons m}^{-2} \text{s}^{-1}$. The average sum of daylight was 5.2 mol photons $\text{m}^{-2} \text{d}^{-1}$. The average photoperiod in run 2 in late-September and October was 12.5 h with a reduced average daylight intensity of 82 $\mu\text{mol photons m}^{-2} \text{s}^{-1}$ impinging upon the surface of the reactor. The maximum daylight impinging upon the reactor was 235 $\mu\text{mol photons m}^{-2} \text{s}^{-1}$. The average sum of daylight was 3.2 mol photons $\text{m}^{-2} \text{d}^{-1}$. Overall, the light intensities and temperatures investigated in this study were lower than other studies in Italy, China, Spain, Chile and Norway (Branco-Vieira et al., 2020; Fernández Sevilla et al., 2004; Steinrücken et al., 2018; Wang et al., 2018a; Zhang et al., 2018).

The average DIC concentration after 1 d was 3327 and 2847 $\mu\text{mol kg}^{-1}$ for the indoor and outdoor PBR respectively (Figure 3.5) and a pH was maintained at 7.8 which ensured >95 % of the carbonic species were in the form of bicarbonate. The supply rate was expected as reported by Chen et al. (2016).

3.4.2.2. Growth and biomass productivity

In the current study *P. tricornutum* CCAP 1055/1 always predominated as the fusiform morphotype (>97 %) with the remainder being a mixture of oval and triradiate (data not shown). CCAP 1055/1 has previously been observed to dominate in the fusiform morphotype (De Martino et al., 2007).

The final biomass concentration attained indoors was 1.56 and 1.59 g L^{-1} DW after 15 days for the first and second run respectively (Figure 3.5). Comparatively outdoors the biomass productivity was higher in the first run (1.13 g L^{-1} DW) than the second run (0.93 g L^{-1}). The lower biomass concentration in the second run was likely due to lower light and colder temperatures towards the end of the run. A similar biomass concentration (1.3 g L^{-1}) was achieved in indoor cultivation using a 20 L hanging bag PBR at a similar light intensity and temperature to the current study (120 $\mu\text{mol photons m}^{-2} \text{s}^{-1}$ and 23°C) with continuous CO_2 supply at 1 % (Wang et al., 2018).

The volumetric biomass productivity indoors (0.10 $\text{g L}^{-1} \text{d}^{-1}$) was significantly higher than the final volumetric productivities outdoors for run 1 (0.07 $\text{g L}^{-1} \text{d}^{-1}$) and run 2 (0.05 $\text{g L}^{-1} \text{d}^{-1}$) ($p < 0.05$) (Table 3.2). The average areal biomass productivity for the indoor cultivation (4.26 $\text{g m}^{-2} \text{d}^{-1}$) was higher than run 1 and run 2 outdoors (2.90 and 2.34 $\text{g m}^{-2} \text{d}^{-1}$ respectively). The average yield on light was lower for the indoor run (0.54 g mol^{-1}), compared with 0.43 and 0.82 g mol^{-1} for the outdoor runs, 1 and 2 respectively. This could be attributable to the higher average light intensity indoors.

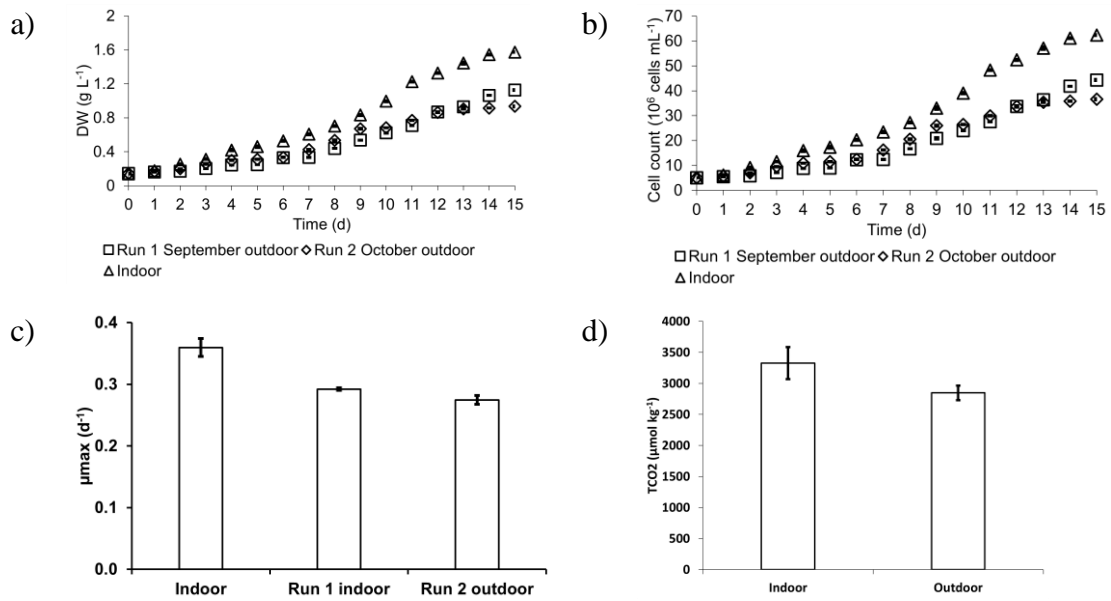


Figure 3.5 – a) Biomass concentration over time, b) cell count, c) μ_{max} (d⁻¹) and d) dissolved inorganic carbon supply (DIC supply) after day 1. The indoor run is the average of two repeated fed-batch runs

Table 3.2 – Biomass (specific growth rate and productivity) of *P. tricornutum* after 15 d cultivation indoors and outdoors using a fed-batch approach

| | | Indoor | Outdoor run 1 | Outdoor run 2 |
|---|--|---------------------------------|---------------|---------------|
| Mean temperature (°C) | | 22 ± 1 | 12.56 ± 0.78 | 12.41 ± 0.82 |
| Mean total daily light (mol photons m ⁻² d ⁻¹) | | 6.22 (first 7 d), 9.61 (8-15 d) | 5.19 ± 2.07 | 3.22 ± 1.29 |
| Mean light intensity (μmol photons m ⁻² s ⁻¹) | | 143 (first 7 d), 221 (8-15 d) | 117 ± 45 | 82 ± 33 |
| Biomass | Specific growth rate (d ⁻¹) | Average | 0.16 ± 0.00 | 0.14 ± 0.00 |
| | | Maximum | | 0.12 ± 0.00 |
| | Biomass concentration (g L ⁻¹ d ⁻¹) | Final | 1.57 ± 0.01 | 1.13 ± 0.01 |
| | Volumetric productivity (g L ⁻¹ d ⁻¹) | Final | 0.10 ± 0.00 | 0.07 ± 0.00 |
| | Areal productivity (g m ⁻² d ⁻¹) | Final | 4.26 ± 0.01 | 2.90 ± 0.01 |
| | Yield on light (g mol ⁻¹) | Final | 0.54 ± 0.00 | 0.43 ± 0.01 |

Typically higher biomass productivities, have been achieved in southern latitudes, with $1.4 \text{ g L}^{-1} \text{ d}^{-1}$ attained in Spain for UTEX 640 with a higher mean daily irradiance ($1100 \mu\text{mol photons m}^{-2} \text{ s}^{-1}$) (Acién Fernández et al., 2003). In Italy, biomass productivities of $0.31 \text{ g L}^{-1} \text{ d}^{-1}$ were obtained with flat-panels in spring and increased to $0.43 \text{ g L}^{-1} \text{ d}^{-1}$ in summer after 6 d batch cultivation (Rodolfi et al., 2017). However, information in Western Europe is lacking. In The Netherlands, the biomass productivity has been found to range from $0.02\text{-}0.27 \text{ g L}^{-1} \text{ d}^{-1}$ for *P. tricornutum* (Necton) cultivated in outdoor flat panel PBRs in October (average of $9.58 \text{ mol photons m}^{-2} \text{ d}^{-2}$, $200 \mu\text{mol photons m}^{-2} \text{ d}^{-1}$, temperature control at $20\text{-}22^\circ\text{C}$), with a higher biomass productivity attained at lower biomass densities ($0.4 \text{ g L}^{-1} \text{ DW}$ compared with 1.1 g L^{-1}) (Gao et al., 2020a). When three different *P. tricornutum* strains (B58, M28 and Fito) were cultivated under Norwegian climate conditions, it was observed that a higher biomass productivity ($0.25\text{-}0.30 \text{ g L}^{-1} \text{ d}^{-1}$) was obtained under a higher light intensity in Spring ($39 \text{ mol photons m}^{-2} \text{ d}^{-1}$), compared with summer and autumn ($0.09\text{-}0.16 \text{ g L}^{-1} \text{ d}^{-1}$ at $20 \text{ mol photons m}^{-2} \text{ d}^{-1}$) (Steinrücken et al., 2018). At $20 \text{ mol photons m}^{-2} \text{ d}^{-1}$ biomass productivities of 0.16 and $0.10 \text{ g L}^{-1} \text{ d}^{-1}$ were achieved at 0.4 g L^{-1} and 1.1 g L^{-1} respectively (Steinrücken et al., 2018). Comparatively in winter conditions in Italy (January and February), lower biomass productivities ($0.03\text{-}0.08 \text{ g L}^{-1} \text{ d}^{-1}$) were obtained in vertical column PBRs (270 L, column height 220 cm, diameter 55 cm) using semi-continuous mode (Simonazzi et al., 2019).

The lower biomass productivities in our study were most likely attributable to the limited irradiance ($82\text{-}117 \mu\text{mol photons m}^{-2} \text{ s}^{-1}$, $3\text{-}5 \text{ mol photons m}^{-2} \text{ d}^{-1}$) as higher productivities have been observed in Spring and Summer in The Netherlands and Norway (Gao et al., 2020a; Steinrücken et al., 2018). Photorespiration at night could also have accounted for lower biomass productivities (Han et al., 2013). Nitrate and phosphate were not found to be limiting throughout growth (data not shown). Media optimisation, higher light intensity/duration through the supplementation of artificial illumination, and using a

chemostat or turbidostat mode rather than a fed-batch approach could result in higher biomass productivities.

3.4.2.3. Product yields

In the indoor run, the protein (33 % DW), chlorophyll *a* (1.3 % DW) and fucoxanthin content (0.85 % DW) were higher than in outdoor cultivation but only chlorophyll *a* and fucoxanthin were significantly higher ($p < 0.05$). Whereas, in outdoor runs 1 and 2, carbohydrate (15 and 19 % DW), FAME (8.0 and 8.4 % DW), and EPA (2.5 and 2.6 % DW) were higher but only EPA was significantly higher ($p < 0.05$).

The indoor biochemical composition; protein (26-38 % DW), carbohydrate (10-19 % DW), FAME (5-7 % DW), EPA (1.2-2.2 % DW) and fucoxanthin (0.5-1.1 % DW) was observed to be more stable than in outdoor cultivation. In outdoor cultivation the protein (21-48 % DW), carbohydrate (14-27 % DW), FAME (5-12 % DW), EPA (1.7-3.6 % DW) and fucoxanthin (0.4-1.2 % DW) was more variable.

Lipid content and EPA yield has been observed to increase with cultivation time up to 18 d, whereas fucoxanthin has been observed to reach a maximum at 6 days cultivation in the mid-linear growth phase (Wang et al., 2018). With a decrease in light intensity fucoxanthin has been shown to increase (Wang et al., 2018). Low *P. tricornutum* biomass densities (0.4 g L⁻¹) resulted in a lower fucoxanthin content (1.09 % DW) compared with higher biomass densities (1.1 g L⁻¹) at 9.58 mol photons m⁻² d⁻¹ (200 μmol photons m⁻² s⁻¹) (Gao et al., 2020a). Fucoxanthin is part of the light harvesting complex and high fucoxanthin contents have been observed under low light intensity or by the self-shading effect of cells to absorb sufficient light for photosynthesis (Gao et al., 2020a; Gómez-Loredo et al., 2016; H. Wang et al., 2018). Fucoxanthin content has been found to decrease as the culture enters stationary phase (Wang et al., 2018). However, no trends in biochemical composition over time were observed in the current study and that is likely due to the large fluctuations in temperature and light in outdoor cultivation and the fact nitrate and phosphate were

supplemented after 7 d to avoid limitation. As there was a long dark period (~12 h) it is possible that short term storage molecules such as protein and carbohydrate were utilised for dark respiration.

There was no statistically significant difference in FAME composition between the indoor and outdoor runs. During indoor cultivation C16:0 (20 % TFAs), C16:1 (32 % TFAs) and C20:5 (33 % TFAs) accounted for 84 % of TFAs. During outdoor cultivation in September (run 1) C16:0 (19 % TFAs), C16:1 (34 % TFAs) and C20:5 (32 % TFAs) accounted for 86 % of TFAs (Appendix A). During outdoor cultivation in late-September/October (run 2) C16:0 (15 % TFAs), C16:1 (28 % TFAs) and C20:5 (30 % TFAs) accounted for 73 % of TFAs (Appendix A). In bubble column and airlift PBRs in outdoor cultivation in Almería, Spain, EPA represents between 27-30 % of TFAs and little variation was observed in EPA content (2.6-3.1 % DW) (Mirón et al., 2003).

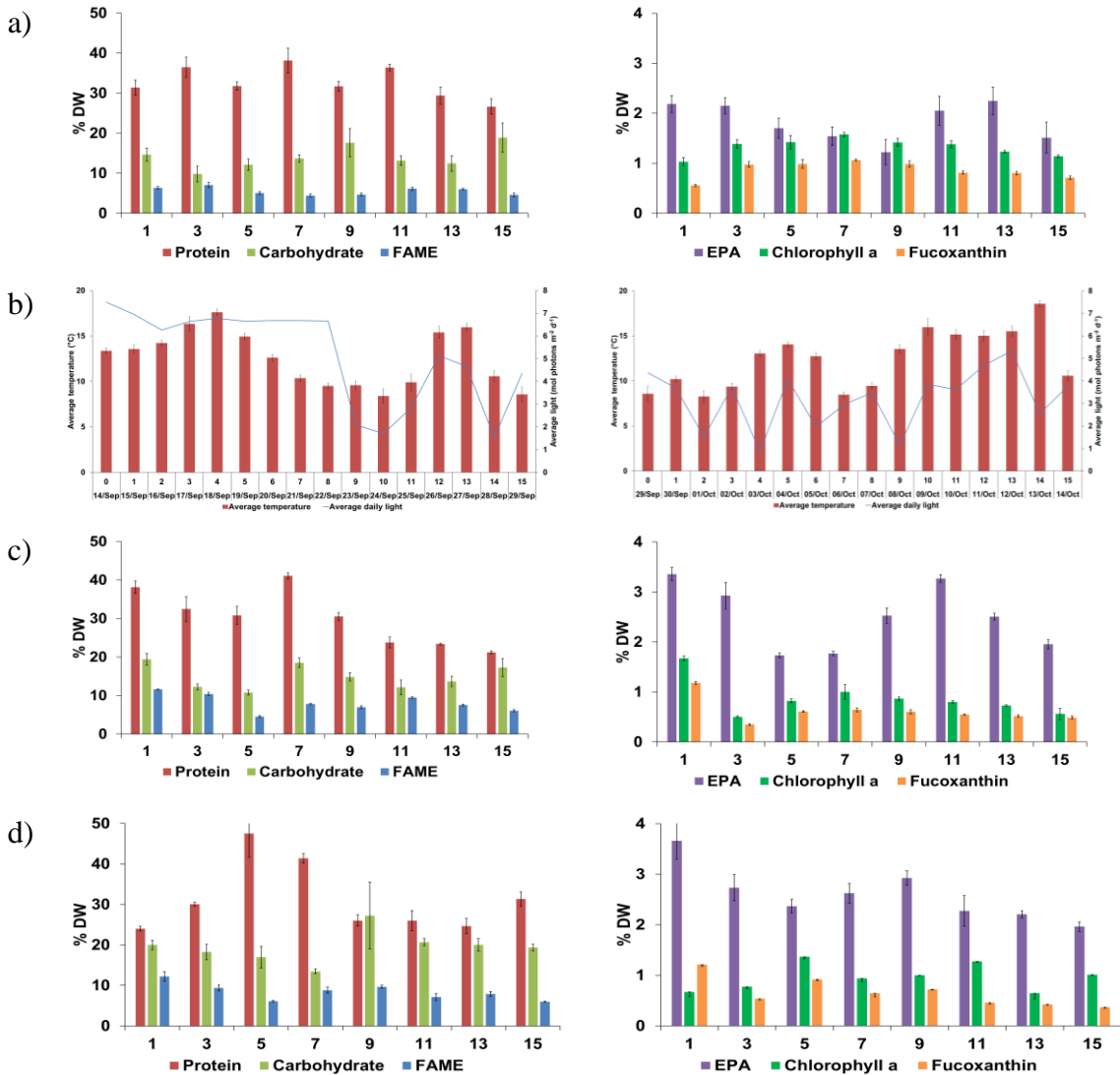


Figure 3.6 – Airlift PBR indoor biochemical composition (protein, carbohydrate, FAME, EPA, chlorophyll *a* and fucoxanthin); b) temperature (°C) and light (mol photons m⁻² d⁻¹) daily profiles during outdoor run 1 (September) and outdoor run 2 (late-September/October) with c) and d) outdoor biochemical composition for run 1 and 2 respectively

No relationships were observed between light/temperature and any of the biochemical components (protein, carbohydrate, chlorophyll *a*, fucoxanthin and, FAMES) or biomass concentration/productivity, but there was a weak inverse relationship between temperature and EPA (Figure 3.7). EPA is known to be accumulated under low temperature and a reduction in temperature to 10°C from 25°C for 12 h has been shown to result in a 120 % increase in EPA yield (Jiang and Gao, 2004). The rapid accumulation of EPA in colder conditions appears to be a response to maintain membrane fluidity , allowing acclimation to low temperature stress (Jiang and Gao, 2004)

The lower temperatures observed outdoor likely resulted in an increase in EPA. Another interesting finding was that fucoxanthin and chlorophyll *a* were positively correlated and this appears to indicate that chlorophyll *a* could be a good indicator of fucoxanthin content in the airlift PBR.

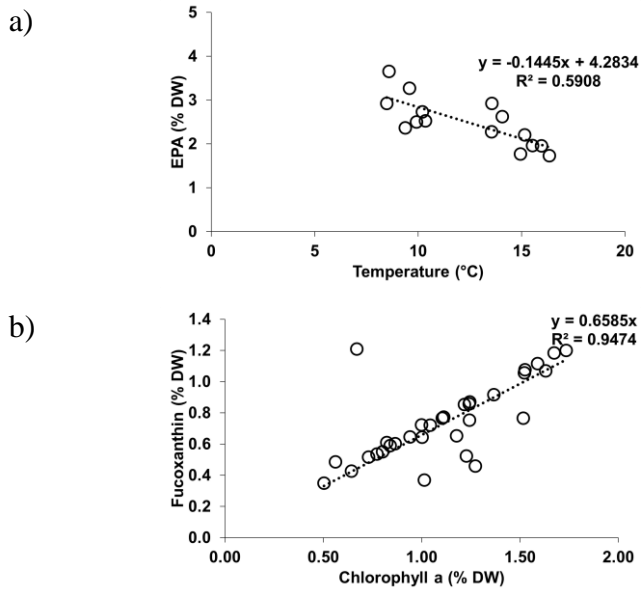


Figure 3.7 - Relationship between a) temperature and EPA content and b) chlorophyll *a* and fucoxanthin over the course of the one month indoor and outdoor run

Table 3.3 - Product (content and productivity) from *P. tricornerutum* after 15 d cultivation indoors and outdoors using a fed-batch approach

| | | | Indoor | Outdoor run 1 | Outdoor run 2 |
|--------------|--|---------|--------------|---------------|---------------|
| Protein | Content (% DW) | Average | 32.58 ± 0.79 | 30.18 ± 1.36 | 31.37 ± 1.64 |
| | Productivity (mg L ⁻¹ d ⁻¹) | Final | 27.93 ± 2.74 | 15.91 ± 0.15 | 19.52 ± 0.94 |
| Carbohydrate | Content (% DW) | Average | 14.18 ± 0.69 | 14.85 ± 0.61 | 19.48 ± 0.74 |
| | Productivity (mg L ⁻¹ d ⁻¹) | Final | 19.78 ± 5.37 | 12.99 ± 1.48 | 12.03 ± 0.37 |
| FAMES | Content (% DW) | Average | 5.69 ± 0.15 | 8.05 ± 0.44 | 8.40 ± 0.4 |
| | Productivity (mg L ⁻¹ d ⁻¹) | Final | 4.83 ± 0.66 | 4.56 ± 0.2 | 3.74 ± 0.12 |
| EPA | Content (% DW) | Average | 1.89 ± 0.07 | 2.51 ± 0.12 | 2.59 ± 0.1 |
| | Productivity (mg L ⁻¹ d ⁻¹) | Final | 1.59 ± 0.28 | 1.47 ± 0.06 | 1.22 ± 0.06 |
| Fucoxanthin | Content (% DW) | Average | 0.88 ± 0.03 | 0.62 ± 0.05 | 0.66 ± 0.05 |
| | Productivity (mg L ⁻¹ d ⁻¹) | Final | 0.74 ± 0.04 | 0.37 ± 0.02 | 0.23 ± 0.01 |

Protein and carbohydrate content is higher in nitrogen replete conditions compared with nitrogen deprived and deplete conditions but lipid content is the inverse (KaiXian and Borowitzka, 1993). Protein content has been found to increase in the later phases of diatom cultures (maximum in the late stationary culture phase) and typically constitutes 30-60 % DW under nutrient-replete conditions which is used for rapid cell growth (Geider et al., 1985)

P. tricornutum outdoor cultivation in 200 L bubble column PBRs in Concepción city, Chile was reported to result in a protein, lipid, carbohydrate, and fucoxanthin content of 38.40, 9.08, 7.85 and 0.86 % DW after 14 days in batch production (Branco-Vieira et al., 2020).

Lipid content is reported to be lower when cultivated at lower biomass densities (0.3 g L⁻¹ DW) but increases at higher biomass concentrations (>0.6 g L⁻¹ DW) with a subsequent reduction in protein (Silva et al., 2013). In N-deficient conditions with higher light intensity, lipid increases and protein and carbohydrate content decrease (KaiXian and Borowitzka, 1993). In Italy, TFA productivities of 21.75 mg L⁻¹ d⁻¹ were obtained with flat-panels in spring and increased to 31 mg L⁻¹ d⁻¹ in summer after 6 d batch cultivation (Rodolfi et al., 2017). EPA productivities of 7.25 mg L⁻¹ d⁻¹ were obtained with flat-panels in spring and increased to 9.5 mg L⁻¹ d⁻¹ in summer after 6 d batch cultivation (Rodolfi et al., 2017).

It has been found that the carbohydrate content is independent of the biomass concentration in the absence of light limitation in outdoor cultivation (Branco-Vieira et al., 2020). Comparatively in light and nitrogen limited conditions, low irradiance (18 μmol photons m⁻² s⁻¹) results in an increase in carbohydrate content (27.70 % DW) compared with 17.50 % DW using 72 μmol photons m⁻² s⁻¹ (KaiXian and Borowitzka, 1993).

3.4.2.4. Commensal bacterial population dynamics

During cultivation no eukaryotic contaminants were observed indoors or outdoors such as protozoa or rotifers. The *P. tricornutum* culture remained uniagal. Unsurprisingly, commensal bacteria were found to be present and the species present were in agreement with the flask screening; *Halomonas* and *Marinobacter*. The bacteria numbers were higher in outdoor cultivation compared with indoors. Nitrogen depletion can limit bacteria reproduction (Wen et al., 2020). It has been reported that the bacterial load is a function of the concentration of nitrogen and phosphorus and bacterial growth is positively correlated with nutrient availability (Wen et al., 2020). No nitrate limitation was observed during the cultivation period (data not shown). The bacterial populations both indoors and outdoors were less

numerous than *P. tricornutum*. Interestingly, the bacteria showed a sinusoidal profile with a population shift occurring between *Halomonas* and *Marinobacter* both indoors and outdoors.

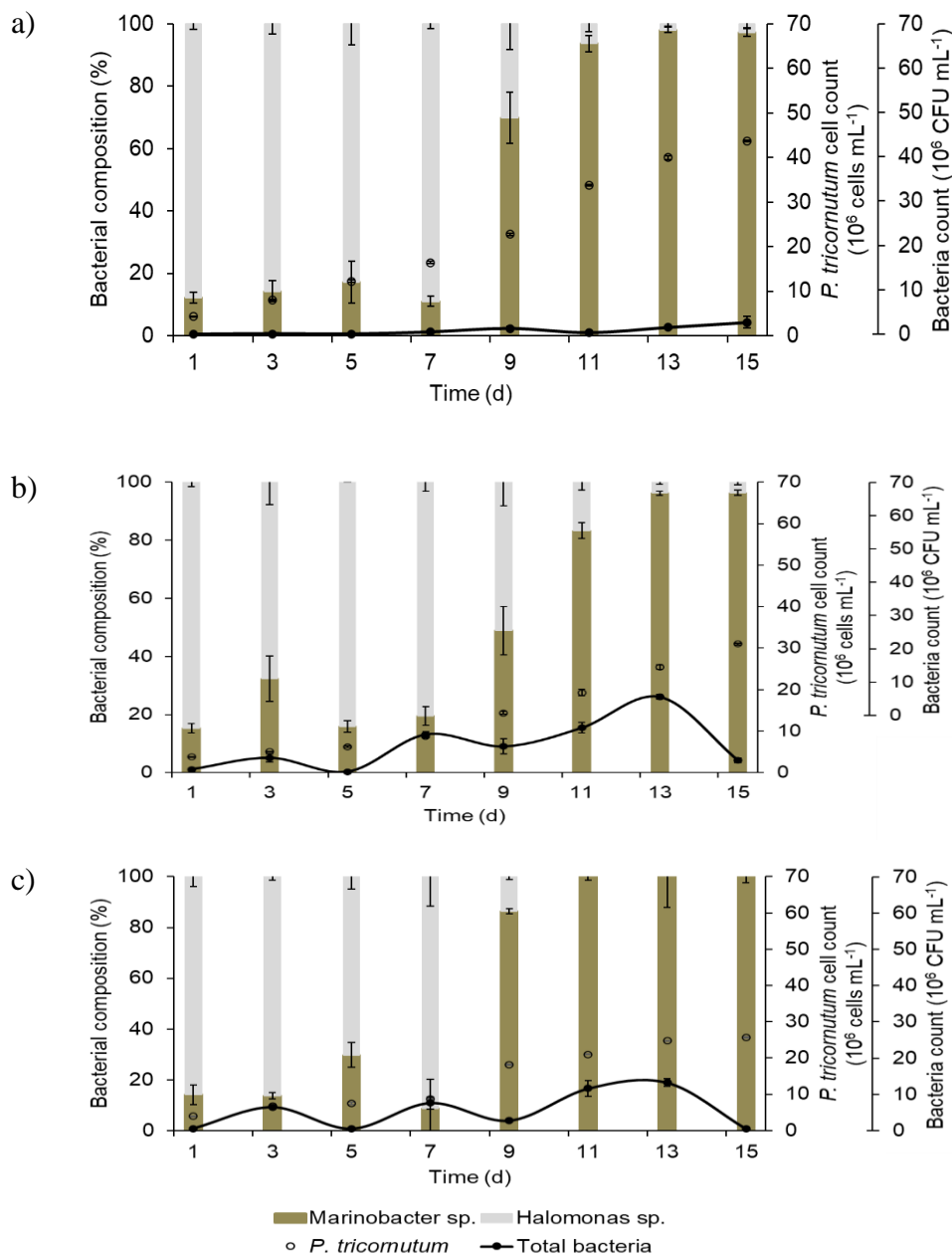


Figure 3.8 – *P. tricornutum* and bacteria profile variation over 15 d cultivation; a) indoor, b) outdoor run 1 and c) outdoor run 2

Ethyl acetate and methanol cell extracts from *P. tricornutum* have antibacterial activity and the fatty acids EPA, C16:1, and hexadecatrienoic acid (C16:3 n-4) were shown to be antibacterial compounds against Gram-positive and Gram-negative bacteria with C16:1 active in micromolar concentrations against multidrug-resistant *Staphylococcus aureus* (Desbois et

al., 2009, 2008). It has been found that fusiform cells show greater antibacterial activity against *Staphylococcus aureus* than oval morphotypes (Desbois et al., 2010). As the bacteria in this study showed a sinusoidal profile it was hypothesized that the antibacterial fatty acids, EPA and C16:1 could be secreted/excreted into the medium which could have responsible for regulating the bacterial numbers.

Fatty acid analysis revealed that C14:0, C16:0 and C18:0 (with C16:0 and C18:0 accounting for >95 % of TFAs detected) were present in the EPS but no even-numbered fatty acids such as EPA or C16:1 was detected over the indoor or outdoor runs (data not shown). It has previously been observed that C14:0, C16:0, C18:0, C16:1, C18:1 and C20:5 (0.1-4.9 $\mu\text{g L}^{-1}$) are secreted into the EPS by *P. tricornutum* and have an important role in regulating the growth of the bacterium *Stappia* sp. K01 (Vuong et al., 2019). High concentrations of fatty acids in the medium downregulate growth-related genes in *P. tricornutum* and cause growth inhibition but it was elucidated that fatty acids are utilized as a nutrient by the bacterium *Stappia* sp. K01 and resulted in upregulation of growth-related genes (Vuong et al., 2019).

Other metabolites could also be responsible for regulating bacterial growth such as nucleotides, pigment derivatives, and peptides (Vuong et al., 2019). A homolog to the antioxidant galactose oxidase (forms hydrogen peroxide) has previously been detected in *P. tricornutum* and there is evidence for a reactive oxygen substance based defence system (Buhmann et al., 2016), but it remains unclear whether diatoms are able to selectively discriminate between beneficial and antagonistic bacteria. Further work is required to understand the interactions between bacteria and *P. tricornutum* through whole-transcriptome and metabolome analyses and future work should determine under which conditions bacterial levels are elevated and suppressed. Further work should also be conducted on determining which bacteria are beneficial for growth and product formation. It has been shown that *Stappia* sp. K01 increases growth, chlorophyll and fucoxanthin content in *P. tricornutum* (Vuong et al., 2019).

3.4.3. Growth and characterisation of commensal bacteria identified during cultivation

Only dominant and cultivable bacteria were recovered from *P. tricornutum* cultures after conducting spread plates using a modified marine agar medium. The bacteria were all found to grow in co-culture with *P. tricornutum* (without any added organic carbon source) implicating that *Halomonas*, *Marinobacter* and *Algoriphagus* solely utilise diatom-derived carbon. The commensal bacteria could also grow on f/2 modified marine agar and in liquid

f/2 marine medium when supplemented with peptone and yeast extract but could not grow in f/2 medium or seawater nutrient agar alone. The bacteria were osmotolerant and could be grown on freshwater and seawater modified marine agar. As the bacterial strains developed in microalgal cultures without organic carbon supplementation, it is suspected that they were able to grow on organic carbon released by the microalgal cells, indicating interactions between the bacteria and *P. tricornutum*.

All bacteria associated with the *P. tricornutum* strains were Gram-negative (by Gram staining). There were two different bacterial species observed indoors using JWP medium in flasks (*Halomonas neptunia* and *Marinobacter alkaliphilus* sp.) and the same two species were observed outdoors. Interestingly *Algoriphagus marincola* (red colony) was only observed in f/2 medium and F2P in flask studies (albeit low in number) but it was not detected indoors or outdoors when using Cell-Hi JWP medium. *Halomonas* sp. was a large white colony and *Marinobacter* was a small white colony.

When the growth rates of all three bacterial species were compared, *Halomonas neptunia* had the highest growth rate but this was not significantly higher than *Algoriphagus marincola*, and *Marinobacter alkaliphilus* was found to have the slowest growth rate (Figure 3.9, a). *Marinobacter alkaliphilus* had a long lag phase (24 h) but then was observed to have a high growth rate (maximum doubling time of 3.5 h). The bacteria were all found to have a unique fatty acid profile which could be used as biomarkers for their presence (Figure 3.9, b). The predominant fatty acids for *Halomonas* sp. and *Algoriphagus* sp. were C18:1 (57 and 51 % TFA respectively) which has also been found in the literature (Sánchez-Porro et al., 2010), and C16:0 was dominant in *Marinobacter* sp. In comparison *P. tricornutum* had only <2 % C18:1. It was also confirmed that only *P. tricornutum* was capable of the synthesis of the long-chain polyunsaturated fatty acids (LC-PUFAs) EPA and DHA.

During the outdoor cultivation a bacterial biofilm was observed on areas of low flow in the PBR. This was surprising as the total run outside was only 45 days. *P. tricornutum* has been cultivated at pilot scale in a BIOCOIL reactor up to 700 L for periods greater than 4 months under semi-continuous conditions. This reactor enabled uniform mixing and minimised fouling in bioreactors (Borowitzka, 1999).

The biofilm appeared to primarily be composed of *P. tricornutum* which was confirmed by 16 S sequencing, SEM, and fatty acid analysis but *Halomonas* and *Marinobacter* were also present. The bacteria were observed to adhere to *P. tricornutum* cells (Figure 3.9, c). *Marinobacter* sp. has previously been reported to attach to *P. tricornutum* over time and enhances growth and single cell carbon fixation (Samo et al., 2018). The planktonic *P.*

tricornutum in suspension culture predominated as the fusiform morphotype but the benthic form predominated as the oval morphotype but both cell types were shown to have a similar fatty acid profile but the fusiform morphotype appeared to have a higher EPA composition of TFAs (Figure 3.9, b and c). This is similar to reported by Desbois et al. (2010) who found that fusiform cells had a higher EPA content than the oval morphotype cells. The transition to the oval morphotype in the benthic stage is likely because only oval morphotypes can adhere strongly to surfaces (Buhmann et al., 2016).

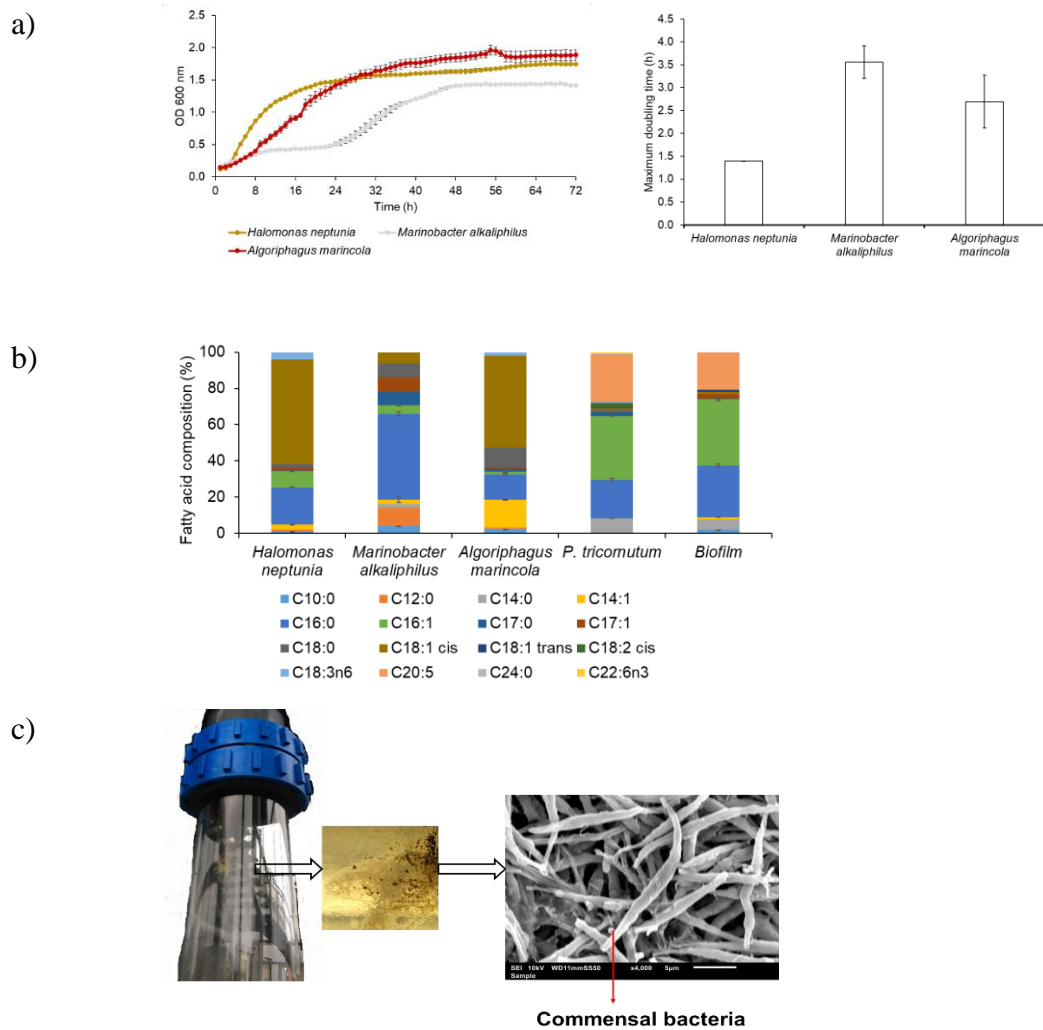


Figure 3.9 - Characterisation of bacteria detected in outdoor cultivation a) fouling biofilm formation on the airlift photobioreactor (ALR) at low flow zones, scanning electron micrograph (SEM) sample from biofilm and bacteria could clearly be observed adhering to cells b) 2000 x magnification and 4000 x magnification, c) growth of bacteria, d) average doubling time of bacteria and e) fatty acid analysis of bacteria, *P. tricornutum* (after 15 d growth outdoor run 2) and biofilm obtained after 15 d growth for outdoor run 2 showcasing commensal bacteria attached to *P. tricornutum*

Further work should be conducted on determining the conditions which result in biofouling in PBRs, to prevent production downtime. Further work should also be conducted on understanding the microalgal-bacterial relationships in PBRs to determine which bacteria are ‘friend’ and ‘foe’ and if they can be exploited for improved biomanufacturing for the implementation of a biorefinery chassis (Padmaperuma, 2017).

3.5. Conclusion

The optimal cost effective medium for obtaining relatively high biomass, fucoxanthin, EPA, and protein yields, utilising a biorefinery approach for the model strain *P. tricornutum* CCAP 1055/1 was Cell-Hi JWP from Varicon Aqua Solutions Ltd. A prototype airlift PBR (PhycoLift) was designed which has a low areal footprint. It was determined that outdoor UK cultivation was possible utilising a prototype airlift PBR under low light and temperatures (8-18°C) and there was an inverse relationship between temperature and EPA content. It was concluded that indoor cultivation resulted in a higher volumetric and areal productivity, and higher EPA, fucoxanthin and protein yields compared with outdoor cultivation. As the lighting conditions were similar it seems plausible that temperature control was important to ensure higher biomass productivities. Further work should be conducted utilising artificial light outdoors to increase photosynthetic activity and minimise photorespiration at night. Employing temperature control could also help increase biomass and product yields. During cultivation indoors in flasks and the airlift PBR, and outdoors in the airlift PBR the total commensal bacteria content showed a sinusoidal profile. *Halomonas* sp. was dominant at low *P. tricornutum* densities but *Marinobacter* sp. was more dominant at higher *P. tricornutum* densities. Further work should be conducted to determine what metabolites are responsible for controlling commensal bacteria population.

Acknowledgements

TOB acknowledges financial assistance from UK-EPSRC (DTA 1912024). Phyconet (now Algae-UK) provided funding for the equipment and reagents involved (PHYCBIV-28). ML and JM provided the airlift PBR and media as in kind contribution.

Author contributions

TOB conceived and wrote the paper with guidance from SV. TOB and GP enacted the experimentation.

Conflicts of interest

The authors declare no conflict of interest. The founding sponsors had no role in the writing of the manuscript. Joe McDonald and Dr Marco Lizzul from Varicon Aqua Solutions Ltd. supplied the powders and air-lift PBR and offered expert advice on experimental setup.

Chapter 4: *Phaeodactylum tricornutum* – culture condition manipulation towards biorefinery chassis development

Thomas O. Butler^{1*} and Seetharaman Vaidyanathan¹

¹Department of Chemical and Biological Engineering, The University of Sheffield, Sheffield, S1 3JD, UK;

S.vaidyanathan@sheffield.ac.uk (S.V.)

Highlights

- Algem[®] used for pre-optimisation studies; 21°C and continuous light optimal for biomass productivity
- f/2 is a maintenance medium and not a production medium. 5 x f/2 NP medium resulted in >3-fold increase in fucoxanthin content and a relatively high fucoxanthin and EPA productivity
- Nitrate and especially phosphate rapidly assimilated by cells
- A reduction and increase in salinity above 33 ‰ resulted in decreased fucoxanthin and EPA yield
- A combination of 5 x f/2 NP, 33 ‰ salinity, 2 ‰ CO₂ and 0.01 M glycerol resulted in up to a 10-fold improvement in biomass productivity and fucoxanthin, EPA, protein and carbohydrate yield

4.1. Abstract

Phaeodactylum tricornutum is well known as a potential cell factory for biofuels, bioplastics, omega-3 fatty acids (eicosapentaenoic acid and docosahexaenoic acid) and recombinant antibodies, but most production processes have focussed on a single product approach. In this study we focus on a multi-product approach. It was observed that bicarbonate supplementation (5-125 mM) resulted in a decrease in biomass and product yields. In addition, decreased or increased salinity from the optimum resulted in a reduction in product yields. However, a culture medium consisting of nitrate and phosphate at 4.41 mM and 0.18 mM (5-fold those employed in the traditional f/2 medium), salinity at 33 ‰, 2 % CO₂ (v/v in air), and a transition to mixotrophy using glycerol (0.01 M) were found to result in increased biomass (0.20 g L⁻¹ d⁻¹), fucoxanthin (1.78 mg L⁻¹ d⁻¹), EPA (7.54 mg L⁻¹ d⁻¹), and protein yields (15.65 mg L⁻¹ d⁻¹), up to ten-fold higher than the f/2 control medium.

Keywords: microalgae; biorefinery, media screen, cultivation optimisation

4.2. Introduction

Microalgae have been of great interest as biobased cell factories for biofuels and bioactive molecules due to their high biomass productivities (60-75 ton dry weight ha⁻¹y⁻¹ at commercial scale) and high photosynthetic efficiencies (3-10 % of solar energy) (Sethi et al., 2020). Microalgae can grow in seawater, brackish water, using marginal land or remediating wastewater (nitrogen, phosphorous, heavy metals and pharmaceutical waste) without the requirement for fertile arable soil, and they can use CO₂ from flue gases of power stations containing SO_x and NO_x (Ma et al., 2016). Of the microalgae, marine diatoms are the dominant primary producers in the ocean and amongst the most productive and environmentally adaptive in the world, being responsible for 20 % of global carbon fixation (Branco-Vieira et al., 2020).

The microalga *P. triornutum* is a model diatom species cultivated at pilot and industrial scale that is known to accumulate a spectrum of natural (the fatty acids eicosapentaenoic acid - EPA and docosahexaenoic acid - DHA, the primary storage carbohydrate, chrysolaminarin and the pigment fucoxanthin) and engineered marketable products (the triterpenoid lupeol, bioplastics and antibodies) (Butler et al., 2020; Sethi et al., 2020). At laboratory and pilot scale, *P. triornutum* has been shown to dominate and outcompete other microalgal species with a tolerance for high pH, an ability to grow under low light, and it does not require silica for growth (Remmers et al., 2018).

Using a biorefinery is an essential approach towards a circular economy and sustainability where the *P. triornutum* biomass is used as a feedstock for multiple products to add value in the process for commercial viability (Butler et al., 2020). For a future production process to be adopted industrially, incorporating *P. triornutum* for bulk products (protein, biofuels, and aquafeed) it is crucial that the biomass is fucoxanthin and EPA rich as these are the highest value known natural products. Implementing a 'high value product first' principle should enable a more economically viable process for exploitation (Li et al., 2015).

Fucoxanthin is valued at US \$175 kg⁻¹ (biomass containing 1 % fucoxanthin) (Leu and Boussiba, 2014) and US \$0.20-0.74 in capsular/softgel form (Leu and Boussiba, 2014; Timmermans, 2017; Wu et al., 2016). In 2016, the global fucoxanthin production was approximately 500 tons and the market grew at an annual rate of 5.3 % up to 2021 (Gao et al., 2020). Comparatively the market size for EPA is US \$300 million and the selling price is US \$200-500 kg⁻¹ (Alam et al., 2020). These two high value products will be fundamental for an economically viable biorefinery process utilising *P. triornutum*. However, for *P. triornutum*

to reach market potential, regulatory hurdles have to be overcome for selling in Europe. To date *P. tricornutum* has not been granted Novel Food status and is currently restricted to sales outside the European Union such as the US.

Fucoxanthin is a xanthophyll carotenoid and is widely found in brown macroalgae (0.01-0.1 % DW) and diatoms (0.19-5.92 % DW) (McClure et al., 2018; Reboloso-Fuentes et al., 2001; Wang et al., 2018). *P. tricornutum* typically exhibits a content between 1.02-2.61 % DW (Derwenskus et al., 2020b). As with all diatoms, fucoxanthin is one of the principal light harvesting pigments (along with chlorophyll *a* and *c*) in the fucoxanthin-chlorophyll protein (FCP) complex of *P. tricornutum* which traps light energy and offers photoprotection (Wang et al., 2018). Fucoxanthin has a plethora of health benefits (animal and human trials) including anti-inflammatory, anti-tumour, anti-obesity, antimalarial and anti-diabetes (Bae et al., 2020).

EPA would have added value as a whole cell byproduct that could be used for aquaculture feed (along with the protein, carbohydrate and mineral fraction) to replace fishmeal and fish oil (for shrimps, fish and bivalves). Currently fishmeal and fish oil are used to satisfy the growing aquaculture industry which consumes >70 % of fish meal and fish oil (Shah et al., 2018). Global production of fish oil is estimated at one million tonnes annually, but this is unsustainable and the cost is rising to >US \$3000 ton⁻¹ (Chen et al., 2016; Shah et al., 2018). Alternatively, EPA could be sold as a nutraceutical as a vegan alternative to fish, which is currently marketed by Simris. EPA is an essential fatty acid for human nutrition with the recommended daily intake (RDI) of 250 mg each day (Ryckebosch et al., 2014). EPA is a precursor for signalling molecules such as eicosanoids and has defined benefits in cardiovascular health, cancer treatment, and for numerous mental health diseases (Deckelbaum & Torrejon, 2012; Oscarsson & Hurt-Camejo, 2017). EPA is currently mainly derived from fish oil and to meet the RDI 0.8 g of fish oil must be consumed daily, whereas for microalgae the daily intake would range from 1.3-12.5 g oil/day (Ryckebosch et al., 2014).

EPA is highly dependent on the strain, PBR system and cultivation conditions and can range from 3.1-5 % DW (Derwenskus et al., 2020). *P. tricornutum* contains almost exclusively EPA and provides a preferential pure form (Derwenskus et al., 2020a). In *P. tricornutum* EPA constitutes around one-third of the total fatty acids (Fernández Sevilla et al., 2004; Derwenskus et al., 2019).

To date the highest volumetric productivity of EPA and fucoxanthin obtained using a biorefinery approach was in a flat-panel photobioreactor (9.6 and 4.7 mg L⁻¹ d⁻¹) during the exponential phase (day 6) with high nitrogen (14.5 mM) and phosphorous (0.88 mM) (Gao et

al., 2017). High fucoxanthin and EPA content are typically obtained under low light and high nitrate (8.82 mM) (Acién Fernández et al., 2000; McClure et al., 2018) but under nutrient-rich conditions EPA content has been found to be independent of the applied light intensity (Remmers et al., 2017). To maximise the value from the biomass, fucoxanthin should be extracted first, followed by EPA, protein, and chrysolaminarin (Zhang et al., 2018).

To date most studies have focussed on *P. tricornutum* UTEX 640 for EPA (Yongmanitchai & Ward, 1993; Cerón García et al., 2000; Fernández Sevilla et al., 2004a; Rodolfi et al., 2017), UTEX 640, UTEX 646 and CS-29 for fucoxanthin (Dambek et al., 2012; Nur et al., 2019), an unknown strain as a biorefinery chassis for EPA, fucoxanthin, and chrysolaminarin (Gao et al., 2017), and UTEX 646 and CCAP 1055/1 as a cell factory for recombinant antibodies, bioplastics, and heterologous terpenoids (Hempel et al., 2017, 2011a; Hempel and Maier, 2012). However, to date, only CCAP 1055/1 has been fully sequenced and annotated, (isolated off Blackpool, UK in ca. 1956) with extensive omics studies and molecular mapping conducted (Bowler et al., 2008; Rastogi et al., 2018). To the authors knowledge there have been no studies on evaluating CCAP 1055/1 as a biorefinery chassis for biotechnological exploitation; fucoxanthin, EPA, carbohydrate and protein. Only recently the biochemical composition has been investigated for CCAP 1055/1 (Song et al., 2020), and it will be interesting to look at the behaviour of this strain to be utilised as a biorefinery chassis.

Process optimisation is critical to increase biomass productivity and product yields. In this study the initial aim was to determine the optimal temperature and photoperiod for maximising biomass productivity in *P. tricornutum* CCAP 1055/1. The next aim was to investigate medium composition (nitrate and phosphate) and culture conditions: salinity and carbon supply (bicarbonate, CO₂, and glycerol) to increase biomass and product (EPA, protein, carbohydrate and fucoxanthin) yields from the standard f/2 medium.

4.3. Materials and methods

4.3.1. *Phaeodactylum tricornutum* culture and routine maintenance

P. tricornutum CCAP 1055/1 stock cultures were routinely maintained by the transfer of a 10% (v/v) inoculum into a 1 L Erlenmeyer flask, containing 800 mL f/2 medium (0.882 mM nitrate and 0.036 mM phosphate) (Guillard, 1975), using 33 g L⁻¹ Instant Ocean (Aquarium Systems, UK) (Appendix B). The stock culture was incubated at continuous irradiance with white lights ca. 150 μmol photons m⁻² s⁻¹ surface irradiance (2700 k Hansa

ECO Star silver lamps), at 21 °C (± 1 °C). The stock culture was sparged with air at 1 lpm (1.25 vvm) (using a ACO-9620, Hailea pump) through a 0.22 μm air filter.

4.3.2. *P. tricornutum* growth in Algem[®] for initial growth optimisation

P. tricornutum was cultivated in an Algem[®] Labscale Photobioreactor (Algenuity, UK) for culture condition optimisation using a standardised 1 L Erlenmeyer flask with 0.4 L working volume. A schematic of the system is shown in Whitton et al. (2018). Cells from the stock culture were harvested during late-log, centrifuged (4000 rpm for 10 mins), washed twice with 20 mL f/2 medium and inoculated at a cell density of 1×10^6 cells mL^{-1} (~ 0.02 g L^{-1} DW). Initially different temperatures (21, 23, 25 and 27°C) were compared using 150 $\mu\text{mol photons m}^{-2} \text{s}^{-1}$ white and red LEDs (85 and 15 % respectively) provided to the base of the photobioreactor over a surface area of 133 cm^2 . The optimal temperature of 21°C was then used for determining the effect of lighting regime (continuous sunlight at 150 $\mu\text{mol photons m}^{-2} \text{s}^{-1}$, 12:12 photoperiod and flashing light with 100 Hz (10 m/s) and a duty cycle of 50 %). The medium used for both experiments was f/2 with artificial seawater and agitation at 120 rpm, with 10 $\text{cm}^3 \text{min}$ (0.01 lpm: 0.025 vvm) aeration with 5 % CO_2 (n=2), pH 7.5. The OD 740 nm was monitored online every 10 minutes and the dry weight (DW) was obtained every 24 h.

4.3.3. Experimental culture setup for high throughput flask screening setup

P. tricornutum CCAP 1055/1 was harvested during late-log, centrifuged (4000 rpm, 10 mins), washed twice with 20 mL of medium and re-suspended in 250 mL Erlenmeyer flasks with 200 mL of autoclaved medium (121°C, 15 mins). The initial inoculum density was $\sim 10^6$ cells mL^{-1} (~ 0.02 g L^{-1} DW) and growth was monitored daily by measuring cell count, OD 750 nm, and dry weight (DW). The cultures were incubated under $21 \pm 0.5^\circ\text{C}$ in a temperature-controlled incubator (LMS Series 4 1200) with continuous light at 142 ± 33 $\mu\text{mol photons m}^{-2} \text{s}^{-1}$ (827 fluorescent bulbs as above) using the high throughput system shown in Figure 4.9. Each culture was aerated at 15 lpm with 0.5 % CO_2 and the gas mixture was delivered through a 0.22 μm air filter. The supplied carbon dioxide concentration was confirmed using a gas analyser (BlueInOne FERM, Blue Sense) coupled to a computer with BlueVis software. The cultures were buffered with 20 mM Tris buffer which maintained the

pH at 7.5-7.65. Samples for determining the biochemical composition (chlorophyll *a*, fucoxanthin, fatty acids, carbohydrate and protein) and elemental analysis were taken after 7 d.



Figure 4.9 - Experimental setup for high throughput screening of culture condition optimisation for biorefining. Cultures contained 200 mL of liquid volume and were aerated with a sterile gas mixture of air and 0.5 % CO₂

4.3.4. Effect of modified f/2 medium on biochemical composition

The *P. tricorutum* flask cultures were cultivated with f/2 medium with elevated nitrate and phosphate (2 x, 5 x, 10 x and 20 x), and f/2 was used as the control medium (Appendix B).

4.3.5. Effect of salinity on biochemical composition

The *P. tricorutum* flask cultures were cultivated with modified f/2 medium with 5 x f/2 NP (Appendix B) with different salinities (0, 16.5, 33, 49.5, 66 and 82.5 practical salinity unit - psu). An artificial seawater medium to replicate Instant Ocean (33 g L⁻¹) was formulated using CaCl₂ (9.4 mM), Na₂SO₄ (25.2 mM), MgCl₂ (51.2 mM), KCl (10.1 mM), NaCl (442.1 mM), and sodium bicarbonate (3.1 mM) and the ionic composition altered to match the

required salinity. Bromide, strontium, fluoride and iodide were omitted. Biochemical analysis was only conducted for 16.5, 33, 49.5, 66 and 82.5 psu.

4.3.6. Effect of carbon source on biochemical composition; bicarbonate, CO₂ and glycerol

For the bicarbonate trial 5 x f/2 NP medium was supplemented with bicarbonate at 5, 10, 25, 50, 100 and 125 mM. For the CO₂ experiment, 0.5, 1 and 2 % CO₂ were tested. For the glycerol trial, 5 x f/2 NP with 2 % CO₂ was supplemented with 0.01, 0.025, 0.05 and 0.1 M glycerol. Glycerol was diluted with deionised water and filter sterilised into the medium after autoclaving.

4.3.7. Analytical methods

4.3.7.1. Biomass sampling and determination of microalgal cell growth

The optical density (OD) was monitored at OD 750 nm using a SPECTROstar spectrophotometer (BMG Labtech, Germany). For cell counts 100 µL of each algal culture was removed and fixed with 10 µL Lugol's iodine prior to counting with an Advanced Neubauer haemocytometer (BS-748, Hawksley) using a microscope (BX51, Olympus) and the cells were counted using ImageJ (<http://rsb.info.nih.gov/ij/>). The average growth rate (μ) was calculated according to Butler et al. (2017) but as a function of each day and the maximum growth rate (μ_{max}) was the maximum value of this. Trypan blue staining was used for viability assays. One mL of each sample was centrifuged at 6000 rpm for 5 mins and the supernatant was discarded. The pellet was then re-suspended in 1 mL phosphate buffered saline (PBS). The viability of flocculated cells was tested by dye exclusion using 0.4 % Trypan blue (Sigma Aldrich, UK), which is excluded by viable cells. To 100 µL of cells, 100 µL 0.4 % Trypan blue solution was added, cells were incubated for three minutes at room temperature and they were counted using a haemocytometer.

Dry weight was performed by centrifugation at (4000 rpm, 10 mins) of 5 mL of samples, washed with 20 mL of 0.01 M phosphate buffered saline (PBS) to remove any adhering medium etc. transferred to a 2 ml Eppendorf safe-lock tube, centrifuged at 13,000 rpm for 5 mins (12,500 g) and stored at -20°C. The samples were then lyophilized and the powder weighted using a 5 d.p. balance.

4.3.7.2. *Determination of dissolved inorganic nitrogen (DIN), dissolved inorganic phosphate (DIP) and dissolved inorganic carbon (DIC) from the supernatant*

Dissolved inorganic nitrogen (DIN) in the media was determined at OD₂₂₀ nm as described in Collos et al. (1999). Dissolved Inorganic Phosphate (DIP) in the media was determined following the method of Strickland and Parsons (1968) and the OD₈₈₅ nm reading was taken after 15 mins (longer times did not result in significantly different values, data not shown). Dissolved inorganic carbon (DIC) was calculated using the back-titration procedure described by Chen et al. (2016).

4.3.7.3. *Inductively coupled plasma mass spectroscopy (ICP-MS) analysis*

From the f/2 media modification experiment after 7 d the dried biomass was analysed for elemental analysis in the f/2 and 5 x f/2 sample. Elemental quantification was achieved by inductively coupled plasma-mass spectroscopy (ICP-MS), using an Agilent 7500CE spectrometer. ~100 mg dried microalgal biomass was digested with 3 mL nitric acid and 1 mL perchloric acid and heated to 200°C. The samples were then made to 25 mL using 1 % nitric acid and elements showing high concentrations were diluted accordingly with deionised water. Anions were quantified using a Metrohm 883 Basic IC plus IC system, fitted with a Metrosep A Supp 5-4 × 150 mm column and using Na₂CO₃/NaHCO₃ eluent.

4.3.7.4. *Biochemical composition (protein and carbohydrate)*

Combined extraction of carbohydrate and protein was carried out according to Chen and Vaidyanathan (2013) with slight modification (Appendix B) using approximately 2 mg dry biomass.

4.3.7.5. *Fatty acid analysis and EPA determination using direct transesterification*

A modified version of Kapoore et al. (2014) was used for FAME direct transesterification. To a 2 mL Eppendorf, 1-2 mg dried biomass and acid washed glass beads (425-600 µm i.d) were added. A bead beating step was introduced where the cells were

disrupted using the Disrupter Genie[®]. Five cycles of disruption were performed with 2 mins disruption, with an interval of 1 min on ice. Ethanolic-HCl (7%) replaced BF₃ as the acid catalyst for the formation of fatty acid ethyl esters (FAEEs) (Appendix B).

4.3.7.6. *Chlorophyll and fucoxanthin* analysis using high-performance liquid chromatography (HPLC)

Chlorophyll *a* and fucoxanthin were analysed using a modified method of Grant et al. (2001). One mg of dried microalgal biomass was extracted with 1.5 mL HPLC grade absolute ethanol (Sigma Aldrich, UK) with 250 mg L⁻¹ butylated hydroxytoluene (BHT) and bead beaten using bead beater tubes with lysing matrix E (Bertin Technologies, USA) three times at 90 s x 5000 rpm with a 45 s break. After cell disruption the bead beating tubes were then centrifuged at 13,000 rpm for 3 mins. 1 mL of the supernatant was pipetted to a 5 mL glass tube (FischerBrand, USA). To the bead beating tube, 1 mL ethanol/BHT mixture was added and the tubes vortexed for 10 s. The tubes were then centrifuged (13,000 rpm, 3 mins) and 1 mL was transferred to the 5 mL glass tube. This procedure was repeated until the pellet was colourless (5 extractions necessary in total and confirmed by microscopy). The extracts in the glass tubes were then evaporated under nitrogen, re-suspended in 1 mL absolute ethanol (Sigma Aldrich, UK) and transferred to a 2 mL safelock Eppendorf tube. The tubes were then centrifuged (13,000 rpm, 2 mins) before transferring the supernatant to amber coloured HPLC vials. To avoid photo-oxidation, all procedures were carried out under darkness.

Ultra-high-performance liquid chromatography (UHPLC) (Thermo Scientific, USA) was used to quantify the fucoxanthin content. HPLC analysis was performed using a Nexera X2 system (Shimadzu, Japan) coupled with a photo-diode array detector (SPD-M20A) and a Kinetex C18 reversed-phase column (100A 150 x 4.6 mm, 5 µm particle size) (Phenomenex, UK) was used. The HPLC method adopted was a modified version of Grant, 2011. Three mobile phases were used: (A) 0.5 M Ammonium acetate in methanol/water 85:15, (B) Acetonitrile/water 90:10 and (C) Ethyl acetate 100 % using the gradient procedure described. The flow rate was set at 1 mL min⁻¹ and the column temperature at 25°C. The concentration of fucoxanthin was quantified by measuring at the absorbance at 450 nm. A linear calibration curve ($R^2 = 0.99$) covering the range 0-20 µg mL⁻¹ was constructed using a fucoxanthin, chlorophyll *a* and antheraxanthin standard (Sigma Aldrich, UK). The retention time of the

extracts matched the standards for fucoxanthin (6.7 mins) and chlorophyll *a* (25.2 mins) as shown in (Appendix B).

4.3.7.7. Elemental composition

Elemental analysis was conducted according to Al-shathr (2019) with slight modification (Appendix B). Helium was used as a carrier gas to transport all the combustion gases through the system and high-purity oxygen was used to aid the combustion

4.3.8. Statistical analysis

Each treatment was performed in triplicates and the mean and standard error of the dependent variables are presented in the results. Statistical analysis of the experimental data was conducted using SPSS statistical software (SPSS Statistics 26, IBM). The data was tested for normality using a Kolmogorov-Smirnov test and if these data were normally distributed ($P > 0.05$) they were subsequently tested for equal variance using Levene's test. If variances were considered equal then a one-way ANOVA/MANOVA and a *post-hoc* Tukey's test was utilised to understand where the differences were. If samples were not normally distributed ($P < 0.05$) then a Kruskal-Wallis and *post-hoc* Dunn's non-parametric comparison was undertaken to understand the changes. The statistical difference of each set of experiments was studied with the analysis of the *P* value. In addition, this value was used to select parameters that were significant.

4.4. Results and Discussion

4.4.1. Pre-optimisation for growth: effect of temperature and lighting regime on growth of *P. tricornutum*

In indoor cultivation it has been reported that *P. tricornutum* becomes photo inhibited at light intensities above $100 \mu\text{mol photons m}^{-2} \text{ s}^{-1}$ (Remmers et al., 2017). Comparatively, in outdoor growth experiments with *P. tricornutum*, the maximum biomass productivity was

reached at average irradiances of 50-150 $\mu\text{mol m}^{-2} \text{s}^{-1}$ and decreased at light intensities higher than 150 $\mu\text{mol m}^{-2} \text{s}^{-1}$ (Acién Fernández et al., 2003).

Initially using f/2 medium at 150 $\mu\text{mol photons m}^{-2} \text{s}^{-1}$, the Algem[®] (Algenuity, UK), was investigated for optimising biomass concentration in *P. tricornutum* CCAP 1055/1. The highest biomass productivity was attained at 21°C (0.072 g L⁻¹ d⁻¹), which was an improvement of 1.34-fold compared with 27°C and was significantly higher ($p < 0.05$) (Figure 4.10). Similarly, 20°C was optimal for growth for *P. tricornutum* CCAP 1055/2 (Leblond and Chapman, 2000) and 21.5°C was optimal for CCAP 1052/1B / UTEX 640 (Yongmanitchai and Ward, 1991). Microalgae typically show a higher growth rate with increasing temperatures, until the optimum temperature. However, above this optimal temperature, a decrease in growth is observed due to the damage of proteins required for photosynthesis (Allakhverdiev et al., 2008; Ras et al., 2013). It was clear that the biomass productivity was significantly reduced at 25°C compared with 21°C ($p < 0.05$). As 21°C was optimal, a 12:12 photoperiod was compared with 24 h and flashing light. Continuous light doubled the biomass productivity compared with a 12:12 photoperiod. Previously, Megía-Hervás et al., (2020) found that 18:6 photoperiod resulted in an increase in biomass concentration compared with 12:12 photoperiod for the same strain but did not compare continuous light. At a higher light intensity (400 $\mu\text{mol photons m}^{-2} \text{s}^{-1}$), a photoperiod of 20:4 was observed to be optimal for achieving the highest growth rate in TV335 and 24:0 was observed to result in photoinhibition (Regmi, 2014). These conditions were then selected for the high-throughput screening experiments to investigate the effect of media composition and cultivation conditions.

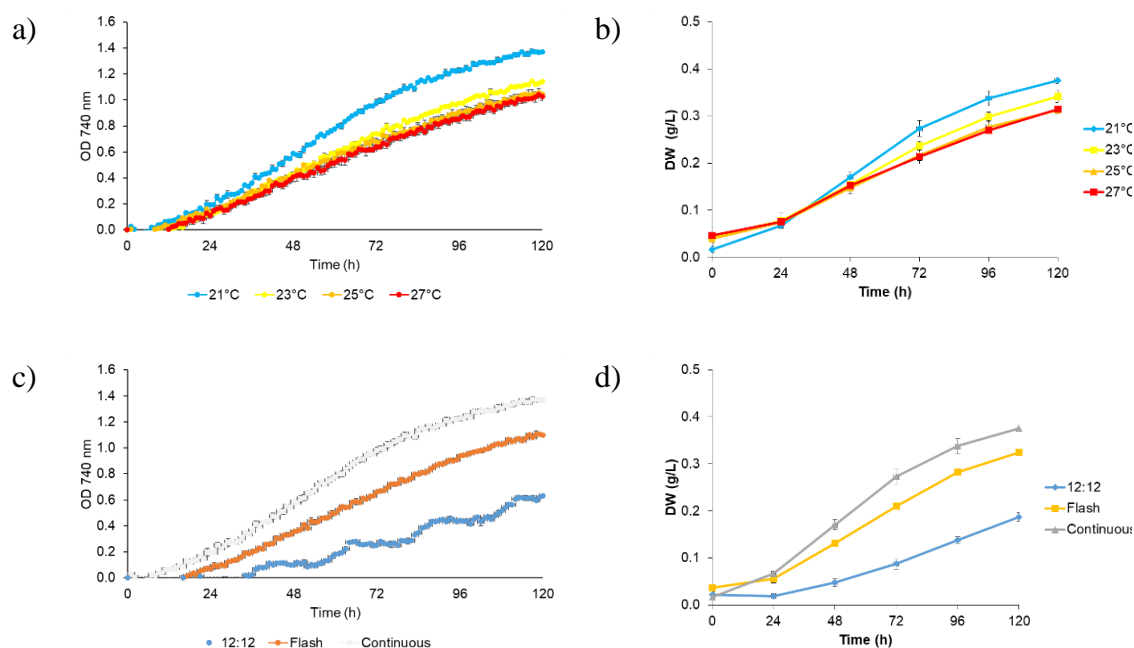


Figure 4.10 - Cultivation in of *P. tricornutum* CCAP 1055/1 for culture condition optimisation (f/2 medium) in Algem[®] (Algenuity, UK); a-b) different temperatures (21, 23, 25 and 27°C) and) light regimes (continuous red: white (85:15) at 150 $\mu\text{mol photons/m}^2/\text{s}$, 12:12 photoperiod and flashing light with 100 Hz (10 m/s) and a duty cycle of 50 %) at 21°C. The medium used was f/2 with artificial salts and agitation at 120 rpm, with 10 cm^3/min (0.01 lpm: 0.025 vvm) aeration with 5 % CO_2 (n=2), pH stat 7.5, 0.4 L working volume.

4.4.2. Effect of f/2 modification on biochemical composition: increasing nitrate and phosphate concentration

Currently there is difficulty in using a standardised but high throughput screening system for comparing environmental factors for effecting growth and biochemical composition. A new setup was designed which could quickly screen different cultivation parameters to observe their effect on biomass productivity and product formation. 20 mM Tris-HCl was used as a buffer and it was found to not adversely affect growth or product formation (Appendix B).

It is well known that fucoxanthin content is higher under low light ($100\text{-}150 \mu\text{mol photons m}^{-2} \text{s}^{-1}$), and a higher biomass productivity has been attained at $150 \mu\text{mol photons m}^{-2} \text{s}^{-1}$ (Gómez-Loredo et al., 2016; McClure et al., 2018). Thus, for the high throughput screening a light intensity of $142 \mu\text{mol photons m}^{-2} \text{s}^{-1}$ was selected.

For the cultivation of diatoms including *P. tricornutum* typically f/2, DAM (diatom artificial medium), and Walnes medium have been used (Sethi et al., 2020). However, it has been observed that these media can be limiting in nutrients (McClure et al., 2018), but this has not been fully quantified. It is well known that nitrate supplementation (8.82 mM) results in

an increase in EPA and fucoxanthin in CS-29 (Baoyan et al., 2017), but it has been reported that phosphate alone does result in an increase in fucoxanthin content or yield (McClure et al., 2018). Therefore, in the current study the effect of elevated macronutrients: nitrate (0.882-17.64 mM) and phosphate (0.036-0.72 mM) in combination, designated 2 x f/2 NP, 5 x f/2 NP, 10 x f/2 NP and 20 x f/2 NP were investigated to determine if biomass productivity, in combination with fucoxanthin, EPA, protein and carbohydrate yield could be increased. To date no study appears to have systematically increased nitrate and phosphate to look at the effect on the biochemical composition of *P. tricornutum*.

Cultivation with f/2 was found to result in a final OD 750 nm, cell count, and biomass concentration of 1.29, 1.55×10^7 cells mL⁻¹ and 0.30 g L⁻¹ DW. When nitrate and phosphate (2 x, 5 x, 10 x and 20 x) were elevated, higher biomass concentrations were obtained (0.40, 0.46, 0.47 and 0.52 g L⁻¹ DW), but 20 x f/2 NP was not significantly higher than 5 x f/2 NP. Cultivation in 5 x f/2 NP resulted in the highest fucoxanthin content (1.23 %) which was >3-fold higher than the content in f/2 medium (0.4 % DW). A subsequent decrease was observed at higher nitrate and phosphate concentrations (1.11 and 0.87% DW at 10 and 20 x f/2 respectively). It is possible that as *P. tricornutum* cultivated with higher nitrate and phosphate concentrations resulted in a higher biomass concentration, there was a lower light per cell/gram of biomass, which could have resulted in an increase in fucoxanthin as this pigment is accumulated under low light.

Cultivation in f/2 medium resulted in the highest FAAE content (13.83 % DW) and increases in nitrate and phosphate resulted in a decrease in FAAE content with the lowest content at 20 x f/2 NP (4.25% DW). It is well known that nitrate and phosphate starvation or deprivation, especially nitrate can result in elevated TFA content in microalgae and *P. tricornutum* (Alipanah et al., 2018; Caballero et al., 2016), and the f/2 and 2 x f/2 treatments were nutrient starved (Figure 4.12). Nitrogen is assimilated into protein and when nitrogen availability decreases, the sink for the tricarboxylic acid (TCA) cycle metabolites declines and acetyl-CoA can be shunted towards fatty acid biosynthesis (Levitan et al., 2015).

The highest EPA content (1.82 % DW) was found when *P. tricornutum* was cultivated in f/2 and 2 x f/2 NP medium but this was not statistically significant compared with other NP elevation treatments, and a further increase in nitrate and phosphate content resulted in a decrease in EPA content **Figure 4.11** Interestingly the highest EPA proportion of FAAE was in 10 x f/2 NP (36.4 % of TFA) compared with only 13.2 % in f/2 medium. The other dominant fatty acids (C16:0 and C16:1) showed a general decrease in proportion with increases in nitrate/phosphate but as the EPA content did not increase, they did not appear to be re-

allocated to EPA synthesis. Under phosphate deprivation or depletion EPA is known to be lower and C16:0 and C16:1 are known to increase (Siron et al., 1989). Under nitrate supplementation, the proportion of C16:0 and C16:1 decreases (Yodsuwan et al., 2017).

5 x f/2 NP (4.41 mM nitrate and 0.18 mM phosphate) resulted in the highest fucoxanthin content (1.2 % DW), which was >3-fold higher than f/2 medium (p<0.01). In *P. tricornutum* CS-29 nitrate supplementation alone in f/2 medium (8.82 mM) resulted in ~3-fold increase in fucoxanthin content (5.9 % DW) but nitrate and phosphate supplementation in combination (8.82 and 0.36 mM) did not result in an increase in fucoxanthin content and this is likely due to the different experimental setup and high error that was reported in the McClure et al. (2018) study.

5 x f/2 NP also resulted in the highest protein content (52.0 % DW) and the protein content was found to increase with nitrate and phosphate content but this was not significantly higher than 10 x f/2 NP (50.6 % DW). The protein content was much higher than previously reported for CCAP 1055/1 (16 % DW) cultivated in f/2 medium without CO₂ supply (Song et al., 2020) and other strains in the literature; unknown Spanish isolate (32 % DW) (Fidalgo et al., 1995), CICESE strain (37 % DW) (Valdez-Flores et al., 2017) and Chilean strain (38 % DW) (Branco-Vieira et al., 2020).

The highest carbohydrate content was obtained using f/2 medium (18.1 % DW) and decreased with an increase in nitrate and phosphate content, with the minimum content obtained with 10 x f/2 NP (12.6 %) which is similar to values reported in the literature for other *P. tricornutum* strains (Valdez-Flores et al., 2017; Branco-Vieira et al., 2020).

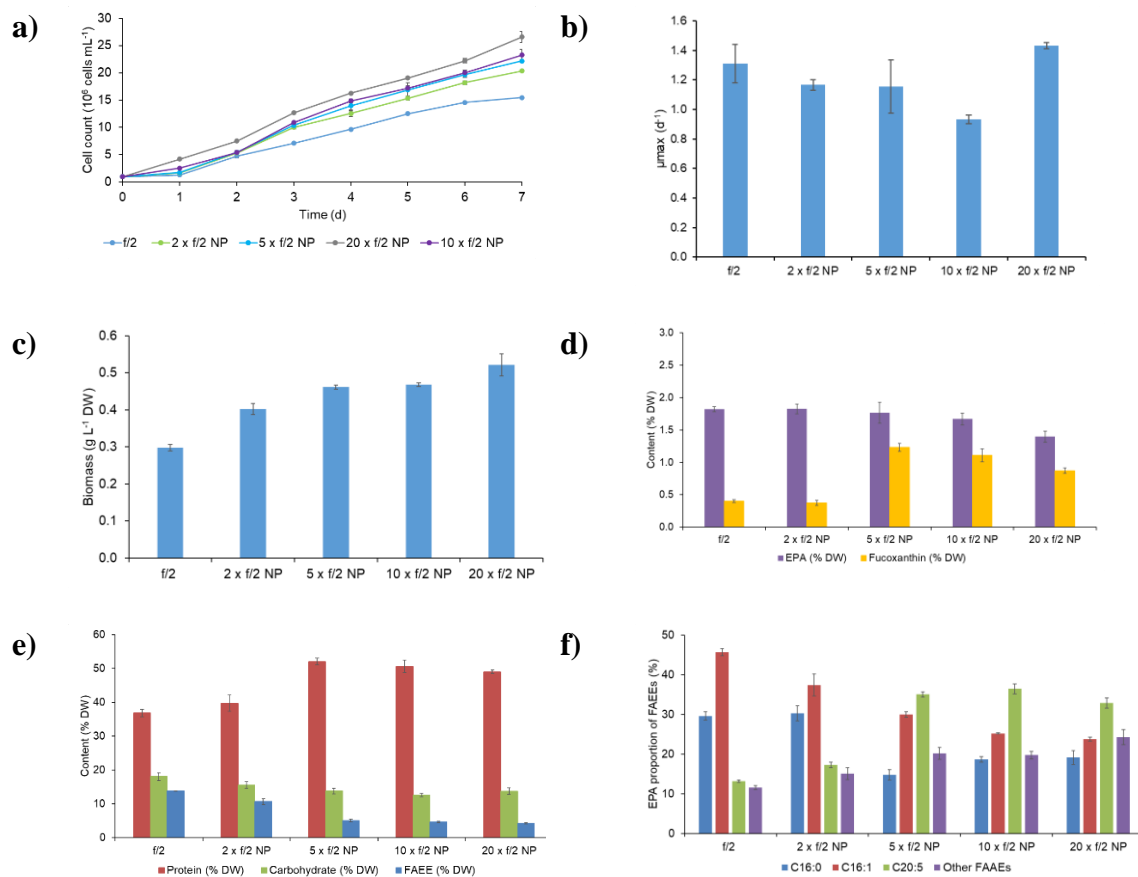


Figure 4.11 – Effect of f/2 modification on biochemical composition of *P. tricornutum*; a) cell count, b) μ_{max} (d⁻¹), c) final biomass concentration, d) eicosapentaenoic acid (EPA), chlorophyll *a*, and fucoxanthin content f) protein, carbohydrate and fatty acid ethyl ester (FAEE) content, g) FAEE composition

The medium with 20 x f/2 NP resulted in the highest biomass concentration (0.52 g L⁻¹ DW) and biomass productivity (74.45 mg L⁻¹ d⁻¹) after only 7 d. A maximum specific growth rate of 0.68 d⁻¹ has been reported for CCAP 1055/1 cultivated in f/2 medium without CO₂ addition and were reported to reach a final biomass concentration of 0.50 g L⁻¹ after three weeks (Song et al., 2020). 20 x f/2 NP also resulted in the highest protein (36.51 mg L⁻¹ d⁻¹) and carbohydrate yield (10.15 mg L⁻¹ d⁻¹) (Table 4.4). 2 x f/2 NP resulted in the highest FAEE yield (6.07 mg L⁻¹ d⁻¹). However, 5 x f/2 NP resulted in the highest fucoxanthin (0.81 mg L⁻¹ d⁻¹) and EPA yields (1.16 mg L⁻¹ d⁻¹) (Table 4.4). Gao et al (2017) explored the biorefinery potential of a Chinese *P. tricornutum* strain in flat-panel PBRs, and found the highest volumetric productivity of EPA (9.6 mg L⁻¹ d⁻¹), chrysolaminarin (93.6 mg L⁻¹ d⁻¹), and fucoxanthin (4.7 mg L⁻¹ d⁻¹) in the exponential phase after 6 days cultivation under high nitrate and phosphate (14.5 and 0.88 mM respectively). In the current study an increase in

fucoxanthin, EPA and carbohydrate content was not observed at higher nitrate and phosphate concentrations beyond 4.41 mM and 0.18 mM respectively. It is possible the lower productivities in our study were likely due obtaining a lower biomass concentration which was due to the longer light path of the flasks compared with the flat plate, lower light employed, and the lower inoculation density.

Table 4.4 - Biomass (volumetric productivity) and product yields with different f/2 media formulations

| | f/2 | 2 x f/2 NP | 5 x f/2 NP | 10 x f/2 NP | 20 x f/2 NP |
|--|--------------|--------------|--------------|--------------|--------------|
| Biomass productivity (mg L ⁻¹ d ⁻¹) | 42.55 ± 1.26 | 57.45 ± 2.19 | 65.90 ± 0.86 | 66.84 ± 0.77 | 74.45 ± 4.23 |
| Carbohydrate (mg L ⁻¹ d ⁻¹) | 7.71 ± 0.69 | 8.91 ± 0.65 | 9.08 ± 0.55 | 8.42 ± 0.29 | 10.15 ± 0.18 |
| Protein (mg L ⁻¹ d ⁻¹) | 15.65 ± 0.23 | 22.91 ± 2.28 | 34.28 ± 0.72 | 33.82 ± 1.45 | 36.51 ± 2.25 |
| Fucoxanthin (mg L ⁻¹ d ⁻¹) | 0.17 ± 0.01 | 0.21 ± 0.02 | 0.81 ± 0.04 | 0.74 ± 0.07 | 0.65 ± 0.05 |
| FAEE (mg L ⁻¹ d ⁻¹) | 5.58 ± 0.17 | 6.07 ± 0.27 | 3.32 ± 0.28 | 3.07 ± 0.19 | 3.17 ± 0.28 |
| EPA (mg L ⁻¹ d ⁻¹) | 0.77 ± 0.01 | 1.05 ± 0.02 | 1.16 ± 0.09 | 1.12 ± 0.07 | 1.04 ± 0.10 |

Higher nutrient containing media (10 x f/2) has been found to result in an increase in final dry weight (0.59 g/L DW) compared to conventional f/2 medium (0.29 g/L DW) (McClure et al., 2018) which was similar to that reported in the current study with 10 x f/2 NP (0.52 g L⁻¹ DW). It has been reported that increasing the phosphate concentration alone in f/2 (from 0.036 mM to 0.36 mM) did not result in an increase in fucoxanthin content (McClure et al., 2018). However, increasing nitrate 10-fold (8.82 mM) resulted in a near 3-fold increase in fucoxanthin content (5.7 % DW) and a 3-fold increase in fucoxanthin productivity (2.16 mg L⁻¹ d⁻¹) compared with f/2. However, when nitrate supplementation was tested in this study alone, no significant increase in fucoxanthin was observed (data not shown). The effect of increasing nitrate alone to rapidly increase fucoxanthin content has only been observed by McClure et al. (2018) and it is the highest content to date, so it could be strain specific.

4.4.3. Effect of f/2 modification on nutrient uptake rate

P. tricornutum cultivated in f/2 and 2 x f/2 medium were near nitrate deprivation with <7 and 18 μM remaining after 7 d cultivation respectively. With the higher NP treatments (5-20 x f/2 NP) there was no nitrate limitation observed with >94-9171 μM nitrate remaining

after 7 d. The highest nitrate uptake rate was on the first day and surprisingly was with 20 x f/2 NP (1535 pmol cell⁻¹ d⁻¹). Generally, an increase in average daily nitrate uptake rate was observed with an increase in nitrate and phosphate content in the medium up to 15.5 mM g⁻¹ biomass DW for 10 x f/2 NP **Figure 4.12**. However, there was no significant difference between 10 x f/2 NP and 20 x f/2 NP. The ability for *P. tricornutum* to scavenge high concentrations of nitrate is interesting. McClure et al. (2018) stated that cultures grown with f/2 medium are limited by nutrient availability after day 7 with <0.01 mg/L remaining but, similar to that reported here but their study did not look at nutrient assimilation.

For phosphate there was <1 μM after 2 d cultivation in f/2 medium and the phosphate was depleted after 3 d. Similarly, phosphate was depleted after 4 d cultivation in 2 x f/2 medium. Residual phosphate remained in the higher N/P containing f/2 media (1.9-8 μM) and this showed that phosphate was rapidly assimilated. The highest phosphate uptake rate was on the first day but there was no significant difference between 20 x f/2 NP and f/2 (12 pmol/cell). Generally, an increase in average daily phosphate uptake rate was observed with an increase in nitrate and phosphate content in the medium up to 1.0 mM g⁻¹ biomass DW for 20 x f/2 NP which was significantly higher than the other treatments ($p < 0.01$) (Figure 4.4). From ICP analysis it appeared that the phosphate in the biomass increased from 0.4 % DW when cultivated in f/2 medium, to 1.0 % DW when cultivated in 5 x f/2 NP (data not shown). It has previously been revealed that during phosphate deprivation, gene expression for proteins involved in phosphate acquisition and scavenging are upregulated, whereas proteins involved in photosynthesis and nitrogen assimilation are downregulated (Alipanah et al., 2018). In the current study, phosphate was indeed rapidly assimilated, but at higher nitrate and phosphate concentrations a higher phosphate uptake rate was observed.

It appeared that the higher nitrate and phosphate uptake rates at 10 x f/2 NP translated into increased biomass concentration and protein, but not an increase in fucoxanthin or EPA compared with 5 x f/2 NP. The nitrogen deprivation and phosphate starvation is likely why the FAEE (TFA) content and carbohydrate content was higher in f/2 medium which has been reported extensively in the literature (Abida et al., 2015).

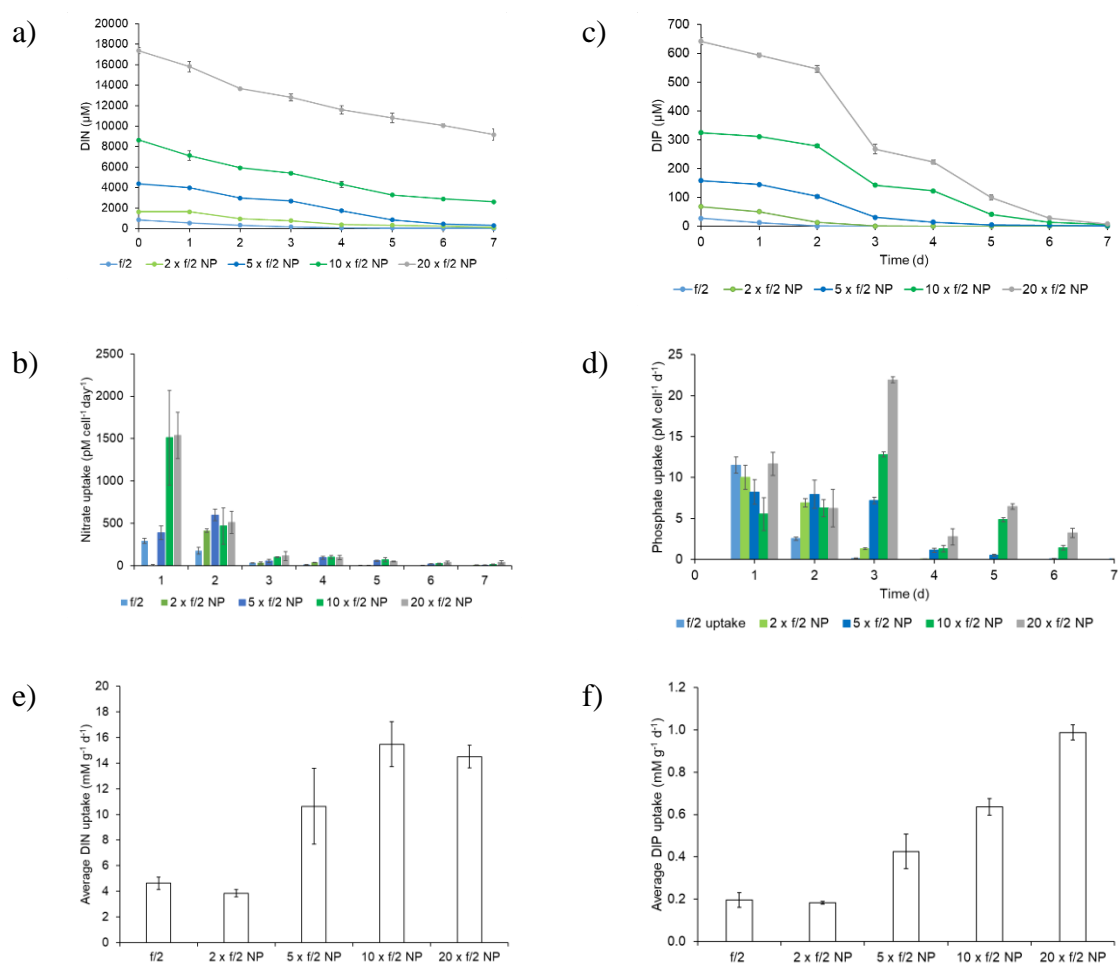


Figure 4.12 - Effect of modified f/2 medium on nitrate (DIN and pmol/cell) and phosphate uptake (DIP and pmol/cell)

As 5 x f/2 NP medium resulted in a significantly higher fucoxanthin (>4.5-fold), EPA (>1.5-fold) and protein (>2-fold) yield, along with an increased carbohydrate yield, and resulted in a higher EPA and fucoxanthin yield than the other elevated nitrate and phosphate treatments 5 x f/2 NP was selected for further increasing the biomass and product yields for CCAP 1055/1.

4.4.4. Effect of salinity on biochemical composition

Seldom reports have been conducted on the effect of salinity on the biochemical composition of *P. tricornutum* but UTEX 640 has been observed to have a higher growth rate in freshwater (Yongmanitchai and Ward, 1991) and CS-29/7 has been observed to grow up to 75 % salinity (Ishika et al., 2018). Typically, *P. tricornutum* CCAP 1055/1 is cultivated in natural seawater at 35 salinity (De Martino et al., 2007; Réveillon et al., 2016) or artificial

seawater using ~33-35 psu e.g. Instant Ocean, Tropic Marine (35 % salinity) (Caballero et al., 2016; Jallet et al., 2020; Song et al., 2020).

A high salinity in the culture medium can create oxidative stress minimise contamination from unwanted species (Das et al., 2011). In addition, if seawater is used in photobioreactors (PBRs), bags or open ponds, evaporation will occur and it is important that *P. tricornutum* is able to tolerate a wide range of salinities. A salinity increase is known to result in an increase in lipid content and β -carotene in some species, but a decrease in lutein in others (Ishika et al., 2017). Some diatoms such as *Amphora* sp. were observed to have the highest content and fucoxanthin yield at higher salinities (85 %), but others have a higher salinity at that optimal for growth (Ishika et al., 2017).

In this study we investigated two lower salinities (0 and 16.5 psu) and three higher salinities (49.5, 66 and 82.5 psu) as a broad range of salinities have not been tested to the authors knowledge to evaluate the effect on the biochemical composition and product yield.

The protein (53.33 % DW), FAEE (6.97 % DW), EPA (2.22 % DW) and fucoxanthin (1.02 % DW) contents were highest at 33 g L⁻¹ salinity and were found to decrease with a reduction in salinity (to 16.5 psu) and an increase in salinity (up to 82.5 psu). The carbohydrate content (14.83 % DW) was highest at 16.5 psu and was found to decrease with an increase in salinity. It has been determined that a salinity of 35 psu resulted in an increase in biomass yields compared with 20 psu in *P. tricornutum* CS 29/8, but salinity had no effect on EPA content (Cui et al., 2020). For *P. tricornutum* UTEX 646 the maximum biomass concentration and EPA content was obtained at 30 psu but the highest lipid and fucoxanthin contents were observed at 20 psu showing that the effect of salinity on the biochemical composition is strain dependent (H. Wang et al., 2018). This is in contrast to the current study where EPA decreased with a decrease or increase in salinity from 33 g L⁻¹ at the concentrations tested. For CS-29/7 the optimal salinity for maximum fucoxanthin content was at 45 psu (Ishika et al., 2017).

Yongmanitchai & Ward (1991) tested 0-24 psu and found for UTEX 640 (only freshwater strain known) that the highest EPA yield was obtained with cultivation in freshwater. However, increasing the salinity up to 24 psu there was an apparent increase in EPA yield compared with 12 g L⁻¹ (Yongmanitchai & Ward, 1991). Comparatively, Qiao et al. (2016) tested four salinities (15-35 ppt) and found there was no effect on fatty acid composition.

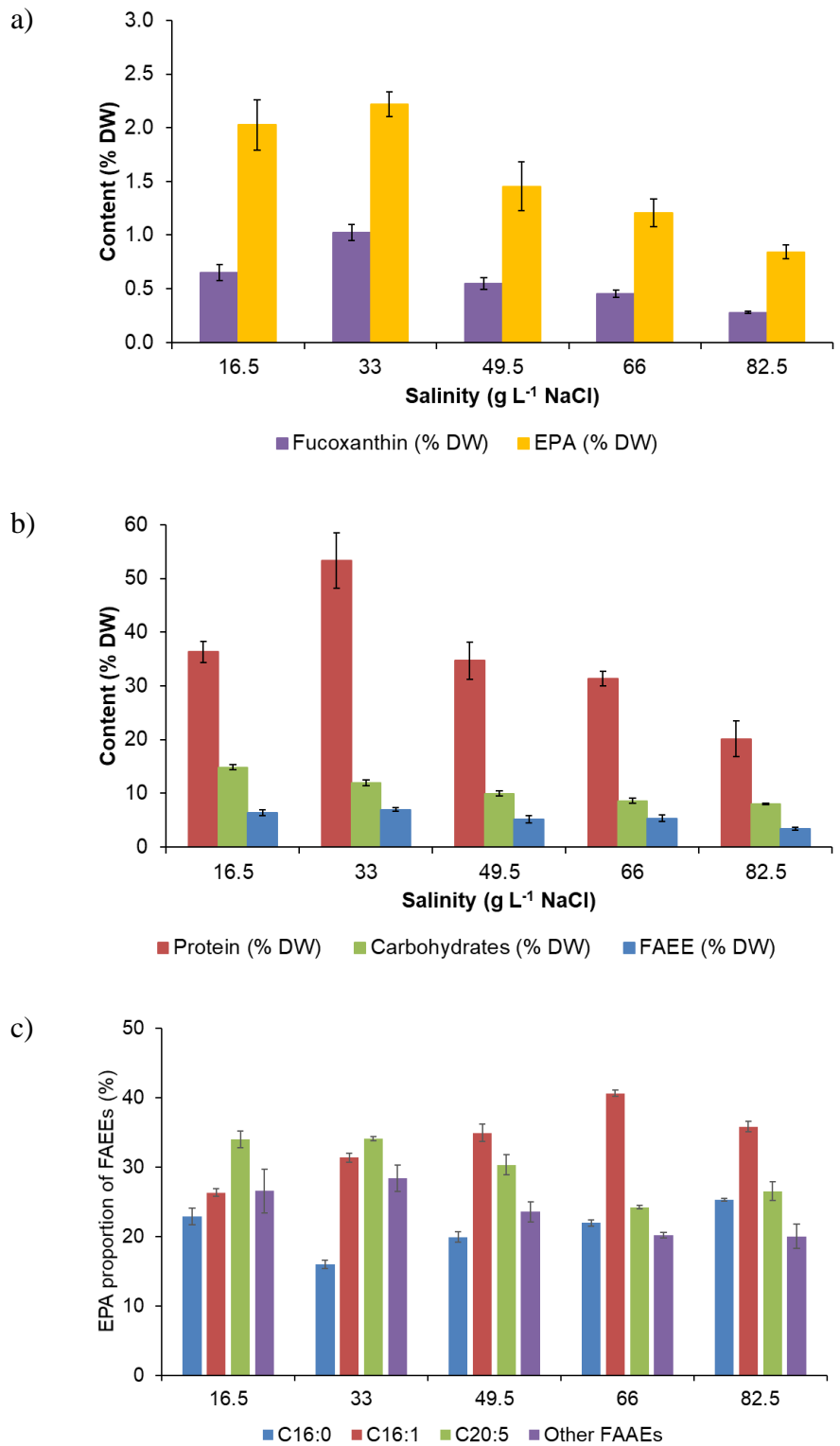


Figure 4.13 - Effect of salinity on biochemical composition of *P. tricornutum*; a) EPA and fucoxanthin content and b) protein, carbohydrate and FAEE content. CCAP 1055/1 did not grow in freshwater and this was not analysed

Wang et al. (2018) compared growth of *P. tricornutum* UTEX 646 cultivated in 2f enriched medium under different salinities (5, 10, 20 and 30 %) under 70 $\mu\text{mol photons m}^{-2} \text{s}^{-1}$ and found that the highest biomass concentration was attained at 30 %. The minimum lipid content was obtained at a salinity of 10 % but the maximum lipid content was obtained at a salinity of 20 % (44.44 % DW). It was found that the EPA content decreased to 12.54 % TFAs from 16.46 % of TFAs (salinity decrease from 30 to 10 %), showcasing that low salinity appears to benefit EPA accumulation which was also found by Ye et al. (2015). The highest fucoxanthin content (0.74 % DW) was obtained at a salinity of 20 %, but other salinities did not significantly affect the fucoxanthin content (Wang et al., 2018).

The highest biomass concentration (0.83 g L^{-1} DW) and productivity (115 $\text{mg L}^{-1} \text{d}^{-1}$) was attained with 66 psu in the current study. For *P. tricornutum* MACC/B221 the highest photosynthetic activity was observed at 20-30 psu and salinity stress (<20 psu and >50 psu) resulted in major impairments of photochemical efficiency and inhibition of PSII electron transport (Liang et al., 2014) and it appeared CCAP 1055/1 was more halotolerant.

Using 66 psu resulted in the highest productivity of protein (35.84 $\text{mg L}^{-1} \text{d}^{-1}$) and FAEE (6.02 $\text{mg L}^{-1} \text{d}^{-1}$). The highest carbohydrate productivity (10.09 $\text{mg L}^{-1} \text{d}^{-1}$) was attained with 49.5 psu. Comparatively the highest fucoxanthin and EPA productivity was attained with 33 psu (0.73 and 1.35 $\text{mg L}^{-1} \text{d}^{-1}$).

Table 4.5 - The effect of salinity (16.5, 33, 49.5, 66 and 82.5 g L^{-1}) on biomass concentration and volumetric productivity) and product yields

| | 16.5 psu | 33 psu | 49.5 psu | 66 psu | 82.5 psu |
|---|------------------|------------------|-------------------|-------------------|------------------|
| Biomass concentration (g L^{-1}) | 0.48 \pm 0.08 | 0.53 \pm 0.07 | 0.73 \pm 0.08 | 0.83 \pm 0.10 | 0.69 \pm 0.08 |
| Biomass productivity ($\text{mg L}^{-1} \text{d}^{-1}$) | 65.57 \pm 0.03 | 71.43 \pm 0.03 | 101.71 \pm 0.03 | 114.91 \pm 0.04 | 95.68 \pm 0.03 |
| Carbohydrate ($\text{mg L}^{-1} \text{d}^{-1}$) | 9.76 \pm 0.43 | 8.51 \pm 0.32 | 10.09 \pm 0.31 | 9.80 \pm 0.26 | 7.65 \pm 0.24 |
| Protein ($\text{mg L}^{-1} \text{d}^{-1}$) | 23.72 \pm 0.53 | 37.97 \pm 0.82 | 34.99 \pm 0.60 | 35.84 \pm 0.46 | 19.56 \pm 0.87 |
| Fucoxanthin ($\text{mg L}^{-1} \text{d}^{-1}$) | 0.42 \pm 0.07 | 0.73 \pm 0.09 | 0.55 \pm 0.07 | 0.52 \pm 0.06 | 0.27 \pm 0.04 |
| FAEE ($\text{mg L}^{-1} \text{d}^{-1}$) | 4.23 \pm 0.35 | 4.97 \pm 0.23 | 5.15 \pm 0.33 | 6.02 \pm 0.24 | 3.26 \pm 0.19 |
| EPA ($\text{mg L}^{-1} \text{d}^{-1}$) | 1.35 \pm 0.21 | 1.58 \pm 0.13 | 1.46 \pm 0.18 | 1.37 \pm 0.11 | 0.81 \pm 0.12 |

Yongmanitchai & Ward (1991) found the highest biomass concentration (3.1 g L^{-1} DW) at low salinity for *P. tricornutum* UTEX 646 in a test tube setup and the biomass concentration decreased with an increase in salinity with the lowest reported biomass density

at 24 psu (2.8 g L⁻¹ DW). It has been reported that the highest EPA and fucoxanthin production was obtained at a salinity of 20 psu for UTEX 646 (Wang et al., 2018). For CS-29/7 the optimal salinity for maximum fucoxanthin yield (0.041 % ash free dry weight (AFDW)) was at 45 psu (Ishika et al., 2017).

As 33 psu resulted in the highest fucoxanthin, EPA and protein yields, further work was conducted to increase the yields.

4.4.5. Effect of carbon on biochemical composition

CO₂ can be supplied in either solid form (as carbonate or bicarbonate), in the gaseous form as CO₂ or an organic carbon form (e.g. glycerol). All three carbon sources were tested sequentially to determine if a further increase in biomass productivity and product yield could be obtained.

4.4.6. Effect of bicarbonate on biochemical composition

The presence of an efficient uptake system for CO₂ and bicarbonate (HCO₃⁻) has been identified in *P. tricornutum* (Burkhardt et al., 2001). *P. tricornutum* is known to assimilate bicarbonate and a 'chloroplast pump' facilitates as the main active transporter (Hopkinson et al., 2016b). When *P. tricornutum* was supplied with bicarbonate as an inorganic carbon source, between 73-99.99 % was consumed or remained dissolved in the medium (resulting in a CO₂ consumption rate of 2.3 g CO₂ g⁻¹ biomass but a reduction in growth and biomass production was observed (Piiparinen et al., 2018). Bicarbonate addition at 10 mM was observed to result in an increase in biomass by 12 % and a 10 % higher maximum growth rate (Seo et al., 2018).

In this study bicarbonate was tested in the concentration range of 5-125 mM and compared to the control (5 x f/2 NP) to see if bicarbonate resulted in an improvement in biomass and product yield. When sodium bicarbonate was >10 mM no growth was observed and the bicarbonate precipitated out of solution which was likely due the pH increase, as Tris at 20 mM did not provide sufficient buffering capacity (Appendix B).

Supplementation with 5- and 10-mM sodium bicarbonate resulted in a decrease in carbohydrate content (7.99 and 6.60 % DW respectively), a decrease in protein content (43.02 and 35.95 % DW respectively), decrease in fucoxanthin (1.27 and 1.09 % DW respectively) and a decrease in EPA content (2.29 and 2.24 % DW). However, an increase in FAEE content

was observed (8.00 and 11.52 % DW). The addition of bicarbonate (25 mM) to nitrate depleted *P. tricornutum* CCAP 1055/1 has been shown to induce TAG accumulation (nile red determination) without cell division arrest (Gardner et al., 2012). In the presence of 15 mM sodium bicarbonate an increase in lipid accumulation was also reported for CCAP 1055/1 (Mus et al., 2013), but no increase in EPA was observed in UTEX 646 and a decrease in growth was observed (Hamilton et al., 2015). *P. tricornutum* UTEX 646 cultivated in f/2 medium supplemented with 60 mM bicarbonate supplementation resulted in an increase in growth, protein content (up to a 3-fold increase), and TFA content, but there was no clear trend in EPA content compared to the control without bicarbonate addition (Nunez and Quigg, 2016). The differences reported in this study could have been because the cells were carbon limited and bicarbonate use improves significantly when cells are grown in air (Matsuda et al., 2001).

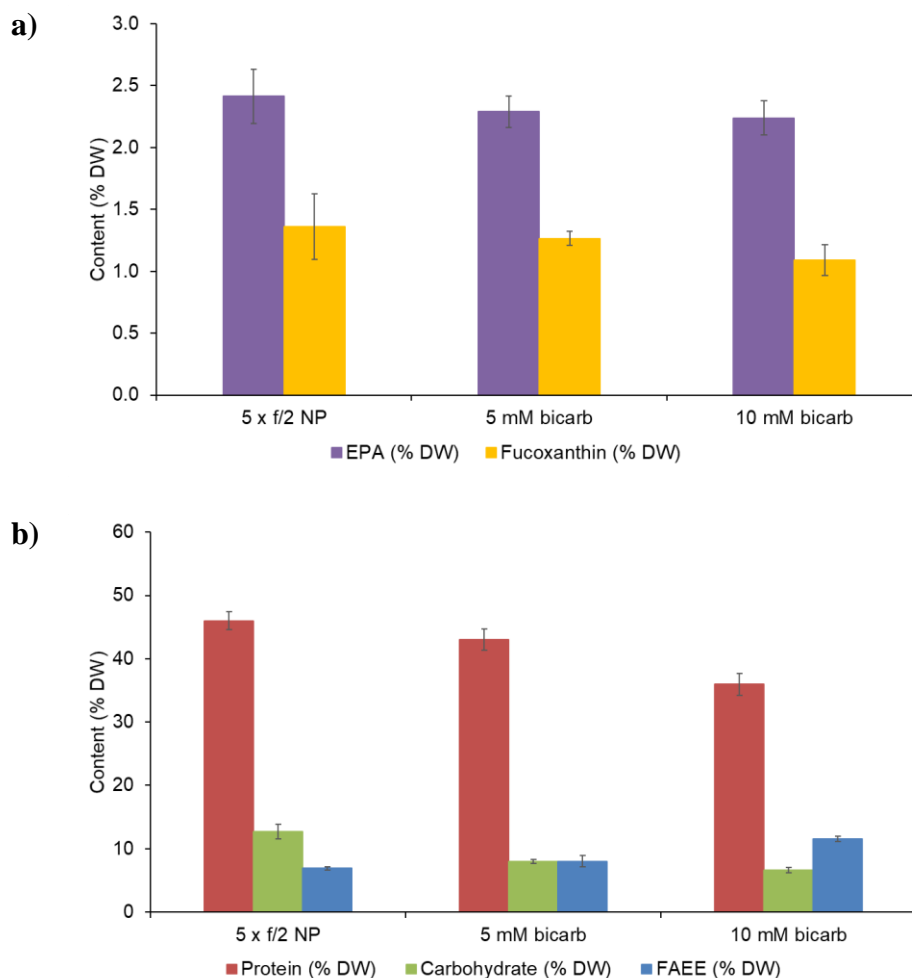


Figure 4.14 - Effect of bicarbonate (5 and 10 mM) on biochemical composition of *P. tricornutum*; a) EPA and fucoxanthin content and b) protein, carbohydrate and FAEE content.

Supplementation with 5- and 10-mM sodium bicarbonate resulted in a decrease in biomass concentration (0.44 and 0.33 g L⁻¹ respectively) compared to the 5 x f/2 NP control (0.52 g L⁻¹). A decrease in the carbohydrate, protein, fucoxanthin, FAEE and EPA productivity was observed with sodium bicarbonate.

Table 4.6 - The effect of bicarbonate (5 and 10 mM) on biomass concentration and volumetric productivity) and product yields

| | 5 x f/2 NP | 5 mM bicarb | 10 mM bicarb |
|--|--------------|--------------|--------------|
| Biomass concentration (g L ⁻¹) | 0.52 ± 0.04 | 0.44 ± 0.01 | 0.33 ± 0.02 |
| Biomass productivity (mg L ⁻¹ d ⁻¹) | 66.75 ± 4.73 | 54.85 ± 1.17 | 38.87 ± 3.18 |
| Carbohydrate (mg L ⁻¹ d ⁻¹) | 8.46 ± 0.92 | 4.39 ± 0.26 | 2.59 ± 0.36 |
| Protein (mg L ⁻¹ d ⁻¹) | 30.57 ± 1.28 | 23.61 ± 1.16 | 13.87 ± 0.59 |
| Fucoxanthin (mg L ⁻¹ d ⁻¹) | 0.91 ± 0.19 | 0.69 ± 0.02 | 0.42 ± 0.06 |
| FAEE (mg L ⁻¹ d ⁻¹) | 4.59 ± 0.31 | 4.41 ± 0.56 | 4.49 ± 0.44 |
| EPA (mg L ⁻¹ d ⁻¹) | 1.60 ± 0.11 | 1.26 ± 0.09 | 0.86 ± 0.05 |

As an optimal biomass productivity and product yields were obtained without sodium bicarbonate supplementation, it was omitted.

4.4.7. Effect of CO₂ concentration on biochemical composition

Carbon capture in *P. tricornutum* predominates in the form of bicarbonates and bicarbonate transporters (Hopkinson et al., 2016b). It has been found that the optimal CO₂ concentration for biomass accumulation is in a narrow range (1-1.25 % CO₂ in air (v/v), at a gas supply rate of 0.66 vvm, but 90 % of the CO₂ left the medium unused (Meiser et al., 2004). Several carbonic anhydrases have been described in *P. tricornutum* which participate in carbon capture to ensure sufficient partial pressure of CO₂ in the pyrenoid for CO₂ fixation by Rubisco (Hopkinson et al., 2016b). Plasma membrane-type aquaporins are known to function in CO₂ transport and provide photoprotection (Matsui et al., 2018). It has been found that CO₂ concentration does not have a significant impact on the cell concentration and fucoxanthin content (McClure et al., 2018).

The highest protein content (52.02 % DW) was obtained with 0.5 % CO₂ and an increase in CO₂ up to 2 % resulted in a decrease in protein, but with an apparent re-allocation to FAEE, EPA, and fucoxanthin (13.83, 3.37 and 1.42 % DW respectively). There seemed to be no significant decrease in carbohydrate content and no significant increase in fucoxanthin content with an increase in CO₂ concentration. In *P. tricornutum* CS-29, CO₂ concentration was not observed to have a significant impact on fucoxanthin (McClure et al., 2018).

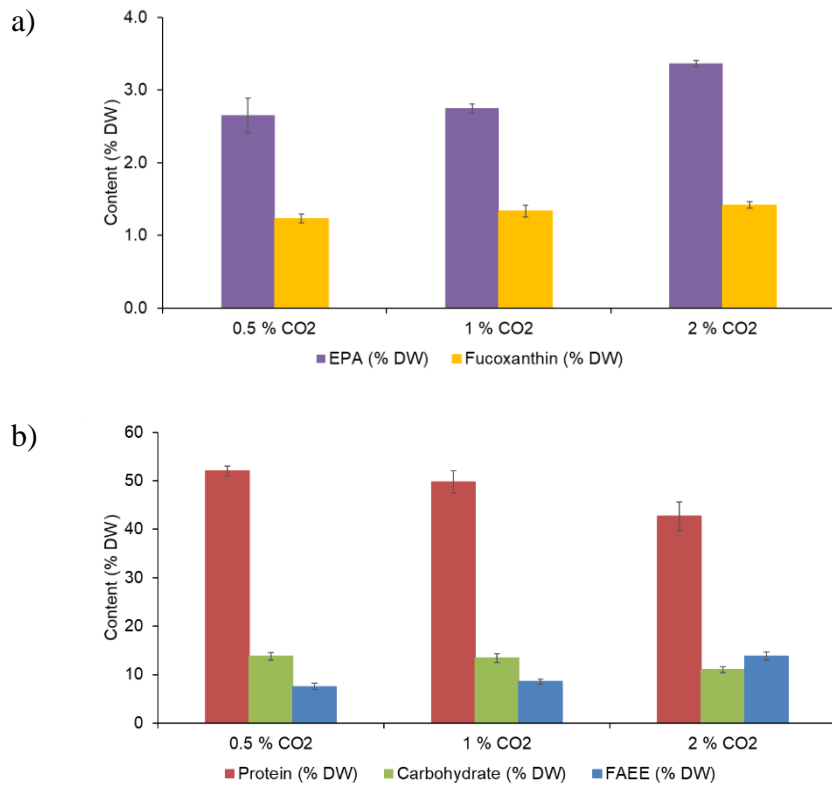


Figure 4.15 - Effect of CO₂ concentration (0.5, 1 and 2 %) on biochemical composition of *P. tricornutum*; a) EPA and fucoxanthin content and b) protein, carbohydrate and FAEE content.

A 5-fold increase in dry biomass concentration from 0.5 g L⁻¹ to 2.5 g L⁻¹ was observed when *P. tricornutum* UTEX 640 was cultivated for 7 days in Mann and Myers medium when CO₂ was increased from 0 to 1 % (Yongmanitchai and Ward, 1991). *P. tricornutum* (PHAE02) in modified f/2 seawater (enriched with four-fold nitrate and phosphate) with a supply of 15 % CO₂ resulted in an increased biomass productivity to 0.15 g L⁻¹ d⁻¹ (Negoro et al., 1991).

The highest biomass concentration and productivity (108.15 mg L⁻¹ d⁻¹) was obtained with 2 % CO₂. In *P. tricornutum* CS-29, 2 % CO₂ resulted in a decrease in biomass

concentration but this was because the culture was acidified (McClure et al., 2018). All biochemical components were increased with an increase in CO₂ to 2 % CO₂ with a final protein (46.24 mg L⁻¹ d⁻¹), carbohydrate (11.95 mg L⁻¹ d⁻¹), FAEE (15.00 mg L⁻¹ d⁻¹), fucoxanthin (1.42 mg L⁻¹ d⁻¹) and EPA yield (1.18 mg L⁻¹ d⁻¹) significantly higher than the control (0.5 % CO₂). Compared with 0.5 % CO₂, the biomass productivity was 1.8-fold higher with 2 % CO₂. An increase of >3-fold FAEE and >2.4-fold EPA was also observed. For UTEX 640 the highest EPA content was obtained at 5 % CO₂ but the highest EPA productivity (7.5-fold higher) was obtained at 1 % CO₂ and a dramatic decrease in culture pH was observed with CO₂ supplementation due to the absence of a buffer (Yongmanitchai and Ward, 1991).

Table 4.7 - The effect of CO₂ concentration (0.5, 1 and 2 %) on biomass concentration and volumetric productivity) and product yields

| | 0.5 % CO ₂ | 1 % CO ₂ | 2 % CO ₂ |
|--|-----------------------|---------------------|---------------------|
| Biomass concentration (g L ⁻¹) | 0.47 ± 0.01 | 0.59 ± 0.01 | 0.88 ± 0.02 |
| Biomass productivity (mg L ⁻¹ d ⁻¹) | 57.81 ± 1.52 | 73.39 ± 1.24 | 108.15 ± 2.47 |
| Carbohydrate (mg L ⁻¹ d ⁻¹) | 7.97 ± 0.57 | 9.85 ± 0.72 | 11.95 ± 0.76 |
| Protein (mg L ⁻¹ d ⁻¹) | 30.06 ± 0.72 | 36.53 ± 1.88 | 46.24 ± 3.92 |
| Fucoxanthin (mg L ⁻¹ d ⁻¹) | 1.23 ± 0.06 | 1.34 ± 0.08 | 1.42 ± 0.05 |
| FAEE (mg L ⁻¹ d ⁻¹) | 4.36 ± 1.53 | 6.48 ± 2.02 | 15.00 ± 3.64 |
| EPA (mg L ⁻¹ d ⁻¹) | 1.53 ± 0.10 | 2.02 ± 0.01 | 3.64 ± 0.09 |

As 2 % CO₂ supplementation resulted in a significant increase in biomass and product yields this concentration was selected for further improvement.

4.4.8. Effect of glycerol and 2 % CO₂ on biochemical composition

P. tricornutum is a successful photoautotroph but is also capable of mixotrophic growth under glucose, fructose, acetate and glycerol, with glycerol known to result in the highest biomass and EPA productivity compared with photoautotrophy (Cerón-García et al., 2013). Glycerol uptake has a lower requirement for photosynthetically derived ATP than other carbon sources (Droop, 1974). To date, mixotrophy has not been adopted for large-scale cultivation systems because of the technological barriers to maintain sterile conditions

(Matsumoto et al., 2017). Even though a high biomass and EPA productivity is obtained with glycerol, currently it is difficult to achieve a high biomass and fucoxanthin content simultaneously.

Glycerol at 0.1 M is the most commonly adopted concentration and has been reported in UTEX 640 to result in an increase in cell density tenfold compared to photoautotrophic production (Cerón García et al., 2000). Glycerol at 0.06 M has been used for CCAP 1055/1 and was found to result in an increase in cell density fourfold compared to the photoautotrophic control (Penhaul Smith et al., 2020). As low light is required for increasing fucoxanthin and EPA content, glycerol has the potential to overcome photolimitation. It has been suggested that glycerol has a similar effect to nitrogen limitation and leads to an increased synthesis of TAG (via the Kennedy pathway) and unsaturated fatty acids through conversion of existing glycolipids with a resultant increase in biomass without the loss of photosynthetic capacity in the cell (Villanova et al., 2017).

In this study the effect of glycerol under low light ($142 \mu\text{mol photons m}^{-2} \text{s}^{-1}$) and high CO_2 concentration was investigated which has not been conducted before to look at further improvements in biomass productivity and product yield.

The protein content was observed to be highest in the photoautotrophic control (5 x f/2 NP) medium (42.09 % DW) but decreased with an increase in glycerol to 28.60 % DW. The highest carbohydrate content was observed with 0.01 M glycerol (16.15 % DW) but was found to decrease with a further increase in glycerol concentration to a minimum of 10.02 % DW at 0.1 M glycerol. This is in contrast to Villanova et al. (2017) and Penhaul Smith et al., (2020) who found that glycerol increases carbon storage carbohydrates in CCAP 1055/3 (0.05 M glycerol) and CCAP 1055/1 (0.06 M glycerol) respectively. The FAEE content was found to increase from 12.63 % DW in 5 x f/2 NP medium to 18.05 % DW in 0.1 M glycerol. This is similar to that reported by Cerón García et al. (2000) and Villanova et al. (2017) who reported an increase in the synthesis of TAG in CCAP 1055/3 and UTEX 640 respectively.

The fucoxanthin content was highest without glycerol addition (1.07 % DW) and decreased with glycerol supplementation to 0.34 % DW at 0.1 M glycerol. Reduced photosynthetic activity has been reported in *P. tricornutum* (Liu et al., 2009) which could have an impact on the FCP complex. Penhaul Smith et al. (2020) also observed a decrease in carotenoid content at higher glycerol concentrations.

The EPA content was found to increase to 3.80 % DW with 0.01 M glycerol but a decrease in EPA content was observed with a further increase in glycerol concentration. In the literature (without CO_2 addition) it has been found that EPA content increases up to 2.38

% DW with 0.01 M glycerol supplementation (1.90 % DW with phototrophic cultivation) and then decreases in UTEX 640 (Cerón García et al., 2000). The TFA content has also been observed to increase from 7.24 % DW in phototrophic cultivation to 15.52 % DW with 0.1 M glycerol supplementation (Cerón García et al., 2000).

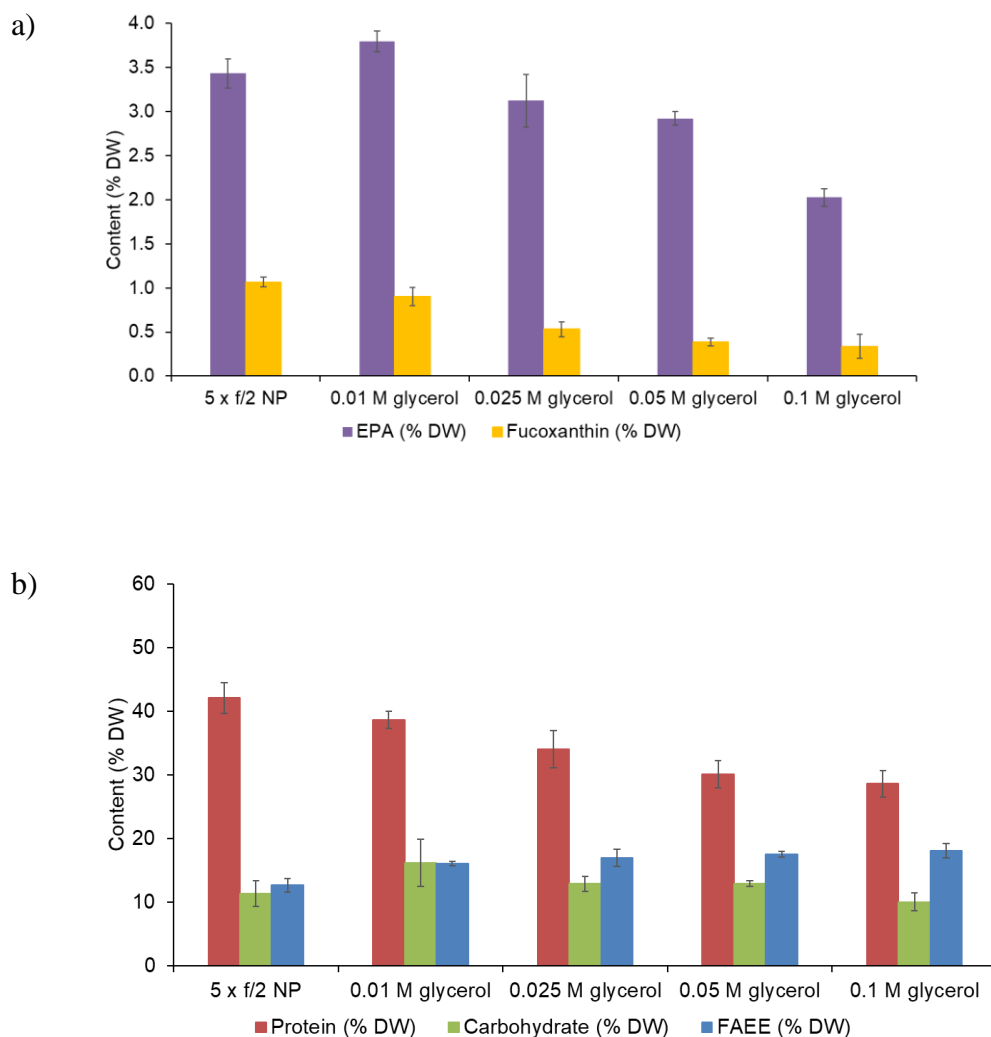


Figure 4.16 - Effect of glycerol (0.01-0.1 M) on biochemical composition of *P. tricornutum*; a) EPA and fucoxanthin content and b) protein, carbohydrate and FAEE content

The highest biomass concentration was observed with 0.05 M glycerol (1.53 g L^{-1}) which was 1.7-fold higher than phototrophic cultivation with 5 x f/2 NP. However, a further increase to 0.1 M glycerol resulted in a decrease in biomass concentration (1.22 g L^{-1}). Higher biomass concentrations of 3-25 g L^{-1} have been reported in the literature (Fernández Sevilla et al., 2004; Yang and Wei, 2020). However, often the cultivation time is long. Penhaul Smith et al. (2020a) obtained a biomass concentration of 1.13 g L^{-1} after 21 days with 0.1 M glycerol

in CCAP 1055/1. However, in the current study with 0.1 M glycerol we obtained 1.22 g L⁻¹ after only 7 days, which was likely because a higher light intensity, continuous light and CO₂ was supplied.

The highest carbohydrate (32.53 mg L⁻¹ d⁻¹), protein (76.9 mg L⁻¹ d⁻¹), fucoxanthin (1.78 mg L⁻¹ d⁻¹), and EPA productivity (7.54 mg L⁻¹ d⁻¹) was observed with supplementation of 0.01 M glycerol.

Table 4.8 - The effect of glycerol concentration (0.01-0.1 M) on biomass (concentration and volumetric productivity) and product yields

| | 5 x f/2 NP | 0.01 M glycerol | 0.025 M glycerol | 0.05 M glycerol | 0.1 M glycerol |
|--|---------------|-----------------|------------------|-----------------|----------------|
| Biomass concentration (g L ⁻¹) | 0.90 ± 0.05 | 1.40 ± 0.03 | 1.47 ± 0.02 | 1.53 ± 0.05 | 1.22 ± 0.01 |
| Biomass productivity (mg L ⁻¹ d ⁻¹) | 125.79 ± 6.81 | 198.52 ± 4.19 | 206.95 ± 3.60 | 216.87 ± 6.50 | 170.69 ± 1.10 |
| Carbohydrate (mg L ⁻¹ d ⁻¹) | 14.3 ± 2.80 | 32.3 ± 7.7 | 26.6 ± 2.40 | 28.0 ± 0.3 | 17.1 ± 2.4 |
| Protein (mg L ⁻¹ d ⁻¹) | 52.7 ± 2.50 | 76.9 ± 4.29 | 70.6 ± 7.07 | 65 ± 3.16 | 48.78 ± 3.23 |
| Fucoxanthin (mg L ⁻¹ d ⁻¹) | 1.35 ± 0.14 | 1.78 ± 0.17 | 1.10 ± 0.17 | 0.84 ± 0.11 | 0.57 ± 0.24 |
| FAEE (mg L ⁻¹ d ⁻¹) | 16.03 ± 2.15 | 31.92 ± 1.28 | 35.08 ± 2.30 | 37.83 ± 0.19 | 30.83 ± 2.07 |
| EPA (mg L ⁻¹ d ⁻¹) | 4.34 ± 0.43 | 7.54 ± 0.33 | 6.44 ± 0.50 | 6.33 ± 0.05 | 3.46 ± 0.16 |

P. tricornutum UTEX 640 cultivated mixotrophically with 0.1 M glycerol resulted in the highest biomass concentration (25.4 g L⁻¹), biomass productivity (1.7 g L⁻¹ d⁻¹) and EPA productivity (56 mg L⁻¹ d⁻¹) to date (Fernández Sevilla et al., 2004). In the literature 0.1 M seems to consistently result in a high biomass and EPA productivity (1.5 g L⁻¹ d⁻¹ and 40 mg L⁻¹ d⁻¹ respectively) under semi-continuous cultivation (Cerón-García et al., 2013) but there is a high risk of culture collapse from bacterial overgrowth (data not shown). The mechanisms of uptake and metabolism of glycerol are important areas for further study, along with controlling the bacterial population.

4.5. Conclusion

A high throughput flask screening approach was used to optimise product yields, particularly fucoxanthin and EPA using f/2 medium as a baseline in *P. tricornutum* CCAP 1055/1. To the authors knowledge this is the first time CCAP 1055/1 has been explored as a biorefinery chassis for high value (fucoxanthin and EPA) and commodity products (protein and carbohydrate). A culture medium consisting of nitrate and phosphate at 4.41 mM and 0.18 mM (5-fold those employed in the traditional f/2 medium), salinity at 33 %, 2 % CO₂ (v/v

in air), and a transition to mixotrophy using glycerol (0.01 M) were found to result in increased biomass, protein, fucoxanthin, EPA, and protein yields (up to 10-fold). To the authors knowledge this is the first study that has explored the effect of glycerol and CO₂ in combination towards a biorefinery approach with biomass rich in fucoxanthin and EPA.

Acknowledgements

TOB acknowledges financial assistance from UK-EPSRC (DTA 1912024). The authors would like to thank Duncan Schofield for his technical assistance in the CHNS analysis. The authors wish to thank Ms Heather Grievson for the ICP-OES analysis.

Author contributions

TOB conceived and wrote the paper with guidance from SV. All authors declare that they have read and agree with the manuscript.

Conflicts of interest

The authors declare no conflict of interest.

Chapter 5: The transition away from chemical flocculants: commercially viable harvesting of *Phaeodactylum tricornutum*

This chapter is published as:

Butler, T.O., Acurio, K., Mukherjee, J., Dangasuk, M.M., Corona, O. and Vaidyanathan, S., 2021. The transition away from chemical flocculants: Commercially viable harvesting of *Phaeodactylum tricornutum*. *Separation and Purification Technology*, 255, p.117733.

5.1. Abstract

Harvesting can contribute up to 15% of the total production cost for microalgal biomanufacturing. Using flocculants is potentially a cost-effective approach but there has been considerable debate on the efficacy, cost, toxicity to the cell and environment, and the effect on the biomass further downstream. In this study, a range of biobased flocculants (chitosan from crab shells, *Moringa oleifera* seed extract, pectin from bananas, tannic acid-based derivatives from *Acacia* tree bark and egg shell powder) were compared with traditional chemical flocculants (aluminium sulphate, iron chloride and sodium hydroxide) for harvesting the diatom *Phaeodactylum tricornutum*. It was concluded that Tanac's tannin based Tanfloc 8025 (SL range) was the most promising, requiring a low concentration (10.4 kg ton⁻¹ biomass), and low cost (\$27.04 ton⁻¹ microalgal biomass). The flocculant was effective over a wide pH (7.5-10.0) and temperature (15-28°C) range and harvesting (>85% efficiency) occurred in 10 mins, which resulted in a biomass concentration factor of ≥ 5.69 .

Keywords: microalgae; harvesting; biobased; bioflocculant, waste

5.2. Introduction

The microalga *Phaeodactylum tricornutum* is a model diatom that is known to accumulate a spectrum of marketable natural and engineered products (Butler et al., 2020). It is a commercially viable species for large-scale cultivation, and in outdoor mass culture systems, it has been shown to dominate and outcompete other microalgal species with a tolerance for high pH and an ability to grow under low light (Piiparinen et al., 2018; Remmers et al., 2018). *P. tricornutum* is typically cultivated in suspended culture, requiring cell harvest and extraction stages, which represent a target for increasing the cost competitiveness for the development of commercially viable manufacturing processes.

Harvesting alone can contribute up to 15% of the total microalgal production cost (Fasaei et al., 2018). Typically, less than 0.5 g L⁻¹ dry weight (DW) (0.05% solids) is obtained in open raceway ponds, with a higher order of cell density achieved in photobioreactors, and industrial fermenters (Pahl et al., 2013). For commercial viability, the harvesting technique must meet specific criteria: increase the solid content to 10-25% total dry matter, be time efficient (requiring less than 1 h), be of high efficacy (>80%), be cost effective, require a low energy input, leave behind little or no toxic residues, and not affect the quality of the biomass downstream (‘t Lam et al., 2017). Centrifugation (including conventional cream separators, disc stack-, bucket, and super-centrifuges) is the current option, industrially. However, centrifugation is energy intensive (1 KWh m⁻³) and can account for 20-25% of the cultivation costs (‘t Lam et al., 2017; Molina Grima et al., 2003). Using flocculation can result in an energy demand reduction from 13.8 to 1.34 MJ kg⁻¹ when compared to centrifugation (Hesse et al., 2017).

A wide variety of harvesting methods have been suggested for *P. tricornutum*. However, the most well researched area has focussed on flocculation with this method being scalable. Flocculants are well characterised and are effective through different modes; charge neutralisation (inorganic flocculants), sweeping, polymeric bridging (organic flocculants) and electrostatic patch mechanisms (Vandamme et al., 2010).

The concentrations of chemical flocculants required for flocculating marine microalgae are often five to ten-fold higher than for freshwater microalgae (Sukenik et al., 1988; Uduman et al., 2010). Metal salts (ionic) such as aluminium and iron chloride are the most commonly used flocculants for harvesting microalgae and are already applied commercially in breweries, drinking water supplies, mining, and wastewater treatment (Vandamme et al., 2013). However, these metals have been found to remain in microalgal biomass after lipid and carotenoid extraction and the residues can be toxic (Rwehumbiza et

al., 2012; Singh and Patidar, 2018). Consequently, an additional step is required further downstream to remove the flocculant from the biomass, incurring additional expense.

To date, many chemical flocculants have been tested (cationic, anionic, and non-ionic) for harvesting microalgae but there has been an inconsistency with the setup design, flocculant concentration used, the initial biomass density, optimal pH, and the sedimentation time for comparing commercially viable flocculants. In addition, few studies have addressed the impact on final product quality. The efficiency of a flocculant depends on several factors; including the species, strain, culture conditions, ionic environment, stirring rate, concentration of flocculant, pH, and temperature. Flocculant costs in excess of \$0.10 kg⁻¹ DW algae constrain commercial implementation and targets of \$0.04 kg⁻¹ are required (Rogers et al., 2014). In transitioning towards a sustainable circular economy there is a desire to use biobased flocculants. Biobased flocculation offers considerable potential as an environmentally friendly and potentially cost-effective approach. Chitosan (10 mg L⁻¹) has been observed to be the optimal flocculant tested to date (in terms of efficacy and time) for *P. tricornutum* (biomass density 0.2-0.5 g L⁻¹) resulting in a 100% harvesting efficiency after 15 mins at pH 8 (Lubián, 1989). However, the cost of harvesting (\$0.32 kg⁻¹ DW) is prohibitive for commercial harvesting applications. In this investigation, the use of sustainable biobased flocculants were explored which have shown promise in the literature: chitosan from crab shells (Şirin et al., 2012), eggshell powder (Choi, 2015), *Moringa oleifera* seed powder (Abdul Hamid et al., 2016), pectin from bananas (Kakoi et al., 2016), and two commercial *Acacia* tree bark tannin derived products from Tanac (Brazil); Tanfloc 6025 (SG range) and 8025 (SL range) (Roselet et al., 2015). Our focus was to identify the most effective natural or biobased harvesting solution that was commercially viable and environmentally sustainable.

5.3. Materials and methods

5.3.1 *Phaeodactylum tricornutum* culture and growth conditions

P. tricornutum CCAP 1055/1, obtained from the Culture Collection of Algae and Protozoa (CCAP) was cultivated in modified f/2 medium (Guillard, 1975) (elevated nitrate and phosphate: 4.41 mM nitrate and 0.17 mM phosphate) with 33 g L⁻¹ of artificial seawater (Instant Ocean, Aquarium Systems, US), in 5 L Duran bottles, in fed-batch mode to ensure nitrogen and phosphorus replete conditions. A continuous irradiance of ca. 240 µmol photons m⁻² s⁻¹ was used using 45 W red: blue (70:30) 225 LED (Excelvan) with the

cultivation at 21 °C (± 1 °C). The culture was aerated at 3 lpm (0.7 vvm) through a 0.22 μm air filter. The pH of the culture was observed to range from 9.16 to 10.15 over the cultivation period.

5.3.2 Inorganic and biobased flocculants

Unless mentioned otherwise, all chemicals were purchased from Sigma Aldrich, UK. The inorganic chemical flocculants tested as a baseline were iron chloride (Fisher Scientific, UK) and anhydrous aluminium sulphate (stock solution of 10 g L⁻¹). Low molecular weight chitosan (deacylated chitin) was dissolved in 1% acetic acid solution under constant magnetic stirring to form a 10 g L⁻¹ stock (pH approximately 4). In order to form a homogeneous clear solution, the mixture was stirred overnight. Three sources of pectin were used, two commercial sources, CU 201 (high methyl-esterified 70%) and 701 (low methyl-esterified 36%) (Herbstreith and Fox, Sweden) heated to 100°C and dissolved in deionised water, and a pectin extract from banana peels (locally sourced). The banana peels were dried at 60°C for 24 h and then coarsely ground and stored at room temperature prior to extraction of pectin. The pectin was extracted according to Emaga et al. (2008) with minor modification. The pectin was extracted with sulphuric acid (pH 2, 90°C for 1 h), the residue freeze dried using a CoolSafe freeze dryer (Labogene, Denmark) and then a stock solution equivalent of 10 g L⁻¹ was prepared in deionised water. Waste eggshells were prepared after boiling, according to Kothari et al. (2017) with minor modification. The fine powder formed was dissolved in 10 mL of 0.1 mol L⁻¹ of hydrochloric acid solution and the mixture was stirred for 30 mins to obtain a stock solution of 10 g L⁻¹. *Moringa oleifera* (Moringa) seeds were purchased from Herbalii, UK. The seeds were unshelled and mechanically ground as only the seed powder results in flocculation. The powder was sieved with a 600 μm mesh for homogeneity (Abdul Hamid et al., 2014) and used directly for the test. Tanfloc 6025 and 8025, two commercial quaternary ammonium polymers based on tannins extracted from the black wattle tree (*Acacia mearnsii*), were obtained from Tanac (Brazil) in a concentrated solution of 25% (w/w) and were diluted 100-fold with deionised water. These polymers were kindly provided by a distributor of the manufacturer, Lansdown Chemicals (OQEMA, UK).

5.3.3. Harvesting experimental setup

Before beginning the flocculation trials, the concentration of the microalgae suspension was always adjusted to 5×10^6 cells mL^{-1} ($\sim 0.07 \text{ g L}^{-1}$ DW) [determined using an Advanced Neubauer haemocytometer (BS-748, Hawksley) using a microscope (BX51, Olympus)]. Flocculation efficiency was evaluated in 500 mL glass columns (42 cm height with a 25 cm working height, 5.5 cm diameter, height/diameter ratio = 4.55) arranged as shown in Fig. 1. The cylinders were supported on a magnetic stirrer (RT10 Power, IKA, UK). To each glass cylinder, 500 mL of the culture (5×10^6 cells mL^{-1}) at pH 9.16-10.15 was aliquoted, different concentrations of flocculants were added as detailed below, and stirred at 1000 rpm for 10 mins for uniform flocculant dispersal. Preliminary experimentation showed that there was no effect of centrifugation and re-suspension in the fresh medium compared with the cultivated biomass (data not shown). The pH was then adjusted to pH 7.5 and pH 9.0 with 1 M of HCl or 100% CO_2 and the culture was mixed for 15 mins at 250 rpm to allow floc formation. The pH was monitored using a pH meter (FE20 FiveEasy, Mettler Toledo). After mixing, the microalgae suspension settling time was monitored every 10 mins over a 60 min time period, with a 1 mL aliquot drawn 5 cm from the top layer of the suspension in the glass column, and the optical density at 750 nm measured by spectrophotometry (SPECTROstar Nano, BMG Labtech, Germany). The harvesting efficiency was calculated from the difference in optical density (OD at 750 nm) between the *P. tricornutum* suspension at the start of the harvesting experiment (t_0) and that after a defined settling time (t_t), a commonly utilised method (Şirin et al., 2012; Vandamme et al., 2018):

$$\text{Harvesting efficiency (\%)} = \frac{OD_{750t_0} - OD_{750t_t}}{OD_{750t_0}} * 100$$

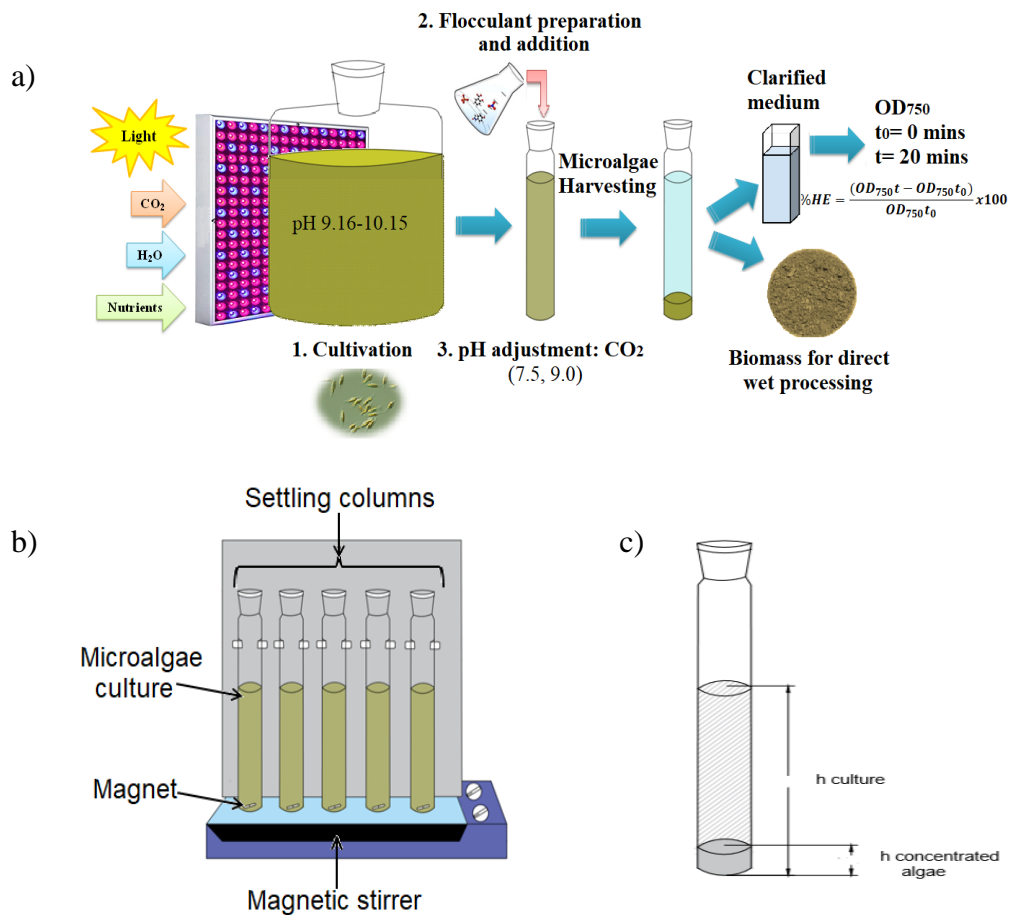


Fig. 5.17. Harvesting experimental setup: a) the experimental workflow, b) Settling column arrangement with 500 ml algal culture and c) concentration factor determination. The cells were cultivated under red: blue light in 5 L Duran bottles, 500 ml was diluted to the required cell density (5×10^6 cells mL⁻¹), the flocculant added, pH adjusted and the samples were withdrawn 5 cm from below the liquid meniscus at ~20 cm height from the bottom of the column.

5.3.4. Flocculation and sedimentation experiments

Sodium hydroxide, calcium oxide, and calcium hydroxide (Sigma Aldrich, UK) were tested for alkaline flocculation. To standardise the dosage of base, the pH of the culture medium was adjusted to pH 6.5 with 1 M HCl and a 1 M stock of the base was used to increase the pH to 10.5. The effect of autoflocculation was explored without the addition of any flocculant to the starting culture (pH 9.16 to 10.15) to determine if high pH alone was responsible for flocculation.

The zeta potential was measured using a phase amplitude light-scattering (PALS) zeta potential analyser (BrookHaven ZetaPALS, UK). The electrode was initially equilibrated to the new medium for 10 mins. Microalgae cultures with sodium hydroxide were centrifuged at 6000 rpm for 5 mins to obtain the mother liquor, and a 50-fold dilution was conducted on the original culture in this mother liquor as recommended by the manufacturer. The Smoluchowski model was applied as the solution was non-aqueous. Measurements were conducted using an electric field of 2.5 V/cm at a frequency of 2.0 Hz. The reported values represent the average of five successive runs of 20 cycles each, using the ZetaPALS. Three replicates of each treatment were used in the analysis.

For the flocculant screening trials, aluminium sulphate and iron chloride (chemical flocculants) and Moringa seeds, eggshell, chitosan, Tanfloc's 8025 and 6025 (bio-based flocculants) were evaluated at 100, 50 and 20 mg L⁻¹. Tests were conducted without the addition of a flocculant to determine if 100% CO₂ could replace 1 M HCl for lowering the pH. As CO₂ did not induce flocculation, the pH value was reduced to pH 7.5 and 9.0 using 100% CO₂ as a more environmental and cost-effective approach. All the tests were performed in triplicates with biomass at different time points of cultivation except the control (nine biological replicates were examined as the pH was highly variable from 9.16 to 10.5).

5.3.5. Effect of flocculant dosage, flocculation time, flocculation temperature, and biomass concentration on flocculation efficiency

Iron chloride was compared to Tanfloc 6025 and 8025 at 5 mg L⁻¹ and the harvesting efficiency was recorded after 10 and 20 mins. To evaluate the performance and behavior of Tanfloc 6025 and Tanfloc 8025 the concentration of the selected bio-flocculant was tested at 100, 50, 20 and 5 mg L⁻¹ over a more rigorous pH range (pH 7.5, 8.0, 8.5, 9.0, 9.5, and 10.0) and a 2D response surface interaction was conducted (Hesse et al., 2017).

The effect of temperature during the harvesting process was studied as this will be applicable when operating in an industrial location. Three different temperatures were tested 15 °C [optimal for eicosapentaenoic acid (EPA) content], 21°C (optimal for biomass and EPA productivity), and 28 °C (upper thermal tolerance for *P. tricornutum* CCAP 1055/1). Those temperatures were chosen between the ranges at which microalgae physiology is not affected and all cells remained viable. Temperature was fixed in the incubator and the tests were conducted after thermal equilibrium was achieved between the culture and the environment.

Different initial cell concentrations were tested by diluting with Instant Ocean Sea Salts (33 g L⁻¹) or concentrating the sample by centrifugation (Sorvall, Thermo Scientific) as required. The concentrations tested were 1, 2, 5, 10, 20 and 40 (x 10⁶) cells mL⁻¹. Dry weights were determined using a speedvac centrifugal freeze dryer (ScanVac Coolsafe 110-4).

The concentration factor (CF) is a parameter which provides information about the residual water content of the particulate phase. The CF is the ratio of final product concentration to the initial concentration (Şirin et al., 2012). The height of the examined microalgal culture ($h_{culture}$) and the final height of the concentrated algae ($h_{conc. algae}$) was used to determine the CF. The CF was calculated after 10 mins as in Şirin et al. (2012).

5.3.6. Effect of flocculants on fatty acid methyl ester (FAME) composition using a wet processing method

For the effect on fatty acid methyl ester (FAME) composition, aliquots of 5 mL of algal culture were harvested by centrifugation at 4000 rpm for 10 mins, the pellets washed with 0.01 M phosphate buffered saline (PBS) and transferred to 2 mL Eppendorf safe-lock tubes, centrifuged at 13,000 rpm for 5 mins and stored at -20°C for analysis. Flocculants which resulted in >80% harvesting efficiency at their lowest respective dose [aluminium sulphate, iron chloride, Tanfloc 6025 and Tanfloc 8025 at 20 mg L⁻¹ and sodium hydroxide at 264 mg L⁻¹ (6.6 mM)] were compared to the control (no flocculant addition). For comparative dry weight calculations, the samples were then freeze dried using a CoolSafe freeze dryer (Labogene, Denmark). These pellets were weighted using a 5 d.p. balance for subsequent data analysis (Sartorius, UK). A modified version of Kapoore (2014) was used for FAME analysis using direct transesterification on the wet biomass with methanolic-HCl (7%) replacing BF₃ as the acid catalyst.

5.3.7. FTIR analysis of Tanfloc 6025 and 8025

Fourier transformation infrared spectroscopy (FTIR) of both Tanfloc 6025 and 8025 flocculants was conducted using an IR Prestige-21 Fourier Transformation Infrared Spectrophotometer (Shimadzu, UK). Samples were dried on a diamond Attenuated Total Reflectance (ATR) apparatus (Pike Technologies, USA) separately attached to the FTIR. A blank spectrum was run as a background using the ATR without the samples and the baseline shift of the spectra was corrected using the IR solution software provided with the Shimadzu FTIR instrument. Two replicates for each sample were analysed. At least 64 scans, with resolution of 4 cm^{-1} using the Happ-Genzel apodization function were collected for all samples. Spectral processing was carried out using the IR solution software, including correction for carbon dioxide, atmospheric water vapour, and baseline correction. A second derivative of the spectra was conducted, and the spectra were overlaid to identify the differences and putatively identify the chemical origins of the regions showing difference.

5.4.1. Statistical analysis

Each treatment was performed in triplicate except for the control culture without pH control ($n=9$), and the mean and standard error of the dependent variable (harvesting efficiency) are presented in the results. Statistical analysis of the experimental data was conducted using SPSS statistical software (SPSS Statistics 26, IBM). The data was tested for normality using a Kolmogorov-Smirnov test and if these data were normally distributed ($P>0.05$) they were subsequently tested for equal variance using Levene's test. If variances were considered equal, then a one-way/two-way ANOVA or MANOVA and a *post-hoc* Tukey's test was utilised to understand where the differences were. If samples were not normally distributed ($P<0.05$) then a Kruskal-Wallis and *post-hoc* Dunn's non-parametric comparison was undertaken to understand the changes. The statistical difference of each set of experiments was studied with the analysis of the P value. In addition, this value was used to select parameters that were significant.

5.4. Results and Discussion

5.4.1. Autoflocculation and alkaline flocculation

The concept of autoflocculation was first devised by Golueke and Oswald (1970) and was understood to occur at high pH due to CO_2 depletion. In later years autoflocculation was determined to be induced by chemical coprecipitation with magnesium and calcium salts in

the culture medium (Shelef et al., 1984). Autoflocculation can also be induced by increased extrapolymeric substance (EPS) production which can neutralise cell surface charge (increasing illumination/temperature/dissolved oxygen/CO₂ or through nutrient deficiency or darkness) and also through increased cell density (ageing of microalgal culture) (González-López et al., 2013; Şirin et al., 2012).

Alkaline flocculation (sometimes incorrectly termed autoflocculation) is another method to induce flocculation. Flocculation for *P. tricornutum* CCAP 1055/1 commences at pH 10 and reaches 90% harvesting efficiency at pH 10.5 when magnesium and calcium are present in the medium, but in the absence of these elements no flocculation occurs (Vandamme et al., 2015b). The harvesting efficiency remains effective up to pH 12 (Vandamme et al., 2015b) but a decrease in photochemical efficiency is observed and the culture becomes lighter brown in colour (Spilling et al., 2011). It has been revealed that 3 mM sodium hydroxide at pH 10.6 resulted in 91% harvesting efficiency in *P. tricornutum* CCAP 1055/1 (Vandamme et al., 2018). However, in an earlier report with the same strain, 4 mM of sodium hydroxide (pH 10.3) was reported to be necessary to maximise harvesting efficiency (71%). However, this resulted in a white sludge with a magnesium content of 5% and a mineral content greater than 10%, requiring hydrochloric acid addition to remove the magnesium from the biomass (Vandamme et al., 2015a), as this is above the recommended level (<10%) for food and feed applications.

In the current investigation, the objective was to determine if autoflocculation was possible without the addition of petrochemically derived chemicals. We altered environmental factors, including flocculation in the dark, high temperature (up to 45°C) and high light (250-1000 $\mu\text{mol photons m}^{-2} \text{ s}^{-1}$), all of which resulted in poor harvesting efficiencies after 1 h (<13%) (data not shown). By manipulating pH it was observed that the culture pH alone (even in the alkaline region), at 9.16-10.15, at different time points during the fed-batch experiments, did not result in 'auto'flocculation even after 1 h (Fig. 2a). However, when the culture pH was reduced to pH 6.5, and sodium hydroxide added to adjust the pH back to the alkaline range, a critical concentration of sodium hydroxide (>5.4 mM-6.6 mM) was required for flocculation (Fig. 2b), suggesting that pH in itself (pH 9.5 – 10) is not sufficient for flocculation. It was further validated through zeta potential analysis that at higher concentrations of sodium hydroxide (>5.4 mM), the zeta potential increased, indicating charge neutralisation of the cells (Fig. 2b). As observed by Vandamme et al. (2015a), the formation of a white precipitate was observed when flocculation occurred (6.6 mM) (Fig. 2b). As autoflocculation could not be induced without chemical addition, and a white sludge was

formed, requiring the addition of hydrochloric/nitric acid for deflocculation, a series of biobased flocculants were explored for more natural flocculation methods.

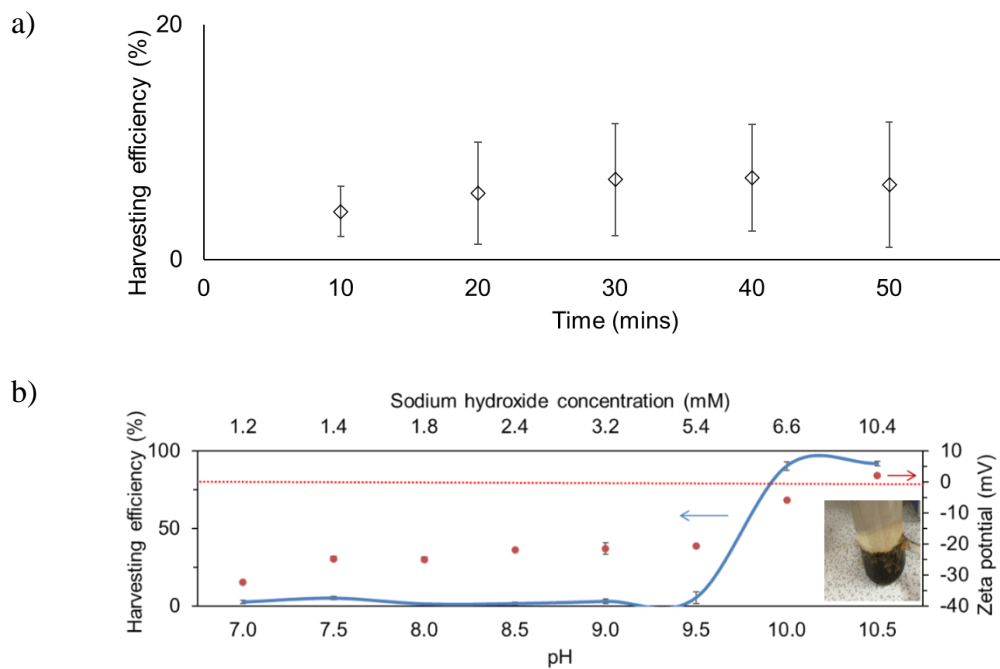


Fig. 5.18 - Autoflocculation and alkaline flocculation: a) autoflocculation with culture obtained directly without pH adjustment (pH of the culture ranged from 9.16 to 10.15) (n=9) from 10 mins to 1 h and b) the effect of sodium hydroxide concentration and pH (starting pH 6.5) on harvesting efficiency and zeta potential after 20 mins (n = 3)

5.4.2 Bio-based flocculation

As autoflocculation was not observed to be effective without the addition of sodium hydroxide, and to avoid chemical addition, a series of non-toxic biobased flocculants (pectin, Moringa seeds, eggshell powder, chitosan, Tanfloc 6025 and Tanfloc 8025) were examined to evaluate their flocculation ability and their performance compared with that of the conventional chemical flocculants (aluminium sulphate and iron chloride) at two pH conditions (7.5 and 9.0).

Typically, pH 7.0 to 8.5 has been used for flocculation studies for *P. tricornutum* (Lam et al., 2014; Schlesinger et al., 2012). As sodium hydroxide was revealed to induce flocculation at 5.4-6.6 mM and given the cultures were already at a high pH (pH 9.16-10.15) the culture pH had to be reduced to accommodate the addition of sufficient sodium hydroxide. This was achieved with 1 M HCl (up to 1.5 mM required to attain pH 7.5) or by sparging the culture medium with 100% CO₂. Either approach for pH reduction did not affect the

harvesting efficiency compared to the control (Fig. 3a) and CO₂ offers an environmentally favourable method with reduced cost.

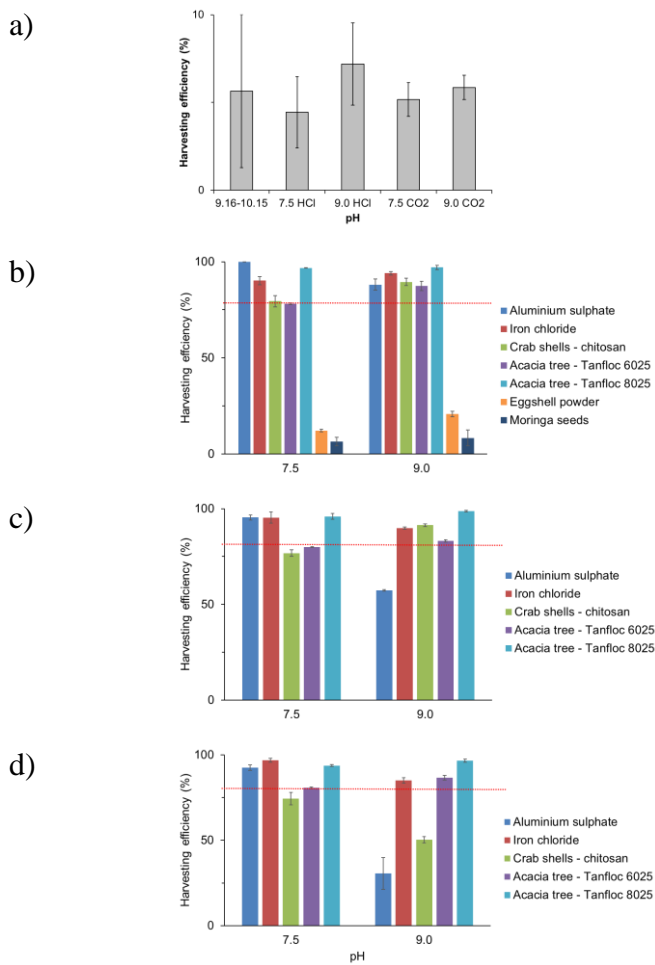


Fig. 5.19. Chemical and bio-based flocculation: a) Effect of adding hydrochloric acid compared with 100% CO₂ for pH reduction with harvesting efficiency reported after 20 mins, b) Performance of bio-based flocculants (chitosan, calcium carbonate from eggshells, Moringa seeds and Tanfloc products from *Acacia* tree bark) compared with conventional chemical-based flocculants (aluminium sulphate and iron chloride) at 100 mg L⁻¹ after 20 mins of flocculation (n= 3 replicates). Effects of lowering the flocculant dosage for the most effective flocculants are shown in c) 50 mg L⁻¹ and d) 20 mg L⁻¹. Red dotted line shows 80% harvesting efficiency.

To date, various chemical flocculants (hydroxides, aluminium sulphate and ammonium chloride), bioflocculants (chitosan, poly-gamma-glutamic acid and cationic starch), and synthetic polymers (e.g. Zetag) have been investigated for harvesting *P. tricornutum* (‘t Lam et al., 2014; Schlesinger et al., 2012; Şirin et al., 2012; Vandamme et al., 2010; Zheng et al., 2012). Typically a biomass concentration of 0.15-0.50 g L⁻¹ DW is used for flocculation studies (Vandamme et al., 2015a, 2010) and the biomass concentration used can have important implications for the dosage of flocculant to be effective, as dosage often

increases with biomass concentration (Vandamme et al., 2010). The minimum concentration of flocculant found to result in >90% harvesting efficiency for *P. tricornutum* was 10 mg L⁻¹ chitosan at pH 8 (100% harvesting efficiency) (Lubián, 1989). For chemical flocculation, the lowest concentration of flocculant tested for harvesting *P. tricornutum* was 25.7 mg L⁻¹ aluminium sulphate which resulted in 94% harvesting efficiency at pH 7 (Vandamme et al., 2018). The concentration of chemical flocculant in the literature has varied considerably up to a maximum of 270 mg L⁻¹ using aluminium sulphate (Şirin et al., 2012). In this study, an intermediate value of 100 mg L⁻¹ was selected to observe if there were any differences at pH 7.5 and 9.0 and this was reduced further (50 and 20 mg L⁻¹) to observe the combined impact of flocculant dosage and pH on the harvesting efficiency of *P. tricornutum*. To date, no data exists on harvesting efficiency using the chemical flocculant iron chloride for harvesting *P. tricornutum*.

Aluminium sulphate was found to be the most effective flocculant at pH 7.5 (>92% harvesting efficiency) at all three concentrations tested, but in all cases the flocculation efficacy decreased at pH 9.0 (30-88% harvesting efficiency) (Fig. 3b-d). In alkaline conditions, monomeric hydroxoaluminium anions dominate the solution and reduce the absorption capacity of microalgal cells and it has been reported that sweeping and enmeshment is responsible for sedimentation (Barros et al., 2015).

Iron chloride was found to operate effectively at pH 7.5 with >90% harvesting efficiency. Iron chloride was equally effective at pH 7.5 and 9.0 at 100 mg L⁻¹ (90-94% harvesting efficiency), but at 50 and 20 mg L⁻¹, the harvesting efficiency was found to decrease at the higher pH (Fig. 3c-d). There was no statistically significant difference between iron chloride and aluminium sulphate at pH 7.5 at the tested concentrations. However, the difference in performance between the two chemical flocculants became apparent at pH 9.0 at reduced concentrations (50 and 20 mg L⁻¹), where iron chloride had a significantly greater harvesting efficiency than aluminium sulphate (ANOVA and *post hoc* Tukey's test, $F = 85.73$, $P < 0.01$, $df = 1$) and was revealed to be suitable as a non-toxic chemical replacement.

In terms of the bio-based flocculants, pectin has not been tested for harvesting microalgae, Moringa seeds and eggshell powder have not been tested on marine microalgae, and tannin based flocculants have only been tested for freshwater microalgae and *Nannochloropsis oculata* in seawater (Roselet et al., 2015). Preliminary experimentation with pectin resulted in no significant difference in harvesting efficiency compared to the control without flocculant addition over both pH ranges (data not shown). Moringa seeds and eggshell powder were ineffective at pH 7.5 and 9.0 (<22% harvesting efficiency) (Fig. 3b). The high

ionic strength of the medium due to the salinity may have caused coiling of the flocculants (Roselet et al., 2015). Moringa seed derivatives and eggshell powder are both natural polymers. Moringa seeds contain an active biocoagulating agent (dimeric protein) with a peptide of 6-20 kDa (Abdul Hamid et al., 2014). The presence of positively charged amino acids causes charge neutralisation through adsorption but it also acts through interparticle bridging (Sapana et al., 2012). For Moringa seeds it is the tertiary protein extract powder (29% protein by weight) and the primary seed powder which are responsible for flocculation (Abdul Hamid et al., 2016; Kandasamy et al., 2018) due to their cationic charges (Sapana et al., 2012). Eggshell has a high cationic charge density and is known to act by sweeping and charge neutralisation due to the presence of divalent cations of calcium and magnesium (Choi, 2015). Eggshells are about 95 % calcium carbonate and the remainder is 5 % calcium phosphate (Kothari et al., 2017). As these flocculants were not effective for *P. tricornutum* in this study they were not used for further experimentation at the lower flocculant dosages.

Chitosan was more effective at pH 9.0 at 100 and 50 mg L⁻¹ (Fig. 3b; c). A reduction in chitosan concentration from 100 to 20 mg L⁻¹ at all pH values tested resulted in a decrease in harvesting efficiency (Fig. 3a-c). Chitosan is proposed to act through a sweeping mechanism induced by the precipitation of the chitosan polymers (Blockx et al., 2018). Other studies have reported that chitosan acts through a combination of charge neutralisation (cationic polymer) and by bridging (Şirin et al., 2012).

Tanfloc 6025 was found to work more effectively at pH 9.0 at all the concentrations tested. The highest harvesting efficiency was attained at pH 9.0 at 20 mg L⁻¹ (82%), but this was not statistically significant compared with 100 and 50 mg L⁻¹. It could be observed that Tanfloc 8025 resulted in a harvesting efficiency >93% at all concentrations tested (100, 50, and 20 mg L⁻¹), at both pH values (pH 7.5 and pH 9.0), and was determined to be the most viable bio-based flocculant screened in this study. Roselet et al. (2016a) reported that the performance of Tanfloc is reduced in saline environments (30‰ salinity) compared to brackish water (10‰ salinity) when applied at 1-10 mg L⁻¹. However, in the current study in a saline medium (33‰ salinity) Tanfloc 8025 was effective, but this could be because the medium we used differed in ionic composition and higher concentrations of flocculant were used (20-100 mg L⁻¹). It was interesting to note that Tanfloc 6025 was not as effective as 8025. The effectiveness of the Tanfloc based products has been attributed to their branched phenolic structure compared with other polysaccharides such as starch (Roselet et al., 2016b). It has been found that Tanfloc POP (>80 mg L⁻¹) resulted in a harvesting efficiency of >80% with a pH range of 7 to 10 (Cassini et al., 2017). Similar results (>90% harvesting efficiency)

were obtained using a modified tannin coagulant (Q-TN) at 5 mg L⁻¹ for *Microcystis aeruginosa* cultivated in BG-11 medium at pH 7 to 8 but at pH 9 the efficacy decreased (Wang et al., 2013). It has been reported that as the Tanfloc concentration increases (69 to 100 mg L⁻¹), the excess cationic charges may destabilise the system and reduce the harvesting efficiency (Roselet et al., 2016b). However, in the current study Tanfloc performed well at 20-100 mg L⁻¹. It is interesting that differences were observed between the two Tanfloc products in the current study for harvesting *P. tricornutum*, as Roselet et al. (2015) reported that there was no significant difference in the performance of four tannic acid-based products (SG 1500, POP, SG and SL) for harvesting *Nannochloropsis oculata* at ≥ 15 mg L⁻¹. It is possible that there is a difference in charge density which accounts for the better performance of Tanfloc 8025.

It was concluded that Tanfloc 8025 is an effective biobased flocculant for *P. tricornutum* requiring no additional inorganic chemicals, such as sodium hydroxide. At pH 9.0 it was the most effective flocculant and at pH 7.5 the harvesting efficiency was similar to aluminium sulphate and iron chloride. In addition, for downstream processing of wet biomass no change in cell morphology, photosynthetic activity (data not shown) or fatty acid composition was observed (Fig. 4) compared with the control (no flocculant addition).

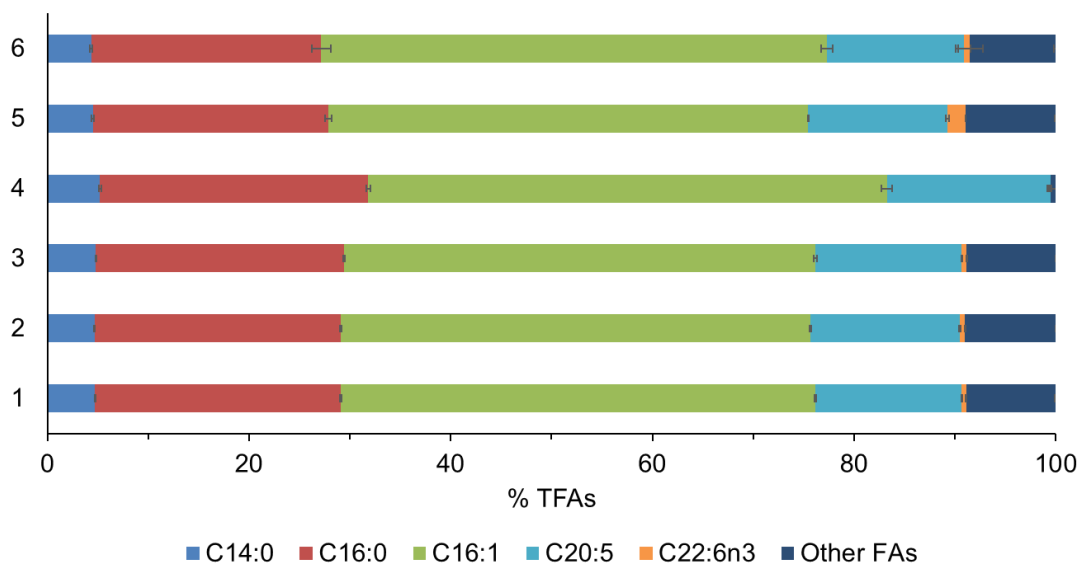


Fig. 5.20. Fatty acid profile of *Phaeodactylum tricornutum* for each treatment (% of total fatty acids). (1) Control - no flocculant addition; (2) aluminium sulphate; (3) iron chloride; (4) sodium hydroxide; (5) Tanfloc 6015 and (6) Tanfloc 8025. Each flocculant (aluminium sulphate, iron chloride, Tanfloc 6025 and Tanfloc 8025) was applied at 20 mg L⁻¹ and sodium hydroxide was added at 264 mg L⁻¹ (6.6 mM) compared to the control (no flocculant addition)

5.4.3. Effect of lowering Tanfloc dosage and flocculation time

In the current study, the ability of Tanfloc 8025 and Tanfloc 6025 to flocculate *P. tricornutum* at a reduced concentration of 5 mg L⁻¹ and in a shorter time period (10 mins) compared with iron chloride was investigated. At pH 7.5 and 9.0, Tanfloc 8025 performed the best and Tanfloc 6025 outperformed iron chloride at pH 9.0. At 20 mg L⁻¹, with Tanfloc 8025, the harvesting efficiency at pH 7.5 was 94% and at pH 9.0 it reached almost 97% (Fig. 5a). When the concentration of Tanfloc 8025 was reduced to 5 mg L⁻¹ the harvesting efficiency was observed to decrease to 83-86%. However, reducing the sedimentation time to 10 mins did not result in a further significant decrease ($P>0.05$). At 5 mg L⁻¹, Tanfloc 8025 performed better at both pH values than Tanfloc 6025 (55-61% harvesting efficiency). Roselet et al. (2015) also found at reduced concentrations (1.66-5 mg L⁻¹) of Tanfloc that the SL range (Tanfloc 8025) was a more effective flocculant for harvesting *N. oculata* and *C. vulgaris*. Here, it was found that Tanfloc 8025 performed equally well at pH 7.5 and 9 with >82% harvesting efficiency and there was no statistically significant difference ($P>0.05$).

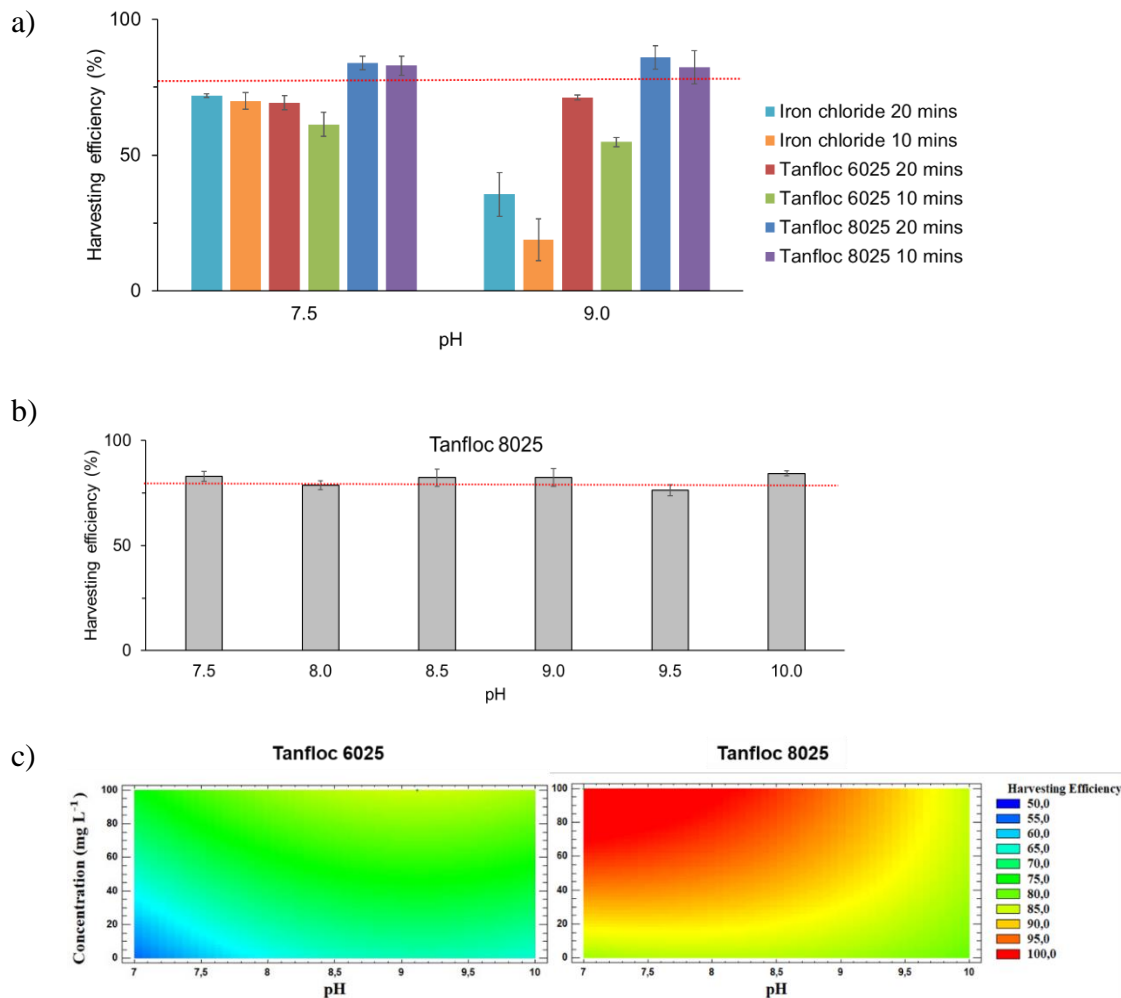


Fig. 5.21. Performance of reduced dosages of Tanfloc: a) effect of reducing the flocculant dosage of iron chloride and Tanfloc 6025 and 8025 to 5 mg L⁻¹ at pH 7.5 and 9.0 and the effect of sedimentation after 10 mins compared with 20 mins, b) performance of Tanfloc 8025 over a wider pH range and c) response surface methodology 2D plot of harvesting efficiency represented by colour after 10 mins for flocculant concentration (100, 50, 20 and 5 mg L⁻¹) and pH (7.5, 8, 8.5, 9, 9.5, and 10) for Tanfloc 6025 compared with Tanfloc 8025. Red dotted line indicates 80% harvesting efficiency

To confirm the ability of Tanfloc 8025 to operate effectively over a wide pH range a more detailed pH range (7.5 to 10.0 at 0.5 increments) was investigated (Fig. 5b). There was no statistically significant difference in the harvesting efficiency over the pH range investigated and an average harvesting efficiency of $81.18\% \pm 3.55$ S.E. was attained ($P > 0.05$). From the 2D response surface graphs it could be observed that Tanfloc 6025 generally performed better at a higher pH (pH 10.0) and concentration (100 mg L⁻¹) (Fig. 5c) but Tanfloc 8025 was found to perform well at all pH values and concentrations (>76% harvesting efficiency) (Fig. 5b; c). At a higher pH of 9.0, Roselet et al. (2017) found that an increased dosage (70 mg L⁻¹) was required for both *Chlorella vulgaris* and *Nannochloropsis oculata* for a harvesting efficiency >90%. The reduced effectiveness at higher pH has been

attributable to the denaturation of the molecule at an alkaline pH (Sánchez-Martín et al., 2009) and could be related to differences in the protonation of the amine group, the macromolecular chain and the structure of the flocs (Selesu et al., 2016). At pH 8.0 and 9.0 Tanfloc had little cationic charge and the mechanism of action was most likely enmeshment (sweep coagulation) in Tanfloc precipitates (Graham et al., 2008).

The minimum concentration of Tanfloc SL (8025) required is reported in the literature to range from 1.66 mg L⁻¹ to 5 mg L⁻¹ which resulted in 94-97% harvesting efficiency for *Nannochloropsis oculata* and 90-100% harvesting efficiency for *Chlorella vulgaris* at pH 8.0 after 30 mins (Roselet et al., 2015). In the current study, reducing the concentration of flocculant to 5 mg L⁻¹ resulted in a decrease in harvesting efficiency compared with 20 mg L⁻¹ for *P. tricornutum*, but still a harvesting efficiency of 81% on average could be obtained over a wide range of pH values and in only 10 mins. It is notable that this is the lowest concentration of flocculant tested in the literature for *P. tricornutum*. One possible reason the lower dosage of Tanfloc 8025 at 5 mg L⁻¹ did not result in ≥94% harvesting efficiency could have been because algal organic matter (AOM) was present. High doses of Tanfloc (60 mg L⁻¹) can be necessary to achieve a harvesting efficiency (>90%) in the presence of AOM, and the organic matter is known to interact with cationic polymers (Henderson et al., 2007; Roselet et al., 2016b). Alternatively, even though the stirring speed used in this study may have been sufficient to disperse the flocculant evenly amongst the cells, the floc formation time may need to be extended for optimal floc formation and altering the mixing conditions would be useful to investigate.

5.4.4. Surface functional groups of Tanfloc

Tanfloc 8025 was observed to outperform Tanfloc 6025 at the pH range investigated (pH 7.5-10.0). An FTIR analysis was undertaken to determine why this may have been the case. The second derivative was applied to the raw FTIR spectra, recorded between 850 and 3800 wavenumbers, to bring out minute differences of the *Acacia* tree extracts of Tanfloc 6025 and Tanfloc 8025 (Fig. 6). Notable differences in the spectral regions include at 1020-1030 cm⁻¹ (C-O stretching of ether group), 1280-1290 cm⁻¹ (C-O stretching, O-H deformations), 1320-1330 cm⁻¹, 1340-1360 cm⁻¹ (C-O stretching of pyrogallol moieties), 1720-1730 cm⁻¹ (C=O stretching from formaldehyde activation), and several peaks in the 3000-3800 cm⁻¹ region (combined effect of O-H stretching and N-H groups) (Fig. 6). These suggest that Tanfloc 8025 is perhaps more activated with formaldehyde and quaternary amine derivatisation (tannin modification by Mannich reaction) (Arbenz and Avérous, 2015), and

hence it is better crosslinked and charged at all pH values to be effective in flocculation. Tanfloc is a moderate-to-high molecular weight C16 polymer (~570,000 g/mol), at 1.7 kDa, with approximately 1000-2000 repeating units with a proposed monomer molecular weight of 399 g mol⁻¹ and an elemental ratio of N:O:C:H of 1:4.2:7.2:12 (Graham et al., 2008; Barrado-Moreno et al., 2016). The cationic nature of the polymer is thought to be a single tertiary amine group (produced by the Mannich reaction) per monomer resulting in a charge density of 3.1 mequiv g⁻¹ at pH 4 and 0.2 mequiv g⁻¹ at pH 9 (Graham et al., 2008). Elemental analysis should be conducted on Tanfloc to provide an indication to the degree of substitution from the precursor tannic acid which may aid in understanding the high flocculation ability.

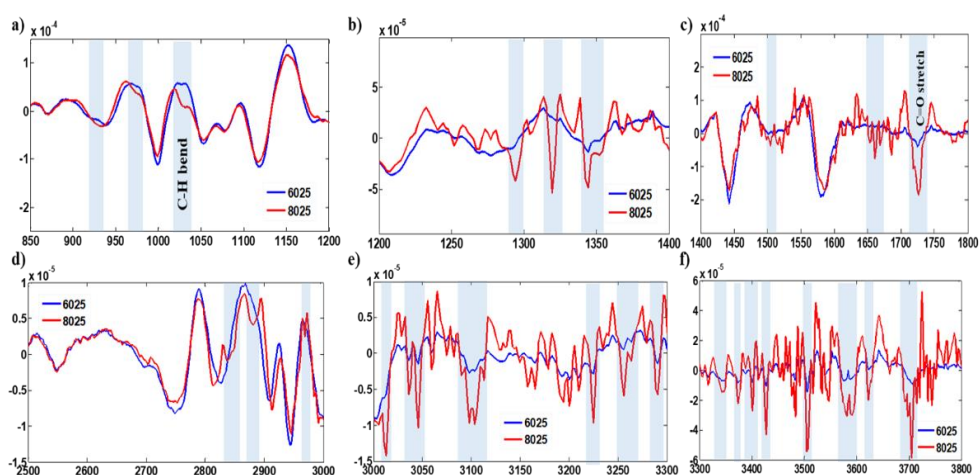


Fig. 5.22. Second derivative FTIR spectra of Tanfloc 6025 and 8025 from 850 – 3800 wavenumbers with a-f showing the differences in the spectra

5.4.5. Effect of temperature and biomass concentration on flocculation with Tanfloc 8025

From a commercial perspective it was important to determine how Tanfloc 8025 would perform at different temperatures and with increasing biomass concentrations which would be more appropriate for industrial facilities. Most species of microalgae can grow at 10 to 35°C (Barrado-Moreno et al., 2016), but the maximum temperature that *P. tricornutum* CCAP 1055/1 can be cultivated at is 28°C (data not shown). It is important in high temperature environments that the biomass is harvested as quickly as possible because the biomass can deteriorate (Gerardo et al., 2015).

Most flocculant screening studies have been conducted at room temperature or under temperature control (20-25°C) (Roselet et al., 2015). To the best of the authors' knowledge only one study has investigated the effect of a flocculant (chitosan) over a range of temperatures (5-20°C) for *P. tricornutum* at pH 8 with no reduction in efficacy observed (Lavoie and de la Noüe, 1983). To the authors' knowledge it is apparent that no study has investigated Tanfloc over a range of temperatures. From the current study, at all temperatures and pH values tested the harvesting efficiency was greater than 82% (Fig. 7a) and there appeared to be no significant effect of pH and temperature ($P>0.05$). Therefore, Tanfloc 8025 offers potential in colder and warmer climates.

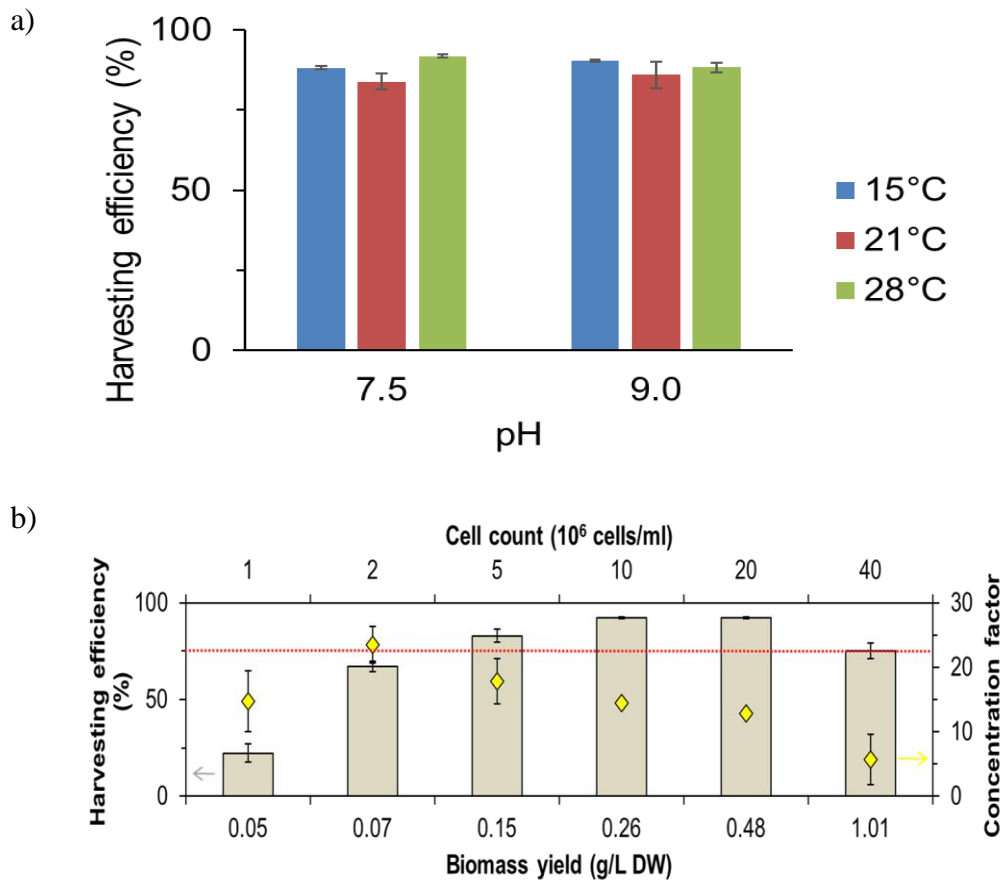


Figure 5.7. Performance of Tanfloc 8025 at different temperatures and biomass densities after 10 mins harvesting: a) Effect of temperature on harvesting efficiency of Tanfloc 8025 applied at 5 mg L⁻¹. b) Effect of biomass concentration (0.05-1.01 g/L DW) on the flocculation potential and concentration factor (CF) of Tanfloc 8025 (5 mg L⁻¹). Red dotted line shows 80% harvesting efficiency.

For *P. tricornutum*, limited studies have been conducted on determining the concentration factor of the flocculant and how it varies with changes in biomass concentration. Furthermore, in calculating the concentration factor few individuals have normalised the data to the harvesting efficiency which has often resulted in overestimates. In the current study, the harvesting efficiency increased up to a maximum (92%) at a biomass density of 0.26-0.48 g L⁻¹ (92% harvesting efficiency) and a further increase to 1.01 g L⁻¹ resulted in a decrease in harvesting efficiency (75%) (Fig. 7b). From 0.07 g L⁻¹ to 1.01 g L⁻¹ there was a decrease in concentration factor from 23.45 to 5.69 (Fig. 7b). It was clear the biomass became less compacted.

Most studies investigating flocculation of *P. tricornutum* have used low biomass densities (<0.5 g L⁻¹) and if the data in the current study is compared, a concentration factor of 12.82 is comparable with sodium hydroxide and chitosan in the literature. Tanfloc 8025 applied to higher biomass densities resulted in a lower concentration factor and further

experimentation is required to improve this. Using properly designed settling vessels with an inclined bottom at an angle would help improve flocculation and is likely to result in higher compaction. Furthermore, optimising the mixing time would likely improve the sedimentation rate and compaction.

5.4.6. Cost analysis of Tanfloc 8025 compared with other commercially viable flocculants

A cost analysis based on the dosage and efficiency can be found in Table 1 for commercially viable flocculants for harvesting *P. tricornutum*. In the current study, with a starting biomass of 0.48 g L⁻¹, 92% of the culture could be harvested in 10 mins with a concentration factor of 12, requiring only 5 mg L⁻¹ of Tanfloc 8025. Tanfloc 8025 was more economically favourable than chitosan, aluminium sulphate and sodium hydroxide (Table 1) but calcium hydroxide has been proposed as a more economically viable alternative. However, calcium hydroxide for harvesting *P. tricornutum* has not been proven and this process would still require a de-flocculation step (addition of hydrochloric or nitric acid) to remove the minerals in the biomass which can cost \$40 ton⁻¹ (Vandamme et al., 2015a) and is environmentally unfavourable. Consequently, Tanfloc 8025 would be more suitable. The flocculant cost per ton of biomass in the current study (\$20.80-27.04) compared favourably to the cost reported for harvesting *Nannochloropsis oculata* with 1.66 to 5 mg L⁻¹ Tanfloc 8025 at \$38 ton⁻¹ (Roselet et al., 2016a).

Table 5.1 - Cost analysis of harvesting *P. tricornutum* with chemical (aluminium sulphate, sodium hydroxide, and calcium hydroxide) and bio-based flocculants (chitosan and Tanfloc 8025). All costs are in US\$.

| | Chitosan a | Aluminium sulphate a | Sodium hydroxide b | Calcium hydroxide b | Tanfloc 8025 |
|--|-----------------|----------------------|--------------------|---------------------|----------------|
| Harvesting efficiency (%) | 91.8 | 82.6 | 73 | - | 92.16 |
| Concentration factor | 8.9 | 7.2 | - | - | 12.82 |
| Flocculant dosage (mg L ⁻¹) | 20 | 30 | 60 | - | 5 |
| Biomass concentration (g L ⁻¹) | 0.105 | 0.105 | 0.5 | 0.5 | 0.48 |
| Flocculant dosage (ton ton ⁻¹ biomass) | 0.18 | 0.27 | 0.12 | - | 0.0104 |
| Flocculant cost (\$ ton ⁻¹) | 2000 to 100,000 | 976 to 2073 | 350 | 150 | 2000c to 2600d |
| Flocculant cost (\$ ton ⁻¹ biomass harvested) | 360 to 18,000 | 263.52 to 559.71 | 42 | 17 | 20.80 to 27.04 |

Data for the efficacy and cost analysis of chitosan and aluminium sulphate was obtained from (Şirin et al., 2012)^a and for sodium hydroxide and calcium hydroxide from Vandamme et al. (2015a)^b. It has already been shown that a de-flocculation step would be

required for sodium hydroxide and calcium hydroxide to remove the magnesium from the biomass which would cost \$40 ton⁻¹ (Vandamme et al., 2015a). The flocculant cost for Tanfloc 8025 was obtained from Roselet et al. (2015)^c and Selesu et al. (2016b)^d.

In addition, the concentration required (10.4 µg g⁻¹ biomass) was vastly lower than the quantities of aluminium and iron required for flocculating *P. tricornutum* (200-270 mg g⁻¹ biomass) (Şirin et al., 2012). As Tanfloc is a natural biopolymer it offers not just an ecological alternative, but it is economically viable and has great potential to replace chemical flocculants. For future studies, the mixing time and optimal harvesting apparatus should be considered as these are critical factors in floc formation and could maximise the performance of this effective biobased flocculant.

5.5. Conclusion

In transitioning towards a biobased and circular economy the replacement of chemical flocculants is essential. Tanfloc 8025 requires a low concentration of flocculant (10.4 g per kg biomass), is cost effective (\$0.03 per kg microalgal biomass), effective over a wide pH (7.5-10.0) and temperature range (15-28°C) with harvesting occurring in as little as 10 mins, resulting in a concentration factor of ≥ 5.69 . Further experimentation needs to be conducted at laboratory scale observing the effect of algal organic matter (AOM) on the behaviour of this flocculant. Further work is required at pilot scale ensuring this method upscales before implementation at a commercial level.

Chapter 6: Evaluating the biorefinery potential of three *Phaeodactylum tricornerutum* strains

Thomas O. Butler^{1*} and Seetharaman Vaidyanathan¹

¹Department of Chemical and Biological Engineering, The University of Sheffield, Sheffield, S1 3JD, UK;

S.vaidyanathan@sheffield.ac.uk (S.V.)

* Correspondence: tbutler2@sheffield.ac.uk

Highlights

- *P. tricornerutum* N017 (Necton S.A.) resulted in the highest fucoxanthin productivity (2 mg L⁻¹ d⁻¹) but UTEX 646 strain resulted in the highest overall biomass (0.16 g L⁻¹ d⁻¹), carbohydrate (39 mg L⁻¹ d⁻¹), protein (42 mg L⁻¹ d⁻¹), FAEE (11 mg L⁻¹ d⁻¹) and EPA (3 mg L⁻¹ d⁻¹) productivities
 - Red: blue (2.25:1) light emitting diodes (LEDs) are 24 % more efficient than white LEDs
 - Red: blue LEDs (2.25:1) resulted in the highest protein, FAEE and EPA productivity, and the biomass, carbohydrate and fucoxanthin productivities were not significantly lower than those obtained under white light
 - Red: blue LEDs resulted in a decrease in commensal bacteria number but there was only a slight difference in community composition
-

6.1. Abstract

Phaeodactylum tricornutum is a model diatom species with the potential to be used as a cell factory and biorefinery chassis. Its two high value products fucoxanthin and eicosapentaenoic acid (EPA) are of commercial interest but determining the best strain and light type is important for commercial exploitation. There are many isolates of *P. tricornutum* around the world. Three different *P. tricornutum* strains (CCAP 1055/1, UTEX 646 and a commercial strain - N017 from Necton, S.A., Portugal) were cultivated in a commercial medium (Nutribloom) and cultivated under warm white LEDs to determine the optimal strain for fucoxanthin and EPA production. UTEX 646 had the highest overall biomass, carbohydrate, protein, fatty acid ethyl ester (FAEE), and EPA productivity, whereas N017 had the highest fucoxanthin productivity. In microalgal production the energy burden is a major issue and by utilising light emitting diodes (LEDs) with red: blue at 2.25:1 light, the electricity consumption can decrease by 24 %. When comparing the lighting source, red: blue LEDs resulted in a higher protein, FAEE, and EPA productivity compared with warm white LEDs but warm white lights resulted in a higher biomass, carbohydrate, and fucoxanthin productivity, but this was not statistically significant. The commensal bacterial community was also profiled during cultivation. *Marinobacter* sp. was present in all strain isolates and dominated at most stages of cultivation. *Halomonas* sp. was only present in *P. tricornutum* CCAP 1055/1 and N017. *Algoriphagus* sp. was only present in *P. tricornutum* CCAP 1055/1 and in low numbers (<4 %). Comparatively, *Sphingorhabdus* (<3 %) and *Croceibacter* spp. (<19 %) were present in N017. This is the first time *Sphingorhabdus* and *Croceibacter* have been observed to be associated with *P. tricornutum* during cultivation. The total bacterial count was observed to be lower under red: blue LEDs for all three strains over the cultivation period, showcasing that red: blue light can affect the community dynamics.

Keywords: microalgae; LEDs, strain screen, biorefinery, bacterial community

6.2. Introduction

Microalgae have been of great interest as cell factories for biofuels and bioactive molecules due to their ability to use natural sunlight, high photosynthetic efficiency, their ability to grow using marginal land, wastewater, whilst remediating nitrogen, phosphorus and CO₂ (Ma et al., 2016). The microalga *P. tricornutum* is a model diatom that is known to accumulate a spectrum of natural products; the omega-3 fatty acids, eicosapentaenoic acid (EPA) and docosahexaenoic acid (DHA), the carbohydrate chrysolaminarin and the pigment fucoxanthin (Butler et al., 2020). It is a commercially viable species for large-scale cultivation, and in outdoor mass culture systems, it has been shown to dominate and outcompete other microalgal species with a tolerance for high pH, an ability to grow under low light, and a non-dependence on silica (Remmers et al., 2017; Sethi et al., 2020; Spilling et al., 2013).

There are >75 known *P. tricornutum* isolates that have been reported in the literature (including synonymous isolates), of which 22 are unique strains maintained in 13 culture collections (Butler et al., 2020). However, there is a lack of knowledge on the biochemical profiles of these strains. All the strains are brackish or marine with the exception of CCAP 1052/1B (UTEX 640) which can uniquely grow in freshwater (Yongmanitchai and Ward, 1991). To date *P. tricornutum* UTEX 640 has been the workhorse for high biomass, lipid and EPA productivities with the highest reported natural EPA content to date in flat-panel airlift PBRs outdoors (5.14 % DW) (Derwenskus et al., 2019). However, recently UTEX 646 has been shown to outperform UTEX 640 and UTEX 642 in terms of biomass and EPA content (Derwenskus et al., 2020a) and has great potential as a recombinant protein factory (Hempel et al., 2011, 2017), antibacterial fatty acids (Desbois et al., 2008), and has been successfully cultivated at >550 L scale in closed photobioreactors and raceway ponds (Hamilton et al., 2015). Bioprospecting has revealed strains such as M21 (from a fjord in Norway) which was of particular interest because it had a high growth rate at 10°C with a high EPA content which increased in the stationary phase to 4.6 % DW (Steinrücken et al., 2017). A high EPA content (4.4 % DW) has been obtained with *P. tricornutum* Fito (obtained from Fitoplankton Marino, Cadiz, Spain – strain CCFM 06) (Steinrücken et al., 2018). Comparatively, two Norwegian isolates (M28 and B58) showed an EPA content of 3.2 and 3.1 % DW respectively (Steinrücken et al., 2018).

Microalgae production is hindered by low biomass and product yields in conjunction with high production costs and energy demands (Norsker et al., 2011). Most methods of large-

scale production use natural sunlight, but in temperate climates light intensities and duration are low in winter and hinder microalgal growth. In addition, in aquaculture production, artificial lighting is usually provided by cool white fluorescent lamps/halogen lamps (where blue, green, yellow and orange light dominate) (del Pilar Sánchez-Saavedra et al., 2016). However, economical, durable, reliable and efficient artificial light sources are needed to increase biomass and product yields. The use of light emitting diodes (LEDs) can decrease production costs through decreased energy costs rather than traditional metal halide filaments (Schulze et al., 2014). Blue LED light could save 50 % energy input compared with fluorescent light (Yang and Wei, 2020). In addition, LEDs are considered an ideal artificial light source and offer advantages over fluorescent bulbs and metal halide lamps due to their long life-span (50,000 h), low heat generation, low energy consumption, and narrow emission band in the blue (465 nm) and red region (660 nm) with a PAR efficiency of 1.91 $\mu\text{mol photons s}^{-1} \text{W}^{-1}$ (Blanken et al., 2013; S. Wang et al., 2018b). A mixture of red: blue light (2.25:1) has been tested successfully for growth optimization in several microalgae (Fu et al., 2013; Kim et al., 2013; Severes et al., 2017). Blue and red wavelengths are the main absorption bands of all chlorophylls and using red LEDs mixed with 10-30 % blue has shown optimal biomass productivities in microalgae (Sirisuk et al., 2018).

Chlorophyll *a* makes up to 74 % of the total chlorophyll in *P. triornutum* and is the major light harvesting pigment with the preferred wavelength absorbance at 420-470 nm and 660-680 nm (de Mooij et al., 2016; Schulze et al., 2014). Fucoxanthin binds with chlorophyll *a + c* and proteins to form the fucoxanthin chlorophyll complex (FCP) and has an important role in light capture and non-photochemical quenching (Yang and Wei, 2020). The specific structure of FCP in *P. triornutum* allows it to absorb blue light, and red mixed with blue light is beneficial for photosynthesis (Kuczynska et al., 2015; Wang et al., 2019).

There have been conflicting reports in the literature on which LED wavelengths to use for optimising *P. triornutum* biomass and product yields. White LEDs have been reported to result in a higher biomass concentration compared with single spectra LEDs (blue, green, yellow and red) for CCMP2561 strain (Oka et al., 2020). Comparatively, using a mixture of red: blue LEDs at different ratios has been found to result in an increase in biomass productivity and fucoxanthin for different strains (Ra et al., 2018; Yang and Wei, 2020). It appears that the effect of the lighting spectra is strain specific.

In this study UTEX 646 (CCAP 1052/6) was selected due to its high growth rate and EPA content, CCAP 1055/1 as a model sequenced strain, and they were compared with a commercial strain from Necton, Portugal. The primary aim of our study was to investigate

which *P. tricornutum* strain had the best biorefinery potential, particularly for fucoxanthin and EPA. Red: blue light (2.25:1) was investigated as an alternative to warm white light to reduce the cost of artificial illumination and to determine if improvements could be observed in fucoxanthin and EPA yield. A final aim was to characterise the bacterial population of three strains under white LED and to determine if red: blue light could affect the commensal bacterial population of all three strains.

6.3. Materials and methods

6.3.1. *Phaeodactylum tricornutum* stock culture and routine maintenance

P. tricornutum CCAP 1055/1 was obtained from the Culture Collection of Algae and Protozoa (CCAP), UTEX 646 (CCAP 1052/6) was obtained from Plymouth Marine Laboratory (PML), and a proprietary strain (N017) was obtained from Necton, S.A., Portugal. Stock cultures were routinely maintained by the transfer of a 10% (v/v) inoculum (every two weeks) and sparged with filtered air (0.22 μm , Millex-FG Vent Filter; Millipore, USA). The stock cultures were cultivated in 1 L Duran bottles with 800 mL natural seawater at 12.1 ppt (20.27 mS), (Eastern Scheldt, The Netherlands) supplemented with 2 ml L⁻¹ of commercial medium (Nutribloom) from Necton (4 mM NaNO₃, 0.2 mM KH₂PO₄, 3.99 μM ZnSO₄ 7H₂O, 2.00 μM MnCl₂ 4H₂O, 0.2 μM Na₂MoO₄ 2H₂O, 0.2 μM CoCl₂ 6H₂O, 0.2 μM CuSO₄ 5H₂O, 52.82 μM Na₂EDTA 2H₂O, 4 μM MgSO₄ 7H₂O, 40 μM FeCl₃ 6H₂O, 0.15 μM vitamin B1, 0.29 μM biotin and 0.004 μM vitamin B12) was filter sterilised (Sartobran 300, 0.2 μm) via a twin-headed peristaltic pump (Model 503S, Watson Marlow, USA). The cultures were incubated at 20.4°C (\pm 0.6 °C), continuous irradiance with either 50 W warm white lights (2700-2900 K, Rohs) (emission peaks at 406, 438, 488, 548, 589, 595, 613 and 632 nm) ca. 134 $\mu\text{mol photons m}^{-2} \text{s}^{-1}$ surface irradiance (44.4 W, 3 $\mu\text{mol W}^{-1}$) or 45 W LED Grow Light 169 LED Red Blue (2.25:1) full spectrum (23.5 W, 5.3 $\mu\text{mol W}^{-1}$) (Roleadro, China) (emission peaks at 459 and 634 nm) ca. 125 $\mu\text{mol photons m}^{-2} \text{s}^{-1}$ surface irradiance for pre-acclimation (Figure 6.). The initial absorption spectra were recorded using an Ocean Optics USB2000 spectrometer with a Mikropack Mini D2 UV-vis-IR light source in the range 350–850 nm (Dunbar et al., 2008). The wattage was measured with an electric energy power meter (Floureon, China) and is shown in Figure 6. Each stock culture was aerated at 7.65 lpm with

2 % CO₂ using a Brooks Mass Flow Controller (Brooks Instrument, USA) and the gas mixture was delivered through a 0.22 µm air filter (Whatman PolyVENT 16, GE Healthcare Life Sciences).

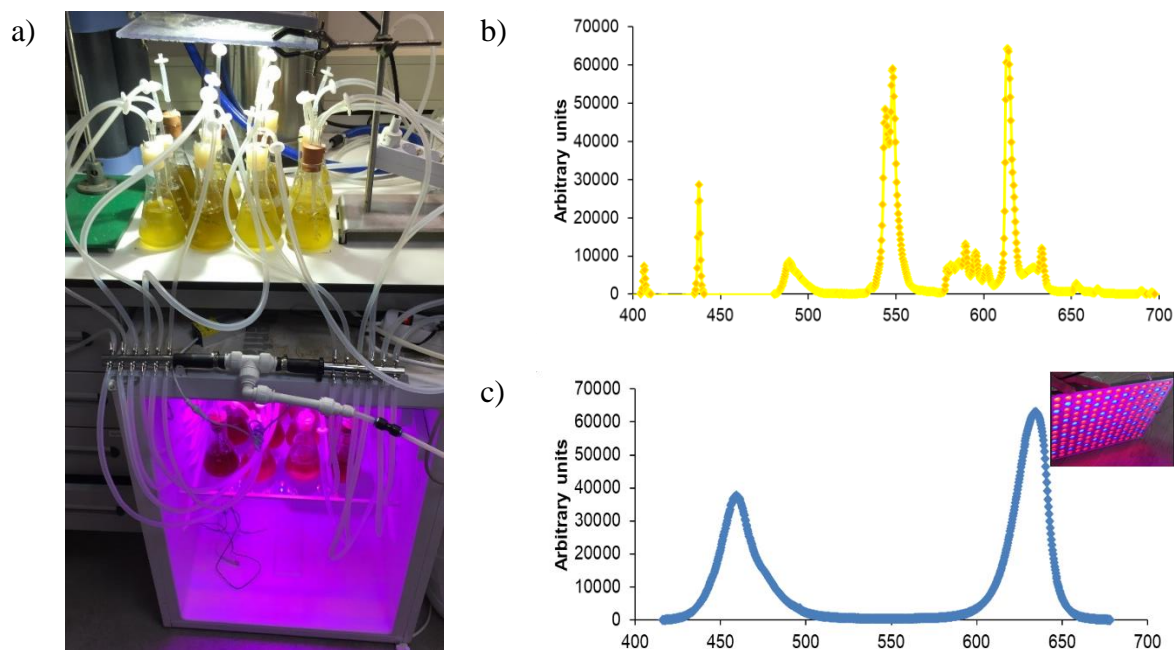


Figure 6.1 - Comparison of white and red: blue LED setups a) experimental setup and the cultures were covered with a blackout material to avoid external light interference, and intensity profile of a) warm white lights (2900-3100 k) (50 W) compared with b) red: blue (2.25:1) (45 W) lights with emission peaks at 459 and 634 nm

6.3.2. Experimental cultures

Cells from the stock culture were harvested during late-log, centrifuged (4000 rpm, 10 mins), washed twice with 20 mL growth medium and re-suspended in 250 mL Erlenmeyer flasks with 200 mL of each medium. The cultures (*P. tricornutum* CCAP 1055/1, UTEX 646 and N017) were incubated under the conditions above and setup according to Figure 1. A humidifying bottle was used in the setup to avoid evaporation from the cultures. The initial inoculum density was $\sim 1 \times 10^6$ cells mL⁻¹.

6.3.3. Biomass sampling

Samples were taken daily for cell concentration and volume determination, using a 50 µm aperture tube (Multisizer III, Beckman Coulter, USA). Samples were diluted in ISOTON II diluents. The average growth rate (μ) was calculated as detailed elsewhere (Butler et al.,

2017) but as a function of each day and the maximum growth rate (μ_{max}) was the maximum value of this. Five mL of culture were taken daily, centrifuged (4000 rpm, 10 mins), the supernatant removed, filtered through a 0.22 μm filter, and stored frozen at -20°C until further analysis of the medium for nutrient analysis. Dissolved inorganic nitrogen (DIN) in the media was determined by measuring the absorbance at 220 nm as described in Collos et al. (1999). Dissolved Inorganic Phosphate (DIP) in the media was determined following the method of Strickland and Parsons (1968) and the reading was taken after 15 mins. On Day 7, the experimental cultures were harvested and 50 mL of microalgal culture was harvested by centrifugation (4000 rpm, 10 mins), the pellets washed twice with 20 mL ammonium formate (0.5 M) to remove adhering inorganic salts from the cells (Guimarães et al., 2021) and transferred to a 2 mL Eppendorf safe-lock tube, centrifuged at 13,000 rpm for 5 mins and stored at -20°C for lyophilisation using a sublimator 2x2x3 (Zirbus Technology, GmbH, Germany) and stored at -20°C for biochemical (chlorophyll *a*, fucoxanthin, protein, carbohydrate, fatty acid ethyl ester (FAEEs)) and elemental analysis.

6.3.4. Dry weight determination

The dry weight of the culture was measured in triplicate in a modified version as described by (Guimarães et al., 2021). Briefly, Whatman glass microfiber filters (55 mm diameter, pore size 0.7 μm) were wetted with deionised water and dried at 95°C overnight and then placed in a desiccator to cool to room temperature. The empty filters were weighed and pre-wet with ammonium formate (0.5 M). Then, 1-5 mL of culture (depending on the density) was filtered and washed twice with ammonium formate, instead of de-mineralised water for maintaining osmotic balance. The dry weight of the samples was then calculated from the difference in weight between the dry filters with and without biomass.

6.3.5. Quantum yield

Pulse amplitude modulation (PAM) fluorometry was utilised to determine the maximum quantum yield (F_v/F_m) as a measure of photosynthetic efficiency at 630 nm (orange-red excitation light) using an AquaPen-C AP 110-C (Photo Systems Instruments, Czech Republic) after 15 mins dark adaptation at room temperature as described by (Janssen et al., 2018). Samples were diluted to an $OD_{750} < 0.4$.

6.3.6. Bacteria isolation and enumeration

Commensal bacteria from the experimental cultures were isolated by streaking out to form single colonies on a 'modified marine agar medium' with the growth medium supplemented with seawater, 5 g L⁻¹ peptone (Sigma, UK), 1 g L⁻¹ yeast extract (Sigma, UK) and 15 g L⁻¹ agar. From each treatment and time point 1 mL of culture was added to 9 mL of Maximum Recovery Diluent (MRD) (with seawater, 1 g L⁻¹ peptone and 8.5 g L⁻¹ sodium chloride and adjusted to pH 7.0) and vortexed for 10 s. Serial 10-fold dilutions were made in triplicate of the homogenate in MRD. From each dilution, the pour plate technique was used, and an aliquot (0.1 mL) of appropriate dilution factor of the homogenate was plated out. The plates were incubated aerobically at room temperature and counted after 3 days (the small, large and halo bacteria appeared after 2 days, the red, pink, orange and yellow bacteria appeared after 3 days). Bacterial cell numbers were estimated by counting colony-forming units (CFU) and only reads between 30 and 300 CFU were used.

6.3.7. Bacteria DNA-amplification, sequencing, and identification

Commensal bacteria identification was conducted by colony PCR with 16S rRNA genes amplified from the bacterial isolates using primer pair 27F (5'-AGAGTTTGATCMTGGCTCAG-3') (Lane et al., 1991) and 1492R (5'-GGTTACCTTGTTACGACTT-3') (Turner et al., 1999) as described previously. The sequences were then aligned using ClustalW and a dendrogram was formulated.

6.3.8. *P. tricornutum* DNA-amplification, sequencing, and identification

P. tricornutum strains from the stock culture were plated out on Nutribloom medium with 15 g L⁻¹ agar to form single colonies. Four-to-five colonies of each *P. tricornutum* strain were re-suspended in 1 mL deionised water and centrifuged for 13,000 rpm for 2 mins to form a pellet, and the supernatant was discarded. The genomic DNA was extracted from the pellet using the DNeasy Plant Pro Kit (Qiagen, USA) according to the manufacturer's instructions except that a Disrupter Genie® (VWR, UK) was used for cell disruption of the microalgal sample in the supplied tissue disruption tubes for 10 mins.

The nuclear SSU rDNA was amplified using PCR with a combination of the universal eukaryotic primers EAF3 (5'-TCGAC AATCT GGTG ATCCT GCCAG-3') and ITS055R

(5'-CTCCT TGGTC CGTGT TTCAA GACGG G-3') (Marin et al., 2003). All PCR reactions with a final volume of 50 µl contained the components previously described. The following PCR conditions were used: initial denaturing step of 1 min at 98°C followed by 35 cycles of denaturing (98°C for 10 s), annealing (69°C for 15 s), and elongation (72°C for 45 s). A final elongation step was performed at 72°C for 8 mins. PCR products formed in gel electrophoresis which showed single clear bands (ca. 3 kbp) determined from the molecular size marker (Quick-Load® Purple DNA ladder (1 kb) (NEB, USA) was purified and sent for sequencing as above in section 2.8.

6.3.9. Fatty acid ethyl ester (FAEE) determination

A modified version of Kapoor et al. (2014) was used for FAME direct transesterification involving bead beating.

6.3.10. Combined extraction of carbohydrate, pigment and protein

Combined extraction of carbohydrate and protein was carried out according to Chen and Vaidyanathan (2013) with slight modification using approximately 2 mg dry biomass.

6.3.11. Pigment analysis by HPLC – chlorophyll *a* and fucoxanthin

For the detection of the chlorophyll *a* and fucoxanthin, a modified method of Grant et al. (2001) was used. One milligram of dried microalgal biomass was extracted with 1.5 mL HPLC grade absolute ethanol (Sigma Aldrich, UK) with 250 mg L⁻¹ butylated hydroxytoluene (BHT) in bead beater tubes using lysing matrix E (Bertin Technologies, USA) three times at 90 s x 5000 rpm with a 45 s break. After cell disruption the bead beating tubes were then centrifuged (13,000 rpm, 3 mins). 1 mL of the supernatant was pipetted to a 5 mL glass tube (FischerBrand, USA). To the bead beating tube, 1 mL ethanol/BHT mixture was added and the tubes vortexed for 10 s. The tubes were then centrifuged (13,000 rpm for 3 mins) and 1 mL was transferred to the 5 mL glass tube. This procedure was repeated until the pellet was colourless (5 extractions necessary in total). The glass tubes were evaporated under nitrogen, the extract re-suspended in 1 mL absolute ethanol (Sigma Aldrich, UK) and transferred to an Eppendorf tube. The tubes were then centrifuged at (13,000 rpm, 2 mins) before transferring the supernatant to amber coloured HPLC vials. To avoid photo-oxidation, all procedures were

carried out under darkness. Ultra-high-performance liquid chromatography (UHPLC) (Thermo Scientific, USA) was used to quantify the fucoxanthin content. HPLC analysis was performed using a Nexera X2 system (Shimadzu, Japan) coupled with a photo-diode array detector (SPD-M20A) and a Kinetex C18 reversed-phase column (100A 150 x 4.6 mm, 5 μ m particle size) (Phenomenex, UK) was used. The HPLC method adopted was a modified version of Grant, 2011. Three mobile phases were used: (A) 0.5 M Ammonium acetate in methanol/water 85:15, (B) Acetonitrile/water 90:10 and (C) Ethyl acetate 100 % using the gradient procedure described. The flow rate was set at 1 mL min⁻¹ and the column temperature at 25°C. The concentration of fucoxanthin was quantified by measuring at the absorbance at 450 nm. A linear calibration curve ($R^2 = 0.99$) covering the range 0-20 μ g mL⁻¹ was constructed using a fucoxanthin, chlorophyll *a* and antheraxanthin standard (Sigma Aldrich, UK). The retention time of the extracts matched the standards for fucoxanthin (6.7 mins), antheraxanthin (10.2 mins), and chlorophyll *a* (25.2 mins) as shown in Appendix D.

6.3.12. Elemental composition

Elemental analysis was conducted according to Al-shathr (2019). Helium was used as a carrier gas to transport all the combustion gases through the system and high-purity oxygen was used to aid the combustion process.

6.3.13. Statistical analysis

Each treatment was performed in triplicates, and the mean and standard error of the dependent variable are presented in the results. Statistical analysis of the experimental data was conducted using SPSS statistical software (SPSS Statistics 26, IBM). The data was tested for normality using a Kolmogorov-Smirnov test and if these data were normally distributed ($P > 0.05$) they were subsequently tested for equal variance using Levene's test. If variances were considered equal then a one-way ANOVA/MANOVA and a *post-hoc* Tukey's test was utilised to understand where the differences were. If samples were not normally distributed ($P < 0.05$) then a Kruskal-Wallis and *post-hoc* Dunn's non-parametric comparison was undertaken to understand the changes. The statistical difference of each set of experiments was studied with the analysis of the *P* value. In addition, this value was used to select parameters that were statistically significant.

6.4. Results and Discussion

The three strains were first pre-acclimated under warm white light and then grown for 7 days under the same conditions. The three strains were then compared in terms of growth and product yield and productivity.

6.4.1. Strain differences in growth and biochemical composition under warm white light

Growth of the three strains was compared under warm white light. *P. tricornutum* CCAP 1055/1 and N017 both predominated as fusiform cells (>95 % of the population) over the 7 d cultivation period. UTEX 646 was found to be of mixed morphology, containing oval and fusiform morphotypes and was smaller in length and volume (data not shown).

The highest biomass concentration and biomass productivity after 7 d cultivation was obtained with UTEX 646 ($1.18 \pm 0.07 \text{ g L}^{-1}$ and $0.16 \text{ g L}^{-1} \text{ d}^{-1}$) but this was not significantly higher than for N017 (Table 6.1). The highest μ_{max} was obtained with N017 from day 1 to 2 under white light ($\mu_{\text{max}} = 1.57$) but this was not significantly higher than for UTEX 646.

The biomass productivity of UTEX 646 in flat-panel PBRs has been found to range from $0.025\text{-}0.158 \text{ g L}^{-1} \text{ d}^{-1}$ (Rodolfi et al., 2017). For *P. tricornutum* N017 the biomass productivity has been found to range from $0.02\text{-}0.27 \text{ g L}^{-1} \text{ d}^{-1}$ in outdoor flat panel PBRs, with a higher biomass productivity attained at lower biomass densities (0.4 g L^{-1} DW compared with 1.1 g L^{-1}) (Gao et al., 2020a).

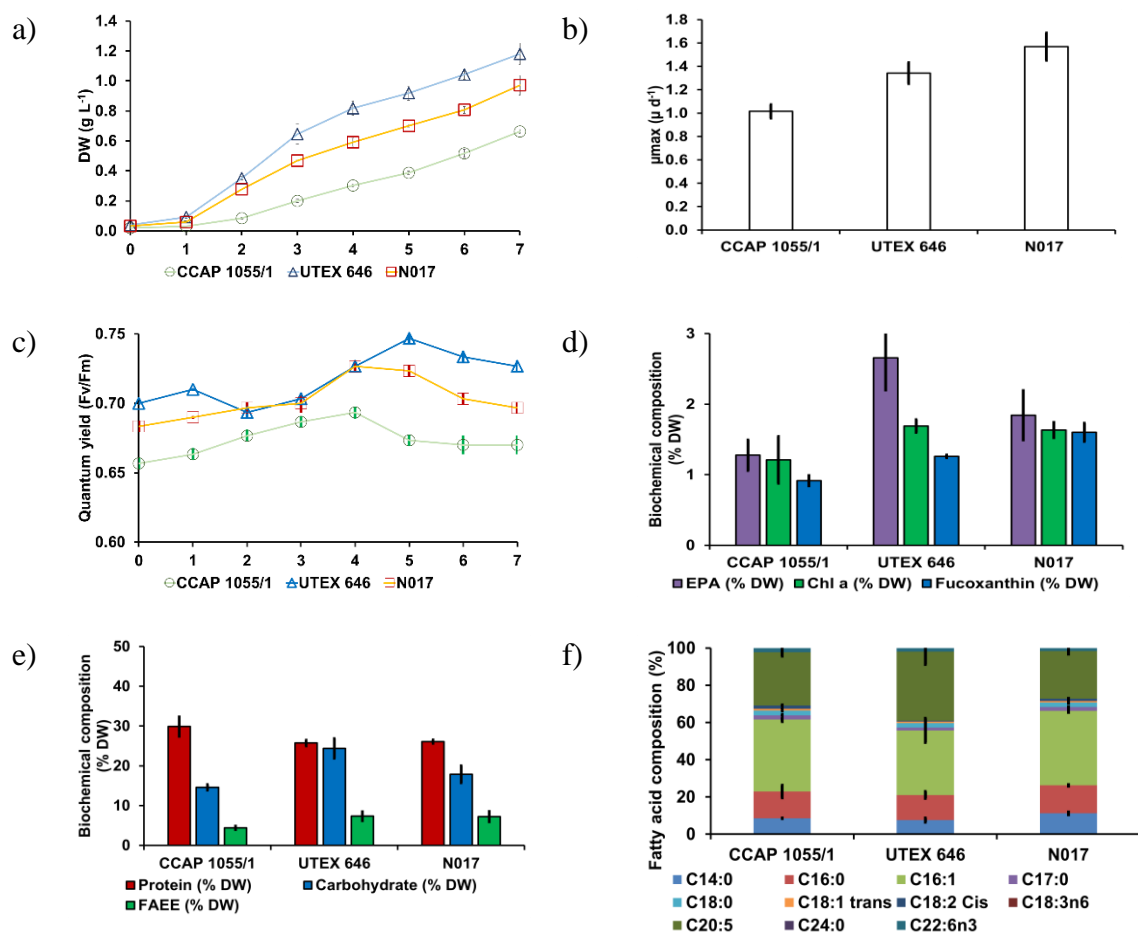


Figure 6.23 - Comparison of three strains of *P. tricornutum*, CCAP 1055/1, UTEX 646 and N017 under warm white light; a) growth as DW (g L⁻¹); b) maximum growth rate (μ d⁻¹), c) quantum yield, d) EPA, chlorophyll *a*, and fucoxanthin, f) fatty acid ethyl ester (FAEE), carbohydrate and protein content, g) FAEE composition

To the authors knowledge, this is the first study to investigate the biochemical composition of N017. The chlorophyll (1.63 % DW), fucoxanthin (1.60 % DW), EPA (1.84 % DW), protein (26.09 % DW), carbohydrate (17.87 % DW) and FAEE (7.21 % DW) contents were similar to those reported in the literature (Reboloso-Fuentes et al., 2001; Breuer et al., 2012; Di Lena et al., 2020). The highest fucoxanthin content (1.60 % DW) was achieved with N017. However, the EPA and fucoxanthin content was lower than previously reported for UTEX 640 (4.28 and 1.91 % DW respectively) (Derwenskus et al., 2020). Comparatively, the highest carbohydrate (24.4 % DW), chlorophyll *a* (1.7 % DW), TFA (7.3 % DW) and EPA content (2.7 % DW) was obtained with UTEX 646 (Figure 6.232). However, the EPA content was lower than reported by Derwenskus et al. (2020) for the strain cultivated in a flat panel PBR (4.45 % DW) and could have been due to the high cell densities employed which

provided mutual shading to the cells. In terms of protein, the highest content was obtained with CCAP 1055/1 (29.87 % DW) but this was not significantly higher than for the other strains.

No significant difference in EPA content has been reported between UTEX 646, 642 and 640 Derwenskus et al. (2020). However, the EPA content of UTEX 646 was found to be higher in the Derwenskus et al. (2020) study for the other strains. The temperature used (20°C) was similar to that used in our study and the higher EPA content could have been due to the higher nitrate and phosphate content in the modified Mann and Myers medium that Derwenskus et al. (2020) and due to the use of flat-panel airlift PBRs which avoid photolimitation and photoinhibition.

P. tricornutum CCAP 1055/1 had the highest C16:0 content of the three strains under white and red: blue light (21 of TFAs) There was no statistically significant difference in C16:1 content of the three strains. *P. tricornutum* UTEX 646 had the highest EPA proportion of TFAs (30 %) which was significantly higher than the other two strains ($p < 0.05$). There was no statistically significant difference in DHA content between the strains and the proportion of TFAs was < 3 % in all strains.

In terms of biorefinery products; UTEX 646 resulted overall in the highest carbohydrate ($39.28 \text{ mg L}^{-1} \text{ d}^{-1}$), protein ($42.01 \text{ mg L}^{-1} \text{ d}^{-1}$), FAEE ($10.66 \text{ mg L}^{-1} \text{ d}^{-1}$), and EPA productivities ($3.19 \text{ mg L}^{-1} \text{ d}^{-1}$). Whereas the highest fucoxanthin yield ($2.12 \text{ mg L}^{-1} \text{ d}^{-1}$) was obtained with the N017 strain but this was not significantly higher than that obtained with UTEX 646 ($2.05 \text{ mg L}^{-1} \text{ d}^{-1}$) (Table 6.1).

Of the strains tested, UTEX 646 appears to be the optimal biorefinery chassis for biomass, carbohydrate, protein, FAEE and EPA. Whereas N017 appears to be optimal for fucoxanthin production. The three strains were next investigated under red: blue light as a more economical artificial light source.

6.4.2. Effect of red: blue LEDs on growth and biochemical composition of *P. tricornutum* CCAP 1055/1, UTEX 646 and Necton

Providing red: blue lights in a 2.25:1 ratio with theoretical maximum photon energy efficacy at a total light intensity of $125 \mu\text{mol photons m}^{-2} \cdot \text{s}^{-1}$ results in a total electrical consumption of 0.0258 kWh, whereas in practice, the realistic white light and the realistic red: blue LED combination under similar conditions cause consumptions of 0.0403-0.0463 kWh

and 0.0353 kWh respectively (Appendix D). By replacing white LEDs with red: blue LEDs (2.25:1), a reduction of 36-44 % in power consumption is theoretically possible. Replacing white LEDs with the realistic red: blue LEDs would save 12-24 % of power consumption.

Applying a red: blue light arrangement can be beneficial as in this case, less electrical power is required because the red blue lights combined provide a higher number of photons for the same amount of energy compared to white light. Red photons (660 nm) contain less energy than blue photons (450 nm) (Appendix D).

The cell physiology and growth was investigated to look at the effect of replacing white LEDs with red: blue LEDs. No difference was observed in the cell morphology (Appendix D) and no significant decrease in final biomass concentration was observed. Another method of monitoring cell health is to look at the quantum yield. A decrease of quantum yield (F_v/F_m) indicates inhibition of electron transport from the PSII reaction centres to the plastoquinone pool (Strasser et al. 2000, Kalaji et al. 2011, Oukarroum 2016) and can be used as an indicator of unfavourable conditions.

The maximum photosynthetic efficiency of PSII was observed for UTEX 646 and N017 under white light with a F_v/F_m of 0.75 and 0.69. Cultivation under red: blue light resulted in a decrease in PSII for days 1 to 7. For the N017 strain the F_v/F_m increased to a maximum on day 4 but for UTEX 646 the maximum was achieved on day 5. With increased culturing age the F_v/F_m was found to decline. A decline in F_v/F_m is generally due to nonphotochemical quenching or acknowledged with reduced photosynthetic efficiency or photo damage (Remmers et al., 2017) (Oukarroum 2016).

A maximum photochemical quantum yield (PSII max) of 0.67 has been reported before for *P. tricornutum* strain CCMA 106 under aeration and under elevated carbon dioxide (1000 μatm at pH 7.7) (Li et al., 2017b). Comparatively the quantum yield has been found to vary between strains; Fito (0.57-0.73), M28 (0.60-0.77) and B58 (0.63-0.79) (Steinrücken et al., 2018). It has been found that after inoculation the quantum yield drops but recovery is observed after two to three days (Steinrücken et al., 2018).

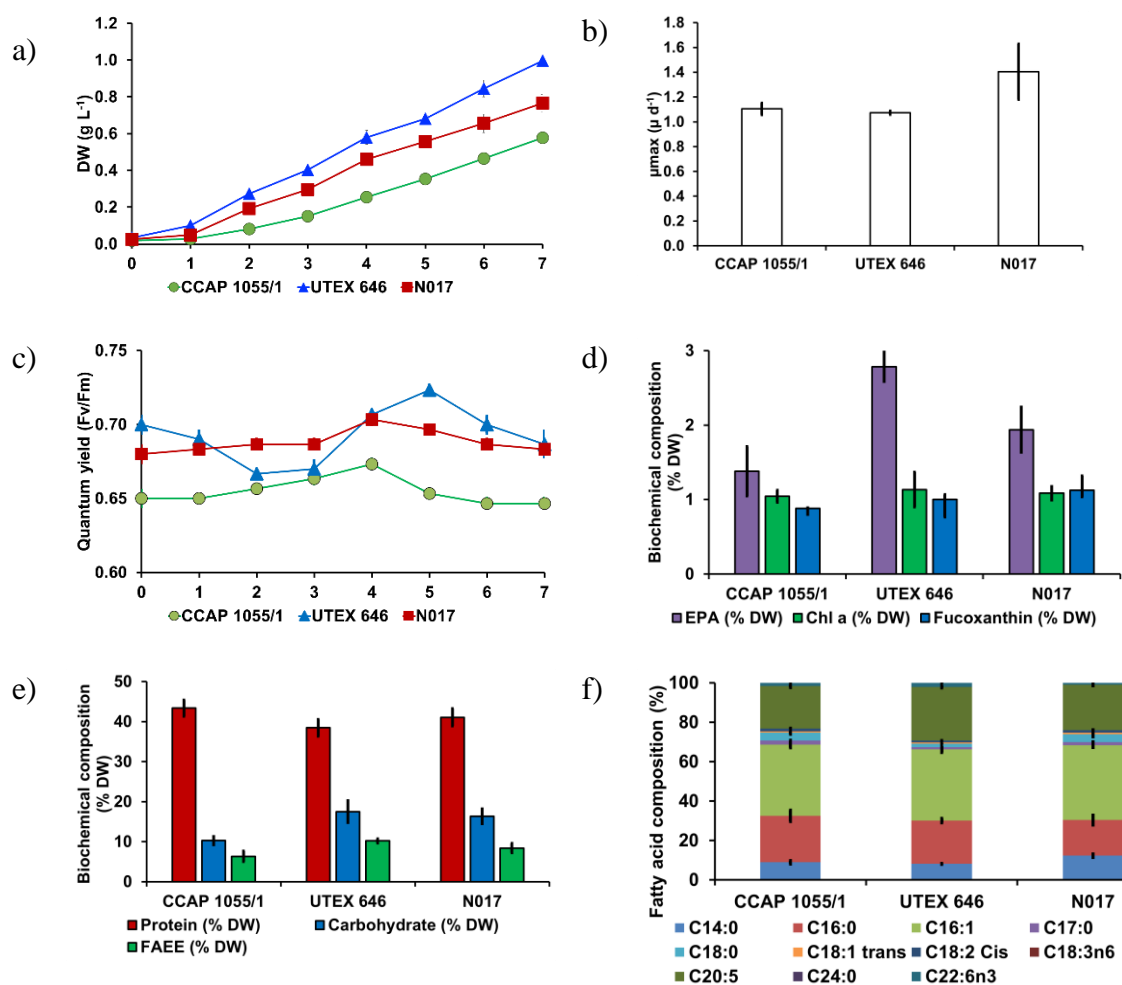


Figure 6.3 - Comparison of three strains of *P. tricornutum*, CCAP 1055/1, UTEX 646 and Necton N017 under red: blue light; a) growth as DW (g L⁻¹); b) maximum growth rate (μ d⁻¹), c) quantum yield, d) EPA, chlorophyll *a*, and fucoxanthin, f) fatty acid ethyl ester (FAEE), carbohydrate and protein content, g) FAEE composition.

The biochemical composition was also monitored to observe differences between strain and the lighting conditions. A higher TFA content was obtained for UTEX 646 and N017 cultivated under red: blue light (10.20 and 8.40 % DW respectively) compared with white light for UTEX 646 and N017 (7.34 and 7.21 % DW). In addition, a higher EPA content was obtained under red: blue lights for UTEX 646 and N017 (2.78 and 1.94 % DW) compared with warm white light (2.65 and 1.84 % DW) which was not statistically significant. Red light has been reported to increase lipid synthesis in *Tisochrysis lutea* (del Pilar Sánchez-Saavedra et al., 2016). Green light has also been shown to result in an increase in lipid content (Jung et al., 2019) but in the current study, green light was shown to be non-essential and red: blue LEDs were responsible for increasing TFA content. EPA is part of the polar lipids (galacto- and phospholipids) that make up the thylakoid membrane and can be affected by the available light (Derwenskus et al., 2020a)

A lower carbohydrate content was obtained for UTEX 646 and N017 under red: blue light (17.52 and 16.36 % DW respectively) compared with 24.38 and 17.87 % DW under warm white light. An increase in protein content was observed for UTEX 646 and N017 under red: blue light (38.45 and 41.07 % DW) compared with 25.72 and 26.09 % DW respectively under warm white light. Blue light has been revealed to cause proteogenesis in *Tisochrysis lutea* (del Pilar Sánchez-Saavedra et al., 2016).

A decrease in fucoxanthin content for UTEX 646 and N017 was obtained under red: blue light (1.00 and 1.13 % DW respectively) compared with warm white light (1.26 and 1.60 % DW respectively). An excessive number of blue photons could result in a higher energy than required for photosynthesis and could cause photosynthetic quenching, resulting in ROS accumulation (Fu et al., 2013). It has been reported that the use of only red and blue wavelengths, which are highly absorbed in the algal spectrum, could result in neglecting green-amber wavelengths, which penetrate deeper in the reactor due to low photo absorption and thus, could be beneficial for high-density cultures or cultures grown in PBRs with a long light path (de Mooij et al., 2016; Schulze et al., 2016).

The FCP complex contains seven molecules of chlorophyll *a*, two molecules of chlorophyll *c* and seven molecules of fucoxanthin which is responsible for harvesting blue-green light and dissipating energy in diatoms (Wang et al., 2019). Chlorophyll *a* has absorbance peaks at 445 and 663 nm, chlorophyll *c* at 450 and 630 nm, and fucoxanthin at 445 nm which suggests that the FCP can harvest blue-green (fucoxanthin and chlorophyll) and red light (chlorophyll *a*) (Wang et al., 2018; Büchel, 2020; Yang et al., 2020). The warm white light had emission peaks at 406, 438, 488, 548, 589, 595, 613 and 632 nm, but the red: blue (2.25:1) light only had two emission peaks at 459 and 634 nm. In diatoms, red and blue light promote photosynthesis and biomass production whilst blue light alone promotes fucoxanthin accumulation (Wang et al., 2018b; Yang et al., 2020). Chlorophylls absorb light in the blue (400-500 nm) and red (600-700 nm) wavelength of the PAR spectrum whilst fucoxanthin is responsible for the capability of diatoms to absorb light in the green region (500-570 nm), but fucoxanthin can also absorb red and blue light (Collier Valle et al., 2014). A mixture of white and blue light (1:1) have been shown to increase fucoxanthin productivity in *Nitzschia laevis* to the highest productivity (16.50 mg L⁻¹ d⁻¹) reported to date (Lu et al., 2018). Green light results in the highest fucoxanthin excitation, followed by white, and then blue light (Shimura and Fujita, 1975), and the presence of green light in the white spectrum could be accountable for the higher fucoxanthin content compared with red: blue LEDs.

For *Tisochrysis lutea*, blue light has been found to result in an increase in growth rate and protein compared with white light, but a decrease in lipid and carbohydrate was observed (del Pilar Sánchez-Saavedra et al., 2016). It has been reported that blue light increases DNA and RNA synthesis and thus growth efficiency (del Pilar Sánchez-Saavedra et al., 2016). Red light was found to result in a decrease in protein, carbohydrate and lipid (del Pilar Sánchez-Saavedra et al., 2016).

In all three strains there appeared to be a lower C/N ratio under red: blue light with a lower carbon content, but there was no statistically significant difference in nitrogen content (Figure 6.4). The supply of CO₂ (2 %) was the same for all strains and lighting arrangements and it could be that carbon uptake is higher under red: blue LEDs and further work is warranted.

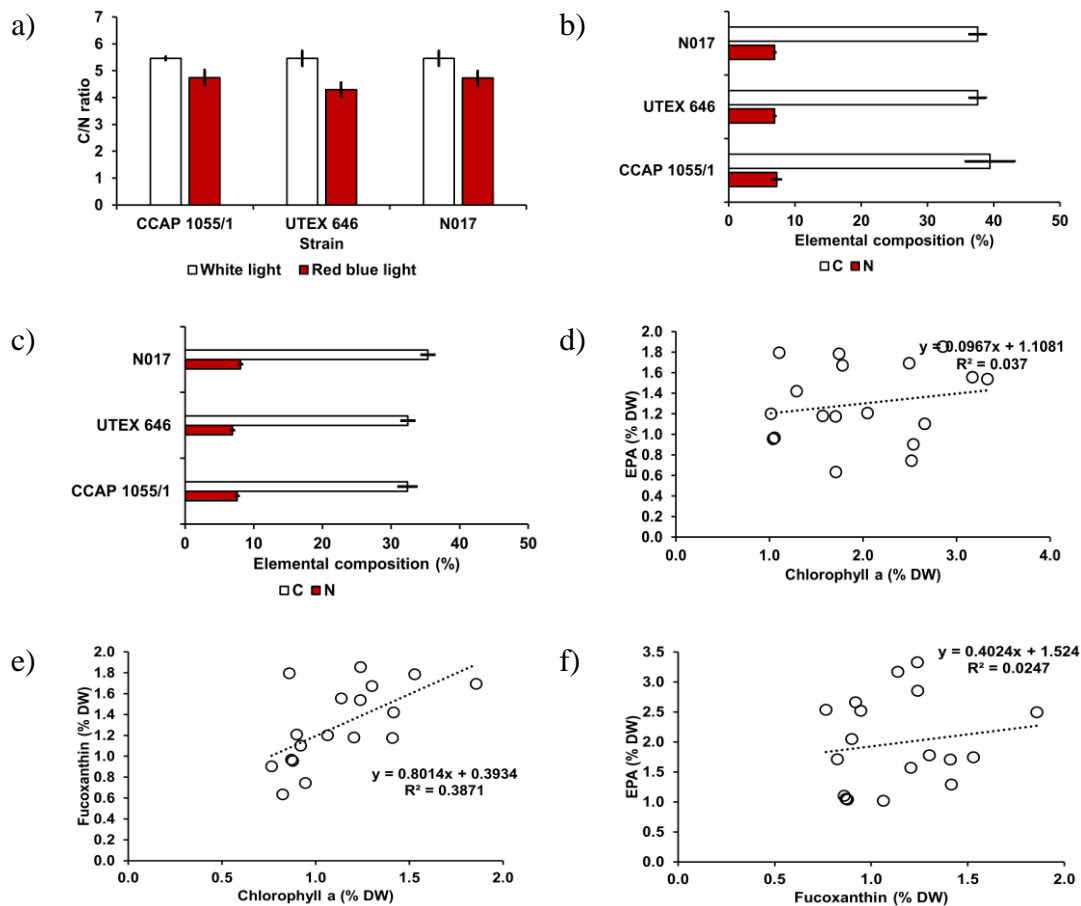


Figure 6.4 – Elemental composition; a) C/N ratio under warm white and red: blue lights, carbon and nitrogen content under b) warm white and c) red: blue light; relationship between d) EPA and chlorophyll a, e) chlorophyll a and fucoxanthin and f) fucoxanthin and EPA

It appears from the current study that a combination of red and blue lights can result in an increase in protein, EPA and FAEEs, but a decrease in fucoxanthin content.

6.4.3. Effect of warm white and red: blue LEDs on productivities in *P. tricornutum* UTEX 646 and N017

UTEX 646 showed the highest overall biomass productivity under white light (0.16 g L⁻¹ d⁻¹) compared with red: blue light (0.14 g L⁻¹ d⁻¹). In terms of biorefinery products; UTEX 646 cultivated under white light resulted overall in the highest carbohydrate yield (39.28 mg L⁻¹ d⁻¹). Whereas the highest fucoxanthin yield (2.12 mg L⁻¹ d⁻¹) was obtained with the N017 strain cultivated under white light but this was not significantly higher than UTEX 646 (2.05 mg L⁻¹ d⁻¹). Interestingly, the highest protein (52.91 mg L⁻¹ d⁻¹), FAEE (14.04 mg L⁻¹ d⁻¹), and EPA yield (3.83 mg L⁻¹ d⁻¹) was recorded under red: blue light with UTEX 646.

Table 6.1 - Biomass and product productivities after 7 d cultivation for *P. tricornutum* UTEX 646 and N017 under white and red: blue LEDs.

| | Warm white light | | Red: blue light | |
|--|------------------|--------------|-----------------|--------------|
| | UTEX 646 | Necton N017 | UTEX 646 | Necton N017 |
| Biomass (g L⁻¹ d⁻¹) | 0.16 ± 0.01 | 0.13 ± 0.01 | 0.14 ± 0.00 | 0.11 ± 0.01 |
| Carbohydrate (mg L⁻¹ d⁻¹) | 39.28 ± 1.98 | 23.92 ± 3.32 | 24.18 ± 4.11 | 17.06 ± 0.96 |
| Protein (mg L⁻¹ d⁻¹) | 42.01 ± 3.35 | 34.92 ± 1.94 | 52.91 ± 3.67 | 43.43 ± 3.35 |
| Fucoxanthin (mg L⁻¹ d⁻¹) | 2.05 ± 0.12 | 2.12 ± 0.04 | 1.38 ± 0.12 | 1.17 ± 0.14 |
| FAEE (mg L⁻¹ d⁻¹) | 10.66 ± 3.65 | 9.43 ± 0.96 | 14.04 ± 0.97 | 9.05 ± 1.87 |
| EPA (mg L⁻¹ d⁻¹) | 3.19 ± 1.08 | 2.41 ± 0.29 | 3.83 ± 0.34 | 1.67 ± 0.27 |

Warm white lights contain a significant fraction of poorly captured regions of the spectrum (e.g. green and yellow) (de Mooij et al., 2016). The light spectrum changes with increasing flask depth with preferential absorption of red and blue light for chlorophyll and green light for fucoxanthin (Oeltjen et al., 2002). The light penetrating becomes greener as the red and blue fractions are rapidly absorbed with the warm white LED light quickly converted into green light with increasing culture depth (de Mooij et al., 2016). It has been found that 53 % of the incoming light energy is absorbed within the first 2 mm and the photosynthetic efficiency in this layer has a dominant effect on the biomass productivity with higher productivities obtained with warm white light at ≥2 mm (de Mooij et al., 2016).

Schulze et al. (2016) concluded the use of dichromatic lights with red and blue LEDs resulting in higher growth rates, as they cover the absorption peaks of chlA at 440, 625 and

680 nm and of antheraxanthin and violaxanthin pigments at 487-490 nm (Lee and Pilon, 2013; Pilon and Kandilian 2011).

Nevertheless, the use of only red and blue wavelengths, which are highly absorbed by algae, results in neglecting of green-amber wavelengths, and allowing penetration to deeper in the reactor due to low photo absorption and thus, could be beneficial for high-density cultures or cultures grown in PBRs with a long light path (de Mooij et al., 2016; Schulze et al., 2014).

As the fucoxanthin content and productivity was lower under red: blue LEDs, other channels of light could be necessary such as green light and further research on light wavelengths and photoperiod is warranted.

6.3.4. Effect of lighting arrangement on commensal bacteria population

To the authors knowledge, no study has looked at the effect of lighting arrangements on the commensal bacterial population associated with *P. tricornutum*. *Marinobacter alkaliphilus* (TB2 – small white colony), *Halomonas neptunia* (TB1 – large white colony) and *Algoriphagus marincola* (TB4 – red colony) were present in *P. tricornutum* CCAP 1055/1. *Marinobacter alkaliphilus* (TB10 – small white colony) was the only bacterial species observed in *P. tricornutum* UTEX 646. *Marinobacter alkaliphilus* (TB3 - Halo and TB5 - small white colonies), *Halomonas titanicae* (TB9), *Sphingorhabdus* sp. (TB11 – yellow colony) and *Croceibacter atlanticus* (TB6 – orange colony) were observed in *P. tricornutum* N017. The fact that *Marinobacter* spp. were found in all strains and that *Halomonas* sp. was found in CCAP 1055/1 and N017 reveals that the bacteria are commensal. *P. tricornutum* typically inhabits brackish water environments such as rock pools where it lives planktonically or adheres to biofilms (De Martino et al., 2007).

Alphaproteobacteria are ubiquitous in diatom cultures and *Roseobacter* has been isolated and characterised from a *P. tricornutum* culture isolated in Ziamen, China (Chen et al., 2019). Marine agar has been widely used to isolate marine bacteria from *P. tricornutum* (Vuong et al., 2019). *Stappia* sp., *Halomonas* sp., *Rhizobium* sp., *Microbacteria* sp., and *Isomarina* sp. have been isolated from *P. tricornutum* UTEX 646 cultures, but *Stappia* sp. was shown to be the most abundant (Vuong et al., 2019).

To the authors knowledge this is the first report of *Croceibacter* and *Sphingorhabdus* being isolated from *P. tricornutum*. *Sphingorhabdus flavimaris* has been isolated from

Skeletonema marinoi and has been found to stimulate the growth of this diatom (Johansson et al., 2019). It would be interesting to investigate the effect of *Croceibacter* and *Sphingorhabdus* for improving productivities and to understand the metabolic interactions through a multi-omics approach.

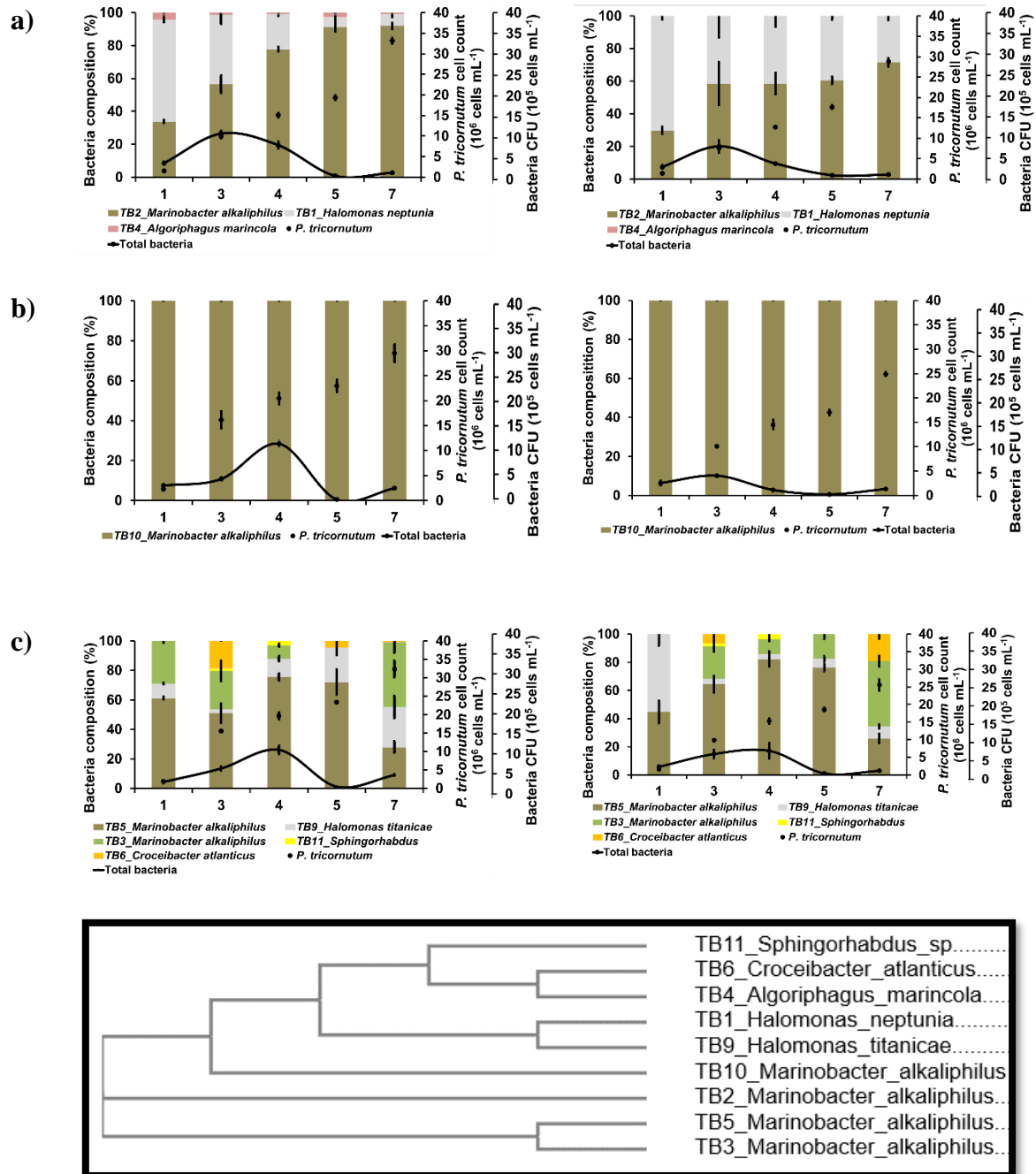


Figure 6.5 – Effect of lighting arrangement on commensal bacterial population; a) *P. tricornutum* CCAP 1055/1 under white and red: blue LEDs, b) *P. tricornutum* UTEX 646 under white and red: blue LEDs, c) *P. tricornutum* Necton N017 under white and red: blue LEDs

In *P. tricornutum* CCAP 1055/1 *Halomonas neptunia* TB1 was found to dominate in the early logarithmic growth stage but then *Marinobacter alkaliphilus* sp. was found to be dominant in later logarithmic growth (day 4-7) under both white and red: blue light. In UTEX 646 *Halomonas* sp. was the only bacterium observed on modified marine agar. For the Necton strain *Marinobacter* dominated at all cultivation stages.

A sinusoidal growth curve was observed for all cultures. The total bacteria numbers were lower under red: blue lighting for all strains. Fatty acids (C14:0, C16:0, C18:0, C16:1, C18:1 and C20:5) secreted into the medium can have an important role in regulating bacteria isolated from *P. tricornutum* (Vuong et al., 2019) which could have accounted for the sinusoidal profile. Other metabolites could also be responsible for regulating bacterial growth such as nucleotides, pigment derivatives, and peptides (Vuong et al., 2019). A homolog to the antioxidant galactose oxidase (forms hydrogen peroxide) has previously been detected in *P. tricornutum* and there is evidence for a reactive oxygen substance based defence system (Buhmann et al., 2016), but it remains unclear whether diatoms are able to selectively discriminate between beneficial and antagonistic bacteria. However, as a decrease in number of bacteria was observed in *P. tricornutum* cultivated with red: blue lights, it appeared that the red: blue LEDs resulted in a decrease in bacterial loading. It has been reported that blue light can kill species of bacteria (Cieplik et al., 2014; Enwemeka, 2013; Enwemeka et al., 2009), but this appears to be the first report that has investigated the effect on commensal bacteria associated with *P. tricornutum*. In future it would be interesting to further understand if blue light is responsible for decreasing the bacterial loading.

6.5. Conclusion

Of the three strains it was identified that UTEX 646 had the highest overall biomass productivity and the highest carbohydrate, protein, FAEE, and EPA productivity, whereas N017 had the highest fucoxanthin productivity. It was found that by using red: blue LEDs, a reduction in electricity consumption of 24 % could be obtained compared with white LEDs without a significant decrease in productivities. When comparing the lighting source, red: blue LEDs resulted in a higher protein, FAEE and EPA productivity. Red: blue light was found to influence the commensal bacterial population in the *P. tricornutum* culture. The total bacterial count was observed to be lower under red: blue LEDs for all three strains over the cultivation period, but the bacterial community composition was similar for each *P.*

tricornutum strain, showcasing that red: blue LEDs could be used as a strategy for controlling the bacterial population. To the authors knowledge this is the first report of *Croceibacter* and *Sphingorhabdus* being isolated from *P. tricornutum* and these co-cultures could offer advantages in biomanufacturing for improving productivities and this warrants investigation.

Acknowledgements

TOB acknowledges financial assistance from UK-EPSRC (DTA 1912024) and Postgraduate Researcher Experience Programme (PREP). The authors would like to thank Prof. Mike Allen for providing the UTEX 646 strain and Necton S.A. for the use of their strain. The authors would also like to thank Prof. Maria Barbosa and Prof. René Wijffels at the Bioprocess Engineering (BPE) department at Wageningen University for the use of the AlgaePARC and Radix facilities and for the valuable interactions. A special thanks goes to Wendy Evers for her technical advice and support. The authors would also like to thank Duncan Schofield for his technical assistance in the CHNS analysis.

Author contributions

TOB conceived and wrote the paper with guidance from SV. All authors declare that they have read and agree with the manuscript.

Conflicts of interest

The authors declare no conflict of interest.

Chapter 7: General discussion: *Phaeodactylum tricornutum*: an emerging cell factory for both fucoxanthin production and aquaculture feed (aquafeed) supplementation

Abstract

Phaeodactylum tricornutum is a well-known microalga with the potential to be a cell factory and biorefinery chassis. This microalga produces a high value product, fucoxanthin, which is of commercial interest and the remaining biomass which is rich in EPA and protein is valued as an aquaculture feed (aquafeed) additive. The main bottlenecks to utilise *P. tricornutum* as a biorefinery chassis for the commercialisation of fucoxanthin and a depigmented microalgal biomass for aquafeed are low biomass productivities, low product yields, coupled with high production costs, primarily due to the high CAPEX involved with photobioreactors (PBRs) (such as glass tubular PBRs) and artificial illumination. Process development can help elevate product contents whilst decreasing the total cost of production. This chapter first discusses the value of the products fucoxanthin and EPA from *P. tricornutum* and strategies to improve their yields. The bottlenecks to overcome for the exploitation of *P. tricornutum* as a biorefinery chassis are then evaluated. Wet extraction is discussed to bypass the costly drying process and an outlook is provided on how to commercially exploit *P. tricornutum* as a biorefinery chassis aimed at fucoxanthin and valuable aquafeed biomass for implementation in the UK.

7.1 Microalgae as a global solution to world issues

With the world population projected to reach 9.6 billion by 2050 (Tripathi et al., 2018), we will require biobased manufacturing practices to meet food and chemical demands. Industrial production of microalgae can provide valuable products including bioplastics, biofuels, pigments (astaxanthin, β -carotene, phycocyanin and fucoxanthin), nutraceuticals (omega-3 fatty acids), cosmetics, and pharmaceuticals (Butler et al., 2020; Sethi et al., 2020).

Several microalgal species are successfully produced at industrial scale (*Chlorella vulgaris*, *Arthrospira maxima*, *Dunaliella* spp., and *Haematococcus pluvialis*), with a total production of 20,000 tonnes dry weight (DW) per year, but primarily they have been exploited for single high-value pigments (Benemann et al., 2018). *Arthrospira* (*Spirulina*) and *Chlorella* bulk selling prices range from US \$10-30 ton⁻¹ and the market is about half a billion dollars annually, with a tenfold increase at the consumer level (Benemann et al., 2018). It has been projected by 2026 the global market for microalgae products could reach US \$53.43 billion (Credence Research, 2020)). The top three microalgae producing countries are in Europe (France, Ireland, and Spain) with a major focus on food-related applications, including the production of high-value products such as nutraceuticals (Araújo and García-tasende, 2021). Microalgae production and consumption in Europe is limited by lack of consumer awareness of the health benefits of microalgae, in conjunction with technological and regulatory hurdles.

7.2 The diatom *Phaeodactylum tricornutum* as an emerging cell factory: products of interest (fucoxanthin and eicosapentaenoic acid)

Microalgae can grow in seawater, brackish water, using marginal land or remediating wastewater (nitrogen or phosphorous recovery, heavy metals absorption and pharmaceutical waste) without the requirement for fertile arable soil, and they can use CO₂ from flue gases of power stations containing SO_x and NO_x (Ma et al., 2016). Within the eukaryotic microalgae, marine diatoms are the dominant primary producers in the ocean and amongst the most productive (responsible for ~40 % of primary production), responsible for 20 % of global carbon fixation (Bowler et al., 2010; Branco-Vieira et al., 2020).

The microalga *P. tricornutum* is a model diatom species that is currently cultivated industrially for single high-value, speciality products; EPA (Simris-Sweden) and fucoxanthin (Alga Technologies-Israel). *P. tricornutum* is also known to accumulate a spectrum of other natural products which have been demonstrated at pilot-scale (the omega-3 docosahexanoic acid for cognitive development and the antioxidant carbohydrate, chrysolaminarin) and engineered marketable products at laboratory scale (the triterpenoid lupeol, bioplastics and antibodies) (Butler et al., 2020; Sethi et al., 2020). At laboratory and pilot scale, *P. tricornutum* has been shown to dominate and outcompete other microalgal species with a tolerance for high pH and an ability to grow under low light (Remmers et al., 2018).

One high-value product which has been studied in detail is fucoxanthin. Fucoxanthin is a xanthophyll carotenoid and is widely found in brown macroalgae (0.01-0.1 % DW) and diatoms (0.19-5.92 % DW) (McClure et al., 2018; Reboloso-Fuentes et al., 2001; S. Wang et al., 2018b) and *P. tricornutum* typically exhibits a content between 1.02-2.61 % DW (Derwenskus et al., 2020a). Fucoxanthin has a plethora of health benefits (animal and human trials) including anti-inflammatory, anti-tumour, anti-obesity, antimalarial and anti-diabetes (Bae et al., 2020). The selling price is estimated at US \$175 kg⁻¹ for biomass containing 1 % fucoxanthin (Leu & Boussiba, 2014) and US \$0.20-0.74 in capsular/softgel form (Timmermans, 2017; Wu et al., 2016). However, to date *P. tricornutum* has not been granted Novel Food status which limits its market potential, especially in Europe. In 2016, the global fucoxanthin production was approximately 500 tons and the market appeared to have grown at an annual rate of 5.3 % to 2021 (Gao et al., 2020). In diatoms, fucoxanthin is one of the primary light harvesting pigments (along with chlorophyll *a* and *c*) in the FCP complex which traps light energy and offers photoprotection (Wang et al., 2018).

Once fucoxanthin is extracted, the remaining biomass is considered of interest for aquafeed (EPA, protein, carbohydrate, minerals, and vitamins), and particularly EPA as an omega-3 fatty acid is crucial for larval development and human nutrition. Currently fishmeal and fish oil are used to satisfy the growing aquaculture industry which consumes >70 % of fish meal and fish oil (Shah et al., 2018). Global production of fish oil is estimated at one million tonnes annually, but this is unsustainable and the cost is rising to >US \$3000 ton⁻¹ (J. Chen et al., 2016; Shah et al., 2018). *P. tricornutum* is either incorporated in the aquafeed for finfish or shrimp (zoea phase and larval phases) or as live prey for rotifers, artemia, copepods and shellfish (pre-set and post set) (<http://phytobloom.com/aquaculture/>). EPA is an essential omega-3 fatty acid for human nutrition with the recommended daily intake (RDI) of 250 mg each day (Ryckebosch et al., 2014). EPA is a precursor for signalling molecules such as eicosanoids and has defined benefits in cardiovascular health, cancer treatment, and for numerous mental health diseases (Deckelbaum & Torrejon, 2012; Oscarsson & Hurt-Camejo, 2017). EPA is currently mainly derived from fish oil (and to some extent krill oil) and to meet the RDI 0.8 g of fish oil must be consumed daily by humans, whereas for microalgae the daily intake would range from 1.3-12.5 g oil day⁻¹ (Ryckebosch et al., 2014). The market size for EPA is US \$300 million and the selling price is US \$200-500 kg⁻¹ (Alam et al., 2020). EPA is highly dependent on the strain, PBR system and cultivation conditions and can range from 3.1-5 % DW without using GMO methods (Derwenskus et al., 2020).

To date, utilising photoautotrophy, microalgae can attain higher biomass productivities (60–75 tons dry weight ha⁻¹ y⁻¹) and higher photosynthetic efficiencies (3-10 % of solar energy) at commercial scale in PBRs (Sethi et al., 2020) when compared with open ponds (45 tons dry weight ha⁻¹ y⁻¹) (Richmond, 2013).

To date the highest volumetric productivities of EPA and fucoxanthin obtained using a biorefinery approach was in a flat-panel photobioreactor (9.6 and 4.7 mg L⁻¹ d⁻¹) during the exponential phase (day 6) with high nitrogen (14.5 mM) and phosphorous (0.88 mM) (Gao et al., 2017). High fucoxanthin and EPA content are typically obtained under low light and high nitrate (Fernández et al., 2000; McClure et al., 2018) but under nutrient-rich conditions EPA content has been found to be independent of the applied light intensity (Remmers et al., 2017). Even though *P. triornutum* is exploited commercially for fucoxanthin and EPA by a few companies, productivities are still low under outdoor conditions (especially cold climates) and the cost of production is high which limits its industrial application. Process optimisation is critical to increase yields, and medium composition, light, salinity and carbon supply can affect growth and biochemical composition and productivity. In addition, a major bottleneck is contamination. Contamination remains an unreported issue due to insufficient monitoring of crop and commercial sensitivity and this is a real industrial problem to overcome.

7.3 The diatom *Phaeodactylum triornutum* as an emerging cell factory: bottlenecks to commercialisation

The major bottlenecks to the commercialisation of *P. triornutum* for bulk production such as aquafeed are the low biomass/product yields, high cost of production (electricity due to pumping and artificial illumination, dewatering, extraction), regulatory (GRAS status in US and Novel Food status in Europe), and marketing of the plethora of health benefits for consumers). In this thesis, biomass and product (fucoxanthin, EPA, and protein) yields were elevated from baseline conditions and a cost-effective harvesting approach was devised. The fact microalgae are largely not economically viable is due to the high cost of production and low selling price where the process is mainly constrained by a single product approach. The reported fucoxanthin and EPA productivities of *P. triornutum* range from 0.041-8.2 mg L⁻¹ d⁻¹ and 0.90-56 mg L⁻¹ d⁻¹ (Table 6.1 and 6.2).

However, using a multi-product biorefinery approach where microalgal biomass is used as a feedstock for multiple products, can contribute to commercial viability. Furthermore, a multi approach to biorefinery can also contribute towards a circular economy and sustainability (Butler et al., 2020).

Table 7.1 - Fucoxanthin production from *P. tricornutum*

| Strain | Cultivation conditions | Content (% DW) | Productivity (mg L ⁻¹ d ⁻¹) | Reference |
|-------------|--|----------------|--|------------------------|
| CCAP 1055/1 | 8 L airlift PBR, JWP powder media, 143-221 $\mu\text{mol photons m}^{-2} \text{s}^{-1}$, 12:12 light:dark cycle, 8-18°C, pH 7.8 control (fed-batch) | 0.88 | 0.74 | Chapter 3 |
| | 8 L airlift PBR, JWP powder media, 21°C, stepwise light increase (82-117 $\mu\text{mol photons m}^{-2} \text{s}^{-1}$), 12:12 light:dark cycle, 21°C, pH 7.8 control (outdoor cultivation, Sheffield, UK) (fed-batch) | 0.62-0.66 | 0.23-0.37 | |
| CCAP 1055/1 | 250 mL flask, 5 x f/2 NP (4.42 mM nitrate, 0.18 mM phosphate), 33 % salinity, 2 % CO ₂ , 0.01 M glycerol, 142 $\mu\text{mol photons m}^{-2} \text{s}^{-1}$, continuous light, 21°C | 1.27 | 1.78 | Chapter 4 |
| N017 | 250 mL flask, Nutribloom (4 mM nitrate, 0.18 mM phosphate), natural seawater (12.1 ppt), 2 % CO ₂ , 142 $\mu\text{mol photons m}^{-2} \text{s}^{-1}$ warm white LEDs, continuous light, 21°C | 1.60 | 2.05 | Chapter 6 |
| SCSIO828 | 2 L flask, f/2, continuous light, 40 $\mu\text{mol photons m}^{-2} \text{s}^{-1}$, 25°C | 0.55 | - | (H. Wu et al., 2016) |
| CS 29/7 | 250 mL flask, 150 $\mu\text{mol photons m}^{-2} \text{s}^{-1}$, 12:12 light:dark cycle, 25°C | 0.19(AFDW) | 0.041 | (Ishika et al., 2017) |
| CS-29 | 5 L flat panel PBR, f/2 (10 x nitrate), 150 $\mu\text{mol photons m}^{-2} \text{s}^{-1}$, 12:12 light:dark cycle, 23°C | 5.92 | 2.3 | (McClure et al., 2018) |
| UTEX 646 | 800 mL column PBR, 2f medium, 30 $\mu\text{mol photons m}^{-2} \text{s}^{-1}$, 23°C | 0.75 | - | (Wang et al., 2018) |
| CCMP 2558 | 100 mL flask, modified f/2 medium, 300 $\mu\text{mol photons m}^{-2} \text{s}^{-1}$, 20 or 25°C | - | 0.0026-0.04 | (Nur et al., 2019) |
| EGE MACC-70 | 1 L aerated bottles, 2-7 L flat plate PBR, f/2 medium, continuous light (45-100 $\mu\text{mol photons m}^{-2} \text{s}^{-1}$), 18°C | - | 0.4-1.1 | (Guler et al., 2019) |
| CCMP 1327 | 250 mL flask, modified f/2 medium, two-phase mixotrophic cultivation: 1:1 red:blue LED, 20 $\mu\text{mol photons m}^{-2} \text{s}^{-1}$ | 0.13 | 8.2 | (Yang and Wei, 2020) |
| CCAP 1055/1 | 250 mL flasks, Mann and Myers, 20 $\mu\text{mol photons m}^{-2} \text{s}^{-1}$, continuous illumination 20°C | 1.20 | 0.4 | (Song et al., 2020) |

*All studies were batch unless otherwise stated

Table 7.2 - EPA production from *P. tricornutum*

| Strain | Cultivation conditions | Content (% DW) | Productivity (mg L ⁻¹ d ⁻¹) | Reference |
|----------------|--|----------------|--|----------------------------------|
| CCAP 1055/1 | 8 L airlift PBR, JWP powder media, 143-221 $\mu\text{mol photons m}^{-2} \text{s}^{-1}$, 12:12 light:dark cycle, 8-18°C, pH 7.8 control (fed-batch) | 1.89 | 1.59 | Chapter 3 |
| | JWP powder media, 8 L airlift PBR, JWP powder media, 21°C, stepwise light increase (82-117 $\mu\text{mol photons m}^{-2} \text{s}^{-1}$), 12:12 light:dark cycle, 21°C, pH 7.8 control (outdoor cultivation, Sheffield, UK) (fed-batch) | 2.51-2.59 | 1.22-1.47 | |
| CCAP 1055/1 | 250 mL flask, 5 x f/2 NP (4.42 mM nitrate, 0.18 mM phosphate), 33 % salinity, 2 % CO ₂ , 0.01 M glycerol, 142 $\mu\text{mol photons m}^{-2} \text{s}^{-1}$, continuous light, 21°C | 3.80 | 7.54 | Chapter 4 |
| UTEX 646 | 250 mL flask, Nutribloom (4 mM nitrate, 0.18 mM phosphate), natural seawater (12.1 ppt), 2 % CO ₂ , 142 $\mu\text{mol photons m}^{-2} \text{s}^{-1}$ 2.25:1 red: blue LEDs, continuous light, 21°C | 2.74 | 3.83 | Chapter 6 |
| UTEX 640 | 75 mL tubes, 20°C, 50 $\mu\text{mol photons m}^{-2} \text{s}^{-1}$, 16:8 light:dark cycle, 21.5°C, 5 % CO ₂ | 3.3 | 19 | (Yongmanitchai and Ward, 1991) |
| UTEX 640 | 50 L external loop airlift PBR, Mann and Myers medium, 21°C, seawater (outdoor cultivation, Almeria, Spain), pH 7.6 control, (fed-batch) | - | 50 | (Acién Fernández et al., 2000) |
| UTEX 640 | 60 L split-cylinder airlift PBR, modified Ukeles medium, 0.1 M glycerol, 0.01 M urea (outdoor cultivation, Almeria, Spain) (fed-batch) | 3 | 56 | (Fernández Sevilla et al., 2004) |
| M26 | 300 mL glass cylinders, 15°C, Walne's medium, 120-150 $\mu\text{mol photons m}^{-2} \text{s}^{-1}$, continuous light, seawater (29 psu), 1 % CO ₂ | 3.4 | 5.32 | (Steinrücken et al., 2017) |
| UTEX 646 | 20 L hanging bag PBR, 23°C, 4 x f/2 medium, 1 % CO ₂ , 20 % salinity, 120 $\mu\text{mol photons m}^{-2} \text{s}^{-1}$, final 3 days 30 $\mu\text{mol photons m}^{-2} \text{s}^{-1}$ | 2.77 | 3.48 | (Wang et al., 2018) |
| SAG 1090-1b | Flat panel Algaemist, 20°C, on-demand CO ₂ sparging, 60-750 $\mu\text{mol photons m}^{-2} \text{s}^{-1}$, 16:8 light:dark cycle (| - | 6-12 | (Remmers et al., 2017) |
| CCFM 06 (Fito) | 40 L Green Wall Panels, modified f/2 medium (29 mM nitrate, 2.9 mM phosphate), salinity 29 PSU, 5-25°C (outdoor cultivation, Bergen, Norway) (fed-batch) | 4.4 | 9.76 | (Steinrücken et al., 2018) |
| CCAP 1055/1 | 250 mL flasks, Mann and Myers, 20 $\mu\text{mol photons m}^{-2} \text{s}^{-1}$, continuous illumination 20°C | 2.6 | 0.90 | (Song et al., 2020) |

*All studies were batch unless otherwise stated

In this thesis, four bottlenecks were focussed upon (outdoor cultivation in a cold climate, low biomass/product yields, cost effective and environmentally friendly harvesting, and low OPEX red: blue LED lighting). First, we aimed to determine if *P. tricornutum* could be grown in cold outdoor conditions in a prototype airlift photobioreactor. It was revealed that *P. tricornutum* could be grown in a prototype airlift PBR using a commercially available powdered media both indoors and outdoors without contamination posing a threat to reduced productivities (**chapter 2**). Indoor cultivation resulted in a higher biomass and fucoxanthin yield (with a higher average protein, chlorophyll *a*, and fucoxanthin content). Outdoor cultivation resulted in a higher protein, carbohydrate, total fatty acid (TFA), and EPA productivity (with a higher TFA, EPA, and carbohydrate content). Trends between environmental conditions (temperature and light) were evaluated and EPA content appeared to be inversely correlated with temperature. A high throughput flask screening approach was used to optimise product yields, particularly fucoxanthin and EPA using f/2 medium as a baseline. A culture medium consisting of nitrate and phosphate at 4.41 mM and 0.18 mM (5-fold those employed in the traditional f/2 medium), salinity at 33 %, 2 % CO₂ (v/v in air), and a transition to mixotrophy using glycerol (0.01 M) were found to result in increased biomass, protein, fucoxanthin, EPA, and protein yields (up to 9-fold) (**chapter 3**). We aimed to develop an economically viable and biobased solution to harvesting. It was shown that *P. tricornutum* could be harvested by a biobased tannic acid derivative of the invasive Acacia tree in only 10 minutes which was more economical than other chemical flocculants and harvesting methods (**chapter 4**). Finally, three different *P. tricornutum* strains (CCAP 1055/1, UTEX 646 and a commercial strain (N017, Necton, Portugal)) were screened for their potential as a biorefinery chassis. Under warm white light emitting diodes (LEDs) it was identified that UTEX 646 had the highest biomass, EPA and protein yield, whereas the commercial *P. tricornutum* N017 resulted in the highest fucoxanthin yield. When comparing the lighting source, warm white LEDs resulted in a higher biomass, fucoxanthin and carbohydrate yield but a lower protein, TFA and EPA yield compared with red: blue LEDs. It was observed that the commensal bacterial community composition was similar under white and red: blue LEDs but the total bacterial count was observed to be lower under red: blue LEDs for all three strains over the cultivation period, showcasing the potential to reduce bacterial loading (**chapter 5**). Knowledge gained from this thesis can be applied to both upstream and downstream processing within industrial *P. tricornutum* production.

7.4 *Phaeodactylum tricornutum*: indoor vs outdoor UK cultivation at cold temperatures and low light

Designing an economical medium which is easy to prepare is a bottleneck to be addressed. The optimal cost effective medium for obtaining relatively high biomass, fucoxanthin, EPA, and protein yields, utilising a biorefinery approach for the model strain *P. tricornutum* CCAP 1055/1 was Cell-Hi JWP from Varicon Aqua Solutions Ltd. This powder could be added straight to the mixing tank and added over filters to the reactor.

P. tricornutum can be cultivated indoors and outdoors in a range of photobioreactors (PBRs) (including tubular, flat-plate, and column) and open (raceway) ponds with biomass and product yields described in Butler et al. (2020). Flat panel configurations are optimal for biomass, EPA and fucoxanthin productivities attributable to their low shear stress and effective illumination (Guler et al., 2019), nevertheless they are constrained by high rates of biofouling and their difficulty to clean (Lizzul, 2016). PBRs result in higher productivities and more hygienic processes than raceway cultivation and can prevent (to some degree) against contamination and grazers (Scott et al., 2010) but they are cost prohibitive for most microalgal production facilities. An airlift PBR (PhycoLift) system was designed mimicking the commercial system which has a low areal footprint. It was determined that outdoor UK cultivation was possible utilising the airlift PBR under low light and temperatures (8-18°C) and there was an inverse relationship between temperature and EPA content. It was concluded that indoor cultivation resulted in a higher volumetric and areal productivity, and higher EPA, fucoxanthin and protein yields compared with outdoor cultivation. As the lighting conditions were similar it seems plausible that temperature control was important to ensure higher biomass productivities. During cultivation indoors in flasks, and indoors/outdoors in the airlift PBR, the total commensal bacteria content showed a sinusoidal profile. *Halomonas* sp. was dominant at low *P. tricornutum* densities but *Marinobacter* sp. was more dominant at higher *P. tricornutum* densities. *Halomonas* had a higher growth rate and this could have ensured early dominance but particular culture conditions could have resulted in a shift to *Marinobacter* sp. Fatty acid analysis revealed that C14:0, C16:0 and C18:0 (with C16:0 and C18:0 accounting for >95 % of TFAs detected) were present in the EPS but no even-numbered antibacterial fatty acids such as EPA or C16:1 was detected over the indoor or outdoor runs which has previously been observed in flask cultures (Vuong et al., 2019). Other metabolites could also be responsible for regulating bacterial growth such as nucleotides, pigment derivatives, and peptides (Vuong et al., 2019). A homolog to the antioxidant galactose oxidase

(forms hydrogen peroxide) has previously been detected in *P. tricornutum* and there is evidence for a reactive oxygen substance based defence system (Buhmann et al., 2016).

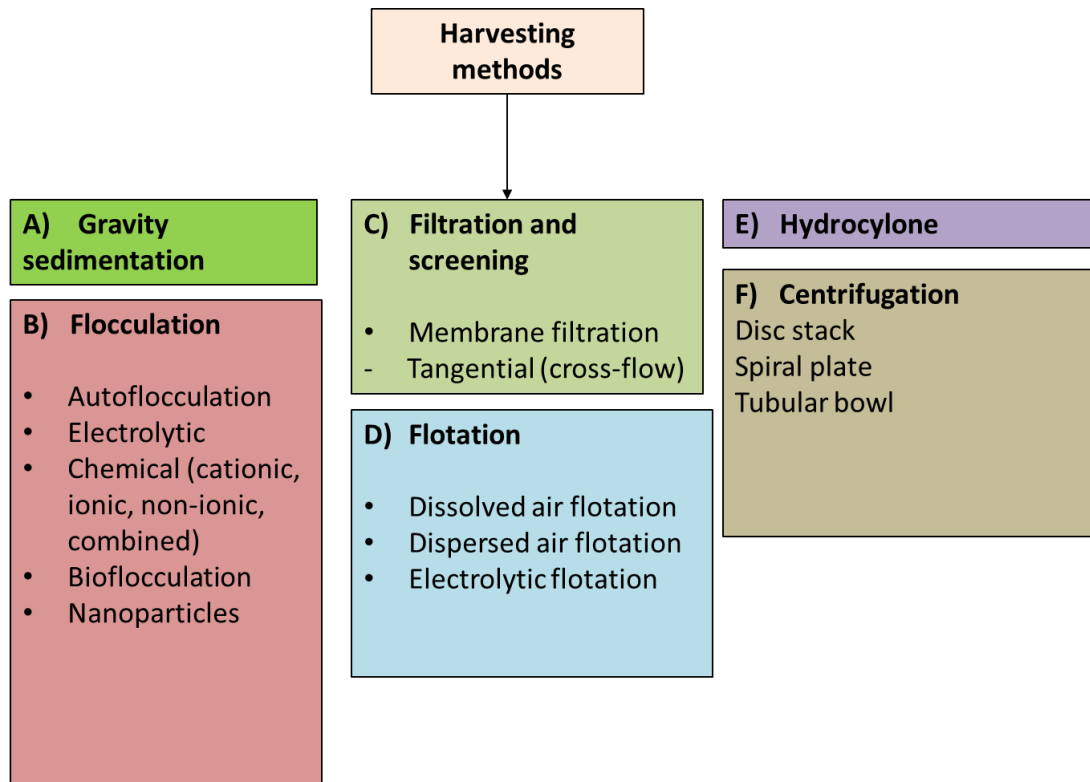
Challenges to overcome within PBRs are reactor design (ensuring high volumetric/areal productivities), high yield on light, lower shear (but minimal fouling), low pumping costs, avoidance of high energy requirement for temperature maintenance, and a requirement to minimise biomass losses due to photorespiration (Meiser et al., 2004; Tredici et al., 2015). Further work should be conducted utilising artificial light outdoors using greenhouses to increase photosynthetic activity and minimise photorespiration at night. Employing temperature control could also help increase biomass and product yields.

7.5 Culture condition manipulation for increased product yields

A high throughput flask screening approach was used to optimise product yields, particularly fucoxanthin and EPA using *f/2* medium as a baseline. It was observed that bicarbonate supplementation (5-125 mM) resulted in a decrease in biomass and product yields. In addition, decreased or increased salinity from the optimum (33%) resulted in a reduction in product yields. However, a culture medium consisting of nitrate and phosphate at 4.41 mM and 0.18 mM (5-fold those employed in the traditional *f/2* medium), salinity at 33 %, 2 % CO₂ (v/v in air), and a transition to mixotrophy using glycerol (0.01 M) were found to result in increased biomass (0.20 g L⁻¹ d⁻¹), fucoxanthin (1.78 mg L⁻¹ d⁻¹), EPA (7.54 mg L⁻¹ d⁻¹), and protein yields (15.65 mg L⁻¹ d⁻¹), up to ten-fold higher than the *f/2* control medium. This high throughput setup has application as a low-cost standardised setup for academia and industry to rapidly screen treatments for elevating biomass and product yield.

7.6 The transition away from chemical flocculants: commercially viable harvesting of *P. tricornutum*

Harvesting can contribute up to 15% of the total production cost for microalgal biomanufacturing (Fasaei et al., 2018). A variety of methods have been investigated for commercial harvesting of microalgae and these are shown below.



Currently, centrifugation (disc-stack) and decanter bowl centrifuges are used as the industry standard and this has remained relatively unchanged since the early 1990s. However, centrifugation has a high CAPEX and OPEX (energy cost of 1 KWh m⁻³), accounting for 20-25 % of the cultivation cost and thus are only used for the high value product markets (Butler et al., 2020; Butler and Guimarães, 2021). Gravity sedimentation would be the most cost-effective method but *P. tricornutum* was not found to auto-flocculate and therefore a series of biobased flocculants (which cause flocculation whereby particles in suspension are sedimented) were explored. For commercial viability, the harvesting technique must meet specific criteria: increase the solid content to 5–25% total dry matter (solids content) depending on the downstream application, be time efficient (requiring <1 h), be of high efficacy (>80%), be cost effective, require a low energy input, leave behind little or no toxic residues, and not affect the quality of the biomass downstream (‘t Lam et al., 2017; Vandamme et al., 2010). A wide variety of harvesting methods have been suggested for *P. tricornutum* (reviewed by Butler et al., 2020). However, the most well researched area has focussed on flocculation with this method being scalable. In this study, a range of biobased flocculants (chitosan from crab shells, *Moringa oleifera* seed extract, pectin from bananas, tannic acid- based derivatives from *Acacia* tree bark and egg shell powder) were compared with traditional chemical flocculants (aluminium sulphate, iron chloride and sodium hydroxide). A standardised harvesting setup

was used for this study regarding the diatom *P. tricornutum*. It was concluded that Tanac's tannin based Tanfloc 8025 (SL range) was the most promising, requiring a low concentration (10.4 kg ton⁻¹ biomass), at low cost (\$27.04 ton⁻¹ microalgal biomass). The flocculant was effective over a wide pH (7.5–10.0) and temperature (15–28 °C) range and harvesting (>85% efficiency) occurred in 10 mins, which resulted in a biomass concentration factor of ≥ 5.69 (0.63 % solids content achieved) (Butler et al., 2021).

Tanfloc 8025 is useful as a primary dewatering step but should not be used as a single harvesting stage since further improvement is necessary. An optimal harvesting apparatus should be used with a conical bottom to aid sedimentation and mixing times for uniform flocculant dispersal and floc formation should be investigated in more detail to maximise the performance of this biobased flocculant.

7.7 Strain screening and potential of white and red: blue LEDs

Three different *P. tricornutum* strains (CCAP 1055/1, UTEX 646 and N017 (a commercial strain, Necton, Portugal)) were compared to determine the optimal strain for producing the highest biomass, protein, fucoxanthin, and EPA yield in natural seawater. It was identified that *P. tricornutum* UTEX 646 had the highest biomass productivity (0.16 g L⁻¹ d⁻¹), along with the highest carbohydrate (39.28 mg L⁻¹ d⁻¹), protein (42.01 mg L⁻¹ d⁻¹), TFA (12.18 mg L⁻¹ d⁻¹) and EPA yield (4.33 mg L⁻¹ d⁻¹). Whereas, *P. tricornutum* N017 from Necton resulted in the highest fucoxanthin yield (2.12 mg L⁻¹ d⁻¹) which was similar to UTEX 646 but 2.5-fold higher than CCAP 1055/1. The second hypothesis tested was that red: blue LEDs could result in higher productivities. When comparing the lighting source, warm white light emitting diodes (LEDs) resulted in a higher biomass, fucoxanthin and protein yield (>12, 18, and 24 % strain improvement) than red: blue LEDs. However, red: blue LEDs resulted in a higher EPA and TFA yield compared with warm white LEDs (13 and 15 % strain improvement).

The third hypothesis tested was the potential of red: blue lights to affect the bacterial community composition and to reduce the bacterial loading of the *P. tricornutum* culture. It was observed that the bacterial community composition was similar under white and red: blue LEDs. *Marinobacter* sp. was present in all strains and dominated at most stages of cultivation indicating a commensal relationship. *Halomonas* sp. was only present in *P. tricornutum* CCAP

1055/1 and the commercial Portuguese (Necton) strain N017. *Algoriphagus* sp. was only present in *P. tricornutum* CCAP 1055/1 and was low in number (<3 % of the population). Comparatively, *Sphingorhabdus* and *Croceibacter* spp. were present in the commercial Portuguese (Necton) strain. The total bacterial count was observed to be lower under red: blue LEDs for all three strains over the cultivation period, showcasing the potential of red: blue LEDs as a contamination mitigation strategy.

7.8 Main conclusion

In this thesis, a cost-effective powdered media formulation (JWP) was shown to involve low preparation time and outperform conventional liquid f/2 medium. JWP resulted in a higher fucoxanthin, EPA, and protein yield. JWP was subsequently used for cultivation of *P. tricornutum* indoors and outdoors in an airlift photobioreactor (PhycoLift) using a repeated fed-batch approach. Indoor cultivation resulted in a higher biomass, protein, and fucoxanthin yield but outdoor cultivation resulted in a higher EPA content which appeared to be inversely correlated with temperature. Commensal bacteria (*Marinobacter* sp. and *Halomonas* sp.) were isolated from the cultures and identified. The total bacteria count showed a sinusoidal growth profile, and it was apparent that *Halomonas* predominated at low microalgal densities, but at higher microalgal densities there was a community shift to *Marinobacter*. It was hypothesised that EPA was secreted by the microalga *P. tricornutum* and could have had an effect on controlling the population. However, when the extracellular matrix was analysed it did not contain EPA, and the metabolites responsible for regulating the bacterial growth remain to be elucidated.

With downstream processing accounting for 70-80 % of the cost of microalgal biomanufacturing, and harvesting accounting for up to 30 % of the production cost, alternative methods for bioflocculation were evaluated. *P. tricornutum* could be economically harvested using a tannic acid-based derivative that was determined to be optimal; Flocculation occurred within 10 minutes, resulting in a high harvesting efficiency (>85 %), a concentration factor ≥ 5.6 , and was economical (US \$21 ton^{-1} microalgae biomass harvested) offering a cost saving of >US \$61 ton^{-1} compared with chemical (US \$82 and 264-560 ton^{-1} for sodium hydroxide and aluminium sulphate respectively) and chitosan as a traditional biobased flocculant (US \$360-18,000 ton^{-1}).

A high throughput screening approach was used to optimise product yields, particularly fucoxanthin and EPA using f/2 medium as a baseline. Conventionally f/2 medium has been used for the cultivation of *P. tricornutum* and we have demonstrated why it is a ‘maintenance’ medium and not a production medium due to its low nitrate and phosphate content. A culture medium consisting of nitrate and phosphate at 4.41 mM and 0.17 mM (5-fold those employed in the traditional f/2 medium), salinity at 33 %, 2 % CO₂ (v/v in air), and a transition to mixotrophy using glycerol (0.1 M) was found to result in increased EPA, fucoxanthin and protein yields up to 9-fold higher.

In summary, this work entitled “The diatom *Phaeodactylum tricornutum* as a microalgal cell factory: utilising a biorefinery approach” has demonstrated that the Phycolift was suitable for the utilisation of *P. tricornutum* as a biorefinery chassis and Tanfloc as a biobased flocculant was commercially viable for harvesting. This thesis has commercial application to rapidly screen treatments for elevating biomass and product yield, whilst decreasing the time taken for harvesting at reduced cost for example, the production of fucoxanthin, and a depigmented by-product as an aquaculture additive.

7.9 Future outlook

7.9.1 Upstream developments

The maximum biomass concentration achieved to date in a fed-batch approach is 25.4 g L⁻¹ with a volumetric productivity of 1.7 g L⁻¹ d⁻¹ in an outdoor airlift PBR in Almería, Spain utilising mixotrophic cultivation with glycerol (0.1 M) (Fernández Sevilla et al., 2004). The highest volumetric productivity of EPA (56 mg L⁻¹ d⁻¹) was also obtained under the same conditions with 3 % DW EPA (Fernández Sevilla et al., 2004). The maximum fucoxanthin productivity (8.22 mg L⁻¹ d⁻¹) was achieved in a two-phase cultivation approach by using red: blue light (6:1) in phase 1 with high nitrate and 0.1 M glycerol, and a transition to red: blue light (5:1) by enhancing blue light and the addition of tryptone in phase 2 (Yang and Wei, 2020)

Utilising a biorefinery approach the highest fucoxanthin, EPA, and chrysolaminarin productivities (4.7, 9.6, and 93.6 mg L⁻¹ d⁻¹ respectively) were obtained in indoor flat-plate PBRs under photoautotrophic conditions with high nitrate with fucoxanthin, EPA and

chrysolaminarin yields of 0.7, 2.3 and 14 % DW respectively, but the EPA/fucoxanthin productivities and yields were lower than using a single-product approach (Baoyan et al., 2017).

Tubular systems have been the most widely developed of the commercialised systems with global suppliers such as Varicon Aqua Solutions Ltd. and Lgem having constructed and deployed numerous systems for both commercial and academic applications. Tubular configurations are favourable over plate configurations as they have higher liquid velocities, lower biofouling rates, they are easier to disassemble and clean, and the modular nature of the tubes allows for easy replacement (Lizzul, 2016). Vertical tubular systems have a low areal footprint and can lead to high volumetric and areal productivities. PBR design will be critical for ensuring most of the light is captured by the algal cells and often the light path will be fixed at 65 mm for tubular PBRs for standard glass tubes. Automated self-cleaning systems should be built in to prevent or minimise downtime.

A daily harvesting mode should be employed using a chemostat approach and the optimal dilution rate needs to be determined (typically 20-40 %) to avoid excessive dilution of the culture, to minimise fouling/contamination, and to ensure operation >3 months (Butler and Guimarães, 2021). It remains to be determined if a turbidostat or chemostat approach is the optimal bioprocess and future harvesting strategies should involve automated harvesting, medium recycling, and culture dilution to reduce OPEX from labour.

For a biorefinery approach (operating at high biomass, fucoxanthin, EPA, and protein productivities), ensuring a high biomass concentration will result in a low light per cell or per gram of biomass and enhance the EPA and fucoxanthin content, but there will be a trade-off with obtaining high biomass productivities (high light per cell). The effect of glycerol addition needs to be studied in more depth for increasing biomass and product yields, looking specifically at uptake rates, avoidance of reduced photosynthetic activity, and the control of contamination.

Red light promotes cell growth and blue light enhances fucoxanthin yield, with blue light more economical than red: blue LED light and white light (50 and 75 % of the energy input) (Yang and Wei, 2020). The FCP complex contains seven molecules of chlorophyll *a*, two molecules of chlorophyll *c* and seven molecules of fucoxanthin which is responsible for harvesting blue-green light and dissipating energy in diatoms (Wang et al., 2019). It has been determined that green light results in the highest fucoxanthin excitation, followed by white, and then blue light (Shimura and Fujita, 1975). The lowest level of chlorophyll content was observed under green light and increased with white and blue light (Shimura and Fujita, 1975).

However, the intracellular amount of fucoxanthin under green light was similar to that under white light (Yang and Wei, 2020). Green light upregulates Zeaxanthin epoxidase (ZEP) and lycopene β -cyclase (LCYB) but the positive effects disappears after greater than 24 h exposure, whereas but blue light upregulates PSY, phytoene desaturase (PDS), ζ -Carotene desaturase (ZDS) and ZEP (Yang et al., 2020). Blue LEDs have been observed to result in the highest fucoxanthin productivity whilst minimising energy consumption compared with white light and a mixture of red: blue LEDs in *Cylindrotheca closterium* (Wang et al., 2018b). A combination of red: blue light appears to be a suitable strategy for elevating biomass, EPA, and fucoxanthin but further work is warranted.

Genome editing tools offer a breakthrough in targeted mutagenesis for the development of *P. tricornutum* as a cell factory, given that the organism is diploid (33 paired chromosomes) and sexual reproduction cannot be controlled in the laboratory, limiting random mutagenesis as a useful tool for trait improvements. Nuclease-driven random integration of plasmid DNA into the genome of *P. tricornutum* has resulted in low transformation efficiencies, off-target cleavage, gene disruptions, and the impossibility to eliminate background mutations or integrated transgenes through outcrossing (Serif et al., 2018). CRISPR/Cas9 with an optimised Cas9 has been effective in *P. tricornutum* for inactivating single target genes and for the generation of stable knockouts (Nymark et al., 2016a; Slattery et al., 2018; Stukenberg et al., 2018). However, CRISPR-Cas9 experiments are challenging in diatoms such as *P. tricornutum* because the organism has two copies of its chromosomes and two individual DNA repair events must occur for the production of homozygous or heterozygous mutations at the target loci (Moosburner et al., 2020). Non-homologous end joining mediated mutagenesis is unpredictable in diploid organisms and requires highly sensitive genotyping methodologies (Moosburner et al., 2020). Genotyping the generated cell lines in *P. tricornutum* has been difficult and time consuming (Moosburner et al., 2020). Recently, bacterial conjugation has been optimised for Cas9 delivery and the mutant cell lines can easily be genotyped and isolated (<3 weeks) without relying on a known phenotype for screening mutants (Moosburner et al., 2020).

7.9.2 Development of wet sequential extraction methods to bypass drying and product formulation

Downstream processing encompasses harvesting, cell disruption, extraction, encapsulation, and formulation of the compound. Depending on the application, downstream processing can account for 20-70 % of the costs of the production process (’t Lam et al., 2017; Kapoore et al., 2018). The cost of centrifugation should be minimised or avoided by dewatering using biobased flocculation (up to 0.6 % solids using Tanfloc 8025) and tangential-flow membrane filtration (up to 15 % solids content) and the medium re-used for cultivation offering a cost and environmental saving.

7.9.3 High cost of drying

Dried biomass (5 % moisture content) is an excellent raw material for extraction of the various components present and is often used to increase the shelf life of the biomass, (Fasaei et al., 2018). However, drying can account for 89 % of the required energy input and 70–75 % of the total cost of processing (Taher et al., 2014). Drying is a costly activity because it takes a lot of energy to evaporate water. The choice of drying technique is related to energy cost, application of the dried biomass downstream (e.g., for animal feed or for extraction), and the processing time. Many common industrial drying technologies use heat, which may lead to degradation of the biochemical fractions. Different technologies are used to dry microalgae, and the most common are freeze drying, solar drying, oven drying, spray drying, and belt drying (de Souza et al., 2019). Other technologies have also been tested, such as vacuum, microwave, agitated thin-film, pulsed combustion, and crossflow air drying. The two most economically feasible drying methods are spray and drum drying (requiring a feedstock of 10-15 % solids) which both can result in a moisture content of 5 %, with >99 % recoveries. The cost of labour is comparable as one operator team can manage more units. Drum and spray drying have the capacity to dry 50 kg dry weight per hour, and the process can be automated enabling 24/7 drying, reducing the cost of labour. The energy consumption of a drum dryer is around 0.9 and a spray dryer is 1.09 kWh kg⁻¹ evaporated water which leads to 0.25- and 0.30-euros kg⁻¹ dried algae as total energy costs (Fasaei et al., 2018). Consumable costs are negligible. The overall costs are just below 0.5 euros kg⁻¹ dried algae for both drying systems with spray drying having lower CAPEX and drum drying having lower OPEX (Fasaei et al., 2018). Of the two methods, drum drying may be optimal as the powder is reported to be more

digestible, and has a dual advantage of sterilising the sample and breaking the cell wall (Show et al., 2015).

7.9.4 Extraction from dry material

A variety of solvents have been used for extracting fucoxanthin but as this compound is a polar molecule extraction is best performed using ethanol as a green solvent for high fucoxanthin recovery and yield (Delbrut et al., 2018). A range of extraction techniques (biochemical, mechanical and physical) have been investigated for microalgae reviewed by (Kapooore et al., 2018) and for *P. tricornutum* as described and reviewed by (Butler et al., 2020). Green solutions include microwave assisted extraction (MAE), pulsed electric field (PEF), ultrasound assisted extraction (UAE), pressurized liquid extraction (PLE), supercritical fluid extraction (SFE) and the use of enzymes and deep eutectic solvents (easier to synthesise, cheaper, and no purification required compared with ionic liquids) (Esquivel-Hernández et al., 2017; Płotka-Wasyłka et al., 2020). Microwave assisted extraction (MAE) has been used to extract fucoxanthin from dry *P. tricornutum* biomass utilising ethanol but only 32 % recovery was obtained (0.46 % DW) (20:1 ratio of solvent to biomass, 2.45 GHz, 850 W, 30°C, 2 mins) (Gilbert-lópez et al., 2017). An issue which should be further explored is a cost effective and environmentally friendly approach to the separation of fucoxanthin and EPA. Zhang et al (2018) developed a protocol for the extraction of fucoxanthin with ethanol from dried biomass and hexane was used for the partition of EPA. However, this process is complex and the extraction yields are low for industrial implementation. Furthermore, utilising hexane would be of environmental and human health concern where the EPA could not be used in many commercial applications and would not be suitable in an industrial context.

7.9.5 Wet extraction

To avoid the cost of drying a wet extraction method should be explored. However, with wet processing, product yields can be lower as shown in this thesis for EPA (Appendix B). The highest yield of fucoxanthin extracted to date was using pressurised liquid extraction (PLE) on wet *P. tricornutum* biomass at 100°C for 10 mins (1.63 % DW). A novel wet method combining cell disruption and extraction has been used to extract astaxanthin which could be applied to fucoxanthin extraction and involves hydrothermal disruption (200°C, 10 minutes, 6 MPa) in a microfluidic platform, which results in uniform and complete cell disruption and is more environmentally friendly than conventional chemical methods as water evaporation is

avoided, reducing the energy input (Cheng et al., 2018, 2017). Using a microfluidics approach with hydrothermal disruption for cell disruption, followed by ScCO₂ extraction (8 MPa, 55°C, with ethanol as a cosolvent, CO₂ /ethanol (4:1), flow rate 100 and 25 $\mu\text{L min}^{-1}$ respectively), astaxanthin could be extracted in 30 s (Cheng et al., 2018). Ethanol is believed to enhance the extraction rate and recovery through the removal of a two-phase interfacial barrier between the solvent and the water-wet surface of the cell and through the increased solubility of astaxanthin (de la Fuente et al., 2006). Olive oil has also been revealed as an attractive cosolvent with ~98% extraction efficiency but requires a longer extraction time (180 s) compared with ethanol, and the olive oil was found to immediately displace the water phase (Cheng et al., 2018).

In order to recover and separate a spectrum of products, a variety of cascade extraction techniques are required, the key is to separate the high-value products first and to enhance the economic feasibility of the process (Branco-Vieira et al., 2020). Few studies have addressed the option for sequentially extracting products from *P. tricornutum* using a biorefinery approach and it has been suggested that fucoxanthin should be extracted first followed by EPA and chrysolaminarin but the economic viability has yet to be shown (Zhang et al., 2018).

Alternatively, a ‘milking’ process where operating parameters are selected which temporarily open pores within the cell wall (as in electroporation) holds promise and can be a viable option for the selective release of fucoxanthin from the cell. Temporarily opening the pores could release fucoxanthin into the media, which would result in a simplified extraction process with a reduction in energy requirement and without disrupting the cells.

7.9.6 Fucoxanthin encapsulation

Post cell disruption and extraction, the final product will likely be a semisolid extract, an ‘oleoresin’, composed of fucoxanthin, some lipid and non-lipid component e.g., carbohydrate and this would then be encapsulated for use as a nutraceutical. Care must be taken to prevent oxidation during processing, handling, encapsulating, tableting, packaging, and storage.

A common method to deliver nutraceuticals into the human body is in a gelatine capsule (Jiang & Zhu, 2019) but they are not suitable for vegan consumers and carbohydrates can interfere with emulsion formation and thus alternative methods would be required (Khalid et al., 2017). The methods for encapsulation have been reviewed in detail by Khalid and Barrow (2018), and the aim is to enhance the stability, solubility, and bioavailability of the pigment. In the formation of an oil-water emulsion, the aim is to reduce the particle size and avoid droplet

aggregation and coalescence (Anarjan and Ping Tan, 2013). Changes in the droplet/particle size can result in changes in coloration, and the effectiveness of the emulsification process is affected by emulsifier concentration, heating temperature, and pH (Khalid et al., 2017). High temperature should be avoided as this can result in changes in stereochemistry (Khalid and Barrow, 2018). Typical methods for encapsulation include high-pressure homogenization, emulsification, phase inversion, nanoparticles, nanodispersions, and microencapsulation (reviewed by Butler and Guimarães, 2021). In the future, membrane and microchannel emulsification appear promising, but more focus is required on developing a cost-effective vegan capsule, using environmentally friendly chemicals, ensuring compliance with food safety and regulatory bodies while making the process scalable. A further emphasis should be on attaining higher encapsulation efficiency, smaller droplet formation, minimising fucoxanthin loss, whilst maintaining stability/functionality of the emulsion.

7.9.7 Aquafeed formulation

After the fucoxanthin is extracted from the *P. tricornutum* biomass for the nutraceutical sector, 90 % of the biomass remains unexploited such as protein, lipid, carbohydrate, vitamin and mineral fractions (Madeira et al., 2017). The remaining biomass could then be incorporated into aquafeed as has been shown for the delivery of omega-3 fatty acids in Salmonid feed (Sørensen et al., 2016). *P. tricornutum* biomass can result in improvements in growth rate, larval survival, feed conversion ratios, immune response and egg fecundity (Becker and Michels, 2004). Fish (in addition to other animals and humans) are unable to synthesise long chain polyunsaturated fatty acids (LC-PUFAs) such as EPA and these must be supplemented in the diet. Preparing aquafeed containing *P. tricornutum* is an extensive process and involves mixing, extrusion, pelletising, and drying. During the aquafeed mixing stage, *P. tricornutum* is mixed with dry ingredients (e.g., fishmeal, bulking agents, vitamins and minerals). The mixture is then extruded or pelletised to improve digestibility of starch and protein, whilst simultaneously minimising degradation of feed ingredients, followed by drying (oven or vacuum drying) to result in a final product with <10 % moisture (Jiang et al., 2019; Lim et al., 2018). Finally, after the pellet is made, the fish oil and water are added (Butler and Guimarães, 2021; Pereira et al., 2020).

7.9.8 Cost effective production of *P. tricornutum* for both fucoxanthin and depigmented microalgal biomass for aquaculture feed

The reference cost price of microalgae biomass (on a dry weight basis) in aquaculture hatcheries (taking into account a 25 m² system) is €290 kg⁻¹ and € 329 kg⁻¹ for tubular reactors under artificial light and a greenhouse, respectively (Oostlander et al., 2020) (dewatering and drying cost excluded). With state of the art technologies a cost price reduction of 92% could be achieved by changing the scale from 25 m² to 1500 m², resulting in a cost price of €43 kg⁻¹ DW, producing 4 tonnes year⁻¹ for tubular reactors in a greenhouse (Oostlander et al., 2020). It was identified that using artificial light could result in the highest cost reduction (35-36 %) for all tested scenarios.

Using a microalgae biorefinery model the cost of production is expected to be 3-7 euros kg⁻¹ DW (production in the south of Spain, 100 hectare scale) with a resulting revenue of 31 euros kg⁻¹ including cultivation (tubular PBRs) and downstream processing (Chauton et al., 2015). Electricity costs required for cultivation are high (62 % of the costs of cultivation in an indoor setting) (Pérez-López et al., 2014), and this can be attributed to LEDs, pumping costs (liquid and air pumps) and temperature regulation (in cost order). Consequently, microalgal products should be produced in an outdoor setting (or a greenhouse exploiting sunlight). Using bioflocculation (Tanfloc) in combination with wet extraction (PEF or MAE) could result in the selective release of fucoxanthin without killing the cells but this remains to be tested.

Currently, only one company globally has achieved large scale production of fucoxanthin (~500 kg year⁻¹ purified fucoxanthin) from macroalgae (Pers. Com. Fengzheng Gao, 2021). From the economic assessment of obtaining fucoxanthin from *P. tricornutum* (0.71 % DW), the minimum cost for purified fucoxanthin (90 % w/w) was 32,042 euros kg⁻¹ (Derwenskus et al., 2020b). An EPA oil has been developed by Simris, Sweden which has been granted Novel Food status but fucoxanthin is still not registered as a Novel Food and accepted for market in Europe.

For ensuring a sustainable and cost-effective, environmentally friendly production approach in the UK for fucoxanthin and aquafeed, a microalgae farm will need to be at least 1-hectare in scale and should be arranged in a greenhouse setting with 'outdoor cultivation' to utilise natural sunlight, with supplementation from low CAPEX/OPEX LEDs with energy sourced from solar renewable energy sources (wind/solar from the grid or solar panels on the greenhouse), organic fertilisers should be used and the media should be recycled (using membrane filtration for the removal of bacteria and inhibitory metabolites), with cooling using a cooling coil and misting in summer (to minimise energy expense and water footprint).

Further reductions in cost and increases in product yield will be required utilising an optimised PBR design (vertical tubular systems for lower land space occupation and higher areal productivities), utilising artificial light for increasing biomass productivity/yield on light/photosynthetic efficiency. An optimal harvesting regime needs to be designed using automation (daily harvesting using a turbidostat or chemostat). Combined omics studies (transcriptomics, proteomics and metabolomics) will determine bottlenecks in pathways for implementation of advanced genetic engineering for increasing biomass and product yields. If a genetically engineered strain is to be utilised for commercial production, caution is warranted because there are regulatory hurdles to overcome such as Directive 2001/18/EC in the European Union (EU) where the approval procedure can take 4–6 years and cost 7–15 million Euros (Hartung et al. 2014).

Utilising a stepwise increase in light during early stages of cultivation can avoid photoinhibition and culture crashes. Higher biomass concentrations, coupled with higher light intensities will lead to higher biomass productivities. Finally, before harvesting the light intensity should be reduced to maximise the fucoxanthin content and productivity. Furthermore, the biomass could be concentrated by flocculation using Tanfloc with submergible LEDs to supply low light to induce fucoxanthin accumulation.

Appendix A

This section contains supplementary figures, tables that resulted from Chapter 3 of this work.

Supplementary files

Table S3.1 - Microalgae cultivated with Cell-Hi F2P Powdered Media

| Organism | F2P concentration (g/L) | Product | Reference |
|---|-------------------------|--|--------------------------|
| <i>Chlorella minutissima</i> | 0.3 | Biomass, CO ₂ sequestration | Papazi et al., 2008 |
| <i>Chaetoceros muelleri</i> | - | Aquaculture feed | Liu et al., 2010 |
| <i>Isochrysis</i> Tahitian strain (CCAP 927/14) | - | | |
| <i>Nannochloropsis</i> sp. (Floria Aqua Farms Inc.) | - | Biomass, carotenoids, chlorophyll | Encarnação et al., 2012 |
| <i>Amphiprora</i> | 0.1 | Biomass | Hrafnisdóttir, 2012 |
| <i>Phaeodactylum tricornum</i> UTEX 642 | | | |
| <i>Tetraselmis suecica</i> PLY 305 | | | |
| <i>Isochrysis</i> Tahitian strain (CCAP 927/14) | 0.15 | Aquaculture feed | Naumann et al., 2013 |
| <i>Nannochloropsis</i> sp. (CCAP 211/78) | | | |
| <i>Nannochloropsis oculata</i> CCAP 849/1 | 0.15 0.45 | Biofuels | Sui, 2013 |
| Mixed algae | - | Biomass | Buchanan et al., 2013 |
| <i>Marinichlorella</i> KAS 603 | - | Molecular toolbox development | Schurr and Kuehnle, 2014 |
| <i>Tetraselmis chuii</i> | | | |
| <i>Pavlova lutheri</i> | 0.1 | Aquaculture feed | Rolton et al., 2014 |
| <i>Chaetoceros calcitrans</i> | | | |
| <i>Isochrysis</i> Tahitian strain (CCAP 927/14) | - | | |
| <i>Tetraselmis chuii</i> | - | Aquaculture feed | Rolton et al., 2015 |
| <i>Chaetoceros muelleri</i> | - | | |
| <i>Porphyridium purpureum</i> CCAP 1380/3 | 0.1 | Biomass, exopolysaccharides | Grünwald et al., 2015 |
| <i>Chaetoceros muelleri</i> CS-176 | 0.1 | Aquaculture feed | Schmitz et al., 2015 |
| <i>Tetraselmis chuii</i> CS-26 | | | |
| <i>Isochrysis galbana</i> Proaqua | | | |
| <i>Chlorella sorokiniana</i> KAS908 | 0.2 | Biomass | Perez et al., 2015 |
| <i>Porphyridium purpureum</i> CCAP 1380/3 | 0.1 | Biomass, EPA, zeaxanthin, Beta-carotene, exopolysaccharides, phycobiliproteins | Coward et al., 2016 |
| <i>Isochrysis</i> Tahitian strain (CCAP 927/14) | - | | |
| <i>Rhodomonas salina</i> CSIRO | | Aquaculture feed | Siqwepu, 2016 |
| <i>Tetraselmis chuii</i> CCAP 8/6 | | | |
| <i>Chlorella</i> sp. CCAP 211/53 | 0.1 | Rheology - flow of microalgae | Cagney et al., 2017 |
| <i>Phaeodactylum tricornum</i> CCAP 1052/1A | | | |
| <i>Pavlova lutheri</i> SAG 926-1 | 0.1 | Biomass, EPA, DHA | Ljubic et al., 2017 |
| <i>Chlorella vulgaris</i> CCAP 211/11R | 0.5 | Biomass, wastewater treatment | Mayhead et al., 2018 |
| <i>Scenedesmus</i> SCCPK-1826 | 0.1 | Biomass, wastewater treatment, CO ₂ removal | Farinacci, 2018 |
| <i>Phaeodactylum tricornum</i> | | | |
| <i>Rhodomonas lens</i> | - | Aquaculture feed | Randazzo et al., 2018 |
| <i>Isochrysis galbana</i> | | | |
| <i>Nannochloropsis oceanica</i> | 0.1 | Biomass, wastewater treatment | Silkina et al., 2019 |
| <i>Scenedesmus quadricauda</i> | | | |
| <i>Nannochloropsis gaditana</i> SAG 2.99 | | | |
| <i>Pavlova lutheri</i> SAG 926-1 | | Biomass, fatty acids | Eser et al., 2019 |
| <i>Nannochloropsis oceanica</i> | 0.1 | Biomass, wastewater treatment | Silkina et al., 2019 |

Table S3.2 - Microalgae cultivated with Cell-Hi WP Powdered Media

| Organism | WP concentration (g/L) | Product | Reference |
|--|------------------------|--|--------------------------|
| | 0.1 | Biomass, fatty acids | Halldórsdóttir, 2009 |
| <i>Amphiprora</i> | 0.1 | Biomass | Hrafnadóttir, 2012 |
| <i>Amphiprora</i> | | | |
| <i>Phaeodactylum tricornerutum</i> CCAP 1055/1 | 0.1 | Biomass, fatty acids | Spilling et al., 2013 |
| <i>Phaeodactylum tricornerutum</i> TV 335 | | | |
| Blue-green algae | 0.3 | Biomass, phycocyanin | Svavarsson et al., 2014 |
| <i>Tisochrysis lutea</i> T-Iso CCMP 1324 | 0.1 | Aquaculture feed | Rolton et al., 2014 |
| <i>Cyanobacterium aponinum</i> | 0.67 | Biomass | Arnardóttir et al., 2015 |
| <i>Tisochrysis lutea</i> T-Iso CCMP 1324 | 0.1 | Fucoxanthin | Beuzenberg et al., 2017 |
| <i>Cyanobacterium aponinum</i> | 0.3 | Skin care, CO ₂ sequestration | Svavarsson et al., 2018 |

Table S3.3 - Working stock formulation for Cell-Hi all-in-one powdered media

| Medium | Powder (kg) | Water (L) | Final concentration (mL L ⁻¹) | Final concentration (g L ⁻¹) |
|-------------|-------------|-----------|---|--|
| Cell-Hi F2P | 1 | 10,000 | 1 | 0.1 |
| Cell-Hi WP | 1.5 | 10,000 | 1 | 0.15 |
| Cell-Hi JWP | 1 | 20,000 | 2 | 0.1 |

Cell-Hi powdered (Varicon Aqua Solutions Ltd.) stock solutions (1 kg 10 L⁻¹ for Cell-Hi F2P, 1.5 kg 10 L⁻¹ for WP, and 1 kg 20 L⁻¹ for JWP) were prepared by thoroughly mixing at room temperature (20°C) with a magnetic stirrer (N2400-2000 Starlab, UK) until the product dissolved. The final concentrations of Cell-Hi F2P, WP and JWP were 0.1, 0.15, and 0.1 g L⁻¹ respectively as recommended by the manufacturers.

S3.4 - Hydroponics medium pre-screening methodology

Economical and easy application ‘Hydroponics media’ were prepared by mixing two components of the FloraSeries Hydroponic fertiliser (GHE, Fleurance, France); FloraMicro (M) and FloraBloom (B) at previously described concentrations; M1B1, M1B2, M1B5, M2B1, M2B2, M2B5 (M1-M5, 1-5 mL L⁻¹ FloraMicro; B1-B5 1-5 mL L⁻¹ FloraBloom) (Butler et al., 2017; Tocquin et al., 2012) and were compared to f/2 as the control in 250 mL Erlenmeyers with 100 mL media.

Table S3.5 – Hydroponics cost assessment

| | Medium cost per m ³ | | | | | | | |
|---|--------------------------------|-------|-------|-------|-------|-------|-------|-------|
| | Commercial f/2 | f/2 | M1B1 | M1B2 | M1B5 | M2B1 | M2B2 | M2B5 |
| Cost (£s) per m ³ | 954 | 5.8 | 14.83 | 20.63 | 38.01 | 23.87 | 29.67 | 47.05 |
| Cost (£s) per m ³ (media/mixing/labour) | 966.03 | 53.89 | 26.94 | 32.74 | 50.12 | 35.98 | 41.78 | 59.16 |

Stock cultures were harvested during late-log, centrifuged at 4000 rpm for 10 mins (3500 g), washed with 20 mL phosphate buffered saline and re-suspended in 250 ml Erlenmeyer flasks for experimental flask screening. The experimental cultures were incubated at 21°C (Series 4, LMS incubator, UK) and agitated at 120 rpm using a Stuart reciprocating table shaker (SSL2, UK) under continuous light at $125 \pm 9 \mu\text{mol photons m}^{-2} \text{s}^{-1}$ for the hydroponics medium pre-screening (provided by 2700 k Hansa ECO Star silver lamps) for 7 d. The initial inoculum density was an optical density of 750 nm (OD_{750}) = 0.12 (equivalent to ca. 1×10^6 cells/mL, 0.02 g L⁻¹ DW) and growth was monitored daily by measuring cell count.

The media were filter sterilised using bottle-top vacuum filtration (Nalgene, 291-3320, Thermo Scientific, UK). From the culture, 50 mL was harvested and the biochemical composition (fatty acids, fucoxanthin, chlorophyll *a*, protein, and carbohydrate) were analysed after 7 d.

S3.6 Evaluation of FloraMicroBloom formulations

The aim was to compare six hydroponics medium formulations (FloraMicroBloom) which were found to be economical alternatives, previously untested for *P. tricornutum* to determine if they offered an improvement in growth and product yield (fucoxanthin, EPA, and protein) compared with conventional f/2 medium. Amongst the six screened media, a maximum cell density (1.68×10^7) and biomass density (0.31 g/L DW) was observed with M2B1 (i.e. 2 mL L⁻¹ FloraMicro and 1 mL L⁻¹ FloraBloom) corresponding to a maximum growth rate of $\mu_{\max} = 0.90 \text{ d}^{-1}$ (doubling time of 18.5 h) and an average growth rate of $\mu = 0.40 \text{ d}^{-1}$ (doubling time of 42 h). However, there was no significant increase in final cell density or biomass concentration compared with the f/2 control medium (1.77×10^7 and 0.36 g L⁻¹ respectively). One characteristic of M2B1 and f/2 was that they had a higher N/P ratio (20.4) than the other media and this could have accounted for the increased growth (Figure S3.9). Previously, FloraMicroBloom has only been tested for *Haematococcus pluvialis* and the formulation M1B5 (1 mL L⁻¹ FloraMicro and 5 mL L⁻¹ FloraBloom) resulted in the highest cell count and biomass concentration which was attributable to the high phosphate content and low N/P ratio (Tocquin et al., 2012). Comparatively for *P. tricornutum* M1B5 resulted in a low biomass yield and M2B1 was optimal and thus the optimal formulation appears species specific.

Biochemical analysis conducted after 7 days of cultivation revealed a difference in composition between the media treatments. M1B5 and M2B5 were not analysed for their biochemical components due to their low biomass yield. The highest fucoxanthin ($0.50 \pm 0.05 \text{ mg L}^{-1} \text{ d}^{-1}$), EPA ($1.25 \pm 0.05 \text{ mg L}^{-1} \text{ d}^{-1}$), and protein ($15.07 \pm 0.33 \text{ mg L}^{-1} \text{ d}^{-1}$) productivities were observed with M2B1 which was significantly higher than all other treatments ($p < 0.05$). The highest fucoxanthin ($1.14 \pm 0.12 \%$ DW), EPA ($2.87 \pm 0.10 \%$ DW), protein ($34.62 \pm 0.70 \%$ DW), and chlorophyll *a* content ($1.17 \pm 0.16 \%$ DW) was observed with M2B1.

As M2B1 resulted in a reasonably high cell density along with a higher product yield of fucoxanthin, EPA, and protein it was further compared with a variety of commercial powdered media under non-sterile conditions to select the optimal economical medium for investigation in the airlift PBR under indoor and outdoor conditions.

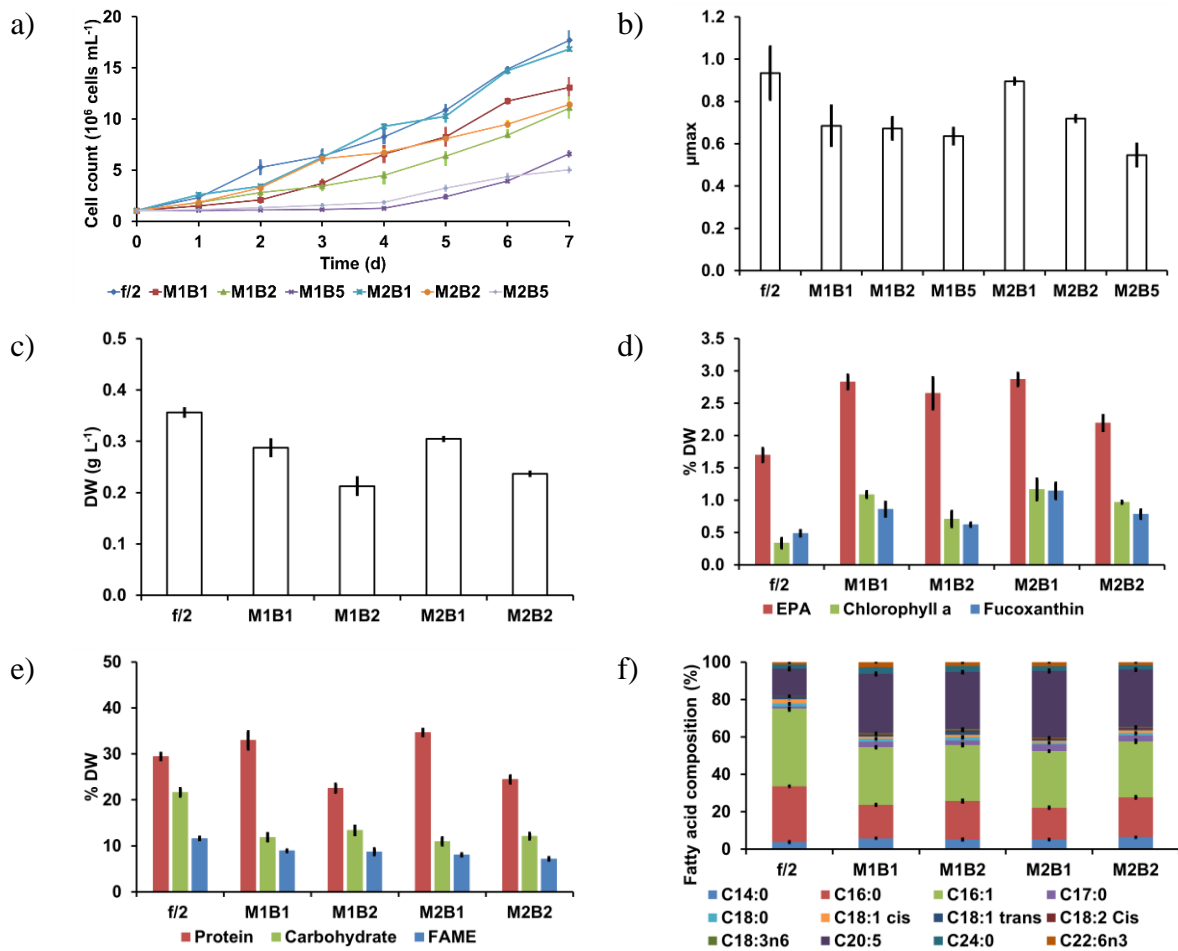


Figure S3.7 - Effect of FloraMicroBloom formulations compared with f/2 medium for growth; a) cell count; b) μ_{max} and analysis after 7 d cultivation; c) dry weight (DW), d) chlorophyll *a*, EPA, fucoxanthin, e) FAME, protein, carbohydrate (% DW) and f) fatty acid composition (%)

Table S3.8 – FloraMicroBloom hydroponics pre-screening composition.

| | FloraMicroBloom | | | | | | |
|---------------------------------|------------------------|-------------|-------------|-------------|-------------|-------------|-------------|
| mM | f/2 | M1B1 | M1B2 | M1B5 | M2B1 | M2B2 | M2B5 |
| Total N | 0.88 | 3.57 | 0.36 | 3.57 | 7.14 | 7.14 | 7.14 |
| Phosphate | 0.04 | 0.35 | 0.71 | 1.77 | 0.35 | 0.71 | 1.77 |
| Sodium | 0.93 | - | - | - | - | - | - |
| Potassium | - | 0.56 | 0.86 | 2.26 | 0.70 | 1.13 | 2.40 |
| Magnesium | - | 1.23 | 2.47 | 6.17 | 1.23 | 2.47 | 6.17 |
| Sulfur | 0.12 | 1.56 | 3.12 | 7.80 | 1.56 | 3.12 | 7.80 |
| Calcium | - | 1.75 | 0.17 | 1.75 | 3.49 | 3.49 | 3.49 |
| Bicarbonate | - | - | - | - | - | - | - |
| μM | f/2 | M1B1 | M1B2 | M1B5 | M2B1 | M2B2 | M2B5 |
| Copper | 0.04 | 1.57 | 0.16 | 1.57 | 3.15 | 3.15 | 3.15 |
| Cobalt | 0.08 | - | - | - | - | - | - |
| Iron | 11.65 | 21.49 | 2.15 | 21.49 | 42.98 | 42.98 | 42.98 |
| Manganese | 0.91 | 7.28 | 0.73 | 7.28 | 14.56 | 14.56 | 14.56 |
| Molybdenum | 0.02 | 0.42 | 0.04 | 0.42 | 0.83 | 0.83 | 0.83 |
| Zinc | 0.08 | 2.29 | 0.23 | 2.29 | 4.59 | 4.59 | 4.59 |
| Boron | - | 9.25 | 0.92 | 9.25 | 18.50 | 18.50 | 18.50 |
| mg L⁻¹ | f/2 | M1B1 | M1B2 | M1B5 | M2B1 | M2B2 | M2B5 |
| Vitamin B12 (cyanocobalamin) | 0.03 | 0.03 | 0.03 | 0.03 | 0.03 | 0.03 | 0.03 |
| Vitamin B1 (Thiamine HCl) | 0.10 | 0.10 | 0.10 | 0.10 | 0.10 | 0.10 | 0.10 |
| Vitamin H (Biotin) | 0.03 | 0.03 | 0.03 | 0.03 | 0.03 | 0.03 | 0.03 |
| | f/2 | M1B1 | M1B2 | M1B5 | M2B1 | M2B2 | M2B5 |
| N/P ratio | 24.50 | 10.20 | 0.51 | 2.02 | 20.40 | 10.06 | 4.03 |

S3.9 - Dissolved inorganic nitrate (DIN) and dissolved inorganic phosphate analysis (DIP)

The culture was centrifuged at 4000 rpm for 10 mins, the supernatant was removed, filtered through a 0.22 μm filter, and stored frozen at $-20\text{ }^{\circ}\text{C}$ until further analysis of the medium for nutrient composition. Dissolved inorganic nitrogen (DIN) in the media was determined by measuring the absorbance at 220 nm as described in Collos et al. (1999). Instant ocean (33 g L^{-1}) was used as a blank. A standard curve was made using sodium nitrate from 0-500 μM .

Dissolved Inorganic Phosphate (DIP) in the media was determined following Strickland and Parsons (1968). To 50 mL 1.5 g ammonium molybdate tetrahydrate was dissolved. To 90 mL deionized water, 14 mL sulphuric acid was added. To 5 mL deionized water 0.27 g ascorbic acid was added. In 250 mL of deionized water 0.34 g potassium antimonyl tartrate trihydrate was added. Mixed reagent was made with ammonium molybdate: sulphuric acid: ascorbic acid: potassium antimonyl tartrate trihydrate solution (1:2.5:1:0.5). To 1 mL of sample 0.1 mL of mixed reagent was added. A spectrophotometric reading was taken at 885 nm after 15 mins (longer times did not result in significantly different values, data not shown). A standard curve was made using sodium dihydrogen phosphate dihydrate (0-20 μM).

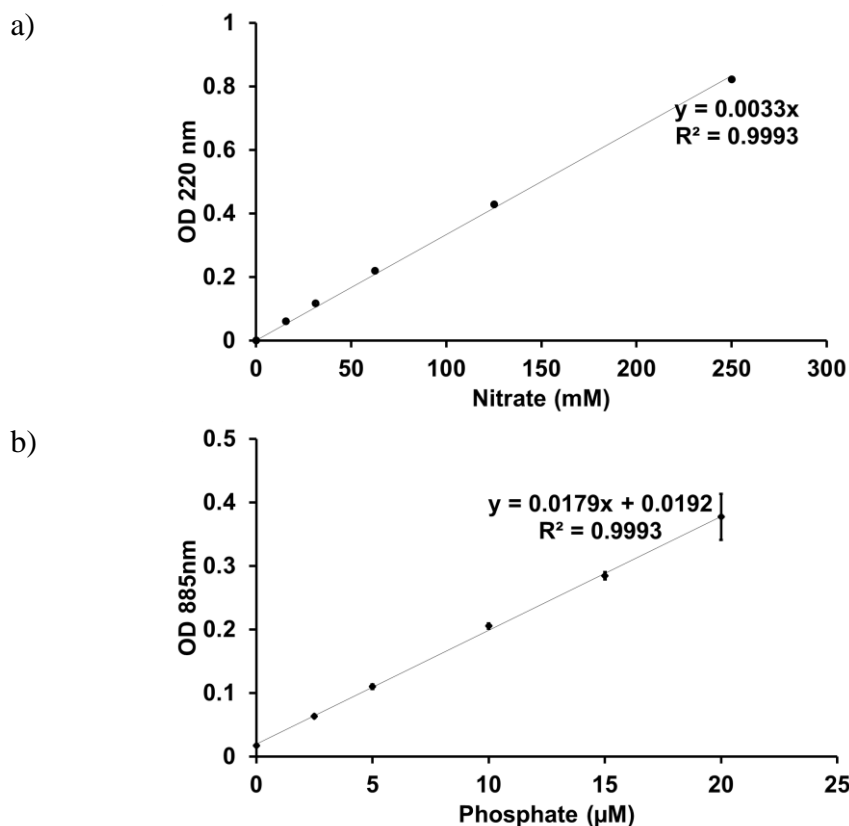


Figure S3.10 – a) DIN standard curve and b) DIP standard curve

S3.11 - Dissolved inorganic carbon (DIC) analysis of outdoor culture

Another 5 ml of culture from the indoor and outdoor PBR was centrifuged at 4000 rpm for 10 mins, and the supernatant was removed, filtered through a 0.22 μm filter, and stored frozen at $-20\text{ }^{\circ}\text{C}$. Within one month the sample was analysed for DIC. The back-titration procedure was conducted according to Chen et al. (2016). The sample was defrosted, transferred to a 20 mL glass beaker, and weighed using a PA 214 precision balance (Ohaus Pioneer, UK). The pH (FE20 FiveEasy, Mettler Toledo), temperature (RC-4 temperature logger (Ellitech, UK) and conductivity (HI 98304, HANNA) were measured. The pH of the supernatant was reduced to pH 7 (pH of bicarbonate) with 0.1 M HCl. The sample was subsequently subjected to two titrations in tandem. In the first titration the pH was reduced to around pH 3.5 with 0.1 M (or 0.5 M) HCl and this amount was recorded for calculating total alkalinity. The sample was then aerated with N_2 to remove the acidified CO_2 and recovered to the pH of bicarbonate by a second titration with the addition of 0.1 M NaOH (or 0.5 M). The concentration of NaOH added was used to calculate the non-carbonate species.

S3.12 - Biochemical composition (chlorophyll *a*, protein, carbohydrate)

Extraction

Combined extraction of carbohydrate, proteins, and chlorophyll *a* was carried out according to Chen and Vaidyanathan (2013) with slight modification. The dry microalgal samples were extracted using 24.3 μL Phosphate buffer (pH 7.4), 1.8 mL of 25% methanol in 1M NaOH and glass beads in 2 mL Safe lock Eppendorf tubes. The tubes were covered with aluminium foil and bead beaten for 10 mins (3 cycles, 2 minutes cool down time) using the Disruptor Genie®.

Carbohydrate

After the extraction process two aliquots of 200 μL of extract were transferred to 2 mL PTFE capped glass vials and analysed for carbohydrate. One vial was used as a control and the other as a sample. Standards of D-glucose (Sigma Aldrich, UK) in deionised water were prepared at the following concentrations: 400, 200, 100, 80, 60, 40, 20, 0 mg mL^{-1} in 2 mL Eppendorf tubes. From each standard, two aliquots of 200 μL were removed and placed in 2 mL PTFE capped glass vials. To the control sample, 1.2 mL pre-chilled 75% H_2SO_4 was added and for the sample, 0.4 mL of pre-chilled 75% H_2SO_4 plus 0.8 mL of freshly prepared Anthrone

reagent. The samples, standards and controls were incubated at 100°C for 15 minutes. Absorbance measurements were taken at 578 nm.

Chlorophyll *a*

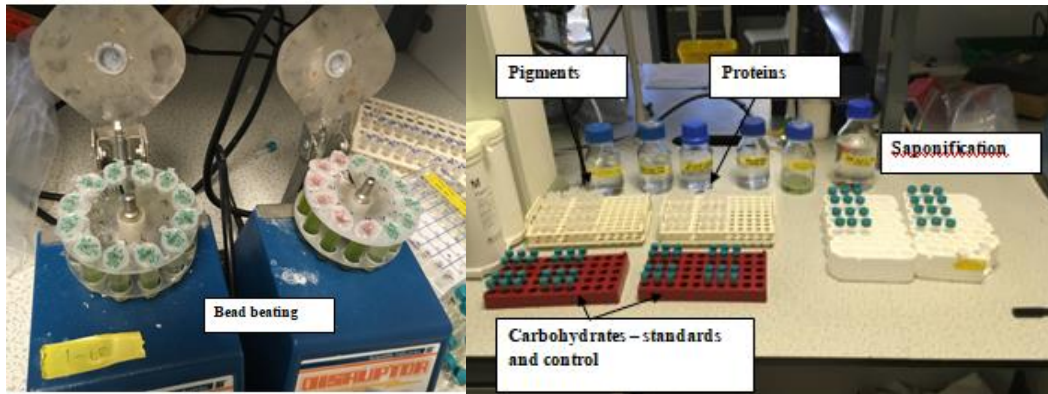
The remainder of the extracts were saponified. The extracts were placed in 4 mL PTFE vials and incubated for 30 mins at 100°C. The vials were inverted four times and 0.7 mL of sample was removed and used for chlorophyll *a* quantification. The remaining saponified samples were transferred to 2 mL Eppendorfs and stored at -20°C for protein analysis. To the 0.7 mL of saponified extract, 1.05 mL of chloroform:methanol (2:1) was added. The samples were vortexed and centrifuged at 13,000 rpm for 10 mins. For chlorophyll analysis the resulting top layer (methanol fraction) was analysed in a quartz cuvette at 416 nm, 453 nm and 750 nm using methanol as a blank. The following equation was used to calculate the chlorophyll *a* concentration:

$$\text{Chl } a \text{ (}\mu\text{g/mL)} = 6.4 * A_{416} - 0.79 * A_{453}$$

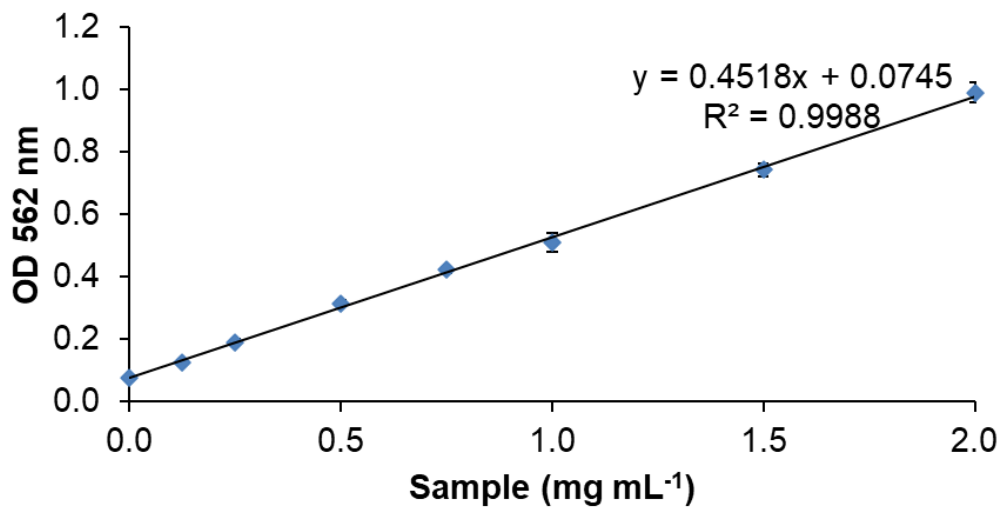
Protein

The remaining saponified samples stored in the freezer were centrifuged at 13,000 rpm for 10 mins. A BCA Protein Assay kit (cat. no. 23225, PierceTM, UK) was used to quantify the protein content. The BCA kit consisted of Reagent A and Reagent B (a copper solution). Using a 96-well plate, 25 μ L was pipetted. As in the carbohydrate assay, one well, then acted as a control (200 μ L of Reagent A added) and the other as sample (Reagent B). The plate was incubated for 30 mins at 37°C. Readings were taken with the plate reader facility on the SPECTROstar Nano spectrophotometer (BMG LABTCH, Germany), at 562nm. BSA standards; 2, 1.5, 1, 0.75, 0.5, 0.25, 0.125 and 0 in 25% methanol in 1 M NaOH were prepared and analysed using the kit.

a)



b)



c)

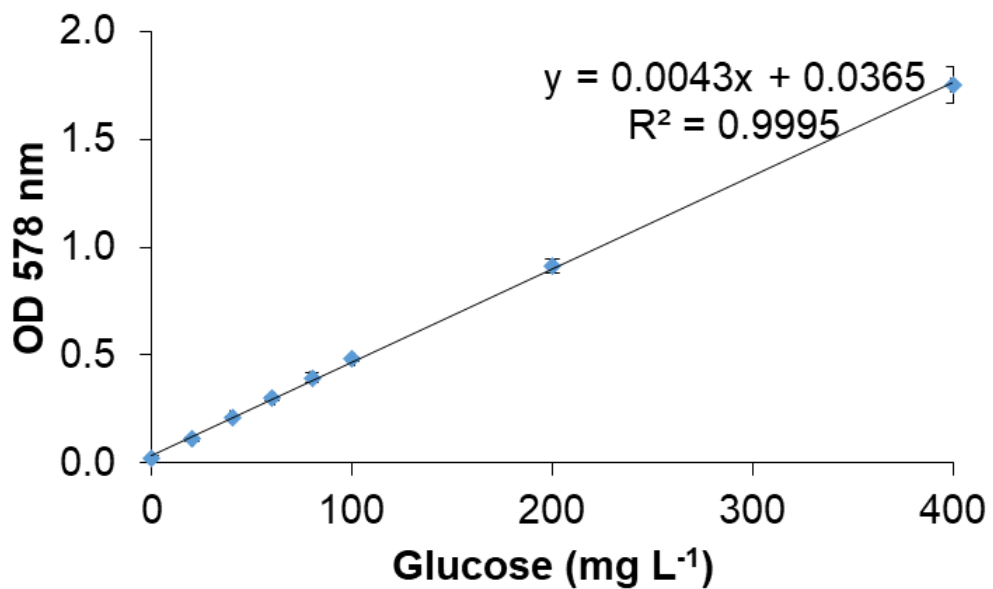


Figure S3.13 – a) setup of biochemical assay, b) typical protein standard curve with bovine serum albumin (BSA) and c) typical carbohydrate standard curve

S3.14 – fatty acid analysis and EPA determination using direct transesterification

All chemicals used were of HPLC grade (Sigma-Aldrich, UK) unless otherwise stated. A modified version of Kapoore et al. (2019) was used for FAME direct transesterification. To the dry biomass in 2 mL Eppendorfs (and wet biomass of the bacteria and biofilm), 300 μ L of toluene and 250 μ L of pentadecanoic acid (C15:0) internal standard dissolved in chloroform at 0.33 mM (equivalent to 1.52 μ M per sample) were added, along with acid washed glass beads (425-600 μ m i.d) (Sigma Aldrich, UK) and the samples were vortexed for 1 min. Then 300 μ L of 0.5 M sodium methoxide was added and vortexed for 1 min. The mixture was then transferred to 2 mL glass vials with polytetrafluoroethene (PTFE) caps (cat. no. 27134, Supelco, Sigma Aldrich, UK) and incubated at 80 °C for 20 min in a dual block dry bath heating system (Starlab, UK). After cooling to room temperature, 300 μ L of 7% HCl in methanol was added and the mixture incubated at 80 °C for 20 min. After cooling to room temperature, the mixture was transferred to a 2 mL Eppendorf tube containing 300 μ L water and 600 μ L of hexane. The resulting biphasic mixture was vortexed for 1 min and centrifuged at 13,000 rpm at 4 °C for 10 mins to facilitate phase separation. The top organic phase was transferred to a fresh 2 mL Eppendorf tube and evaporated to dryness under inert nitrogen gas using a Multivap (Sigma Aldrich, UK). The samples were then frozen at -20°C before use. The dried fatty acid methyl esters (FAMES) were reconstituted in 80 μ L toluene and centrifuged for 2 mins at 13,000 rpm prior to identification and quantification.

To a polypropylene injection vial (12 x 32 mm. crimp seal and snap ring cap 11 mm, Chromatography Direct, UK) 30 μ L of the toluene-FAMES mixture was added. The prepared FAMES were identified and quantified using a Thermo Finnigan TRACE 1300 GC-FID system (Thermo, Hertfordshire, UK) onto a TR-FAME capillary column (25 m x 0.32 mm x 0.25 μ m) with helium as a carrier gas. The derivatisation sample volume of 1 μ l was injected in split injection mode at 250°C. The split flow was 75 mL min⁻¹ and purge flow was 5 mL min⁻¹. The GC was operated at a constant flow of 1.5 mL min⁻¹ helium. The temperature program was started at 150°C for 1 min, followed by temperature ramping at 10°C min⁻¹ to a final temperature of 250°C and held at 250°C for 1 min. The total analysis time was 12 minutes with detector temperature at 250°C. The retention time and identity of each FAME peak was calibrated using the Supelco 37 component FAME mix (Sigma Aldrich, UK).

S3.15 – fucoxanthin analysis by spectrophotometry

Five mL of culture was centrifuged (13,000 rpm, 5 mins), washed with 10 mL of deionised water, and the supernatant discarded. The cells were re-suspended in an equal volume of HPLC grade ethanol, incubated at 45°C for 20 mins and left to stand for 2 h (vortexing every 30 mins). Subsequent to extraction, the mixture was centrifuged (4000 rpm, 10 min) and the supernatant analysed for pigment analysis using a quartz cuvette. Samples were protected from light by using foil and the lights were turned off. The A_{445} and A_{663} values were detected after dilution with HPLC grade ethanol (A_{445} and A_{663} range from 0.2 to 1) and fucoxanthin was calculated using the following formula as described by Wang et al. (2018):

$$\text{Fucoxanthin (mg L}^{-1}\text{)} = 6.39 \times A_{445} - 5.18 \times A_{663} + 0.312 \times A_{750} - 5.27$$

S3.16 - Scanning electron micrograph imaging of biofilm

The scanning electron micrograph (SEM) image was prepared as follows. The biofilm was spread evenly on a glass slide and allowed to dry in a laminar flow. The slides were then placed in a petri dish (roughly requiring 25 ml for each plate for washing). Stages proceeded in the laminar flow. Specimens were fixed in 3% Glutaraldehyde (G7776 – 10 ml) in 0.1M Sodium Phosphate overnight. Specimens were washed twice (0.1M phosphate buffer) with 10 min intervals at 4°C. The cells were post-fixed in a 1% aqueous osmium tetroxide solution for 1 hour at room temperature. The fixated cells were rinsed and dehydrated at room temperature through a graded series of ethanol: 75, 95, 100 and 100 % ethanol for 15 mins, followed by a final dehydration step with 100% ethanol for 15 mins. The samples were then lyophilized mounted on aluminium stubs, attached with Carbon Sticky Tabs, and coated with approximately 25 nm of gold in an Edwards S150B sputter coater. Fixed cells were examined using a JSM-6010LA InTouchScope™ Multiple Touch Scanning Electron Microscope (JEOL Ltd., Japan) at an accelerating voltage of 15Kv.

Table S3.17 – Media cost calculations

| Medium | Price (US \$/m ³) media | Mixing time laboratory (h) | Mixing time 1 m ³ tank (h) | Media preparation time (h) | Price (US \$/m ³) labour/mixing/media | Relative cost - labour/mixing/media |
|--------------------|--|-------------------------------|--|-------------------------------|--|--|
| Commercial f/2 | 1230.66 | 0 | 1 | 1 | 1246.17 | 100 |
| Laboratory f/2 | 7.6 | 2 | 2 | 4 | 69.62 | 5.58 |
| Commercial BBM | 1127.46 | 0 | 1 | 1 | 1142.97 | 91.72 |
| Laboratory BBM | 78.73 | 2 | 2 | 4 | 140.87 | 11.3 |
| Cell-Hi F2P powder | 0.33 | 0 | 1.5 | 1.5 | 23.6 | 1.89 |
| Cell Hi-JW powder | 6.94 | 0 | 1.5 | 1.5 | 30.21 | 2.42 |
| Cell Hi-HP powder | 3.82 | 0 | 1.5 | 1.5 | 27.09 | 2.17 |
| Cell-HI WP powder | 5.73 | 0 | 1.5 | 1.5 | 29 | 2.33 |

1. Prices of media were based on Sigma Aldrich and commercial media tested were used from Sigma Aldrich
2. For laboratory mixing a IKA C-MAG HS4 mixer was assumed at 0.27 KW
3. For mixing in the 1 m³ tank a Synera ADV 5.5 Water Pump was assumed at 0.05 KW
4. The electricity cost assumed was US \$0.186/KWh based on the average UK electricity price (https://www.ukpower.co.uk/home_energy/tariffs-per-unit-kwh)
5. The labour cost was assumed to be for a technician employed in the UK at US \$32,250 and assuming a 40 hour working week (US \$15.50/h)
6. The conversion factor for £s to US \$ was 1.29
7. For the saltwater species it is assumed the facility would be located next to the ocean and seawater would be free

Table S3.18 Laboratory f/2 formulation and cost

| Compound | mM | Final amount (mg/L) | Final amount (g/L) | Cost (£'s per m3) |
|--|------|---------------------|--------------------|-------------------|
| NaNO ₃ | 0.88 | 75 | 0.08 | 3.84 |
| NaH ₂ PO ₄ 2H ₂ O | 0.04 | 5.65 | 0.01 | 0.73 |
| | μM | | | |
| Na ₂ EDTA | 0.01 | 4.16 | 0 | 0.59 |
| FeCl ₃ 6H ₂ O | 0.01 | 3.15 | 0 | 0.51 |
| CuSO ₄ 5H ₂ O | 0 | 0.01 | 0 | 0 |
| ZnSO ₄ 7H ₂ O | 0 | 0.02 | 0 | 0 |
| CoCl ₂ 6H ₂ O | 0 | 0.01 | 0 | 0.01 |
| MnCl ₂ 4H ₂ O | 0 | 0.18 | 0 | 0.04 |
| Na ₂ MoO ₄ 2H ₂ O | 0 | 0.01 | 0 | 0 |
| Cyanocobalamin (B12) | 0 | 0 | 0 | 0.03 |
| Thiamine HCl (B1) | 0 | 0.1 | 0 | 0.04 |
| Biotin (H) | 0 | 0 | 0 | 0.02 |
| Total cost | | | | 0 5.8 |

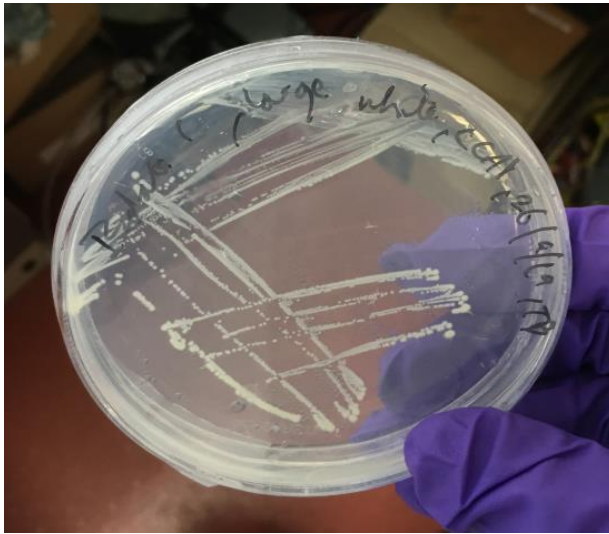
Medium formulation obtained from: <https://www.ccap.ac.uk/media/documents/f2.pdf>

Cost determined from Sigma Aldrich, UK

S3.19 Bacteria sequences

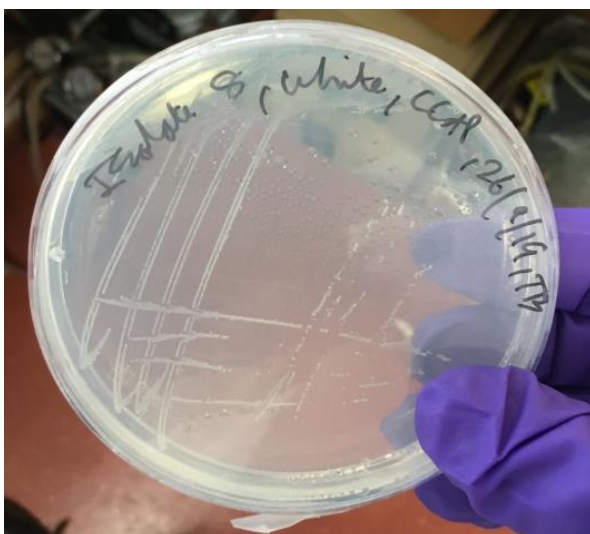
Bacteria isolate 1 – *Halomonas* sp.

>KC354707.1:73-1126 *Halomonas neptunia* strain MAT-17 16S ribosomal RNA gene, partial sequence
AGCTTGCTAGATGCTGACGAGCGGCGGACGGGTGAGTAATGCATAGGAATCTGCC
GGTAGTGGGGGATAACCTGGGGAAACCCAGGCTAATACCGCATACTGCTACGGGAGAAAG
GGGGCTCCGGCTCCCGCTATTGGATGAGCCTATGTCCGATTAGCTAGTTGGTGAGGTAATGG
CTCACCAAGGCAACGATCCGTAGCTGGTCTGAGAGGATGATCAGCCACATCGGGACTGAGA
CACGGCCCGAACTCTACGGGAGGCAGCAGTGGGGAATATTGGACAATGGGGGCAACCCTG
ATCCAGCCATGCCGCGTGTGTGAAGAAGGCCCTCGGGTTGTAAAGCACTTTCAGCGAGGAA
GAACGCCTAGTGGTTAATACCCATTAGGAAAGACATCACTCGCAGAAGAAGCACC GGCTAAC
TCCGTGCCAGCAGCCGCGGTAATACGGAGGGTGCAAGCGTTAATCGGAATTACTGGGCGTA
AAGCGCGCTAGGTGGCTTGATAAGCCGTTGTGAAAGCCCCGGGCTCAACCTGGGAACGG
CATCCGAACTGTCAGGCTAGAGTGCAGGAGAGGAAGGTAGAATTCCCGGTGTAGCGGTGA
AATGCGTAGAGATCGGGAGGAATACCAGTGGCGAAGGCCGCCTTCTGGACTGACACTGACA
CTGAGGTGCGAAAGCGTGGGTAGCAAAACAGGATTAGATACCCTGGTAGTCCACGCCGTAA
CGATGTCGACACAGCCGTTGGGTGCCTAGAGCACTTTGTGGCGAAGTTAACGCGATAAGTCGA
CCGCCTGGGGAGTACGGCCGCAAGGTTAAACTCAAATGAATTGACGGGGGCCCGCACAAAG
CGGTGGAGCATGTGGTTTAAATTCGATGCAACGCGAAGAACCTTACCTACCCTTGACATCTAC
AGAAGCCGGAAGAGATTCTGGTGTGCCTTCGGGAACTGTAAGACAGGTGCTGCATGGCTGT
CGTCAGCTCGTGTGTGAAATGTTGGGTTAAGTCCCGTAACGAGCGCAACCCTTGTCTTAT
TTGCCAGCACGTAATGG



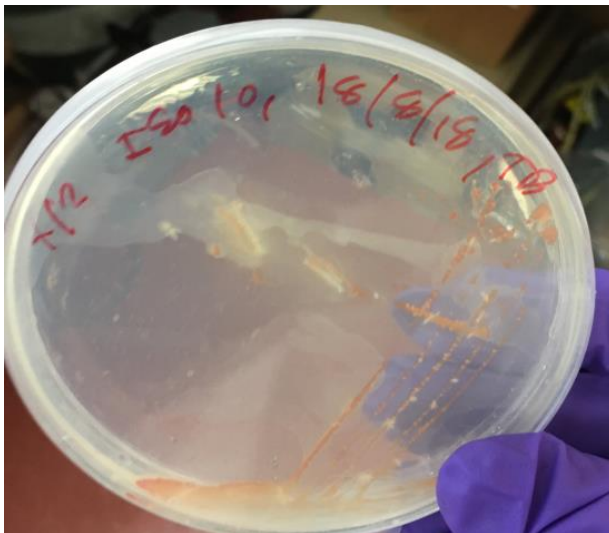
Bacteria isolate 2 – *Marinobacter* sp.

>JQ286003.1:24-1099 *Marinobacter alkaliphilus* strain SYNH ARB 16S ribosomal RNA gene, partial sequence
 AGGTGCTTGACACCCCGCTGACGAGCGGCGGACGGGTGAGTAATGCTTAGGAATCTG
 CCCAGTAGTGGGGGATAGCCCGGGGAAACCCGGATTAATACCGCATAACGTCCTACGGGAGA
 AAGCAGGGGATCTTCGGACCTTGCCTACTGGATGAGCCTAAGTCGGATTAGCTAGTTGGTG
 GGGTAAAGGCCTACCAAGGCGACGATCCGCTAGCTGGTCTGAGAGGATGATCAGCCACATCG
 GGACTGAGACACGGCCCGAACTCCTACGGGAGGCAGCAGTGGGGAATATTGGACAATGGGG
 GCAACCTGATCCAGCCATGCCGCGTGTGTGAAGAAGGCTTTCGGGTTGTAAAGCACTTTCA
 GCGAGGAGGAAGGCCTTAAAGTTAATACCTTTGAGGATTGACGTTACTCGCAGAAGAAGCAC
 CGGCTAACTCCGTGCCAGCAGCCGCGGTAATACGGAGGGTGCAAGCGTTAATCGGAATTAC
 TGGGCGTAAAGCGCGTAGGTGGTTAGGTAAGCGAGATGTGAAAGCCCCGGGCTTAACT
 GGAACGGCATTTCGAACTGTCTGACTAGAGTGTGGTAGAGGGTAGTGGAAATTTCCGTGTGA
 GCGGTGAAATGCGTAGATATAGGAAGGAACACCAGTGGCGAAGGCGGCTACCTGGACCAAC
 ACTGACACTGAGGTGCGAAAGCGTGGGAGCAAACAGGATTAGATACCCTGGTAGTCCAG
 CCGTAAACGATGTCAACTAGCCGTTGGGACTCTTGAAGTCTTAGTGGCGCAGCTAACGCACT
 AAGTTGACCGCTGGGGAGTACGGCCGCAAGGTTAAAACCTCAAATGAATTGACGGGGGCC
 GCACAAGCGGTGGAGCATGTGGTTTAAATTCGACCGCAAGCAAGAACCTTACCTGGCCTTGA
 CATCCAGAGAATTTCCAGAGATGGATTGGTGCCTTCGGGAACTCTGAGACAGGTGCTGCAT
 GGCCGTCGTCAGCTCGTGTGTCGTGAGATGTTGGGTTAAGTCCCGTAACGAGCGCAACCCCTAT
 CCCTGGTTGCTAGCAGGTAATGCTGAGAACTCCAGG



Bacteria isolate 3 – *Algoriphagus* sp.

>MK583623.1:171-995 *Algoriphagus marincola* strain NBP 16S ribosomal RNA gene, partial sequence
TGATTAGCTAGTTGGTGGGGTAACGGCCCACCAAGGCGACGATCAGTAGGGGTTCT
GAGAGGAAGGTCCCCACACTGGCACTGAGATACGGGCCAGACTCCTACGGGAGGCAGCAG
TAGGGAATATTGGGCAATGGACGAGAGTCTGACCCAGCCATGCCGCGTGCAGGAAGACGGC
CTATTGGGTTGTAAACTGCTTTTATACGGGAAGAAAAGGCCCATGCGTGGGACATTGCCGGT
ACCGTATGAATAAGCACCGGCTAACTCCGTGCCAGCAGCCGCGGTAATACGGAGGGTGCAA
GCGTTGTCGGATTTATTGGGTTTAAAGGGTGCGTAGGCGGCTGATTAAGTCAGCGGTGAAA
GACTCCGGCTCAACCGGAGCAGTGCCGTTGATACTGGTTGGCTTGAGTGCTGCAGGGGTAC
ATGGAATTGATGGTGTAGCGGTGAAATGCATAGATAACCATCAGGAACACCGATAGCGAAGG
CATTGTA CTGGGCAGCAACTGACGCTGATGCACGAAAGCGTGGGGAGCGAACAGGATTAGA
TACCCTGGTAGTCCACGCCGTAACGATGATTACTCGCTGTTATGCCTTTAGGTGTAGCGGC
CAAGCGAAAGCGTTAAGTAATCCACCTGGGGAGTACGCCGGCAACGGTGAAACTCAAAGGA
ATTGACGGGGGTCCGCACAAGCGGTGGAGCATGTGGTTTAAATTCGATGATACGCCGAGGAAC
CTTACCTGGGCTAGAATGTGAAGGAATGATTGGAGACAGATCAGTCAGCAATGACCTGAAA
CAAGGTGCTGCATGGCTGTCGTCAGCTCGTGCC



S3.20 Reactor design

Conventionally horizontal tubular bioreactors have been selected in the past due to their high volumetric productivity, but the merits of vertical tubular split cylinder bioreactors have been showcased with having a higher areal productivity, relatively cheap to construct, easy to operate and maintain and scalable (0.01-100 m³) (Fernández Sevilla et al., 2004; Lizzul, 2016). Tubular systems have been the most widely developed of the commercialized systems with global suppliers such as Varicon Aqua Solutions and Lgem having constructed and deployed numerous systems for both commercial and academic applications. Tubular configurations are

favourable over plate configurations as they have higher liquid velocities, they are easier to disassemble and clean, and the modular nature of the tubes allows for easy replacement (McDonald, 2013; Lizzul, 2016). Vertical systems are often mixed pneumatically, which allows for superior mass transfer compared with conventional liquid pumps in horizontal systems (Lizzul, 2016). Vertically arranged reactors have the benefit of providing greater strength to the reactor than horizontal configurations and thus require less supporting framework which can reduce the capital expenditure (CAPEX) involved (Lizzul, 2016).

A simple vertical airlift reactor arrangement was constructed (ALR) based on Lizzul (2016) which is a simple modular design (capable of being arranged in linear arrays) and could be extended for higher production volumes, allowing for high mass transfers, rapid-de gassing, and a reduction in material costs compared to horizontal systems. There are no mechanical parts internally ensuring lower levels of equipment 'wear and tear' and fouling, and the constant tube diameter reduces shear (Lizzul, 2016). The design is considered a hybrid reactor and is able to operate under bubble column and airlift mixing regimes (Lizzul, 2016). In the airlift operational mode, adjacent columns form alternating riser and downcomer columns, mixing in the form of an external loop airlift column, with the top horizontal manifold being the degasser zone. The planar arrangement of the system allows for the PBR to be angled towards the sun and maximises solar penetration. For a sustainable, resilient and economical design, durable materials were chosen (standard pipe fittings from PVC) and the manifold sections had internal diameter of 63 mm and were glued with PVC cement. The photo-collecting tubes had walls of 3 mm thickness and were made from borosilicate glass (Schott, Germany) (lower UV damage than PVC tubing and lower rates of fouling), giving a total outer diameter (OD) of 54 mm. This tube diameter allowed for a trade-off between high solar penetration and maintaining a reasonable areal volume. The total height of each riser and downcomer was 1.4 m with each vertical solar collecting region 1.25 m in length and the total area occupied was 0.18 m². A ¼ bsp brass fitting was threaded to the riser section at the base for introducing mixing air and a sampling port was introduced on the downcomer side. The final working volume of the system was 8 L. A flow rate of 0.625 vvm was chosen because higher values result in a plateau of gas hold-up and liquid velocity which results in energy loss (Hernández-Melchor et al., 2017). It was theorised at higher mixing rates that there would be poor gas disengagement and the higher liquid velocity would draw more air back into the downcomer.

S3.21 Relationships in outdoor cultivation

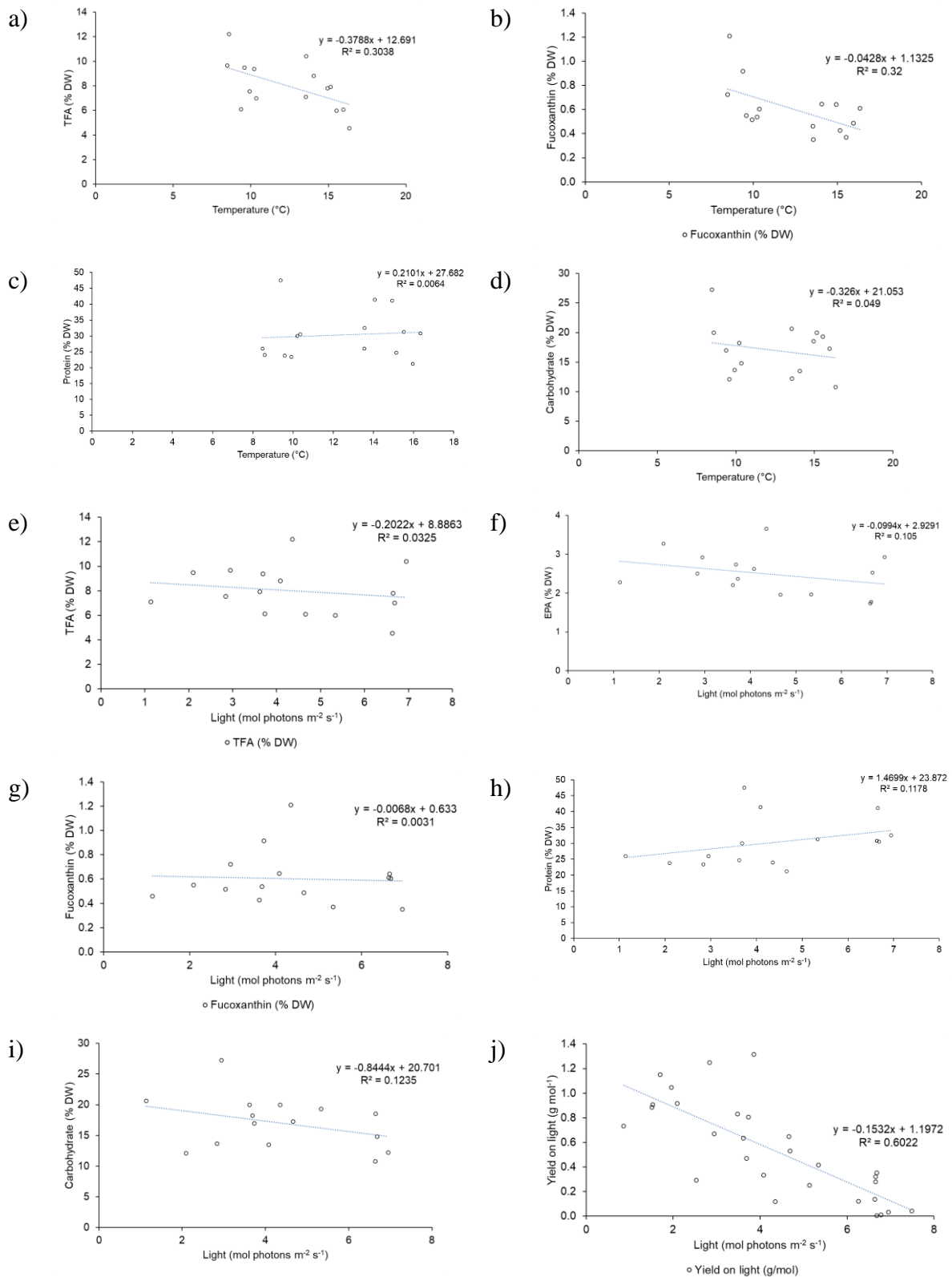


Figure S3.22 – Relationship between a) temperature and TFA, b) temperature and fucoxanthin, c) temperature and protein, d) temperature and carbohydrate, e) light and TFA, f) light and EPA, g) light and fucoxanthin, h) light and protein, i) light and carbohydrate, j) light and yield on light

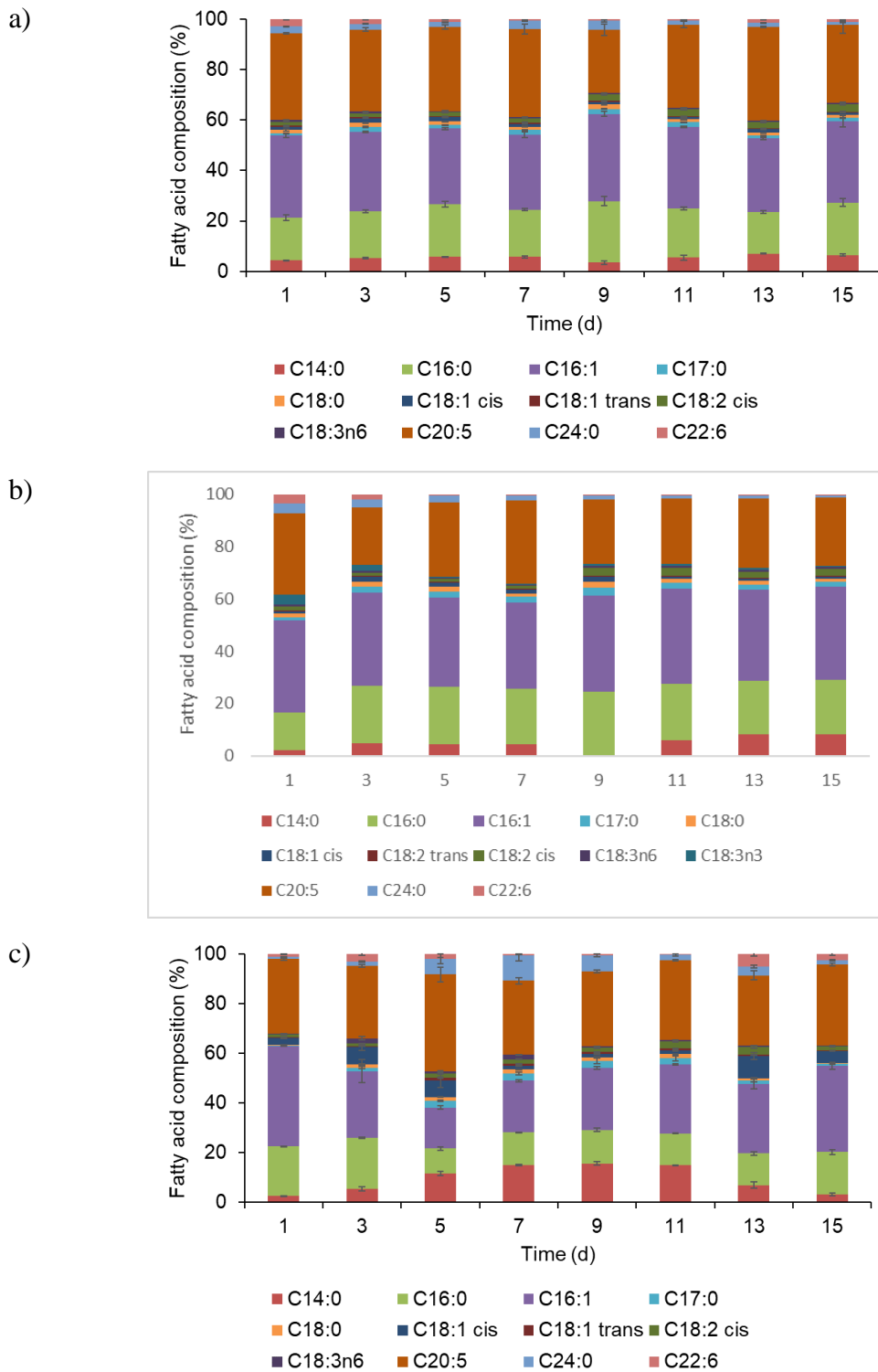


Figure S3.23 – Fatty acid composition of *P. tricornutum*; a) indoor cultivation, b) outdoor run 1 and c) outdoor run 2

Appendix B

This section contains supplementary figures, tables that resulted from Chapter 4 of this work.

Supplementary files

Calibration curves between OD, cell count and DW

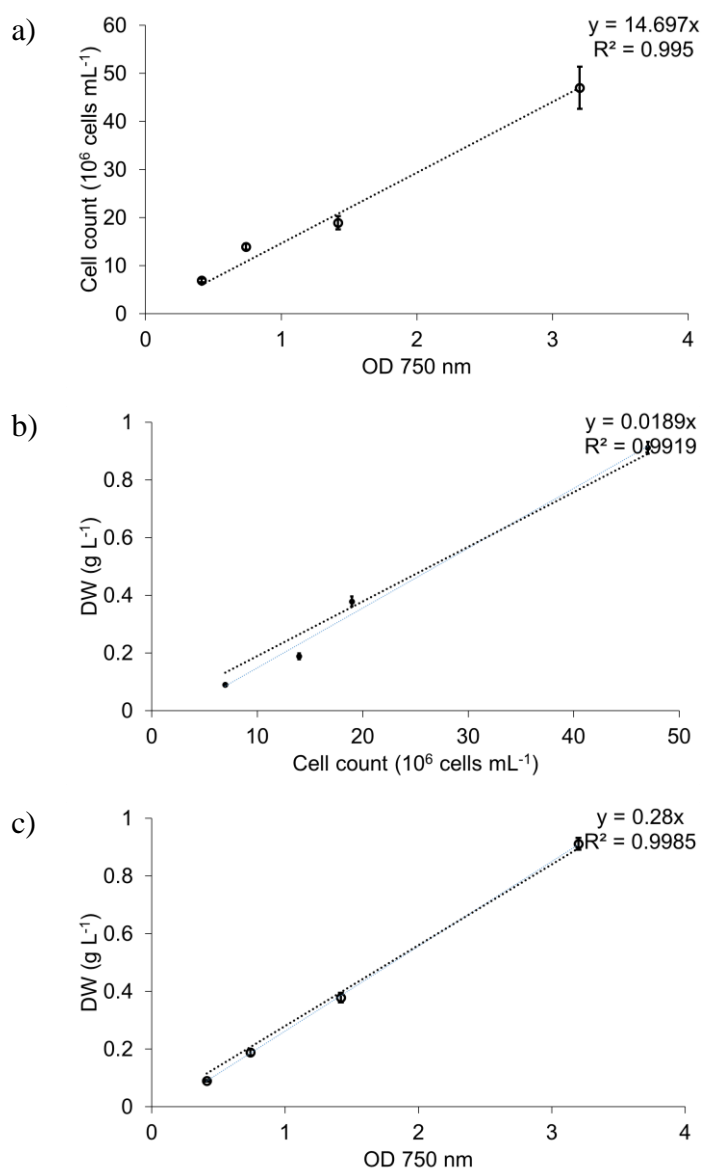


Figure S4.1 - Correlation between a) OD 750 nm and cell count, b) cell count and dry weight (DW), c) OD 750 nm and DW

Effect of vitamins and Tris-HCl on growth

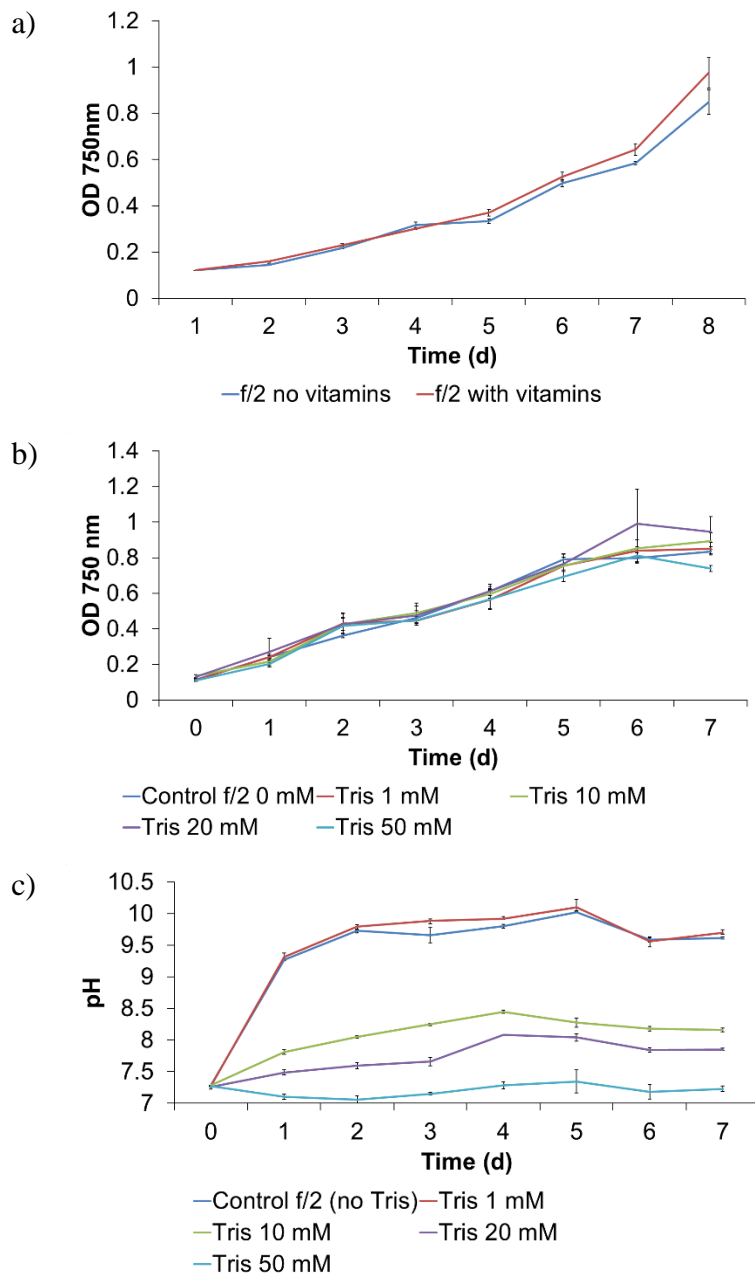


Figure S4.2 - a) Effect of vitamins on *P. tricornutum* growth; effect of Tris-HCl on *P. tricornutum* a) growth, b) pH.

Table S4.3 - Elemental composition of f/2 media modifications

| | f/2 | 2 x f/2 NP | 5 x f/2 NP | 10 x f/2 NP | 2 x f/2 | 5 x f/2 | 10 x f/2 |
|-------------------------------|------------|-------------------|-------------------|--------------------|----------------|----------------|-----------------|
| | mM | | | | | | |
| NO ₃ ⁻ | 0.88 | 1.76 | 4.41 | 8.82 | 1.76 | 4.41 | 8.82 |
| PO ₄ ³⁻ | 0.04 | 0.07 | 0.18 | 0.36 | 0.07 | 0.18 | 0.36 |
| Cl ⁻ | 513.01 | 513.01 | 513.01 | 513.01 | 513.01 | 513.01 | 513.01 |
| Na ⁺ | 442.11 | 442.11 | 442.11 | 442.11 | 443.04 | 445.83 | 450.48 |
| Mg ²⁺ | 51.21 | 51.21 | 51.21 | 51.21 | 51.21 | 51.21 | 51.21 |
| K ⁺ | 10.13 | 10.13 | 10.13 | 10.13 | 10.13 | 10.13 | 10.13 |
| Ca ²⁺ | 9.41 | 9.41 | 9.41 | 9.41 | 9.41 | 9.41 | 9.41 |
| HCO ₃ ⁻ | 3.09 | 3.09 | 3.09 | 3.09 | 3.09 | 3.09 | 3.09 |
| | μM | | | | | | |
| Fe | 11.65 | 11.65 | 11.65 | 11.65 | 23.31 | 58.27 | 116.54 |
| Cu | 0.04 | 0.04 | 0.04 | 0.04 | 0.08 | 0.2 | 0.4 |
| Zn | 0.08 | 0.08 | 0.08 | 0.08 | 0.15 | 0.38 | 0.77 |
| Co | 0.08 | 0.08 | 0.08 | 0.08 | 0.15 | 0.39 | 0.77 |
| Mn | 0.91 | 0.91 | 0.91 | 0.91 | 1.82 | 4.55 | 9.1 |
| Mo | 0.02 | 0.02 | 0.02 | 0.02 | 0.05 | 0.12 | 0.25 |
| N/P | 24.37 | | | | | | |
| EC | 60.92 mS | | | | | | |

Table S4.4. f/2 medium modification cost (£ per m3)

| f/2 | 2 x f/2 NP | 5 x f/2 NP | 10 x f/2 NP |
|------------|-------------------|-------------------|--------------------|
| 7.49 | 13.38 | 31.06 | 60.53 |

S4.5 - Elemental composition analysis

Ten mg of vanadium pentoxide (V₂O₅) was added to a tin capsule pressed (light) (CE Instruments, UK) which acted as a catalyst for complete conversion of inorganic sulphur in the sample to sulphur dioxide. Then 2.5-5 mg of 2,5-Bis (5-tert-butyl-benzoxazol-2-yl) thiophene (BBOT) standard reference material or microalgal sample was added and this weight was noted using a Sartorius precision weighing microbalance CPA2P (Fisher Scientific, UK) at a precision of 0.001 mg. The tin capsules were folded to ensure no powder escaped before being placed inside the MAS 200R auto sampler (Thermo Scientific, UK) for combustion using a Flash 2000 CHNS Elemental Analyser (Thermo Scientific, UK).

The BBOT standard gave the calibration reference of 72.53% carbon, 6.09% Hydrogen, 6.51% Nitrogen and 7.44% Sulphur. When the tin crucible with sample is dropped into the furnace, it is combusted at 900°C and the oxygen environment triggers a strong exothermic reaction. The tin aids the combustion process by increasing the local temperature to 1800°C. The combustion gases pass through a reaction tube inside the instrument containing copper (II) oxide and electrolytic copper which reduces the gases such as nitrogen oxide and sulphur trioxide to a gas mixture containing N₂, CO₂, H₂O, and SO₂. These four compounds are then separated by the gas chromatography column and then passed through a Thermal Conductivity Detector (TCD) to give N, C, H and S. Helium was used as a carrier gas to transport all the combustion gases through the system and high-purity oxygen was used to aid the combustion process. Initially a blank tin capsule was run to ensure no peaks formed, followed by two BBOT standards and then two BBOT standards run as unknowns to confirm the identity and then every 24 samples this was repeated. For the samples biological triplicates were used.

S4.6 - Effect of different kelvin lights

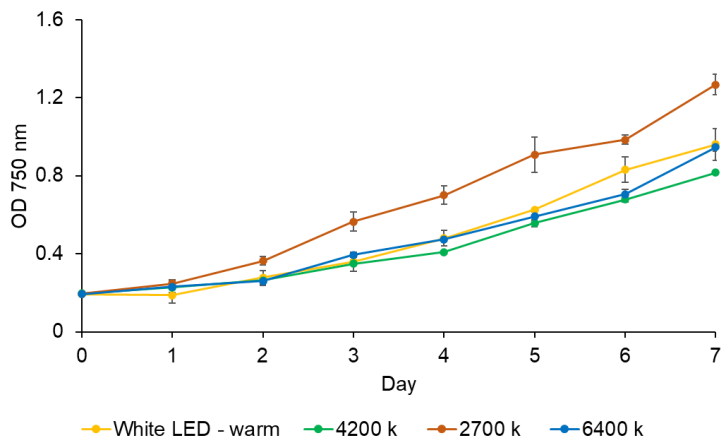


Figure S4.7 – Effect of fluorescent bulbs and white LEDs on growth of *P. tricornutum*.

S4.8 - Effect of sodium bicarbonate on pH when buffered with Tris-HCl

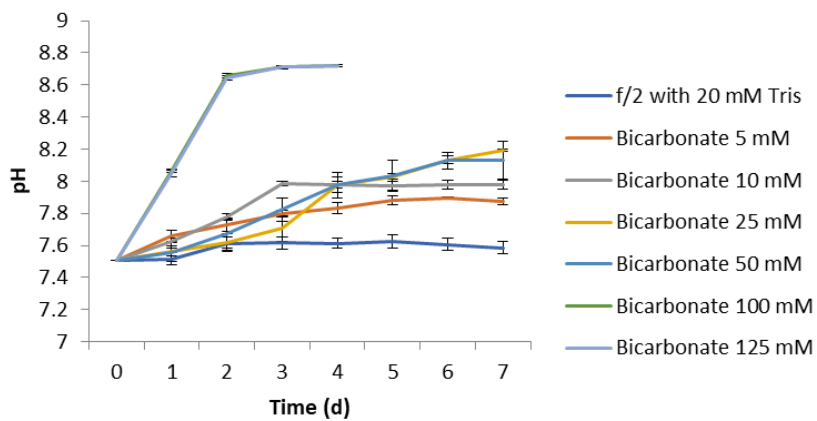


Figure S4.9 – Effect of sodium bicarbonate on pH compared with control (no sodium bicarbonate).

S4.10 - Fatty acid method development

Effect of direct transesterification method

A variety of solvents (e.g. hexane, chloroform: methanol and methanol) have been used for lipid extraction using dry and wet methods with hexane commonly used due to its efficacy of neutral lipid extraction, cost (threefold cheaper than other non-polar solvents) and ability to be reused (up to 95 % solvent recovery) (Kapoore et al., 2018). The lipid content is then quantified by gravimetric analysis but this is an inaccurate method and is often an overestimate due to the presence of non-lipid components such as pigments and proteins and no internal standard is used to account for error in weight and volume measurements (Kapoore, 2014).

Direct transesterification can be used where extraction and transesterification are used in a single step which minimises solvent use (Kapoore et al., 2018). The issue with transesterification is that it requires large volumes of methanol with an acid and base and operates under high temperature (Kapoore et al., 2018). Methanol is readily available at a relatively low price and has been extensively used as an alcohol for transesterification at commercial scale worldwide where triglycerides are transesterified to fatty acid methyl esters (FAMEs) (Reddy et al., 2014). However, methanol is mainly produced from petroleum-derived sources and has toxic properties. Replacing methanol with ethanol results in a more sustainable and renewable process as it can be produced exclusively from renewable sources (García et al., 2011). In addition fatty acid ethyl esters (FAEE) are superior to fatty acid methyl esters in terms of fuel properties (including cetane number, cold flow properties and oxidation stability (Reddy et al., 2014).

The main challenges of acid catalysis compared to base catalysis is that the reaction is 4000 times slower, higher molar ratios of alcohol to oil are required, higher temperatures are employed (60-90°C) and longer reaction times are required (Kapoore, 2014). Common acid catalysts are methanolic-HCl, sulphuric acid and boron trifluoride (Kapoore, 2014). Homogenous alkaline catalysts are the most commonly used route for biodiesel production due to the ability to operate at low temperature/atmospheric pressure, lower cost, less corrosive nature and higher biodiesel conversion efficiency (Kapoore, 2014; Yacob et al., 1998).

Fatty acid methyl ester (FAME) and fatty acid ethyl ester (FAEE) determination

P. tricornutum was cultivated in 250 ml flasks in triplicate with 150 ml f/2 medium for 7 d at 21°C, 125 µmol photons/m²/s continuous light (2700 k) with shaking at 120 rpm. The samples were then pooled and used for fatty acid analysis.

Direct transesterification of wet microalgal biomass

Aliquots of 5 mL of algal culture were harvested by centrifugation at 4000 rpm for 10 mins, the pellets washed with 0.01 M phosphate buffered saline (PBS) and transferred to 2 mL Eppendorf safe-lock tubes, centrifuged at 13,000 rpm for 5 mins and stored at -20°C for analysis. 15 ml aliquots $\sim 1 \times 10^7$ cells ml^{-1} were passed through an OS Cell Disrupter (Constant Systems Ltd., UK) (flow rate 5 mL min^{-1}) at 15,000, 20,000 and 25,000 psi. The machine was pre-washed with runs of 200 mL deionised water-100 % ethanol-deionised water (200 mL each). The samples were then lysed, collected on ice and centrifuged and stored as above to observe the effect of cell disruption through homogenisation compared with bead beating.

A modified version of Kapoore et al. (2014) was used to look at the effect of FAME direct transesterification using acid and base catalysts. All chemicals used were of HPLC grade (Sigma-Aldrich, UK) unless otherwise stated.

Table S4.11 - Effect of acid and base catalysts on direct transesterification of wet microalgal biomass

| | |
|----|--|
| 1) | Base catalyst only (0.5 M sodium methoxide) |
| 2) | Acid catalyst only (7 % ethanolic-HCl) |
| 3) | Base (0.5 M sodium methoxide) and acid (10 % boron trifluoride) catalyst |
| 4) | Base (0.5 M sodium methoxide) and acid (7 % ethanolic-HCl) catalyst |
| 5) | Base (0.5 M sodium methoxide) and acid (7 % methanolic-HCl) catalyst |
| 6) | Base (0.5 M sodium methoxide) and acid (5 % acetyl chloride) catalyst |

To the frozen wet pellets 300 μL of toluene, 300 μL of 0.5 M sodium methoxide (or ethanolic-HCl in the case of the base catalyst only treatment), and 200 μL of tripentadecanoin (C15:0 TAG) internal standard dissolved in chloroform at 100 mg/L (equivalent to 20 μg per sample) were added. The mixture was then transferred to 2 mL glass vials with polytetrafluoroethene (PTFE) caps (cat. no. 27134, Supelco, Sigma Aldrich, UK) and incubated at 80°C for 20 min in a dual block dry bath heating system (Starlab, UK). After

cooling to room temperature, 300 μL of acid catalyst (7% HCl in methanol, 7 % HCl in ethanol, 5 % acetyl chloride in methanol, 10 % boron trifluoride or methanol for base catalyst only) was added and the mixture incubated at 80 °C for 20 min. After cooling to room temperature, the mixture was transferred to a 2 mL Eppendorf tube containing 300 μL water and 600 μL of hexane. The resulting biphasic mixture was vortexed for 1 min and centrifuged at 13,000 rpm at 4 °C for 10 mins to facilitate phase separation. The top organic phase was transferred to a fresh 2 mL Eppendorf tube and evaporated to dryness under inert nitrogen gas using a Multivap (Sigma Aldrich, UK). The samples were then frozen at -20°C before use. The dried fatty acid methyl esters (FAMES) were reconstituted in 80 μL toluene and centrifuged for 2 mins at 13,000 rpm prior to identification and quantification.

To a polypropylene injection vial (12 x 32 mm. crimp seal and snap ring cap 11 mm, Chromatography Direct, UK) 30 μL of the toluene-FAMES mixture was added. The prepared FAMES were identified and quantified using a Thermo Finnigan TRACE 1300 GC-FID system (Thermo, Hertfordshire, UK) onto a TR-FAME capillary column (25 m x 0.32 mm x 0.25 μm) with helium as a carrier gas. The derivatisation sample volume of 1 μl was injected in split injection mode at 250°C. The split flow was 75 mL min^{-1} and purge flow was 5 mL min^{-1} . The GC was operated at a constant flow of 1.5 ml min^{-1} helium. The temperature program was started at 150°C for 1 min, followed by temperature ramping at 10°C min^{-1} to a final temperature of 250°C and held at 250°C for 1 min. The total analysis time was 12 minutes with detector temperature at 250°C. The retention time and identity of each FAME peak was calibrated using the Supelco 37 component FAME mix and only direct hits of three samples were included (Sigma Aldrich, UK).

Direct transesterification of wet vs dry microalgal biomass

To a 2 mL Eppendorf, 1-2 mg dried biomass and acid washed glass beads (425-600 μm i.d) (Sigma Aldrich, UK) were added. For the wet samples (5 ml aliquots) comparative dry weights were calculated. The samples were centrifuged and washed as above and freeze dried using a CoolSafe freeze dryer (Labogene, Denmark). These pellets were weighted using a 5 d.p. balance for subsequent data analysis (Sartorius, UK) and the FAME extraction method above was used using 7 % ethanolic-HCl as the acid catalyst.

Effect of bead beating and mechanical cell disruption on direct transesterification of dry microalgal biomass

After the glass beads, toluene and sodium methoxide addition a bead beating step was introduced where the cells were disrupted using the Disrupter Genie® and fatty acid and EPA extraction was compared with homogenisation (Constant Systems) and no bead beating. Kapoore (2014) found that 5 cycles with a disruption time of 2 mins and 1 min was optimal for FAME extraction from *C. reinhardtii* and *N. salina* respectively and they were selected as tests in this study. They were compared with 1 cycle of 5 mins and 10 mins to determine if disruption time was more important than cycle time. After each disruption step the samples were placed on ice. The mixture was then transferred to 2 mL glass vials and the FAME method followed as above using 7 % ethanolic-HCl as the acid catalyst. Five cycles of disruption with 2 mins disruption, with an interval of 1 min on ice was determined to be optimal and was used for analysis in subsequent experiments.

Fatty acid method development

In this study sodium methoxide as a base catalyst and ethanolic HCl were tested as base catalyst alone and in combination. Sodium methoxide as a base catalyst alone did not result in direct transesterification (Figure S4.5). The possible reason behind no yield with the base catalyst alone could be the high free fatty acid content in *P. tricornutum* and a FFA content >3 % can result in the formation of soap (Kapoore, 2014). Thus, employing sodium methoxide as the only catalyst is not suitable for fatty acid production using direct transesterification. Using 7 % ethanolic-HCl alone as an acid catalyst resulted in poor transesterification to FAEE. The best performing acid and base catalyst combination for FAME extraction was sodium methoxide and 7 % methanolic-HCl (83.55 mg L⁻¹) followed by ethanolic-HCl (81.14 mg L⁻¹) but there was no significant difference between the acid catalysts employed. Sodium methoxide and ethanolic-HCl resulted in the highest extraction of EPA (20.13 mg/L) and thus due to its efficacy and safety profile was chosen for further development to compare wet and dry direct transesterification.

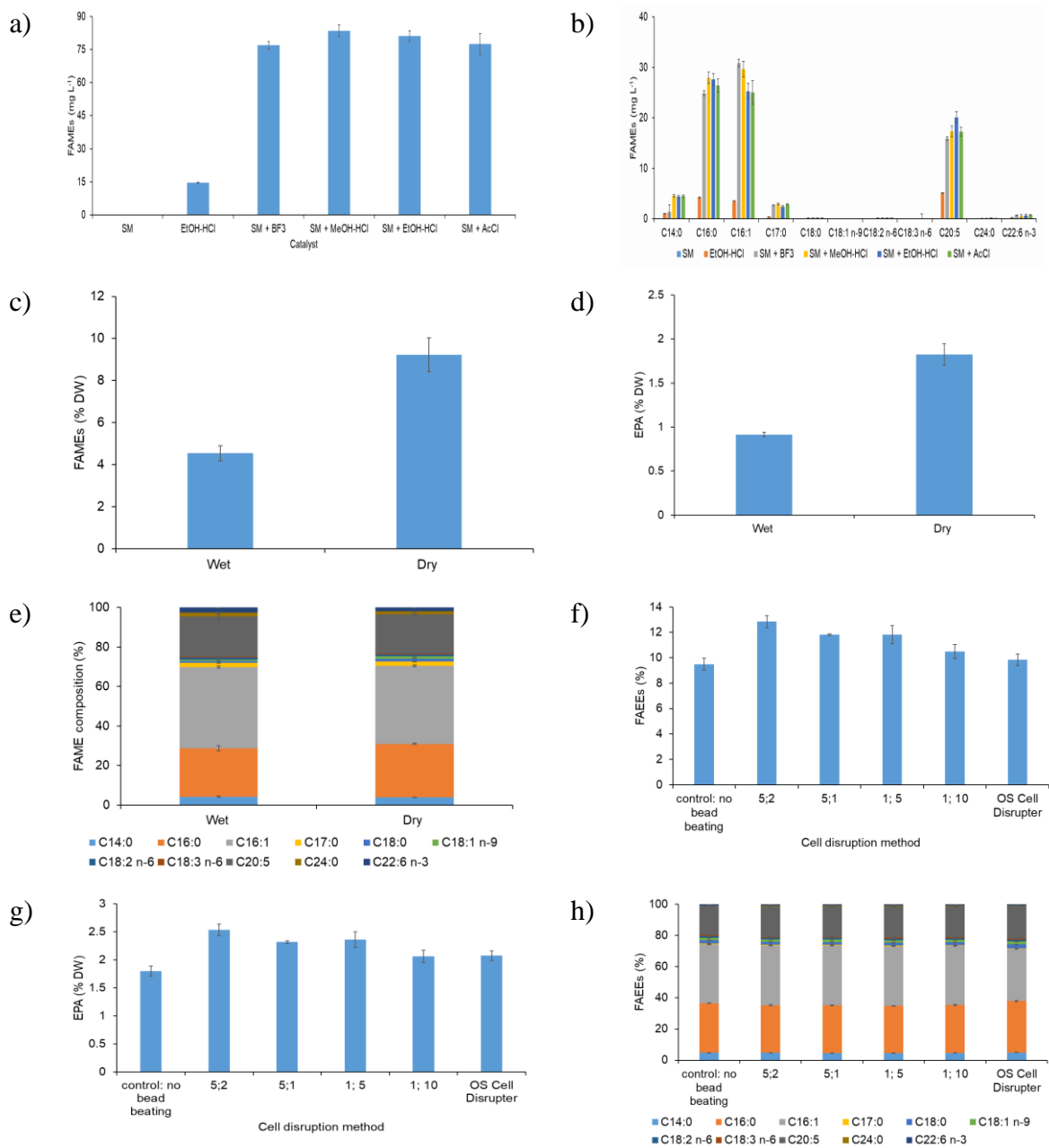


Figure S4.12 – Fatty acid method modification. Effect of direct transesterification method (acid and base) on wet biomass for: a) TFA content (mg/L) and b) individual fatty acid content. Sodium methoxide (SM), methanolic-HCl (MeOH-HCl), boron trifluoride (BF₃), ethanolic-HCl (EtOH-HCl), acetyl chloride (AcCl). Effect of direct transesterification method on wet and dry biomass; c) TFA, d) EPA content and e) FAMEs composition. Effect of bead beating on f) FAEE, g) EPA content and h) FAEE composition.

Effect of lyophilising biomass compared with wet direct transesterification and the effect of cell disruption

Lyophilisation is reported to have an adverse effect on the recovery of short chain SFAs (Kapoor, 2014) and therefore the effect of direct transesterification methods on fatty acid and EPA production was conducted on wet and dry samples. Extraction of dry biomass resulted in a significantly higher TFA (9.23 % DW) and EPA (1.82 % DW) content ($P < 0.05$).

For microalgal cell disruption and fatty acid extraction many techniques have been tested including Soxhlet, microwave assisted extraction, homogenisation, mechanical cell presses, hydrothermal liquefaction and bead beating (Butler et al., 2020; Kapoor, 2014; Kapoor et al., 2018). Amongst mechanical methods bead beating has been reported as the most effective cell disruption method in laboratories (Kapoor, 2014; Lee et al., 2010; Ryckebosch et al., 2012). An optimal cycle time of 5 and disruption times of 2 mins and 1 min have been found for *C. reinhardtii* and *N. salina* respectively with a bead size of 0.5 mm determined as optimal and multiple samples can be processed simultaneously (>12) (Kapoor, 2014). Agitated beads are often used for large-scale application (Gong and Bassi, 2016). Bead milling using the DYNO-Mill has also resulted in 97 % cell disintegration for the notoriously difficult algaenan containing *Chlorella vulgaris* at 25-145 g L⁻¹ (Postma et al., 2015). During bead beating care has to be considered for overheating which can result in product degradation (Lee et al., 2010).

In this investigation bead beating was compared with cell disruption by an OS Cell Disrupter which resulted in 97.60-98.04 % cell disruption at 20,000-30,000 psi respectively (data not shown). For bead beating it was determined that 2 mins cell disruption via bead beating with 5 cycles resulted in the highest FAEE content (12.85 % DW) and EPA content (2.54 % DW) compared to no bead beating (9.50 % and 1.80 % DW respectively) leading to a 35 and 41 % increase in FAEE and EPA content respectively. The other bead beating treatments with varied cycling and disruption times also resulted in higher FAEE and EPA contents compared to the control. The FAEE profiles were similar with C16:0 (30.18-32.97 % FAEEs), C16:1 (35.55-38.34 % FAEEs) and EPA (18.97-21.07 % FAEEs) being predominant. As 2 mins bead beating with 5 cycles resulted in the highest FAEE and EPA content this method was adopted for culture optimisation studies.

Effect of ethanol and methanol on chlorophyll a and fucoxanthin recovery

As with chlorophyll, fucoxanthin is a polar molecule and can be extracted with polar solvents such as methanol and ethanol. However, ethanol resulted in a higher total recovery of fucoxanthin and chlorophyll *a*.

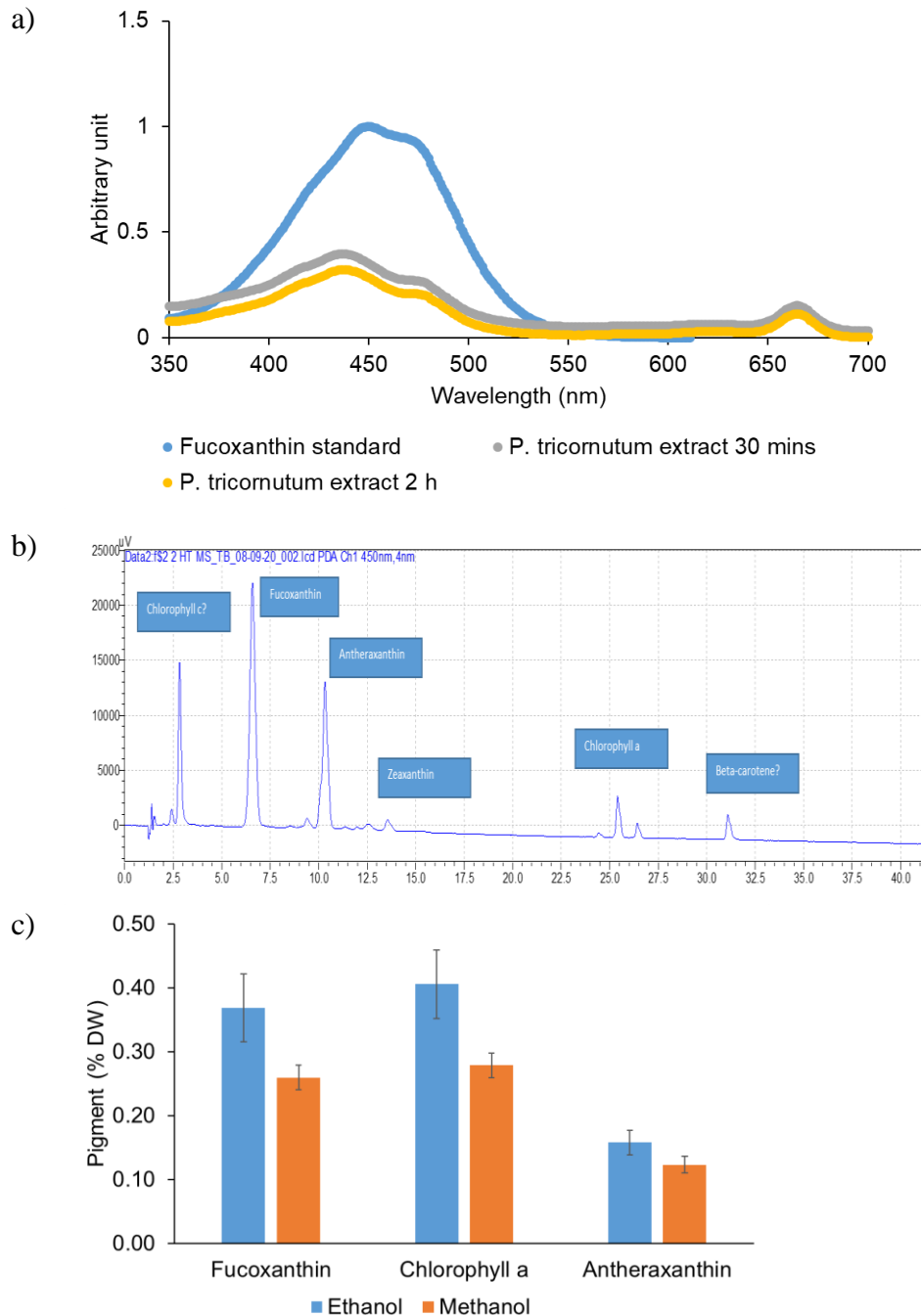


Figure S4.13 – a) Maximum absorbance of fucoxanthin, b) retention times of pigments observed using UHPLC with fucoxanthin, antheraxanthin, chlorophyll *a* with retention times of 6.6, 10.4, and 25.5 respectively, c) effect of solvent (methanol and ethanol) on pigment extraction; fucoxanthin, antheraxanthin and chlorophyll *a*.

Appendix C

This section contains supplementary figures, tables that resulted from Chapter 6 of this work.

Supplementary files

S5.1. Ionic composition of modified f/2 and Instant Ocean

Table 5.2 - Concentrations of the main ions in the medium used to cultivate *Phaeodactylum tricornutum* CCAP 1055/1 (modified f/2 with 33 g L⁻¹ Instant Ocean seawater).

| | Synthetic seawater (mM) |
|--|----------------------------|
| Cl ⁻ | 513.0 |
| Na ⁺ | 442.1 |
| Mg ²⁺ | 51.2 |
| K ⁺ | 10.1 |
| Ca ²⁺ | 9.4 |
| HCO ₃ ⁻ | 3.1 |
| Conductivity (mS cm ⁻¹) | 13.9 |

S5.3. Alkaline flocculation

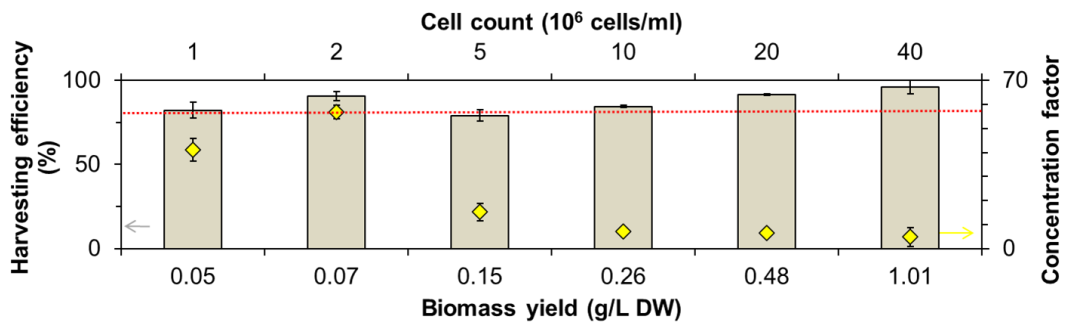


Figure 5.4 - Alkaline flocculation: the effect of biomass concentration (0.05-1.01 g/L DW) on the flocculation potential and concentration factor (CF) of sodium hydroxide (6.6 mM) after 10 mins harvesting. Red dotted line shows 80 % harvesting efficiency line.

S5.5. Testing the effect of the harvesting protocol on cell viability

A culture at 5×10^6 cells mL^{-1} , pH 7.5 (obtained as in section 2.5) was sedimented for 30 mins. The control had no flocculant addition and then aluminium sulphate, iron chloride and both Tanfloc 6025 and 8025 were tested at 20 mg L^{-1} and sodium hydroxide at 6.6 mM (264 mg L^{-1}) (tested in triplicate). For determining the effect on the photosynthetic apparatus, the quantum yield was determined, and 1 ml of culture was used directly. Pulse amplitude modulation (PAM) fluorometry was utilised to determine the maximum quantum yield (F_v/F_m) as a measure of photosynthetic efficiency at 630 nm (orange-red excitation light) using an AquaPen-C AP 110-C (Photo Systems Instruments, Czech Republic) after 15 mins dark adaptation at room temperature. Cells treated with 15 % H_2O_2 for 30 mins were used as a negative control as recommended by (Vandamme et al., 2015a). F_v/F_m is reported as the ratio of variable fluorescence to maximum fluorescence in the following equation.

F_m = maximum level of fluorescence after a short pulse of high intensity light

F_v = variable fluorescence, difference between F_m and F_0 and is the difference between fluorescence intensities with open and closed reaction centres.

$$\frac{F_v}{F_m} = (F_m - F_0) / F_m$$

Images were taken using a Leica DM750 microscope equipped with a Lecia DFC 450 camera for light microscopy at x400 magnification with oil to observe changes in microalgal physiology and the effect of each flocculant after 30 mins. Trypan blue staining was used for viability assays. One milliliter of each sample was centrifuged at 6000 rpm for 5 mins and the supernatant was discarded. The pellet was then re-suspended in 1 mL phosphate buffered saline (PBS). The viability of flocculated cells was tested by dye exclusion using 0.4 % Trypan blue (Sigma Aldrich, UK), which is excluded by viable cells. To 100 μL of cells, 100 μL 0.4 % Trypan blue solution was added and the cells were incubated for three minutes at room temperature and they were counted using a haemocytometer.

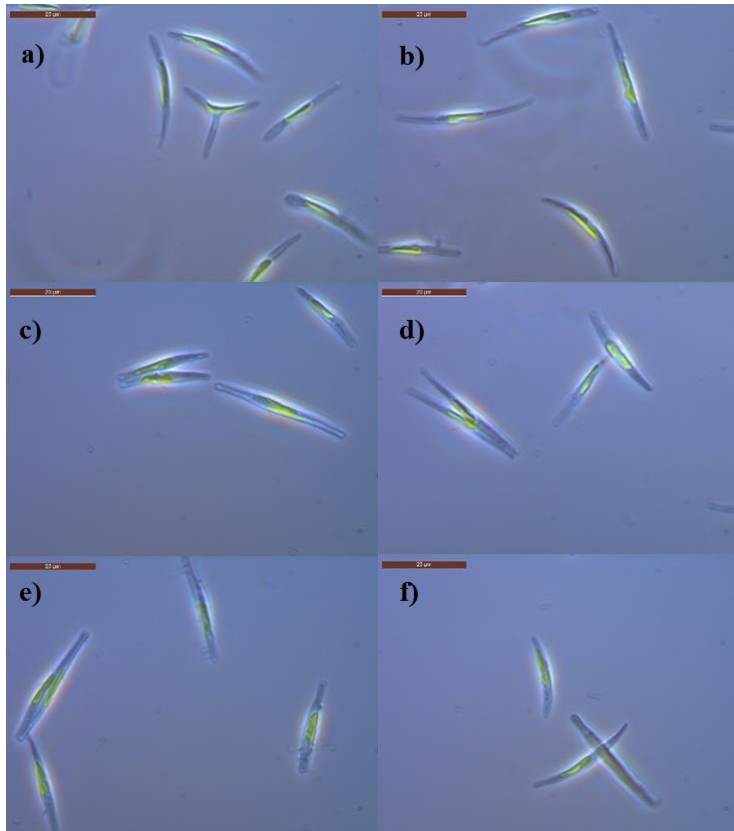


Figure 5.6 - Effect of no flocculant compared with flocculant addition on cell morphology based on light microscopy after 30 mins exposure: a) control, b) aluminium sulphate, c) iron chloride, d) sodium hydroxide, e) Tanfloc 6025 and f) Tanfloc 8025. Images were taken using a Leica DM750 microscope equipped with a Lecia DFC 450 camera for light microscopy at x400 magnification with oil.

S5.7. Testing the effect of the harvesting protocol on product accumulation

For the effect on product accumulation (chlorophyll *a*, protein, carbohydrate, FAMES and fucoxanthin) aliquots of 5 mL of algal culture were harvested by centrifugation at 4000 rpm for 10 mins, the pellets washed with 0.01 M phosphate buffered saline (PBS) and transferred to a 2 ml Eppendorf safe-lock tube, centrifuged at 13,000 rpm for 5 mins and stored at -20°C for analysis. For comparative dry weight calculations, the samples were then freeze dried using a CoolSafe freeze dryer (Labogene, Denmark). These pellets were weighted using a 5 d.p. balance for subsequent data analysis (Sartorius, UK).

A modified version of Kapoore (2014) was used for FAME analysis using direct transesterification on the wet biomass with methanolic-HCl (7 %) replacing BF₃ as the acid catalyst. All chemicals used were of HPLC grade (Sigma-Aldrich, UK) unless otherwise stated. Combined extraction of chlorophyll *a*, carbohydrate, and protein was carried out according to Chen and Vaidyanathan (2013) and Padmaperuma (2017).

For determination of fucoxanthin content, the pellet was extracted with 1.5 mL ethanol with 250 mg L⁻¹ butylated hydroxytoluene (BHT) and disrupted by bead beating in bead beater tubes (Bertin Technologies) three times at 90 s x 5000 rpm with a 45 s break. After cell disruption the bead beating tubes were then centrifuged at 13,000 rpm for 3 mins. One millilitre of the supernatant was pipetted to a 5 mL glass tube. To the bead beating tube, 1 mL ethanol/BHT mixture was added and the tubes vortexed for 10 s. The tubes were then centrifuged at 13,000 rpm for 3 mins and 1 mL was transferred to the 5 mL glass tube. This procedure was repeated until the pellet was colourless (5 extractions necessary in total). The glass tubes were evaporated under nitrogen, the extract re-suspended in 1 mL absolute methanol (Sigma Aldrich, UK) and transferred to a 2 mL safe lock Eppendorf tube. The tubes were then centrifuged at 13,000 rpm for 2 mins before transferring the supernatant to amber coloured HPLC vials. To avoid photo-oxidation, all procedures were carried out under darkness.

Ultra-high-performance liquid chromatography (UHPLC) was used to quantify the fucoxanthin content. The HPLC method adopted was a modified version of Grant (2011). Three mobile phases were used: (A) 0.5 M Ammonium acetate in methanol/water 85:15, (B) Acetonitrile/water 90:10 and (C) Ethyl acetate 100 % using the gradient procedure described. The flow rate was set at 1 mL min⁻¹ and the column temperature at 25°C. The concentration of fucoxanthin was quantified by measuring at the absorbance at 450 nm. A linear calibration curve (R² = 0.99) covering the range 0-20 µg mL⁻¹ was constructed using a fucoxanthin

standard (Sigma Aldrich, UK). The retention time of the extracts matched the standard for fucoxanthin (6.7 mins).

Overall sodium hydroxide was found to result in the highest ranking, followed by iron chloride (Table D.2). Tanfloc 6025 and 8025 performed the worst in the ranking. If chlorophyll *a*, fucoxanthin, and fatty acids are to be produced Tanfloc 6025 and 8025 were shown to be suitable relative to the control samples but protein and carbohydrate were shown to be adversely affected, but this was the case with the other flocculants as well, and this could have been due to interference in the multi-assay procedure using wet biomass and further work is required to confirm this.

Table 5.8 - Effect of flocculant addition on quantum yield and biochemical composition of *Phaeodactylum tricornutum* for each treatment. (1) Control - no flocculant addition; (2) aluminium sulphate; (3) iron chloride; (4) sodium hydroxide; (5) Tanfloc 6015 and (6) Tanfloc 8025. Each flocculant (aluminium sulphate, iron chloride, Tanfloc 6025 and Tanfloc 8025) was applied at 20 mg L⁻¹ and sodium hydroxide was added at 264 mg L⁻¹ (6.6 mM) compared to the control (no flocculant addition). Data is displayed as a fold change relative to centrifugation. The function of dry weight composition was normalised according to the control weight of a 5 mL microalgal pellet (0.744 ± 0.001 g). Mean ± S.E. (biological triplicates)

| | 1 | 2 | 3 | 4 | 5 | 6 |
|-------------------|---------------|---------------------------------|---------------|---------------|---------------|---------------|
| Pellet weight (g) | 0.744 ± 0.001 | 0.752 ± 0.006 | 0.768 ± 0.004 | 1.436 ± 0.046 | 0.752 ± 0.006 | 0.751 ± 0.004 |
| Quantum yield | 0.72 ± 0.00 | 0.71 ± 0.00 | 0.71 ± 0.00 | 0.72 ± 0.00 | 0.72 ± 0.00 | 0.72 ± 0.00 |
| | % DW | Fold change relative to control | | | | |
| Chlorophyll | 0.62 ± 0.02 | 0.98 ± 0.01 | 1.04 ± 0.03 | 1.58 ± 0.02 | 1.52 ± 0.04 | 1.26 ± 0.02 |
| Protein | 50.18 ± 2.82 | 0.88 ± 0.06 | 0.78 ± 0.05 | 0.48 ± 0.03 | 0.33 ± 0.02 | 0.6 ± 0.04 |
| Carbohydrates | 16.98 ± 1.63 | 0.92 ± 0.05 | 0.68 ± 0.09 | 0.49 ± 0.03 | 0.48 ± 0.02 | 0.62 ± 0.02 |
| FAMES | 8.89 ± 0.30 | 1.29 ± 0.15 | 1.54 ± 0.10 | 1.38 ± 0.03 | 0.97 ± 0.02 | 0.96 ± 0.07 |
| EPA | 1.29 ± 0.04 | 1.32 ± 0.16 | 1.54 ± 0.10 | 1.54 ± 0.02 | 0.92 ± 0.06 | 0.91 ± 0.12 |
| Fucoxanthin | 0.47 ± 0.02 | 0.97 ± 0.02 | 1.04 ± 0.03 | 1.56 ± 0.03 | 1.44 ± 0.06 | 1.23 ± 0.05 |

Table 5.9 - Effect on biochemical composition with each flocculant using ranking matrix (1-6) with a higher number representing a higher yield

| | Control (no flocculant) | Aluminium sulphate | Iron chloride | Sodium hydroxide | Tanfloc 6025 | Tanfloc 8025 |
|---------------|--------------------------------|---|-------------------------|-------------------------|---------------------|---------------------|
| Quantum yield | 6 | 5 | 5 | 6 | 6 | 6 |
| Chlorophyll | 1 | 2 | 3 | 6 | 5 | 4 |
| Protein | 6 | 5 | 4 | 2 | 1 | 3 |
| Carbohydrates | 6 | 5 | 4 | 2 | 1 | 3 |
| FAMES | 3 | 4 | 6 | 5 | 2 | 1 |
| EPA | 3 | 4 | 6 | 6 | 2 | 1 |
| Fucoxanthin | 2 | 1 | 3 | 6 | 5 | 4 |
| | Control | Al₂(SO₄)₃ | FeCl₃ | NaOH | Tanfloc 6025 | Tanfloc 8025 |
| Total | 27 | 26 | 31 | 33 | 22 | 22 |

Appendix D

This section contains supplementary figures, tables that resulted from Chapter 6 of this work.

Supplementary files

S6.1 – Morphological differences between strains under white and red: blue lights

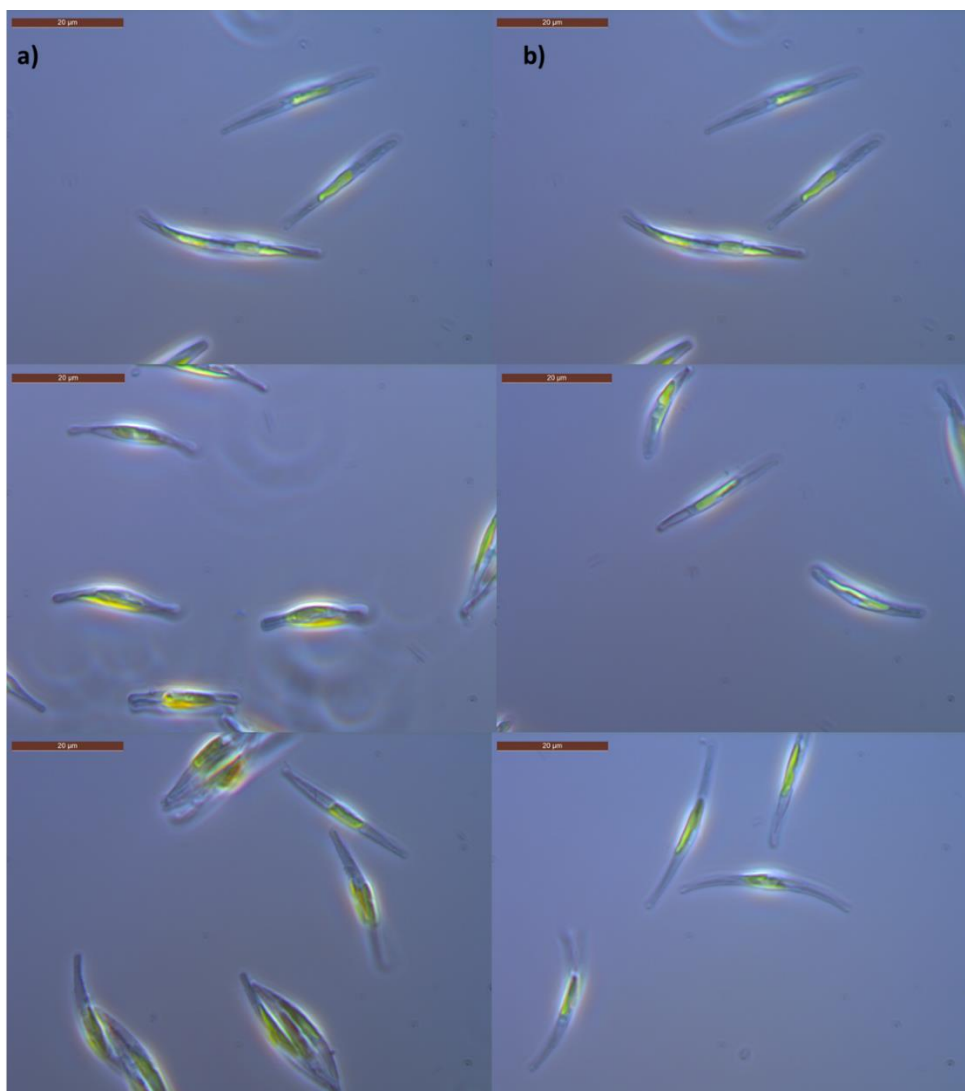


Figure S6.2 – Cell morphology differences between *P. tricornutum* CCAP 1055/1, UTEX 646 and Necton respectively under a) white LEDs and b) red: blue LEDs

Lighting cost

The benefit of applying a red: blue light mix is that less electrical power is needed because red and blue lights in combination can provide a higher number of photons for the same amount of energy compared to white light. Following Blanken et al. (2013), Planck's relation (Equation 1) can be used to obtain the amount of energy for a photon at a specific wavelength and further multiplication with the Avogadro constant N_A provides the amount of energy per mol_{ph} . In Equation 1, the energy of a photon E_{ph} in J or Ws ($1 \text{ J} = 1 \text{ Ws}$), is calculated with Planck's constant h in J.s, speed of light c in m s^{-1} and the wavelength λ in m.

Therefore, the theoretical maximum photosynthetically active radiation (PAR) efficiency can be calculated. As can be taken from Equation and Table, red photons (660 nm) contain less energy than blue photons (450 nm) and consequently provide a better theoretical maximum efficacy. Nevertheless, a theoretical maximum efficacy cannot be achieved as the wall-plug efficiency, the ratio of the radiant flux to the input electrical power, limits the energy conversion. At the moment, Osram Oslon Square LED emitter (Osram Opto Semiconductor) focusing on a wavelength of 660 nm and 450 nm, achieve a high efficacy of $3.91 \mu\text{mol J}^{-1}$ and $2.9 \mu\text{mol J}^{-1}$ (MechaTronix Horticulture Lighting, 2020a). Future development and improving of LED technology is expected to increase the actual photon energy efficacy and wall-plug efficiency (Schulze et al., 2014) The white LEDs can reach a photon energy efficacy of 2.7-3.1 $\mu\text{mol Ws}^{-1}$, obtained from MechaTronix Horticulture Lighting (2020a).

Providing red: blue lights in a 2.25:1 ratio with theoretical maximum photon energy efficacy at a total light intensity of $125 \mu\text{mol photons m}^{-2} \text{ s}^{-1}$ results in a total electrical consumption of 0.0258 kWh, whereas in practice, the realistic white light and the realistic red: blue LED combination under similar conditions cause consumptions of 0.0403-0.0463 kWh and 0.0353 kWh respectively (Appendix D). By replacing white LEDs with red: blue LEDs (2.25:1), a reduction of 36-44 % in power consumption is theoretically possible. Replacing white LEDs with the realistic red: blue LEDs would save 12-24 % of power consumption., presented in Table S6.1.

Equation
1:
$$E_{\text{ph}} = \frac{h \times c}{\lambda}$$

Table S6.3: Power consumption of different light regimes.

| Light | Wavelength [nm] | Photon energy efficacy [$\mu\text{mol}/\text{Ws}$] | [kWh/mol]A | PFD [$\mu\text{mol}/\text{m}^2.\text{s}$] | Consumption [kWh]B | Combined lights consumption [kWh]B |
|--------|-----------------|---|-------------|---|--------------------|------------------------------------|
| RedC | 660 | 5.52 | 0.0503 | 175 | 0.0317 | 0.0516 |
| BlueC | 450 | 3.76 | 0.0739 | 75 | 0.0199 | |
| WhiteD | - | 2.70-3.10 | 0.103-0.090 | 250 | 0.0926-0.0806 | - |
| RedE | 660 | 3.91 | 0.071 | 175 | 0.0448 | 0.0706 |
| BlueE | 450 | 2.9 | 0.0958 | 75 | 0.0259 | |

A $1 \text{ W s} = 2.7778 \times 10^{-7} \text{ kWh}$

B Calculated for $A = 1 \text{ m}^2$ and $t = 1 \text{ h}$

C Theoretical maximum efficacy

D Efficacy obtained from MechaTronix Horticulture Lighting (2020a)

E Efficacy obtained from MechaTronix Horticulture Lighting (2020b)

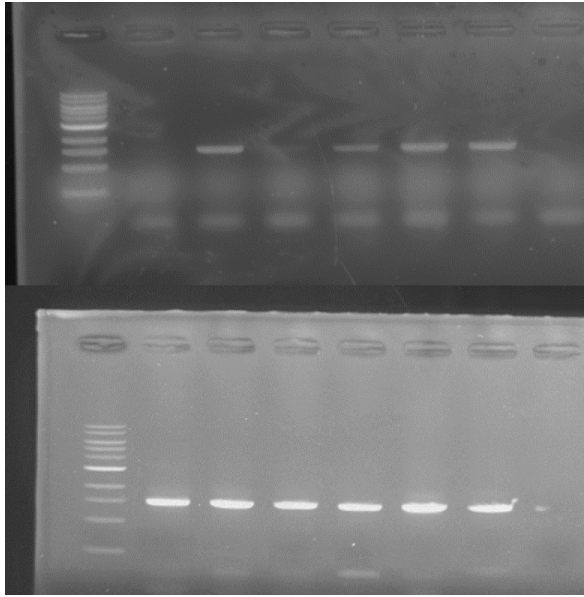


Figure S6.4 Effect of reduced annealing time (15 s) and increased number of cycles (35) on DNA yield; a) 98°C, 1 min, 30 x (98°C, 10 s, 58°C, 20 s, 72°C, 45 s), 72°C, 8 mins, 4°C hold and b) 98°C, 1 min, 35 x (98°C, 10 s, 58°C, 15 s, 72°C, 45 s), 72°C, 8 mins, 4°C hold. Well 1 to 7: TB1, TB2, TB3, TB4, TB6, TB11, -ve control (HN, MA, MA, AM, CA, S, -ve control). Reduced formation of primer dimers

P. tricornutum 18 S sequences

CCAP 1055/1

EAF3

GGAGCCGTNTTNAACACGGACCNNNNNNCCGTNTTGAAACACGGACCANGGAGCCGTCTTG
 AAACNCGGACCANGGAGCCGTNTTGAAACACGGACCANGGAGCCNTNTTGAAACACGGACC
 AAGGAGCCNTNTTGAAACNCGACCANGGAGCCGTCTTGAAACACGGACCANGGAGCCGTN
 TAAAAACATNGACCAGGGAGCCGTCTTAAAAACNCTTCNGACCGATCCGTTTTGAGAGATAGA
 ACATGGACCCNCCATGGANTTNGGGNTAGGGGNANNTTAGGNNTTGATTCCGNNNGGGGA
 NNTTAGANACGNCTACCNCNTCCANGGANNGCNNCANGCNCNTAAATTACCAATCC

ITTS055R

GATTGNCGAANCCACCGGCCCGGANGGGGGAGNCAAGACGCGGGTAACGATGGTTTCGTT
 CACTTCCTTTTCNGGGTTTCNGGNACTCTTAACTCTCTTTTCAAAGTTCTGTTGCNTCTTTCC
 CTCACGGNACTTGTCGCNACCGGNCTCCCNCCANNATTTNNCTTTAGANGGAATTTACCNC
 CCACTGGGAGCTGTNATCCCGAAACAACCTCNACTCNCAACGCGCGCTCCANGGGCCAGGCG
 ANCGGGGGTCTCNCCTCTCAGCCGCCCTGNTCCANGGACTTGGCCCGGCCNNGTAACGC
 ACACGCCTATAGACCACAATTCNGCGCCGCAGAACGGCGCANATTACATCTTGAGCTACTC
 CCGCTTCNGNCGCCCTTACTGAGGGAATCCTGGTTAGTTTCTTTTCTCCGNTTAATNATATG
 CTTAAATTCAGCGGGTCTTCTTGCTTGANCTGANATCNAAACGANGGNATNCTGGNNGGANN
 CNATGGACATNTCATTCAATTCAAAAGATGANCAAGNAANNNNNNNCGCTTNNCNCANTNNNN
 CTGCNGATGNNGCATTCTTANNANNGANGCGCNATACTAGANNNNNNNCTGGNNTGCTGCT
 GCAGNTCACTGNTGCCTNNTAGNATNNNCNCCGANGANGACGACNCTTGCNGCTNNTCCTAC
 ATACTGNNGANNNAANCCNNNNANCNCAATTNNANTGGAGTAGAACNANATNATAGCCNNNCG
 ACNNCCNNGAAGAATACTNCTNCTACGGNNNTTNCNTCGNNTCATATATNCANACGAACN
 NTNNAANANCAGCCANNANTNGNNGCGGCANGNNCNCAGNNCNCNCCCACTCGANNANAANAN
 ANTANNATNAGCNCANNGCTNANGGNTATNGNNGANCACTNAGAACCANCANGCATCCNNA
 GNNNANNNTGNNNNGAAGCCNNNNNGNGCNNTN

UTEX 646

EAF3

AGCTAATACATGCGTCAATACCCTTNTGGGGTAGTATTTATTANATTGAAACCAACCCCTTCG
GGGTGATGTGGTGATTTCATAATAAGCTTGC GGATCGCATGGCTTTTGCCGGCGATGGATCAT
TCAAGTTTCTGCCCTATCAGCTTGGATGGTAGGGTATTGGCCTACCATGGCTTTAACGGGT
AACGGGAAATCAGGGTTTGATTCCGGAGAGGGAGCCTGAGAGACGGCTACCACATCCAAGG
AAGGCAGCAGGCGCGTAAATTACCCAATCCTGACACAGGGAGGTAGTGACAATAAATAACAA
TGCCGGGCCTTTCTAGGTCTGGCTTTTGGAAATGAGAACAATTTAAACCCCTTATCGAGGATC
CATTGGAGGGCAAGTCTGGTGCCAGCAGCCGCGTAATTCCAGCTCCAATAGCGTATATTTAA
TGTGCTGCAGTTAAAAAGCTCGTAGTTGGATTTGTGGTGGGCCCGGTGGCTCGGCCTTAGT
TGNCCGTTGCTGTTTTGGGTCCGCCATCCTTGGGTGGAATCAGTGTGGCATTAAAGTTGTCGC
GCTGGGGATGCCATCGTTTACTGTGAAAAAATTANAGTGTTCAAAGCAGGCTTACGCCGTT
GAATATATTANCATGGAATAATGAGATAGGACCTTGGTACTATTTTGTGGTTTGC GCACCG
AGGNAATGATTAATANGGACAGTTGGGGGTATTCGNATTCATTGT CANANGTGA AATTCTT
GGATTTCTGGAANANNACTACTGCNAAAGCATTACCANNATGTTTTATTATCANAAACGA
AAGTTAGGGNATCGANNATGATTANATACCATCGTAGNCTTAA CATAAACTATGCCGNNCA
NGNATTGGCGGGTT

ITTS055R

GAACGGGGAAGTATGACGCAGCTAACACTGGTTTCNTTCGNTTCCTTTTCAGCAATTCAGG
TACTCTTTAACTCTCTTTTCAAAGTTCTGTTCATCTTTCCCTCACGGTACTTGTACGTCATC
GGTCTCCACAGTATTTAGCTTTAGATGGAATTTACCACCCACTTTGAGCTGCAATCCCAA
CAACTCGACTCGTCGACGCGCTCCAAAGGCCAGGCGAACGGGGTCTCACCCCTCAGC
CGCCCTGTTCCAAGGGACTTGGCCCCGGCCAGGTAACGCACACGCCTATAGACCACAATTCGG
CGCCGCAGAACGGCGCAGATTCACATNTGAGCTACTCCCGCTTCAGTCGCCCTTACTGAGG
GAATCCTGGTTAGTTTCTTTTCTCCGCTTAATTATATGCTTAAATTCAGCGGGTCTTCTTGC
TTGAGCTGAGATCAGGAACGAAGGTATGCTGGTGGAAACGATGGACATTTTCATTTCATCCAA
GATGAACGAAGAAAAACACACCCGCTTTCCACCAATCCGCTCTGCCNATGCCGATTCTTACCAA
GGAAGCGGATTACAGGACTTTGCGCTGGNCTGCTCCTGCAGTTCAGTCTTCTTTTANNA
TCCCNANGGGTGAANNCAAGCCTTGCAGCTTTTCCNTACCTACTGNAGANGGAAACCGAAA
CCGATTTGAGTGGAGTANAACAGATAAAAAGCCCANNANCNTCCNANG

Necton – N017

EAF3

GTCTAAGTATAAATCTTTTACTTTGAAACTGCGAATGGCTCNTTATNTCAGTTATAGTTTATT
TGATAGTCCCTTCACTATTTGGATAACCGTAGTAATTCTAGAGCTAATACATGCGTCAATACC
CTTCTGGGGTAGTATTTATTAGATTGAAACCAACCCCTTCGGGGTGATGTGGTGATTTCATAA
TAAGCTTGC GGATCGCATGGCTTTTGCCGGCGATGGATCATTCAAGTTTCTGCCCTATCAGC
TTTGGATGGTAGGGTATTGGCCTACCATGGCTTTAACGGGTAACGGGAAATCAGGGTTTGAT
TCCGGAGAGGGAGCCTGAGAGACGGCTACCACATCCAAGGAAGGCAGCAGGCGCGTAAATT
ACCCAATCCTGACACAGGGAGGTAGTGACAATAAATAACAATGCCGGGCCTTTCTAGGTCTG
GCTTTTGAATGAGAACAATTTAAACCCCTTATCGAGGATCCATTGGAGGGCAAGTCTGGTG
CCAGCAGCCGCGGTAATTCCAGCTCCAATAGCGTATATTAATGTTGCTGCAGTTAAAAAGCT
CGTAGTTGGATTTGTGGTGGGCCCGGTGGCTCGGCCTTAGTTGGCCGTTGCTGTTTTGGGT
CGCCATCCTTGGGTGGAATCAGTGTGGCATTAAAGTTGTGCGCTGGGGATGCCATCGTTTA
CTGTGAAAAAATTAGAGTGTTCAAAGCAGGCTTACGCCGTTGAATATATTAGCATGGAATAA
TGAGATAGGACCTTGGTACTATTTTGTGGTTTGC GCACCGANGTAATGATTAATAGGGACA
GTTGGGGGTATTTCGATTCCATTGT CANAGGTGAAATTTCTTGGATTTCTGGAANACNAACTA
CTGCGAAAGCATTACCANGATGTTTTTCAATTAATCAANAAACNAAGTTANGGATCGAANATGAT
TANATACCATCGTANTCNTNACCATAANCTATGNCGANNNGNATTGGNCGGNNNTCNTTAC
GTCTNCGTCAGCACCNATGANAAANCANANNNTTGGGNTCCTNNNGANNNTGGNCGCAN
GCT

ITTS055R

CGAACGCAGACACACGCAGGTCTAATCTCCCTACGCGCATTTCNNCANCCNGCCAAGCCT
GACAACGCTGGCCACAGCGCCCNCCGANGNAACGGGGAAGTATGACGCAGCTAACAC
TGGTTTCCTTCGNTTCCTTTTCAGCAATTCAGGTACTCTTTAACTCTCTTTTCAAAGTTCTGT
TGCATCTTTCCCTCACGGTACTTGTACGCTATCGGTCTCCACCAGTATTTAGCTTTAGATGG
AATTTACCACCCACTTTGAGCTGCAATCCCAAACAACCTCGACTCGTCGACGCGCGCTCCAAA
GGCCAGGCGAACGGGGGTCTACCCCTCTCAGCCGCCCTGTTCCAAGGGACTTGGCCCCGCC
AGGTAACGCACACGCCTATAGACCACAATTCGGCGCCGCAGAACGGCGCAGATTCACATCTT
GAGCTACTCCCGCTTCAGTCGCCCTTACTGAGGGAATCCTGGTTAGTTTCTTTTCTCCGCTT
AATTATATGCTTAAATTCAGCGGGTCTTCTTGCTTGAGCTGAGATCAGAAAACGAAGGTATNC
TGGTGGAAACGATGGACATTTCAATTCATTCAAAGATGATGAACGAAGAAAACACNCNGNTTT
CCACCAATCCGNTGCCGATGCCGATTCTTACCNAGGAAGCGCGATTACAGGACTTTGCGC
TGGCCTGCTCCTGCAGTTCNCTGTTTCTTTTAGTATCCCNAGGGTGAAGTCAAGCCTTGC
ANCTTTTCTACTACTGGAGACGGAAACCGAAAACCGCATTGAGTGGAGTAGAACCAGAT
AAAAGCCCAACGACCTCCAAAGAAGAATACTGCATCCAACGGTTTTTCCGTCNCATCAGATA
TGCGAACGTACACTTGAACAGCAGCCAGAGCTGGCAGCGCCAAAGTCCAGCAGTCCNNCN
TTGANAAAAATATATATATNTG

TB-1

>KC354707.1:73-1126 *Halomonas neptunia* strain MAT-17 16S ribosomal RNA gene, partial
sequenceAGCTTGCTAGATGCTGACGAGCGGCGGACGGGTGAGTAATGCATAGGAATCTGCCC
GGTAGTGGGGGATAACCTGGGGAAACCCAGGCTAATACCGCATACGTCCTACGGGAGAAAG
GGGGCTCCGGCTCCCGCTATTGGATGAGCCTATGTCCGATTAGCTAGTTGGTGAGGTAATGG
CTCACCAAGGCAACGATCCGTAGCTGGTCTGAGAGGATGATCAGCCACATCGGGACTGAGA
CACGGCCCGAACTCCTACGGGAGGCAGCAGTGGGGAATATTGGACAATGGGGGCAACCCTG
ATCCAGCCATGCCGCGTGTGTGAAGAAGGCCCTCGGGTTGTAAAGCACTTTCAGCGAGGAA
GAACGCCTAGTGGTTAATACCCATTAGGAAAGACATCACTCGCAGAAGAAGCACCCGGCTAAC
TCCGTGCCAGCAGCCGCGGTAATACGGAGGGTGCAAGCGTTAATCGGAATTACTGGGCGTA
AAGCGCGCGTAGGTGGCTTGATAAGCCGGTTGTGAAAGCCCCGGGCTCAACCTGGGAACGG
CATCCGGAACGTGCAGGCTAGAGTGCAGGAGAGGAAGGTAGAATTCCCGGTGTAGCGGTGA
AATGCGTAGAGATCGGGAGGAATACCAGTGGCGAAGGCGGCCTTCTGGACTGACACTGACA
CTGAGGTGCGAAAGCGTGGGTAGCAAAACAGGATTAGATACCCTGGTAGTCCACGCCGTA
CGATGTCGACACCGCTGGGTGCTAGACACTTTGTGGCGAAGTTAACCGCGATAAGTCTGA
CCGCTGGGGAGTACGGCCGCAAGGTTAAACTCAAATGAATTGACGGGGGCCGACACA
CGGTGGAGCATGTGGTTTAAATTCGATGCAACGCGAAGAACCCTTACCTACCCTTGACATCTAC
AGAAGCCGGAAGAGATTCTGGTGTGCCTTCGGGAACTGTAAGACAGGTGCTGCATGGCTGT
CGTCAGTCTCGTGTGTGAAATGTTGGGTTAAGTCCCGTAACGAGCGCAACCCTTGTCTTAT
TTGCCAGCACGTAATGG

TB-2

>JQ286003.1:24-1099 *Marinobacter alkaliphilus* strain SYNH ARB 16S ribosomal RNA gene, partial
sequenceAGGTGCTTGACACCCCGCTGACGAGCGGCGGACGGGTGAGTAATGCTTAGGAATCTG
CCAGTAGTGGGGGATAGCCCCGGGGAAACCCGGATTAATACCGCATACGTCCTACGGGAGA
AAGCAGGGGATCTTCGGACCTTGCCTACTGGATGAGCCTAAGTCGGATTAGCTAGTTGGTG
GGGTAAAGGCCTACCAAGGCGACGATCCGTAGCTGGTCTGAGAGGATGATCAGCCACATCG
GACTGAGACACGGCCCGAACTCCTACGGGAGGCAGCAGTGGGGAATATTGGACAATGGGG
GCAACCCCTGATCCAGCCATGCCGCGTGTGTGAAGAAGGCTTTCGGGTTGTAAAGCACTTTCA
GCGAGGAGGAAGGCCTTAAAGTTAATACCTTTGAGGATTGACGTTACTCGCAGAAGAAGCAC
CGGCTAACTCCGTGCCAGCAGCCGCGGTAATACGGAGGGTGCAAGCGTTAATCGGAATTAC
TGGGCGTAAAGCGCGCTAGGTGGTTAGGTAAGCGAGATGTGAAAGCCCCGGGCTTAACT
GGGAACGGCATTTCGAACCTGTCTGACTAGAGTGTGGTAGAGGGTAGTGGAAATTTCTGTGTA
GCGGTGAAATGCGTAGATATAGGAAGGAACACCAGTGGCGAAGGCGGCTACCTGGACCAAC
ACTGACACTGAGGTGCGAAAGCGTGGGGAGCAAAACAGGATTAGATACCCTGGTAGTCCACG
CCGTAAACGATGTCAACTAGCCGTTGGGACTCTTGAAGTCTTAGTGGCGCAGCTAACGCACT
AAGTTGACCGCTGGGGAGTACGGCCGCAAGGTTAAACTCAAATGAATTGACGGGGGGCC
GCACAAGCGGTGGAGCATGTGGTTTAAATTCGACGCAACGCGAAGAACCCTTACCTGGCCTTGA
CATCCAGAGAACTTCCAGAGATGGATTGGTGCCTTCGGGAACTCTGAGACAGGTGCTGCAT
GGCCGTCGACGCTGTCGTGATGTTGGGTTAAGTCCCGTAACGAGCGCAACCCTTAT
CCCTGGTTGCTAGCAGGTAATGCTGAGAACTCCAGG

TB-3

>CP045367.1:564449-565491 Marinobacter alkaliphilus
GGTGCTTGCACCCCGCTGACGAGCGGCGGACGGGTGAGTAATGCTTAGGAATCT
GCCAGTAGTGGGGGATAGCCCGGGGAAACCCGGATTAATACCGCATACTGCTACGGGAG
AAAGCAGGGGATCTTCGGACCTTGCCTATTGGATGAGCCTAAGTCGGATTAGCTAGTTGGT
GGGGTAAAGGCCTACCAAGGCGACGATCCGTAGCTGGTCTGAGAGGATGATCAGCCACATC
GGGACTGAGACACGGCCCGAACTCCTACGGGAGGCAGCAGTGGGGAATATTGGACAATGGG
GGCAACCCTGATCCAGCCATGCCGCGTGTGTGAAGAAGGCTTTCGGGTTGTAAAGCACTTTC
AGCGAGGAGGAAGGCCTTAAAGTTAATACCTTTGAGGATTGACGTTACTCGCAGAAGAAGCA
CCGGCTAACTCCGTGCCAGCAGCCGCGGTAATACGGAGGGTCAAGCGTTAATCGGAATTA
CTGGGCGTAAAGCGCGCTAGGTGGTTAGGTAAGCGAGATGTGAAAGCCCCGGGCTTAACC
TGGGAACGGCATTTCGAACTGTCTGACTAGAGTGTGGTAGAGGGTAGTGGAAATTTCTGTGT
AGCGGTGAAATGCGTAGATATAGGAAGGAACACCAGTGGCGAAGGCGGCTACCTGAGCCAA
CACTGACACTGAGGTGCGAAAGCGTGGGGAGCAAACAGGATTAGATACCCTGGTAGTCCAC
GCCGTAAACGATGTCAACTAGCCGTTGGGACTCTTGAAGTCTTAGTGGCGCAGCTAACGCAC
TAAGTTGACCGCCTGGGGAGTACGGCCGCAAGGTTAAAACCTCAAATGAATTGACGGGGGCC
CGACAAGCGGTGGAGCATGTGGTTTAAATTCGACGCAACGCGAAGAACCTTACCTGCGCTTG
ACATCCAGAGAACTTTCAGAGATGGATTGGTGCCTTCGGGAACTCTGAGACAGGTGCTGCA
TGGCCGTCGTCAGCTCGTGTCTGAGATGTTGGGTTAAGTCCCCTAACGAGCGCAACCCCTA
TCCCT

TB-4

>MK583623.1:171-995 *Algoriphagus marincola* strain NBP 16S ribosomal RNA gene, partial sequence
TGATTAGCTAGTTGGTGGGGTAAACCGCCACCAAGGCGACGATCAGTAGGGGTTCT
GAGAGGAAGGTCCCCACACTGGCACTGAGATACGGGCCAGACTCCTACGGGAGGCAGCAG
TAGGGAATATTGGGCAATGGACGAGAGTCTGACCCAGCCATGCCGCGTGCAGGAAGACGGC
CTATTGGGTTGTAAACTGCTTTTATACGGGAAGAAAAGGCCCATGCGTGGGACATTGCCGGT
ACCGTATGAATAAGCACCGGCTAACTCCGTGCCAGCAGCCGCGGTAATACGGAGGGTGCAA
GCGTTGTCCGGATTTATTGGGTTTAAAGGGTGCCTAGGCGGCTGATTAAGTCAGCGGTGAAA
GACTCCGGCTCAACCGGAGCAGTGCCTGATACTGGTTGGCTTGTGAGTGTGCAGGGGTAC
ATGGAATTGATGGTGTAGCGGTGAAATGCATAGATACCATCAGGAACACCGATAGCGAAGG
CATTGTACTGGGCAACTGACGCTGATGCACGAAAGCGTGGGGAGCGAACAGGATTAGA
TACCCTGGTAGTCCACGCGTAAACGATGATTACTCGCTGTTATGCCTTTAGGTGTAGCGGC
CAAGCGAAAGCGTTAAGTAATCCACCTGGGGAGTACGCCGGCAACGGTGAACCTCAAAGGA
ATTGACGGGGTCCGCACAAGCGGTGGAGCATGTGGTTTAAATTCGATGATACGCGAGGAAC
CTTACCTGGGCTAGAATGTGAAGGAATGATTTGGAGACAGATCAGTCAGCAATGACCTGAAA
CAAGGTGCTGCATGGCTGTCGTGAGCTCGTGCC

TB-5

>CP045367.1:564449-565512 *Marinobacter alkaliphilus*
GGTGCTTGCACCCCGCTGACGAGCGGCGGACGGGTGAGTAATGCTTAGGAATCTGCCAGT
AGTGGGGGATAGCCCGGGGAAACCCGGATTAATACCGCATACTGCTACGGGAGAAAGCAG
GGGATCTTCGGACCTTGCCTATTGGATGAGCCTAAGTCGGATTAGCTAGTTGGTGGGGTAA
AGGCTACCAAGGCGACGATCCGTAGCTGGTCTGAGAGGATGATCAGCCACATCGGGACTG
AGACACGGCCCGAACTCCTACGGGAGGCAGCAGTGGGGAATATTGGACAATGGGGGCAACC
CTGATCCAGCCATGCCGCGTGTGTGAAGAAGGCTTTCGGGTTGTAAAGCACTTTCAGCGAGG
AGGAAGGCCTTAAAGTTAATACCTTTGAGGATTGACGTTACTCGCAGAAGAAGCACCGGCTA
ACTCCGTGCCAGCAGCCGCGGTAATACGGAGGGTCAAGCGTTAATCGGAATTACTGGGCG
TAAAGCGCGCTAGGTGGTTAGGTAAGCGAGATGTGAAAGCCCCGGGCTTAACTGGGAAC
GGACTTTCGAACTGTCTGACTAGAGTGTGGTAGAGGGTAGTGGAAATTTCTGTGTAGCGGTG
AAATGCGTAGATATAGGAAGGAACACCAGTGGCGAAGGCGGCTACCTGGACCAACACTGAC
ACTGAGGTGCGAAAGCGTGGGGAGCAAACAGGATTAGATACCCTGGTAGTCCACGCGTAA
ACGATGTCAACTAGCCGTTGGGACTCTTGAAGTCTTAGTGGCGCAGCTAACGCACTAAGTTG
ACCGCTGGGGAGTACGGCCGCAAGGTTAAAACCTCAAATGAATTGACGGGGGCCCCGACAA
GCGGTGGAGCATGTGGTTTAAATTCGACGCAACGCGAAGAACCTTACCTGGCCTTGACATCCA
GAGAACCTTCCAGAGATGGATTGGTGCCTTCGGGAACTCTGAGACAGGTGCTGATGGCCGT
CGTCAGCTCGTGTCTGAGATGTTGGGTTAAGTCCCCTAACGAGCGCAACCCCTATCCCTGG
TTGCTAGCAGGTAATGCTG

TB-6R

>MK130723.1:379-1390 *Croceibacter atlanticus* strain ACBC086 16S ribosomal RNA gene, partial sequence

AACTGCTTTTATACGGGAAGAAACCCACCTACGTGTAGGTGGCTGACGGTACCGTAAGAATA
AGGACCGGCTAACTCCGTGCCAGCAGCCGCGTAATACGGAGGGTCCGAGCGTTATCCGGA
ATCATTGGGTTTAAAGGGTCCGCAGGCGGCCAGATAAGTCAGTGGTCAAATCCGTGGCTCA
ACCACGGAACCTGCCATTGATACTGTTTGGCTTGAATCAGTTCGAGGATGCCGGAATGTGTGG
TGTAGCGGTGAAATGCATAGATATCACACAGAACACCAATTGCGAAGGCAGGTGTCCAGAAC
TGTATTGACGCTGATGGACGAAAGCGTGGGTAGCGAACAGGATTAGATACCTGGTAGTCCA
CGCCGTAAACGATGGTCACTAGCTGTCCGGACTTAGGTCTGGGTGGCCAAGCGAAAGTGAT
AAGTGACCCACCTGGGGAGTACGTTTCGCAAGAATGAAACTCAAAGGAATTGACGGGGGCC
GCACAAGCGGTGGAGCATGTGGTTAATTCGATGATACGCGAGGAACCTTACCAGGGCTTAA
ATGCATTATGACAGGGGTGGAGACACCTTTTCTTCGGACATTTTGCAAGGTGCTGCATGGT
TGTCGTCAGCTCGTGCCGTGAGGTGTCAGGTTAAGTCTATAACGAGCGCAACCCCTGTTGT
TAGTTGCCAGCGAGTAATGTCGGAACTCTAGCAAGACTGCCGGTGCAAACCGCGAGGAAG
GTGGGATGACGTCAAATCATCACGCCCTTACGCCCTGGGCCACACACGTGCTAATGGG
AGGTACAGCAAGCACCCTGGGCGACCAGGAGCGAATCTGTAAAGCCTGTACAGTTCCG
ATCGGAGTCTGCAACTCGACTCCGTGAAGCTGGAATCGCTAGTAATCGCATATCAGCCATGA
TGCGGTGAATACGTTCCCGGGCCTGTACACACCGCCCGTCAAGCCATGGAAGCTGGGAGT
GCCTGAAGTCCGTGCGCCGCAAGGAGC

TB-9

>CP040451.1:82711-83738 *Halomonas titanicae*

TAGCTTGCTACCCGCTGACGAGCGGCGGACGGGTGAGTAATGCATAGGAATCTGCCCGATA
GTGGGGGATAACCTGGGGAAACCCAGGCTAATACCGCATACTCCTACGGGAGAAAGGGGG
CTTCGGCTCCCGCTATTGGATGAGCCTATGTCGGATTAGCTAGTTGGTAAGGTAATGGCTTA
CCAAGGCAACGATCCGTAGCTGGTCTGAGAGGATGATCAGCCACATCGGGACTGAGACACG
GCCCGAECTCCTACGGGAGGCAGCAGTGGGGAATATTGGACAATGGGGGCAACCCCTGATCC
AGCCATCCCGCTGTGTGAAGAAGGCCCTCGGGTTGTAAAGCACTTTCAGCGAGGAAGAAC
GCCTATCGGTTAATACCCGGTAGGAAAGACATCACTCGCAGAAGAAGCACCCGGCTAACTCCG
TGCCAGCAGCCGCGTAATACGGAGGGTGCAAGCGTTAATCGGAATTAAGTGGGCGTAAAGC
GCGCGTAGGTGGCTTGATAAGCCGTTGTGAAAGCCCCGGGCTCAACCTGGGAACGGCATC
CGGAACTGTCAGGCTAGAGTGCAGGAGAGGAAGGTAGAATCCCGGTGTAGCGGTGAAATG
CGTAGAGATCGGGAGGAATACCAGTGGCGAAGGCGGCCTTCTGGACTGACACTGACACTGA
GGTGCGAAAGCGTGGGTAGCAAACAGG

ATTAGATACCTGGTAGTCCACGCCGTAAACGATGTCGACCAGCCGTTGGGTGCCTAGAGCA
CTTTGTGGCGAAGTTAACGCGATAAGTTCGACCGCCTGGGGAGTACGGCCGCAAGGTTAAAA
CTCAAATGAATTGACGGGGGCCCGACAAGCGGTGGAGCATGTGGTTAATTCGATGCAAC
GCGAAGAACCTTACCTACCTTGACATCTACAGAAGCCGGAAGAGATTCTGGTGTGCCCTTCG
GGAAGTGAAGACAGGTGCTGCATGGCTGTCGTCAGCTCGTGTGTGAAATGTTGGGTTAAG
TCCCGTAACGAGCGCAACCC

TB-10

>MG029444.1:5-1055 *Marinobacter alkaliphilus*

TGCAAGTCGAGCGGTAACAGGGGGTGCTTGCACCCCGCTGACGAGCGGCGGACGGGTGAGT
AATGCTTAGGAATCTGCCAGTAGTGGGGGATAGCCCGGGAAACCCGGATTAATACCGCA
TACGTCCTACGGGAGAAAGCAGGGGATCTTCGACCTTGCCTACTGGATGAGCCTAAGTC
GGATTAGCTAGTTGGTGGGGTAAAGGCCTACCAAGGCGACGATCCGTAGCTGGTCTGAGAG
GATGATCAGCCACATCGGGACTGAGACACGGCCCGAACTCCTACGGGAGGCAGCAGTGGGG
AATATTGGACAATGGGGGCAACCCCTGATCCAGCCATGCCGCGTGTGTGAAGAAGGCTTTTCG
GGTTGTAAAGCACTTTCAGCGAGGAGGAAGGCCTTAAAGTTAATACCTTTGAGGATTGACGT
TACTCGCAGAAGAAGCACCCGGCTAACTCCGTGCCAGCAGCCGCGGTAATACGGAGGGTGCA
AGCGTTAATCGGAATTAAGTGGGCGTAAAGCGCGCTAGGTGGTTAGGTAAGCGAGATGTGA
AAGCCCCGGCTTAACTGGGAACGGCATTTCGAACTGTCTGACTAGAGTGTGGTAGAGGG
TAGTGGAATTTCTGTGTAGCGGTGAAATGCGTAGATATAGGAAGGAACACCAGTGGCGAA
GGCGGCTACCTGGACCAACTGACACT

GAGGTGCGAAAGCGTGGGGAGCAAACAGGATTAGATACCCTGGTAGTCCACGCCGTAAACG
ATGTCAACTAGCCGTTGGGACTCTTGAAGTCTTAGTGGCGCAGCTAACGCACCTAAGTTGACC
GCCTGGGGAGTACGGCCGCAAGGTTAAAACTCAAATGAATTGACGGGGGCCGCACAAGCG
GTGGGAGATGTGGTTAATTTCGACGCAACGCGAAGAACCCTTACCTGGCCTTGACATCCAGAG
AACTTCCAGAGATGGATTGGTGCCTTCGGGAACTCTGAGACAGGTGCTGCATGGCCGTCGT
CAGCTCGTGTCTGAGATGTTGGGTTAAGTCCCGTAAACGAGCG

TB-11

>CP022336.1:1530884-1531926 *Sphingorhabdus* sp. SMR4y chromosome, complete genomeTTAGAGTGCCCAACCAAATGGTAGCAACTAAAGATAGGGGTTGCGCTCGTTGCGGGA
CTTAACCCAACATCTCACGACACGAGCTGACGACAGCCATGCAGCACCTGTCACTGATCCAG
CCGAGCTGAAGGAAACCATCTCTGGTATCCGCGATCAGGATGTCAAACGCTGGTAAGGTTCT
GCGCGTTGCGTCGAATTAACCAACATGCTCCACCGCTTGTGCAGGCCCCCGTCAATTCCTTT
GAGTTTAAATCTTGCACCGTACTCCCCAGGCGGATAACTTAATGCGTTAGCTGCGCCACCA
AAGCCCTGTGGGCCCTAGCAGCTAGTTATCATCGTTTACGGCGTGGACTACCAGGGTATCTA
ATCCTGTTTGTCTCCCCACGCTTTCGCACCTCAGCGTCAATACTTGTCCAGCGAGTCGCCTTC
GCCACTGGTGTCTTCCGAATATCTACGAATTCACCTCTACACTCGGAATTCCACTCGCCTC
TCCAAGATTCTAGTCACCTAGTTTCAAAGGCAGTTCCGGAGTTGAGCTCCGGGCTTTCACCT
CTGACTTGAGTAACCGCCTACGCGCGCTTACGCCAGTAATTCCGAACAACGCTAGCTCCC
TCGGTATTACCGCGGCTGCTGGCACGGAGTTAGCCGGAGCTTATTCTCCAGGTACTGTCATT
ATCATCCCTGGTAAAAGAGCTTTACAACCCTAAGGCCTTCATCACTCACGCGGCATTGCTGG
ATCAGGCTTTCGCCATTGTCCAATATTTCCCACATGCTGCCTCCCGTAGGAGTCTGGGCCGT
GTCTCAGTCCCAGTGTGGCTGATCATCCTCTCAGACCAGCTAAAGATCGTCCGCTTGGTGAG
CCTTTACCTACCAACAAGCTAATCTTACGCGGGTTCATCAAAGGGCGATAAATCTTTGGTC
CGAAGACATTATGCGGTATTAGCTCAAATTTCTCTGAGTTATTCCGCACCCTATGGTAGATCC
CCACGCGTTACGCACCCGTGCGCCACTAGATCCGAAGATCTCGTTCGACTTGCA

S6.6 - Cultivation in flat-panel Algaegerm PBRs

Two 2 L bottles were used to inoculate one 25 L Algaegerm (0.27, 0.78 and 1.27 g L⁻¹ DW for repeated batch runs 1, 2 and 3 respectively) with the same medium composition outlined in the methods (filtered natural seawater, Nutribloom with 4 mM nitrate, 2 mL L-1 NutriBloom plus). The Algaegerm was 72 cm Length x 72 cm Width with a 7.5 cm light path (4.5 cm culture, 3 cm temperature jacket). The culture was mixed by enriched air, with 2 % CO₂ under continuous illumination provided by white fluorescent lamps (153 μmol photons m⁻² s⁻¹), resulting in 1 μmol photons m⁻² s⁻¹ outgoing light. The temperature was controlled by a heating-cooling coil (regulated with water) at 21°C for *P. tricornutum*.

Batches 1-2 were run in August and batch 3 was run in early-September 2019. The maximum biomass concentration achieved was 5.65 g L⁻¹ DW after batch 1. After run 1, 2 and 3 biomass productivities of 0.73, 0.29 and 0.33 g L⁻¹ d⁻¹ were achieved respectively (average 0.45 g L⁻¹ d⁻¹). After batch 1 predatory ciliates were observed and these could have resulted in a decrease in biomass productivity, along with difficulties in cooling the system during summer cultivation where the temperature increased up to 31°C and this caused a culture crash after the third run after 6 days. Through taxonomic identification it was speculated that the ciliate could have been *Parallelostrombidium* sp., *Antestrombidium* sp. or *Spirostrombidium* but molecular typing was not conducted.

After the runs 3-4 days of downtime was required to clean the fouling using a combination of sodium hydroxide and sodium hypochlorite (200 ppm) with the culture aerated.

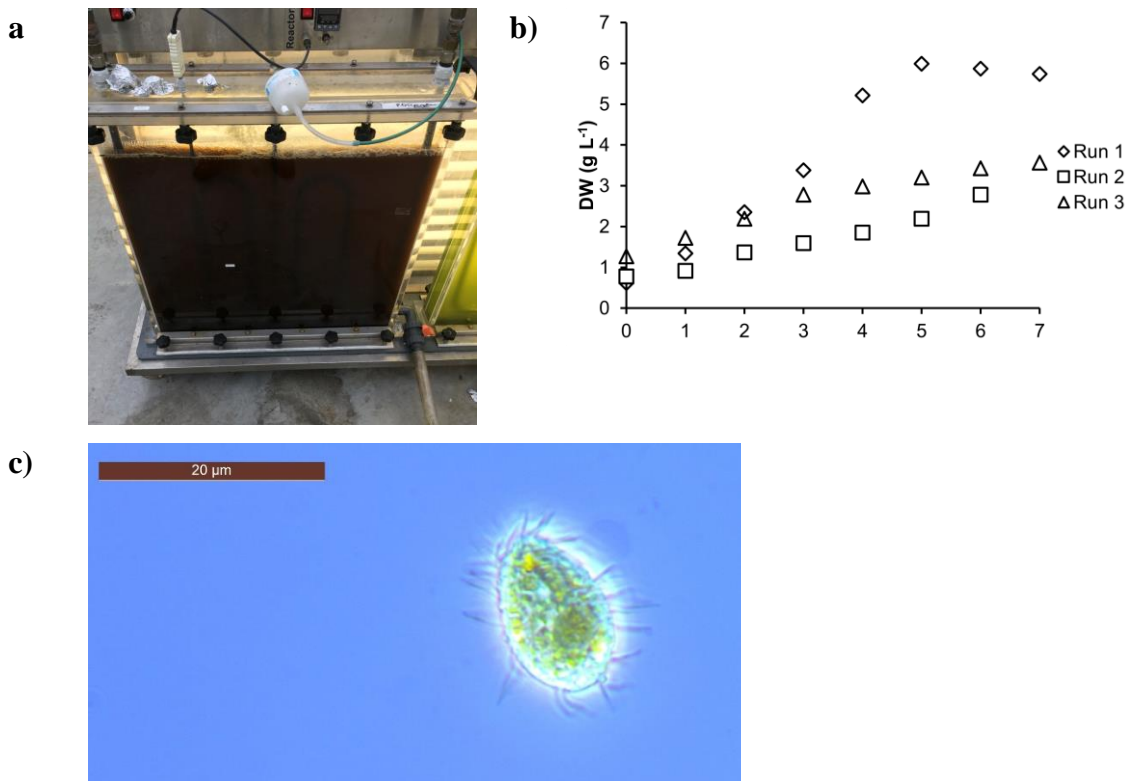


Figure S6.7 – Necton N017 cultivation; a) scaling up of Necton N017 strain in Algaegerm system, b) growth profile over three repeated-batch cultivations in the Algaegerm system in a greenhouse, AlgaePARC, Wageningen University, Netherlands, and d) ciliate contamination

Bibliography

- 't Lam, G.P., Vermuë, M.H., Eppink, M.H.M.M., Wijffels, R.H., van den Berg, C., 2017. Multi-Product Microalgae Biorefineries: From Concept Towards Reality. *Trends Biotechnol.* 36, 216–227. <https://doi.org/10.1016/j.tibtech.2017.10.011>
- 't Lam, G.P., Vermue, M.H., M.H.M., E., Wijffels, R.H., van den Berg, C., 2019. Multi-product microalgae biorefineries: from oncept towards reality. *Cell Press Rev.* 36, 217–227.
- 't Lam, G.P., Vermuë, M.H., Olivieri, G., van den Broek, L.A.M., Barbosa, M.J., Eppink, M.H.M., Wijffels, R.H., Kleinegris, D.M.M., 2014. Cationic polymers for successful flocculation of marine microalgae. *Bioresour. Technol.* 169, 804–807. <https://doi.org/10.1016/j.biortech.2014.07.070>
- Abdul Hamid, S.H., Lananan, F., Din, W.N.S., Lam, S.S., Khatoon, H., Endut, A., Jusoh, A., 2014. Harvesting microalgae, *Chlorella* sp. by bio-flocculation of *Moringa oleifera* seed derivatives from aquaculture wastewater phytoremediation. *Int. Biodeterior. Biodegrad.* 95, 270–275. <https://doi.org/10.1016/j.ibiod.2014.06.021>
- Abdul Hamid, S.H., Lananan, F., Khatoon, H., Jusoh, A., Endut, A., 2016. A study of coagulating protein of *Moringa oleifera* in microalgae bio-flocculation. *Int. Biodeterior. Biodegrad.* 113, 310–317. <https://doi.org/10.1016/j.ibiod.2016.03.027>
- Abel, G.J., Barakat, B., KC, S., Lutz, W., 2016. Meeting the Sustainable Development Goals leads to lower world population growth. *Proc. Natl. Acad. Sci.* 113, 14294–14299. <https://doi.org/10.1073/pnas.1611386113>
- Abida, H., Dolch, L.-J., Meï, C., Villanova, V., Conte, M., Block, M.A., Finazzi, G., Bastien, O., Tirichine, L., Bowler, C., Rébeillé, F., Petroustos, D., Jouhet, J., Maréchal, E., 2015. Membrane Glycerolipid Remodeling Triggered by Nitrogen and Phosphorus Starvation in *Phaeodactylum tricornutum*. *Plant Physiol.* 167, 118–136. <https://doi.org/10.1104/pp.114.252395>
- Acién Fernández, F.G., Hall, D.O., Cañizares Guerrero, E., Krishna Rao, K., Molina Grima, E., 2003. Outdoor production of *Phaeodactylum tricornutum* biomass in a helical reactor. *J. Biotechnol.* 103, 137–152. [https://doi.org/10.1016/S0168-1656\(03\)00101-9](https://doi.org/10.1016/S0168-1656(03)00101-9)
- Acién Fernández, F.G., Sánchez Pérez, J.A., Fernández Sevilla, J.M., Camacho, F.G.G., Molina Grima, E., 2000. Modeling of Eicosapentaenoic Acid (EPA) Production from *Phaeodactylum tricornutum* Cultures in Tubular Photobioreactors. Effects of Dilution Rate, Tube Diameter, and Solar Irradiance. *Biotechnol. Bioeng.* 68, 173–183. [https://doi.org/10.1002/\(SICI\)1097-0290\(20000420\)68:2<173::AID-BIT6>3.0.CO;2-C](https://doi.org/10.1002/(SICI)1097-0290(20000420)68:2<173::AID-BIT6>3.0.CO;2-C)
- Adamo, S.D., Schiano, G., Lowe, G., Szaub-newton, J., Beacham, T., Landels, A., Allen, M.J., Spicer, A., Matthijs, M., 2019. Engineering the unicellular alga *Phaeodactylum tricornutum* for high-value plant triterpenoid production. *Plant Biotechnol. J.* 17, 75–87. <https://doi.org/10.1111/pbi.12948>
- Adamo, S.D., Schiano, G., Lowe, G., Szaub-Newton, J., Beacham, T., Landels, A., Allen, M.J., Spicer, A., Matthijs, M., D'Adamo, S., Schiano di Visconte, G., Lowe, G., Szaub-Newton, J., Beacham, T., Landels, A., Allen, M.J., Spicer, A., Matthijs, M., 2018. Engineering The Unicellular Alga *Phaeodactylum tricornutum* For High-Value Plant Triterpenoid Production. *Plant Biotechnol. J.* 0–2. <https://doi.org/10.1111/pbi.12948>
- Al-shathr, A.R., 2019. Exploiting the Role of Coke in Catalytic Transformations. Doctoatorial Diss. Univ. Sheffield, Sheffiled, United Kingdom.
- Alam, M.A., Xu, J.L., Wang, Z., 2020. Microalgae biotechnology for food, health and high value products. *Microalgae Biotechnol. Food, Heal. High Value Prod.* 1–483. <https://doi.org/10.1007/978-981-15-0169-2>
- Alipanah, L., Rohloff, J., Winge, P., Bones, A.M., Brembu, T., 2015. Whole-cell response to

- nitrogen deprivation in the diatom *Phaeodactylum tricornutum*. *J. Exp. Bot.* 66, 6281–6296. <https://doi.org/10.1093/jxb/erv340>
- Alipanah, L., Winge, P., Rohloff, J., Najafi, J., Brembu, T., Bones, A.M., 2018. Molecular adaptations to phosphorus deprivation and comparison with nitrogen deprivation responses in the diatom *Phaeodactylum tricornutum*. *PLoS One* 13, 1–24. <https://doi.org/10.1371/journal.pone.0193335>
- Allakhverdiev, S.I., Kreslavski, V.D., Klimov, V. V., Los, D.A., Carpentier, R., Mohanty, P., 2008. Heat stress: An overview of molecular responses in photosynthesis. *Photosynth. Res.* 98, 541–550. <https://doi.org/10.1007/s11120-008-9331-0>
- Anarjan, N., Ping Tan, C., 2013. Physico-chemical stability of astaxanthin nanodispersions prepared with polysaccharides as stabilizing agents. *Int. J. Food Sci. Nutr.* 64, 744–748. <https://doi.org/10.3109/09637486.2013.783001>
- Araújo, R., García-tasende, M., 2021. Current Status of the Algae Production Industry in Europe: An Emerging Sector of the Blue Bioeconomy 7, 1–24. <https://doi.org/10.3389/fmars.2020.626389>
- Arbenz, A., Avérous, L., 2015. Chemical modification of tannins to elaborate aromatic biobased macromolecular architectures. *Green Chem.* 17, 2626–2646. <https://doi.org/10.1039/c5gc00282f>
- Bae, M., Kim, M.B., Park, Y.K., Lee, J.Y., 2020. Health benefits of fucoxanthin in the prevention of chronic diseases. *Biochim. Biophys. Acta - Mol. Cell Biol. Lipids* 1865, 158618. <https://doi.org/10.1016/j.bbalip.2020.158618>
- Bai, X., Song, H., Lavoie, M., Zhu, K., Su, Y., Ye, H., Chen, S., Fu, Z., Qian, H., 2016. Proteomic analyses bring new insights into the effect of a dark stress on lipid biosynthesis in *Phaeodactylum tricornutum*. *Sci. Rep.* 6, 1–10. <https://doi.org/10.1038/srep25494>
- Balamurugan, S., Wang, X., Wang, H.-L., An, C.-J., Li, H., Li, D.-W., Yang, W.-D., Liu, J.-S., Li, H.-Y., 2017. Occurrence of plastidial triacylglycerol synthesis and the potential regulatory role of AGPAT in the model diatom *Phaeodactylum tricornutum*. *Biotechnol. Biofuels* 10, 97. <https://doi.org/10.1186/s13068-017-0786-0>
- Banerjee, S., Ramaswamy, S., 2017. Dynamic process model and economic analysis of microalgae cultivation in open raceway ponds. *Algal Res.* 26, 330–340. <https://doi.org/10.1016/j.algal.2017.08.011>
- Baoyan, G., Ailing, C., Wenyuan, Z., Aifen, L., Chengwu, Z., Gao, B., Chen, A., Zhang, W., Li, A., Zhang, C., 2017. Co-Production of Lipids, Eicosapentaenoic Acid, Fucoxanthin, and Chrysolaminarin by *Phaeodactylum tricornutum* Cultured in a Flat-Plate Photobioreactor Under Varying Nitrogen Conditions. *J. Ocean Univ. China (Oceanic Coast. Sea Res.* 16, 916–924. <https://doi.org/10.1007/s11802-017-3174-2>
- Barka, F., Angstenberger, M., Ahrendt, T., Lorenzen, W., Bode, H.B., Büchel, C., 2016. Identification of a triacylglycerol lipase in the diatom *Phaeodactylum tricornutum*. *Biochim. Biophys. Acta - Mol. Cell Biol. Lipids* 1861, 239–248. <https://doi.org/10.1016/j.bbalip.2015.12.023>
- Barrado-Moreno, M.M., Beltrán-Heredia, J., Martín-Gallardo, J., 2016. Microalgal removal with natural coagulants. *Phycologia* 55, 688–695. <https://doi.org/10.2216/15-113.1>
- Barros, A.I., Gonçalves, A.L., Simões, M., Pires, J.C.M.M., 2015. Harvesting techniques applied to microalgae: A review. *Renew. Sustain. Energy Rev.* 41, 1489–1500. <https://doi.org/10.1016/j.rser.2014.09.037>
- Becker, W., Michels, M.H.A., 2004. Microalgae for aquaculture, in: *Handbook of Microalgal Culture: Biotechnology and Applied Phycology*. pp. 380–391.
- Benemann, J.R., Woertz, I., Lundquist, T., 2018. Autotrophic microalgae biomass production: From niche markets to commodities. *Ind. Biotechnol.* 14, 3–10. <https://doi.org/10.1089/ind.2018.29118.jrb>

- Benoiston, A.-S.S., Ibarbalz, F.M., Bittner, L., Guidi, L., Jahn, O., Dutkiewicz, S., Bowler, C., 2017. The evolution of diatoms and their biogeochemical functions. *Philos. Trans. R. Soc. B Biol. Sci.* 372, 20160397. <https://doi.org/10.1098/rstb.2016.0397>
- Blanken, W., Cuaresma, M., Wijffels, R.H., Janssen, M., 2013. Cultivation of microalgae on artificial light comes at a cost. *Algal Res.* 2, 333–340. <https://doi.org/10.1016/j.algal.2013.09.004>
- Blockx, J., Verfaillie, A., Thielemans, W., Muylaert, K., 2018. Unravelling the Mechanism of Chitosan-Driven Flocculation of Microalgae in Seawater as a Function of pH. *ACS Sustain. Chem. Eng.* [acssuschemeng.7b04802](https://doi.org/10.1021/acssuschemeng.7b04802). <https://doi.org/10.1021/acssuschemeng.7b04802>
- Borowitzka, M.A., 1999. Commercial production of microalgae: ponds, tanks, tubes and fermenters. *J. Biotechnol.* 70, 313–321.
- Bowler, C., Allen, A.E., Badger, J.H., Grimwood, J., Jabbari, K., Kuo, A., Maheswari, U., Martens, C., Maumus, F., Otilar, R.P., Rayko, E., Salamov, A., Vandepoele, K., Beszteri, B., Gruber, A., Heijde, M., Katinka, M., Mock, T., Valentin, K., Verret, F., Berges, J. a, Brownlee, C., Cadoret, J.-P., Chiovitti, A., Jae Choi, C., Coesel, S., De Martino, A., Chris Detter, J., Durkin, C., Falciatore, A., Fournet, J., Haruta, M., J Huysman, M.J., Jenkins, B.D., Jiroutova, K., Jorgensen, R.E., Joubert, Y., Kaplan, A., Kröger, N., Kroth, P.G., La Roche, J., Lindquist, E., Lommer, M., Martin-Jézéquel, V., Lopez, P.J., Lucas, S., Mangogna, M., McGinnis, K., Medlin, L.K., Montsant, A., Oudot-Le Secq, M.-P., Napoli, C., Obornik, M., Schnitzler Parker, M., Petit, J.-L., Porcel, B.M., Choi, C.J., Coesel, S., De Martino, A., Detter, J.C., Durkin, C., Falciatore, A., Fournet, J., Haruta, M., Huysman, M.J.J., Jenkins, B.D., Jiroutova, K., Jorgensen, R.E., Joubert, Y., Kaplan, A., Kröger, N., Kroth, P.G., La Roche, J., Lindquist, E., Lommer, M., Martin-Jézéquel, V., Lopez, P.J., Lucas, S., Mangogna, M., McGinnis, K., Medlin, L.K., Montsant, A., Oudot-Le Secq, M.-P., Napoli, C., Obornik, M., Parker, M.S., Petit, J.-L., Porcel, B.M., Poulsen, N., Robison, M., Rychlewski, L., Rynearson, T. a, Schmutz, J., Shapiro, H., Siaux, M., Stanley, M., Sussman, M.R., Taylor, A.R., Vardi, A., von Dassow, P., Vyverman, W., Willis, A., Wyrwicz, L.S., Rokhsar, D.S., Weissenbach, J., Armbrust, E.V., Green, B.R., Van de Peer, Y., Grigoriev, I. V, 2008. The *Phaeodactylum* genome reveals the evolutionary history of diatom genomes. *Nature* 456, 239–244. <https://doi.org/10.1038/nature07410>
- Bowler, C., Vardi, A., Allen, A.E., 2010. Oceanographic and biogeochemical insights from diatom genomes. *Ann. Rev. Mar. Sci.* 2, 333–365. <https://doi.org/10.1146/annurev-marine-120308-081051>
- Branco-Vieira, M., San Martin, S., Agurto, C., Freitas, M.A.V., Martins, A.A., Mata, T.M., Caetano, N.S., 2020. Biotechnological potential of *Phaeodactylum tricornutum* for biorefinery processes. *Fuel* 268, 117357. <https://doi.org/10.1016/j.fuel.2020.117357>
- Brembu, T., Chauton, M.S., Winge, P., Bones, A.M., Vadstein, O., 2017. Dynamic responses to silicon in *Thalassiosira pseudonana* - Identification, characterisation and classification of signature genes and their corresponding protein motifs. *Sci. Rep.* 7, 1–14. <https://doi.org/10.1038/s41598-017-04921-0>
- Breuer, G., Lamers, P.P., Martens, D.E., Draaisma, R.B., Wijffels, R.H., 2012. The impact of nitrogen starvation on the dynamics of triacylglycerol accumulation in nine microalgae strains. *Bioresour. Technol.* 124, 217–226. <https://doi.org/10.1016/j.biortech.2012.08.003>
- Brown, A.J., Gibson, S.J., Hatton, D., Arnall, C.L., James, D.C., 2019. Whole synthetic pathway engineering of recombinant protein production. *Biotechnol. Bioeng.* 116, 375–387. <https://doi.org/10.1002/bit.26855>
- Büchel, C., 2020. Light harvesting complexes in chlorophyll c-containing algae. *Biochim. Biophys. Acta - Bioenerg.* 1861, 148027. <https://doi.org/10.1016/j.bbabi.2019.05.003>

- Buhmann, M.T., Schulze, B., Förderer, A., Schleheck, D., Kroth, P.G., 2016. Bacteria may induce the secretion of mucin-like proteins by the diatom *Phaeodactylum tricoratum*. *J. Phycol.* 52, 463–474. <https://doi.org/10.1111/jpy.12409>
- Burkhardt, S., Amoroso, G., Riebesell, U., Sültemeyer, D., 2001. CO₂ and HCO₃⁻ uptake in marine diatoms acclimated to different CO₂ concentrations. *Limnol. Oceanogr.* 46, 1378–1391. <https://doi.org/10.4319/lo.2001.46.6.1378>
- Butler, T., Kapoore, R.V., Vaidyanathan, S., 2020. *Phaeodactylum tricoratum*: A Diatom Cell Factory. *Trends Biotechnol.* 1–17. <https://doi.org/10.1016/j.tibtech.2019.12.023>
- Butler, T.O., Acurio, K., Mukherjee, J., Dangasuk, M.M., Corona, O., Vaidyanathan, S., 2021. The transition away from chemical flocculants: Commercially viable harvesting of *Phaeodactylum tricoratum*. *Sep. Purif. Technol.* 255, 117733. <https://doi.org/10.1016/j.seppur.2020.117733>
- Butler, T.O., Guimarães, B., 2021. Industrial perspective on downstream processing of *Haematococcus pluvialis*, in: *Global Perspectives on Astaxanthin*. pp. 283–311.
- Butler, T.O., McDougall, G.J., Campbell, R., Stanley, M.S., Day, J.G., 2017. Media Screening for Obtaining *Haematococcus pluvialis* Red Motile Macrozooids Rich in Astaxanthin and Fatty Acids. *Biology (Basel)*. 7, 2. <https://doi.org/10.3390/biology7010002>
- Caballero, M.A., Jallet, D., Shi, L., Rithner, C., Zhang, Y., Peers, G., 2016. Quantification of chrysolaminarin from the model diatom *Phaeodactylum tricoratum*. *Algal Res.* 20, 180–188. <https://doi.org/10.1016/j.algal.2016.10.008>
- Cao, J.Y., Kong, Z.Y., Zhang, Y.F., Ling, T., Xu, J.L., Liao, K., Zhou, C.X., Yan, X.J., 2019. Bacterial community diversity and screening of growth-affecting bacteria from *isochrysis galbana* following antibiotic treatment. *Front. Microbiol.* 10, 1–11. <https://doi.org/10.3389/fmicb.2019.00994>
- Cassini, S.T., Francisco, S.A., Antunes, P.W.P., Oss, R.N., Keller, R., 2017. Harvesting microalgal biomass grown in anaerobic sewage treatment effluent by the coagulation-flocculation method: Effect of pH. *Brazilian Arch. Biol. Technol.* 60, 1–12. <https://doi.org/10.1590/1678-4324-2017160174>
- Cerón-García, M.C., Fernández-Sevilla, J.M., Sánchez-Mirón, A., García-Camacho, F., Contreras-Gómez, A., Molina-Grima, E., 2013. Mixotrophic growth of *Phaeodactylum tricoratum* on fructose and glycerol in fed-batch and semi-continuous modes. *Bioresour. Technol.* 147, 569–576. <https://doi.org/10.1016/j.biortech.2013.08.092>
- Cerón García, M., Fernández Sevilla, J., Acien Fernández, F., Molina Grima, E., García Camacho, F., 2000. Mixotrophic growth of *Phaeodactylum tricoratum* on glycerol: growth rate and fatty acid profile. *J. Appl. Phycol.* 12, 239–248.
- Chen, J., Wang, Y., Benemann, J.R., Zhang, X., Hu, H., Qin, S., 2016. Microalgal industry in China: challenges and prospects. *J. Appl. Phycol.* 28, 715–725. <https://doi.org/10.1007/s10811-015-0720-4>
- Chen, Y., Zhang, L., Xu, C., Vaidyanathan, S., 2016. Dissolved inorganic carbon speciation in aquatic environments and its application to monitor algal carbon uptake. *Sci. Total Environ.* 541, 1282–1295. <https://doi.org/10.1016/j.scitotenv.2015.10.025>
- Chen, Z., Zhang, J., Lei, X., Lai, Q., Yang, L., Zhang, H., Li, Y., Zheng, W., Tian, Y., Yu, Z., Xu, H., Zheng, T., 2019. *Mameliella phaeodactyli* sp. nov., a member of the family Rhodobacteraceae isolated from the marine algae *Phaeodactylum tricoratum*. *Int. J. Syst. Evol. Microbiol.* 65, 1617–1621. <https://doi.org/10.1099/ijs.0.000146>
- Chen, Z., Zheng, W., Yang, L., Boughner, L.A., Tian, Y., Zheng, T., Xu, H., 2017. Lytic and chemotactic features of the plaque-forming bacterium KD531 on *phaeodactylum tricoratum*. *Front. Microbiol.* 8, 1–10. <https://doi.org/10.3389/fmicb.2017.02581>
- Cheng, X., Qi, Z., Burdyny, T., Kong, T., Sinton, D., 2018. Low pressure supercritical CO₂ extraction of astaxanthin from *Haematococcus pluvialis* demonstrated on a microfluidic

- chip. *Bioresour. Technol.* 250, 481–485. <https://doi.org/10.1016/j.biortech.2017.11.070>
- Cheng, X., Riordon, J., Nguyen, B., Ooms, M.D., Sinton, D., 2017. Hydrothermal disruption of algae cells for astaxanthin extraction. *Green Chem.* 19, 106–111. <https://doi.org/10.1039/c6gc02746f>
- Chiaromonti, D., Prussi, M., Casini, D., Tredici, M.R., Rodolfi, L., Bassi, N., Zittelli, G.C., Bondioli, P., 2013. Review of energy balance in raceway ponds for microalgae cultivation: Re-thinking a traditional system is possible. *Appl. Energy* 102, 101–111. <https://doi.org/10.1016/j.apenergy.2012.07.040>
- Choi, H.J., 2015. Effect of eggshells for the harvesting of microalgae species. *Biotechnol. Biotechnol. Equip.* 29, 666–672. <https://doi.org/10.1080/13102818.2015.1031177>
- Chorazyczewski, A.M., Huang, I., Abdulla, H., Mayali, X., Zimba, P. V., 2021. The influence of bacteria on the growth, lipid production, and extracellular metabolite accumulation by *Phaeodactylum tricornutum* (Bacillariophyceae). *J. Phycol.* 57, 931–940. <https://doi.org/10.1111/jpy.13132>
- Chu, L., Ewe, D., R o B artulos, C., Kroth, P.G., Gruber, A., 2016. Rapid induction of GFP expression by the nitrate reductase promoter in the diatom *Phaeodactylum tricornutum*. *PeerJ* 4, e2344. <https://doi.org/10.7717/peerj.2344>
- Cieplik, F., Sp ath, A., Leibl, C., Gollmer, A., Regensburger, J., Tabenski, L., Hiller, K.A., Maisch, T., Schmalz, G., 2014. Blue light kills *Aggregatibacter actinomycetemcomitans* due to its endogenous photosensitizers. *Clin. Oral Investig.* 18, 1763–1769. <https://doi.org/10.1007/s00784-013-1151-8>
- Collier Valle, K., Nymark, M., Aamot, I., Hancke, K., Winge, P., Andresen, K., Johnsen, G., Brembu, T., Bones, A.M., 2014. System Responses to Equal Doses of Photosynthetically Usable Radiation of Blue, Green, and Red Light in the Marine Diatom *Phaeodactylum tricornutum*. *PLoS One* 9. <https://doi.org/10.1371/journal.pone.0114211>
- Collos, Y., Mornet, F., Sciandra, A., Waser, N., Larson, A., Harrison, P.J., 1999. An optical method for the rapid measurement of micromolar concentrations of nitrate in marine phytoplankton cultures. *J. Appl. Phycol.* <https://doi.org/10.1023/A:1008046023487>
- Colusse, G.A., Duarte, M.E.R., de Carvalho, J.C., Nosedo, M.D., 2019. Media effects on laboratory scale production costs of *Haematococcus pluvialis* biomass. *Bioresour. Technol. Reports* 7, 100236. <https://doi.org/10.1016/j.biteb.2019.100236>
- Colusse, G.A., Mendes, C.R.B., Duarte, M.E.R., Carvalho, J.C. de, Nosedo, M.D., 2020. Effects of different culture media on physiological features and laboratory scale production cost of *Dunaliella salina*. *Biotechnol. Reports* 27. <https://doi.org/10.1016/j.btre.2020.e00508>
- Croft, M.T., Lawrence, A.D., Raux-Deery, E., Warren, M.J., Smith, A.G., 2005. Algae acquire vitamin B12 through a symbiotic relationship with bacteria. *Nature* 438, 90–93. <https://doi.org/10.1038/nature04056>
- Cui, Y., Thomas-Hall, S.R., Chua, E.T., Schenk, P.M., 2020. Development of High-Level Omega-3 Eicosapentaenoic Acid (EPA) Production from *Phaeodactylum tricornutum*. *J. Phycol.* 268, 258–268. <https://doi.org/10.1111/jpy.13082>
- Daboussi, F., Leduc, S., Mar echal, A., Dubois, G., Guyot, V., Perez-Michaut, C., Amato, A., Falciatore, A., Juillerat, A., Beurdeley, M., Voytas, D.F., Cavarec, L., Duchateau, P., 2014. Genome engineering empowers the diatom *Phaeodactylum tricornutum* for biotechnology. *Nat. Commun.* 5, 3831–3837. <https://doi.org/10.1038/ncomms4831>
- Dambek, M., Eilers, U., Breitenbach, J., Steiger, S., Buchel, C., Sandmann, G., B uchel, C., Sandmann, G., 2012. Biosynthesis of fucoxanthin and diadinoxanthin and function of initial pathway genes in *Phaeodactylum tricornutum*. *J. Exp. Bot.* 63, 5607–5612. <https://doi.org/10.1093/jxb/ers211>
- Das, P., Aziz, S.S., Obbard, J.P., 2011. Two phase microalgae growth in the open system for

- enhanced lipid productivity. *Renew. Energy* 36, 2524–2528. <https://doi.org/10.1016/j.renene.2011.02.002>
- de Carvalho, J.C., Sydney, E.B., Assú Tessari, L.F., Soccol, C.R., 2019. Culture media for mass production of microalgae, Second Edi. ed, *Biofuels from Algae*. Elsevier B.V. <https://doi.org/10.1016/b978-0-444-64192-2.00002-0>
- de la Fuente, J.C., Oyarzún, B., Quezada, N., del Valle, J.M., 2006. Solubility of carotenoid pigments (lycopene and astaxanthin) in supercritical carbon dioxide. *Fluid Phase Equilib.* 247, 90–95. <https://doi.org/10.1016/j.fluid.2006.05.031>
- De Martino, A., Meichenin, A.S., Shi, J., Pan, K., Bowler, C., Martino, A. De, Meichenin, A.S., Shi, J., Pan, K., Bowler, C., De Martino, A., Meichenin, A.S., Shi, J., Pan, K., Bowler, C., 2007. Genetic and phenotypic characterization of *Phaeodactylum tricornutum* (Bacillariophyceae) accessions. *J. Phycol.* 43, 992–1009. <https://doi.org/10.1111/j.1529-8817.2007.00384.x>
- de Mooij, T., De Vries, G., Latsos, C., Wijffels, R.H., Janssen, M., 2016. Impact of light color on photobioreactor productivity. *Algal Res.* 15, 32–42. <https://doi.org/10.1016/j.algal.2016.01.015>
- de Souza, M.P., Hoeltz, M., Brittes Benitez, L., Machado, Ê.L., de Souza Schneider, R. de C., 2019. Microalgae and Clean Technologies: A Review. *Clean - Soil, Air, Water* 47, 1–18. <https://doi.org/10.1002/clen.201800380>
- del Pilar Sánchez-Saavedra, M., Maeda-Martínez, A.N., Acosta-Galindo, S., 2016. Effect of different light spectra on the growth and biochemical composition of *Tisochrysis lutea*. *J. Appl. Phycol.* 28, 839–847. <https://doi.org/10.1007/s10811-015-0656-8>
- Delbrut, A., Albina, P., Pradelles, R., Dubreucq, E., Lapiere, T., Pradelles, R., Dubreucq, E., 2018. Fucoxanthin and Polyunsaturated Fatty Acids Co-Extraction by a Green Process. *Molecules* 23, 1–15. <https://doi.org/10.3390/molecules23040874>
- Derwenskus, F., Metz, F., Gille, A., Schmid, U., Briviba, K., Schließmann, U., Hirth, T., 2019. Pressurized extraction of unsaturated fatty acids and carotenoids from wet *Chlorella vulgaris* and *Phaeodactylum tricornutum* biomass using subcritical liquids. *GCB Bioenergy* 11, 335–344. <https://doi.org/10.1111/gcbb.12563>
- Derwenskus, F., Schäfer, B., Müller, J., Frick, K., Gille, A., Briviba, K., Schmid-Staiger, U., Hirth, T., 2020a. Coproduction of EPA and Fucoxanthin with *P. tricornutum* – A Promising Approach for Up- and Downstream Processing. *Chemie-Ingenieur-Technik* 92, 1780–1789. <https://doi.org/10.1002/cite.202000046>
- Derwenskus, F., Weickert, S., Lewandowski, I., Schmid-Staiger, U., Hirth, T., 2020b. Economic evaluation of up- and downstream scenarios for the co-production of fucoxanthin and eicosapentaenoic acid with *P. tricornutum* using flat-panel airlift photobioreactors with artificial light. *Algal Res.* 51, 102078. <https://doi.org/10.1016/j.algal.2020.102078>
- Desbois, A.P., Lebl, T., Yan, L., Smith, V.J., 2008. Isolation and structural characterisation of two antibacterial free fatty acids from the marine diatom, *Phaeodactylum tricornutum*. *Appl. Microb. Cell Physiol.* 81, 755–764. <https://doi.org/10.1007/s00253-008-1714-9>
- Desbois, A.P., Mearns-Spragg, A., Smith, V.J., 2009. A fatty acid from the diatom *Phaeodactylum tricornutum* is antibacterial against diverse bacteria including multi-resistant *Staphylococcus aureus* (MRSA). *Mar. Biotechnol.* 11, 45–52. <https://doi.org/10.1007/s10126-008-9118-5>
- Desbois, A.P., Walton, M., Smith, V.J., 2010. Differential antibacterial activities of fusiform and oval morphotypes of *phaeodactylum tricornutum* (bacillariophyceae). *J. Mar. Biol. Assoc. United Kingdom* 90, 769–774. <https://doi.org/10.1017/S0025315409991366>
- Di Lena, G., Casini, I., Lucarini, M., Sanchez del Pulgar, J., Aguzzi, A., Caproni, R., Gabrielli, P., Lombardi-Boccia, G., 2020. Chemical characterization and nutritional evaluation of

- microalgal biomass from large-scale production: a comparative study of five species. *Eur. Food Res. Technol.* 246, 323–332. <https://doi.org/10.1007/s00217-019-03346-5>
- Dinamarca, J., Levitan, O., Kumaraswamy, G.K., Lun, D.S., Falkowski, P.G., 2017. Overexpression of a diacylglycerol acyltransferase gene in *Phaeodactylum tricornutum* directs carbon towards lipid biosynthesis. *J. Phycol.* 53, 405–414. <https://doi.org/10.1111/jpy.12513>
- Dolch, L.J., Maréchal, E., 2015. Inventory of fatty acid desaturases in the pennate diatom *Phaeodactylum tricornutum*. *Mar. Drugs* 13, 1317–1339. <https://doi.org/10.3390/md13031317>
- Dunbar, A.D.F., Richardson, T.H., Hutchinson, J., Hunter, C.A., 2008. Langmuir-Schaefer films of five different free base tetraphenylporphyrins for optical-based gas sensing of NO₂. *Sensors Actuators, B Chem.* 128, 468–481. <https://doi.org/10.1016/j.snb.2007.07.049>
- Enwemeka, C.S., 2013. Antimicrobial blue light: An emerging alternative to antibiotics. *Photomed. Laser Surg.* 31, 509–511. <https://doi.org/10.1089/pho.2013.9871>
- Enwemeka, C.S., Williams, D., Enwemeka, S.K., Hollosi, S., Yens, D., 2009. Blue 470-nm light kills Methicillin-Resistant *Staphylococcus aureus* (MRSA) in vitro. *Photomed. Laser Surg.* 27, 221–226. <https://doi.org/10.1089/pho.2008.2413>
- Erdene-Ochir, E., Shin, B.K., Huda, M.N., Kim, D.H., Lee, E.H., Song, D.G., Kim, Y.M., Kim, S.M., Pan, C.H., 2016. Cloning of a novel endogenous promoter for foreign gene expression in *Phaeodactylum tricornutum*. *Appl. Biol. Chem.* 59, 861–867. <https://doi.org/10.1007/s13765-016-0235-y>
- Esquivel-Hernández, D.A., Rodríguez-Rodríguez, J., Rostro-Alanis, M., Cuéllar-Bermúdez, S.P., Mancera-Andrade, E.I., Núñez-Echevarría, J.E., García-Pérez, J.S., Chandra, R., Parra-Saldívar, R., 2017. Advancement of green process through microwave-assisted extraction of bioactive metabolites from *Arthrospira Platensis* and bioactivity evaluation. *Bioresour. Technol.* 224, 618–629. <https://doi.org/10.1016/j.biortech.2016.10.061>
- Fasaei, F., Bitter, J.H., Slegers, P.M., van Boxtel, A.J.B., 2018. Techno-economic evaluation of microalgae harvesting and dewatering systems. *Algal Res.* 31, 347–362. <https://doi.org/10.1016/j.algal.2017.11.038>
- Fernández Sevilla, J.M., Cerón García, M.C., Sánchez Mirón, A., Belarbi, E.H.E.H., García Camacho, F., Molina Grima, E., 2004. Pilot-plant-scale outdoor mixotrophic cultures of *Phaeodactylum tricornutum* using glycerol in vertical bubble column and airlift photobioreactors: Studies in fed-batch mode. *Biotechnol. Prog.* 20, 728–736. <https://doi.org/10.1021/bp034344f>
- Fidalgo, P., Cid, A., Herrero, C., 1995. Culture of the marine diatom *Phaeodactylum tricornutum* with different nitrogen sources: Growth, nutrient conversion and biochemical composition. *Cah. BioI. Mar* 36, 165–173.
- Flori, S., Jouneae, P.-H., Bailleul, B., Gallet, B., Estrozi, L.F., Moriscot, C., Bastien, O., Eicke, S., Schober, A., Bartulos, C.R., Eric, M., Kroth, P.G., Petroustos, D., Zeeman, S., Breyton, C., Schoehn, G., Falconet, D., Finazzi, G., 2017. Plastid thylakoid architecture optimizes photosynthesis in diatoms. *Nat. Commun.* 8, p.15885. <https://doi.org/10.1038/ncomms15885>
- Flynn, K.J., Opik, H., Syrett, P.J., 1986. Localization of the Alkaline Phosphatase and 5'-Nucleotidase Activities of the Diatom *Phaeodactylum tricornutum* By. *J. Gen. Microbiol.* 132, 289–298.
- Formosa-Dague, C., Gernigon, V., Castelain, M., Daboussi, F., Guiraud, P., 2018. Towards a better understanding of the flocculation/flotation mechanism of the marine microalgae *Phaeodactylum tricornutum* under increased pH using atomic force microscopy. *Algal Res.* 33, 369–378. <https://doi.org/10.1016/j.algal.2018.06.010>

- Fu, W., Guomundsson, Ó., Paglia, G., Herjólfsson, G., Andrésson, Ó.S., Pálsson, B.O., Brynjólfsson, S., 2013. Enhancement of carotenoid biosynthesis in the green microalga *Dunaliella salina* with light-emitting diodes and adaptive laboratory evolution. *Appl. Microbiol. Biotechnol.* 97, 2395–2403. <https://doi.org/10.1007/s00253-012-4502-5>
- Gao, F., Marta, S., Teles, I., Wijffels, R.H., Barbosa, M.J., 2020a. Production and monitoring of biomass and fucoxanthin with brown microalgae under outdoor conditions. *Biotechnol. Bioeng.* 1–11. <https://doi.org/10.1002/bit.27657>
- Gao, F., Teles (Cabanelas, ITD), I., Wijffels, R.H., Barbosa, M.J., 2020b. Process optimization of fucoxanthin production with *Tisochrysis lutea*. *Bioresour. Technol.* 315, 123894. <https://doi.org/10.1016/j.biortech.2020.123894>
- García, M., Gonzalo, A., Sánchez, J.L., Arauzo, J., Simoes, C., 2011. Methanolysis and ethanolysis of animal fats: a comparative study of the influence of alcohols. *Chem. Ind. Chem. Eng. Q.* 17, 91–97. <https://doi.org/10.2298/CICEQ100224058G>
- Gardner, R.D., Cooksey, K.E., Mus, F., Macur, R., Moll, K., Eustance, E., Carlson, R.P., Gerlach, R., Fields, M.W., Peyton, B.M., 2012. Use of sodium bicarbonate to stimulate triacylglycerol accumulation in the chlorophyte *Scenedesmus* sp. and the diatom *Phaeodactylum tricorutum*. *J. Appl. Phycol.* 24, 1311–1320. <https://doi.org/10.1007/s10811-011-9782-0>
- Ge, F., Huang, W., Chen, Z., Zhang, C., Xiong, Q., Bowler, C., Yang, J., Xu, J., Hu, H., 2014. Methylcrotonyl-CoA Carboxylase Regulates Triacylglycerol Accumulation in the Model Diatom *Phaeodactylum tricorutum*. *Plant Cell* 26, 1681–1697. <https://doi.org/10.1105/tpc.114.124982>
- Geider, R.J., Osborne, B.A., Raven, J.A., 1985. Light dependence of growth and photosynthesis in *Phaeodactylum tricorutum* (Bacillariophyceae). *J. Phycol.* 21, 609–619.
- Gerardo, M.L., Van Den Hende, S., Vervaeren, H., Coward, T., Skill, S.C., 2015. Harvesting of microalgae within a biorefinery approach: A review of the developments and case studies from pilot-plants. *Algal Res.* 11, 248–262. <https://doi.org/10.1016/j.algal.2015.06.019>
- Gifuni, I., Pollio, A., Safi, C., Marzocchella, A., Olivieri, G., 2019. Current Bottlenecks and Challenges of the Microalgal Biorefinery. *Trends Biotechnol.* 37, 242–252. <https://doi.org/10.1016/j.tibtech.2018.09.006>
- Gilbert-lópez, B., Barranco, A., Herrero, M., Cifuentes, A., Ibáñez, E., 2017. Development of new green processes for the recovery of bioactives from *Phaeodactylum tricorutum*. *Food Res. Int.* 99, 1056–1065. <https://doi.org/10.1016/j.foodres.2016.04.022>
- Golueke, C., Oswald, W., 1970. Surface Properties and Ion Exchange in Algae Removal. *J. Water Pollut. Control Fed.* 42.
- Gómez-Loredo, A., Benavides, J., Rito-Palomares, M., 2016. Growth kinetics and fucoxanthin production of *Phaeodactylum tricorutum* and *Isochrysis galbana* cultures at different light and agitation conditions. *J. Appl. Phycol.* 28, 849–860. <https://doi.org/10.1007/s10811-015-0635-0>
- Gong, M., Bassi, A., 2016. Carotenoids from microalgae: A review of recent developments. *Biotechnol. Adv.* 34, 1396–1412. <https://doi.org/10.1016/j.biotechadv.2016.10.005>
- González-López, C. V., Cerón-García, M.C., Fernández-Sevilla, J.M., González-Céspedes, A.M., Camacho-Rodríguez, J., Molina-Grima, E., 2013. Medium recycling for *Nannochloropsis gaditana* cultures for aquaculture. *Bioresour. Technol.* 129, 430–438. <https://doi.org/10.1016/j.biortech.2012.11.061>
- Graham, N., Gang, F., Fowler, G., Watts, M., 2008. Characterisation and coagulation performance of a tannin-based cationic polymer: A preliminary assessment. *Colloids Surfaces A Physicochem. Eng. Asp.* 327, 9–16.

- <https://doi.org/10.1016/j.colsurfa.2008.05.045>
- Grant, C., 2011. Light intensity influences on algal pigments, proteins and carbohydrates: implication for pigment-based chemotaxonomy.
- Guillard, R.R.L., 1975. Culture of Phytoplankton for Feeding Marine Invertebrates, in: Culture of Marine Invertebrate Animals. Springer US, Boston, MA, pp. 29–60. https://doi.org/10.1007/978-1-4615-8714-9_3
- Guimarães, B.O., Gremmen, P., Wijffels, R.H.R.H., Barbosa, M.J., D’Adamo, S., Guimaraes, B., Gremmen, P., Wijffels, R.H.R.H., Barbosa, M.J., D’Adamo, S., 2021. Effect of ammonium formate washing on the elemental composition determination in *Nannochloropsis oceanica*. *Aquaculture* 538, 736526. <https://doi.org/10.1016/j.aquaculture.2021.736526>
- Guler, B.A., Deniz, I., Demirel, Z., Oncel, S.S., Imamoglu, E., 2019. Comparison of different photobioreactor configurations and empirical computational fluid dynamics simulation for fucoxanthin production. *Algal Res.* 37, 195–204. <https://doi.org/10.1016/j.algal.2018.11.019>
- Gundermann, K., Buchel, C., 2014. Structure and Functional heterogeneity of Fucoxanthin-Chlorophyll Proteins in Diatoms, in: Advances in Photosynthesis and Respiration. pp. 21–37. https://doi.org/10.1007/978-94-017-8742-0_13
- Hamilton, M., Powers, S., Napier, J., Sayanova, O., 2016. Heterotrophic Production of Omega-3 Long-Chain Polyunsaturated Fatty Acids by Trophically Converted Marine Diatom *Phaeodactylum tricornutum*. *Mar. Drugs* 14, 53. <https://doi.org/10.3390/md14030053>
- Hamilton, M.L., Warwick, J., Terry, A., Allen, M.J., Napier, J.A., Sayanova, O., 2015. Towards the Industrial Production of Omega-3 Long Chain Polyunsaturated Fatty Acids from a Genetically Modified Diatom *Phaeodactylum tricornutum*. *PLoS One* 10. <https://doi.org/10.1371/journal.pone.0144054>
- Han, F., Wang, W., Li, Y., Shen, G., Wan, M., Wang, J., 2013. Changes of biomass, lipid content and fatty acids composition under a light – dark cyclic culture of *Chlorella pyrenoidosa* in response to different temperature. *Bioresour. Technol.* 132, 182–189. <https://doi.org/10.1016/j.biortech.2012.12.175>
- Han, J., Zhang, L., Wang, S., Yang, G., Zhao, L., Pan, K., 2016. Co-culturing bacteria and microalgae in organic carbon containing medium. *J. Biol. Res.* 23, 1–9. <https://doi.org/10.1186/s40709-016-0047-6>
- Happi Emaga, T., Ronkart, S.N., Robert, C., Wathelet, B., Paquot, M., 2008. Characterisation of pectins extracted from banana peels (*Musa AAA*) under different conditions using an experimental design. *Food Chem.* 108, 463–471. <https://doi.org/10.1016/j.foodchem.2007.10.078>
- Helliwell, K.E., Wheeler, G.L., Leptos, K.C., Goldstein, R.E., Smith, A.G., 2011. Insights into the evolution of vitamin B 12 auxotrophy from sequenced algal genomes. *Mol. Biol. Evol.* 28, 2921–2933. <https://doi.org/10.1093/molbev/msr124>
- Hempel, F., Bozarth, A.S., Lindenkamp, N., Klingl, A., Zauner, S., Linne, U., Steinbüchel, A., Maier, U.G., 2011a. Microalgae as bioreactors for bioplastic production. *Microb. Cell Fact.* 10, 81–86. <https://doi.org/10.1186/1475-2859-10-81>
- Hempel, F., Lau, J., Klingl, A., Maier, U.G., 2011b. Algae as Protein Factories: Expression of a Human Antibody and the Respective Antigen in the Diatom *Phaeodactylum tricornutum*. *PLoS One* 6, e28424. <https://doi.org/10.1371/journal.pone.0028424>
- Hempel, F., Maier, U.G., 2016. Microalgae as Solar-Powered Protein Factories. *Adv. Technol. protein Compexe Prod. Charact.* 896, 241–262. <https://doi.org/10.1007/978-3-319-27216-0>
- Hempel, F., Maier, U.G., 2012. An engineered diatom acting like a plasma cell secreting human IgG antibodies with high efficiency. *Microb. Cell Fact.* <https://doi.org/10.1186/1475->

- Hempel, F., Maurer, M., Brockmann, B., Mayer, C., Biedenkopf, N., Kelterbaum, A., Becker, S., Maier, U.G., 2017. From hybridomas to a robust microalgal-based production platform: Molecular design of a diatom secreting monoclonal antibodies directed against the Marburg virus nucleoprotein. *Microb. Cell Fact.* 16, 1–10. <https://doi.org/10.1186/s12934-017-0745-2>
- Henderson, R.K., Baker, A., Parsons, S.A., Jefferson, B., 2007. Characterisation of algogenic organic matter extracted from cyanobacteria, green algae and diatoms. *Water Res.* 42, 3435–3445. <https://doi.org/10.1016/j.watres.2007.10.032>
- Hermann, D., Egue, F., Tastard, E., Nguyen, D.H., Casse, N., Caruso, A., Hiard, S., Marchand, J., Chénais, B., Morant-Manceau, A., Rouault, J.D., 2014. An introduction to the vast world of transposable elements - What about the diatoms? *Diatom Res.* 29, 91–104. <https://doi.org/10.1080/0269249X.2013.877083>
- Hernández-Melchor, D.J., Cañizares-Villanueva, R.O., Terán-Toledo, J.R., López-Pérez, P.A., Cristiani-Urbina, E., 2017. Hydrodynamic and mass transfer characterization of flat-panel airlift photobioreactors for the cultivation of a photosynthetic microbial consortium. *Biochem. Eng. J.* 128, 141–148. <https://doi.org/10.1016/j.bej.2017.09.014>
- Hesse, M.C.S., Santos, B., Selesu, N.F.H., Corrêa, D.O., Mariano, A.B., Vargas, J.V.C., Vieira, R.B., 2017. Optimization of flocculation with tannin-based flocculant in the water reuse and lipidic production for the cultivation of *Acutodesmus obliquus*. *Sep. Sci. Technol.* 52, 936–942. <https://doi.org/10.1080/01496395.2016.1269130>
- Heydarizadeh, P., Boureba, W., Zahedi, M., Huang, B., Moreau, B., Lukomska, E., Couzinet-Mossion, A., Wielgosz-Collin, G., Martin-Jézéquel, V., Bougaran, G., Marchand, J., Schoefs, B., 2017. Response of CO₂-starved diatom *Phaeodactylum tricorutum* to light intensity transition. *Philos. Trans. R. Soc. B Biol. Sci.* 372, 20160396. <https://doi.org/10.1098/rstb.2016.0396>
- Hopkinson, B.M., Dupont, C.L., Matsuda, Y., 2016a. The physiology and genetics of CO₂concentrating mechanisms in model diatoms. *Curr. Opin. Plant Biol.* 31, 51–57. <https://doi.org/10.1016/j.pbi.2016.03.013>
- Hopkinson, B.M., Dupont, C.L., Matsuda, Y., 2016b. The physiology and genetics of CO₂ concentrating mechanisms in model diatoms. *Curr. Opin. Plant Biol.* 31, 51–57. <https://doi.org/10.1016/j.pbi.2016.03.013>
- Huang, W., Haferkamp, I., Lepetit, B., Molchanova, M., Hou, S., Jeblick, W., Río Bártulos, C., Kroth, P.G., 2018. Reduced vacuolar β -1,3-glucan synthesis affects carbohydrate metabolism as well as plastid homeostasis and structure in *Phaeodactylum tricorutum*. *Proc. Natl. Acad. Sci.* 201719274. <https://doi.org/10.1073/pnas.1719274115>
- Huang, W., Río Bártulos, C., Kroth, P.G., 2016. Diatom Vacuolar 1,6- β -Transglycosylases can Functionally Complement the Respective Yeast Mutants. *J. Eukaryot. Microbiol.* 63, 536–546. <https://doi.org/10.1111/jeu.12298>
- Huete-Ortega, M., Okurowska, K., Kapoore, R.V., Johnson, M.P., Gilmour, D.J., Vaidyanathan, S., 2018. Effect of ammonium and high light intensity on the accumulation of lipids in *Nannochloropsis oceanica* (CCAP 849/10) and *Phaeodactylum tricorutum* (CCAP 1055/1). *Biotechnol. Biofuels* 11, 1–15. <https://doi.org/10.1186/s13068-018-1061-8>
- Ishika, T., Bahri, P.A., Laird, D.W., Moheimani, N.R., 2018. The effect of gradual increase in salinity on the biomass productivity and biochemical composition of several marine , halotolerant , and halophilic microalgae 1453–1464.
- Ishika, T., Moheimani, N.R., Bahri, P.A., Laird, D.W., Blair, S., Parlevliet, D., 2017. Halo-adapted microalgae for fucoxanthin production: Effect of incremental increase in salinity. *Algal Res.* 28, 66–73. <https://doi.org/10.1016/j.algal.2017.10.002>

- Jallet, D., Xing, D., Hughes, A., Moosburner, M., Simmons, M.P., Allen, A.E., Peers, G., 2020. Mitochondrial fatty acid β -oxidation is required for storage-lipid catabolism in a marine diatom. *New Phytol.* 228, 946–958. <https://doi.org/10.1111/nph.16744>
- Janssen, J.H., Kastenhofer, J., de Hoop, J.A., Lamers, P.P., Wijffels, R.H., Barbosa, M.J., 2018. Effect of nitrogen addition on lipid productivity of nitrogen starved *Nannochloropsis gaditana*. *Algal Res.* 33, 125–132. <https://doi.org/10.1016/j.algal.2018.05.009>
- Jayme, D., Fike, R., Radominski, R., Dadey, B., Hasset, R., Cady, D., 2002. A novel application of granulation technology to improve physical properties and biological performance of powdered serum-free culture media, in: *Animal Cell Technology: Basic & Applied Aspects*. Springer, Dordrecht, pp. 155–159.
- Jeon, S., Lim, J.M., Lee, H.G., Shin, S.E., Kang, N.K., Park, Y. II, Oh, H.M., Jeong, W.J., Jeong, B.R., Chang, Y.K., 2017. Current status and perspectives of genome editing technology for microalgae. *Biotechnol. Biofuels* 10, 1–18. <https://doi.org/10.1186/s13068-017-0957-z>
- Jiang, G.L., Zhu, M.J., 2019. Preparation of astaxanthin-encapsulated complex with zein and oligochitosan and its application in food processing. *Lwt* 106, 179–185. <https://doi.org/10.1016/j.lwt.2019.02.055>
- Jiang, H., Gao, K., 2004. Effects of lowering temperature during culture on the production of polyunsaturated fatty acids in the marine diatom *Phaeodactylum tricornutum* (Bacillariophyceae). *J. Appl. Phycol.* 40, 651–654. <https://doi.org/10.1111/j.1529-8817.2004.03112.x>
- Jiang, J., Nuez-Ortin, W., Angell, A., Zeng, C., de Nys, R., Vucko, M.J., 2019. Enhancing the colouration of the marine ornamental fish *Pseudochromis fridmani* using natural and synthetic sources of astaxanthin. *Algal Res.* 42, 101596. <https://doi.org/10.1016/j.algal.2019.101596>
- Johansson, O.N., Pinder, M.I.M., Ohlsson, F., Egardt, J., Töpel, M., Clarke, A.K., 2019. Friends With Benefits: Exploring the Phycosphere of the Marine Diatom *Skeletonema marinoi*. *Front. Microbiol.* 10, 1–11. <https://doi.org/10.3389/fmicb.2019.01828>
- Jouhten, P., Boruta, T., Andrejev, S., Pereira, F., Rocha, I., Patil, K.R., 2016. Yeast metabolic chassis designs for diverse biotechnological products. *Sci. Rep.* 6, 1–9. <https://doi.org/10.1038/srep29694>
- Jung, J.H., Sirisuk, P., Ra, C.H., Kim, J.M., Jeong, G.T., Kim, S.K., 2019. Effects of green LED light and three stresses on biomass and lipid accumulation with two-phase culture of microalgae, *Process Biochemistry*. Elsevier Ltd. <https://doi.org/10.1016/j.procbio.2018.11.014>
- Jungandreas, A., Schellenberger Costa, B., Jakob, T., Von Bergen, M., Baumann, S., Wilhelm, C., Subramanyam, R., 2014. The Acclimation of *Phaeodactylum tricornutum* to Blue and Red Light Does Not Influence the Photosynthetic Light Reaction but Strongly Disturbs the Carbon Allocation Pattern. <https://doi.org/10.1371/journal.pone>
- Kadono, T., Miyagawa-Yamaguchi, A., Kira, N., Tomaru, Y., Okami, T., Yoshimatsu, T., Hou, L., Ohama, T., Fukunaga, K., Okauchi, M., Yamaguchi, H., Ohnishi, K., Falciatore, A., Adachi, M., 2015. Characterization of marine diatom-infecting virus promoters in the model diatom *Phaeodactylum tricornutum*. *Sci. Rep.* 5, 18708. <https://doi.org/10.1038/srep18708>
- KaiXian, Q., Borowitzka, M.A., 1993. Light and nitrogen deficiency effects on the growth and composition of *Phaeodactylum tricornutum*. *Appl. Biochem. Biotechnol.* 38, 93–103. <https://doi.org/10.1007/BF02916415>
- Kakoi, B., Kaluli, J.W., Ndiba, P., Thiong'o, G., 2016. Banana pith as a natural coagulant for polluted river water. *Ecol. Eng.* 95, 699–705. <https://doi.org/10.1016/j.ecoleng.2016.07.001>

- Kandasamy, G., Shaleh, S.R.M., Raehanah, S., Shaleh, M., Shaleh, S.R.M., 2018. Flotation removal of the microalga *Nannochloropsis* sp. using Moringa protein–oil emulsion: A novel green approach. *Bioresour. Technol.* 247, 327–331. <https://doi.org/10.1016/j.biortech.2017.08.187>
- Kapooore, R., 2014. Mass spectrometry based hyphenated techniques for microalgal and mammalian metabolomics.
- Kapooore, R.R.V., Butler, T., Pandhal, J., Vaidyanathan, S., 2018. Microwave-Assisted Extraction for Microalgae: From Biofuels to Biorefinery. *Biology (Basel)*. 7, 1–25. <https://doi.org/10.3390/biology7010018>
- Kapooore, R.V., Huete-Ortega, M., Day, J.G., Okurowska, K., Slocombe, S.P., Stanley, M.S., Vaidyanathan, S., 2019. Effects of cryopreservation on viability and functional stability of an industrially relevant alga. *Sci. Rep.* 9, 1–12. <https://doi.org/10.1038/s41598-019-38588-6>
- Karas, B.J., Diner, R.E., Lefebvre, S.C., McQuaid, J., Phillips, A.P.R.R., Noddings, C.M., Brunson, J.K., Valas, R.E., Deerinck, T.J., Jablanovic, J., Gillard, J.T.F.F., Beerli, K., Ellisman, M.H., Glass, J.I., Hutchison, C.A., Smith, H.O., Venter, J.C., Allen, A.E., Dupont, C.L., Weyman, P.D., 2015. Designer diatom episomes delivered by bacterial conjugation. *Nat. Commun.* 6, 1–10. <https://doi.org/10.1038/ncomms7925>
- Kazamia, E., Czesnick, H., Nguyen, T.T. Van, Croft, M.T., Sherwood, E., Sasso, S., Hodson, S.J., Warren, M.J., Smith, A.G., 2012. Mutualistic interactions between vitamin B12-dependent algae and heterotrophic bacteria exhibit regulation. *Environ. Microbiol.* 14, 1466–1476. <https://doi.org/10.1111/j.1462-2920.2012.02733.x>
- Kern, D.G., 1994. Methods and containment system for storing, reconstituting, dispensing and harvesting cell culture media.
- Khalid, N., Barrow, C.J., 2018. Critical review of encapsulation methods for stabilization and delivery of astaxanthin. *J. Food Bioact.* 1, 104–115. <https://doi.org/10.31665/jfb.2018.1129>
- Khalid, N., Shu, G., Kobayashi, I., Nakajima, M., Barrow, C.J., 2017. Formulation and characterization of monodisperse O/W emulsions encapsulating astaxanthin extracts using microchannel emulsification: Insights of formulation and stability evaluation. *Colloids Surfaces B Biointerfaces* 157, 355–365. <https://doi.org/10.1016/j.colsurfb.2017.06.003>
- Kikutani, S., Nakajima, K., Nagasato, C., Tsuji, Y., Miyatake, A., Matsuda, Y., 2016. Thylakoid luminal Θ -carbonic anhydrase critical for growth and photosynthesis in the marine diatom *Phaeodactylum tricornutum*. *Proc. Natl. Acad. Sci. U. S. A.* 113, 9828–9833. <https://doi.org/10.1073/pnas.1603112113>
- Kim, J., Brown, C.M., Kim, M.K., Burrows, E.H., Bach, S., Lun, D.S., Falkowski, P.G., 2017. Effect of cell cycle arrest on intermediate metabolism in the marine diatom *Phaeodactylum tricornutum*. *Proc. Natl. Acad. Sci.* 201711642. <https://doi.org/10.1073/pnas.1711642114>
- Kim, T.H., Lee, Y., Han, S.H., Hwang, S.J., 2013. The effects of wavelength and wavelength mixing ratios on microalgae growth and nitrogen, phosphorus removal using *Scenedesmus* sp. for wastewater treatment. *Bioresour. Technol.* 130, 75–80. <https://doi.org/10.1016/j.biortech.2012.11.134>
- Kimbrel, J.A., Samo, T.J., Ward, C., Nilson, D., Thelen, M.P., Siccardi, A., Zimba, P., Lane, T.W., Mayali, X., 2019. Host selection and stochastic effects influence bacterial community assembly on the microalgal phycosphere. *Algal Res.* 40. <https://doi.org/10.1016/j.algal.2019.101489>
- Kira, N., Ohnishi, K., Miyagawa-Yamaguchi, A., Kadono, T., Adachi, M., 2016. Nuclear transformation of the diatom *Phaeodactylum tricornutum* using PCR-amplified DNA fragments by microparticle bombardment. *Mar. Genomics* 25, 49–56.

- <https://doi.org/10.1016/j.margen.2015.12.004>
- Kothari, R., Pathak, V. V., Pandey, A., Ahmad, S., Srivastava, C., Tyagi, V. V., 2017. A novel method to harvest *Chlorella* sp. via low cost bioflocculant: Influence of temperature with kinetic and thermodynamic functions. *Bioresour. Technol.* 225, 84–89. <https://doi.org/10.1016/j.biortech.2016.11.050>
- Krohn-Molt, I., Alawi, M., Förstner, K.U., Wiegandt, A., Burkhardt, L., Indenbirken, D., Thieß, M., Grundhoff, A., Kehr, J., Tholey, A., Streit, W.R., 2017. Insights into Microalga and bacteria interactions of selected phycosphere biofilms using metagenomic, transcriptomic, and proteomic approaches. *Front. Microbiol.* 8, 1–14. <https://doi.org/10.3389/fmicb.2017.01941>
- Kuczynska, P., Jemiola-Rzeminska, M., Strzalka, K., 2015. Photosynthetic pigments in diatoms. *Mar. Drugs* 13, 5847–5881. <https://doi.org/10.3390/md13095847>
- Lavoie, A., de la Noüe, J., 1983. Harvesting Microalgae With Chitosan. *J. World Maric.* 694, 685–694.
- Le Chevanton, M., Garnier, M., Bougaran, G., Schreiber, N., Lukomska, E., Bérard, J.B., Fouilland, E., Bernard, O., Cadoret, J.P., 2013. Screening and selection of growth-promoting bacteria for *Dunaliella* cultures. *Algal Res.* 2, 212–222. <https://doi.org/10.1016/j.algal.2013.05.003>
- Le Costaouec, T., Unamunzaga, C., Mantecon, L., Helbert, W., 2017. New structural insights into the cell-wall polysaccharide of the diatom *Phaeodactylum tricornutum*. *Algal Res.* 26, 172–179. <https://doi.org/10.1016/j.algal.2017.07.021>
- Lebeau, T., Robert, J.M., 2003. Diatom cultivation and biotechnologically relevant products. Part I: Cultivation at various scales. *Appl. Microbiol. Biotechnol.* 60, 612–623. <https://doi.org/10.1007/s00253-002-1176-4>
- Leblond, J.D., Chapman, P.J., 2000. Combined effects of temperature and iron on the growth and physiology of the marine diatom *Phaeodactylum tricornutum* (Bacillariophyceae). *J. Phycol.* 36, 1096–1102. <https://doi.org/10.1046/j.1529-8817.2000.99042.x>
- Lee, J.Y., Yoo, C., Jun, S.Y., Ahn, C.Y., Oh, H.M., 2010. Comparison of several methods for effective lipid extraction from microalgae. *Bioresour. Technol.* 101, S75–S77. <https://doi.org/10.1016/j.biortech.2009.03.058>
- Lei, X., Zheng, W., Ding, H., Zhu, X., Chen, Q., Xu, H., Zheng, T., Tian, Y., 2018. Effective harvesting of the marine microalga *Thalassiosira pseudonana* by *Marinobacter* sp. FL06. *Bioresour. Technol.* 269, 127–133. <https://doi.org/10.1016/j.biortech.2018.08.077>
- Leu, S., Boussiba, S., 2014. Advances in the production of High Value Products by Microalgae: Current Status and Future Prospectives. *Ind. Biotechnol.* 10, 169–183.
- Levering, J., Broddrick, J., Dupont, C.L., Peers, G., Beerli, K., Mayers, J., Gallina, A.A., Allen, A.E., Palsson, B.O., Zengler, K., 2016. Genome-scale model reveals metabolic basis of biomass partitioning in a model diatom. *PLoS One* 11, 1–22. <https://doi.org/10.1371/journal.pone.0155038>
- Levitan, O., Dinamarca, J., Zelzion, E., Lun, D.S., Guerra, L.T., Kim, M.K., Kim, J., Van Mooy, B.A.S., Bhattacharya, D., Falkowski, P.G., 2015. Remodeling of intermediate metabolism in the diatom *Phaeodactylum tricornutum* under nitrogen stress. *Proc. Natl. Acad. Sci. U. S. A.* 112, 412–7. <https://doi.org/10.1073/pnas.1419818112>
- Li, F., Beardall, J., Collins, S., Gao, K., 2017a. Decreased photosynthesis and growth with reduced respiration in the model diatom *Phaeodactylum tricornutum* grown under elevated CO₂ over 1800 generations. *Glob. Chang. Biol.* 23, 127–137. <https://doi.org/10.1111/gcb.13501>
- Li, F., Beardall, J., Collins, S., Gao, K., 2017b. Decreased photosynthesis and growth with reduced respiration in the model diatom *Phaeodactylum tricornutum* grown under elevated CO₂ over 1800 generations. *Glob. Chang. Biol.* 23, 127–137.

<https://doi.org/10.1111/gcb.13501>

- Li, J., Liu, Y., Cheng, J.J., Mos, M., Daroch, M., 2015. Biological potential of microalgae in China for biorefinery-based production of biofuels and high value compounds. *N. Biotechnol.* 32, 588–596. <https://doi.org/10.1016/j.nbt.2015.02.001>
- Liang, Y., Sun, M., Tian, C., Cao, C., Li, Z., 2014. Effects of salinity stress on the growth and chlorophyll fluorescence of *Phaeodactylum tricornutum* and *Chaetoceros gracilis* (Bacillariophyceae). *Bot. Mar.* 57, 469–476. <https://doi.org/10.1515/bot-2014-0037>
- Lim, K.C., Yusoff, F.M., Shariff, M., Kamarudin, M.S., 2018. Astaxanthin as feed supplement in aquatic animals. *Rev. Aquac.* 10, 738–773. <https://doi.org/10.1111/raq.12200>
- Lima-Mendez, G., Faust, K., Henry, N., Decelle, J., Colin, S., Carcillo, F., Chaffron, S., Ignacio-Espinosa, J.C., Roux, S., Vincent, F., Bittner, L., Darzi, Y., Wang, J., Audic, S., Berline, L., Bontempi, G., Cabello, A.M., Coppola, L., Cornejo-Castillo, F.M., d’Ovidio, F., De Meester, L., Ferrera, I., Garet-Delmas, M.-J., Guidi, L., Lara, E., Pesant, S., Royo-Llonch, M., Salazar, G., Sanchez, P., Sebastian, M., Souffreau, C., Dimier, C., Picheral, M., Searson, S., Kandels-Lewis, S., Gorsky, G., Not, F., Ogata, H., Speich, S., Stemmann, L., Weissenbach, J., Wincker, P., Acinas, S.G., Sunagawa, S., Bork, P., Sullivan, M.B., Karsenti, E., Bowler, C., de Vargas, C., Raes, J., 2015. Determinants of community structure in the global plankton interactome. *Science* (80-.). 348, 1262073–1262073. <https://doi.org/10.1126/science.1262073>
- Lin, H.Y., Yen, S.C., Kuo, P.C., Chung, C.Y., Yeh, K.L., Huang, C.H., Chang, J., Lin, H.J., 2017. Alkaline phosphatase promoter as an efficient driving element for exogenic recombinant in the marine diatom *Phaeodactylum tricornutum*. *Algal Res.* 23, 58–65. <https://doi.org/10.1016/j.algal.2017.01.007>
- Liu, X.J., Duan, S.S., Li, A.F., Sun, K.F., 2009. Effects of glycerol on the fluorescence spectra and chloroplast ultrastructure of *Phaeodactylum tricornutum* (Bacillariophyta). *J. Integr. Plant Biol.* 51, 272–278. <https://doi.org/10.1111/j.1744-7909.2008.00767.x>
- Lizzul, A., 2016. Integrated production of algal biomass. Dr. thesis, UCL (University Coll. London).
- Longworth, J., Wu, D., Huete-Ortega, M., Wright, P.C., Vaidyanathan, S., 2016. Proteome response of *Phaeodactylum tricornutum*, during lipid accumulation induced by nitrogen depletion. *Algal Res.* 18, 213–224. <https://doi.org/10.1016/j.algal.2016.06.015>
- Lu, X., Sun, H., Zhao, W., Cheng, K.W., Chen, F., Liu, B., 2018. A hetero-photoautotrophic two-stage cultivation process for production of fucoxanthin by the marine diatom *Nitzschia laevis*. *Mar. Drugs* 16. <https://doi.org/10.3390/md16070219>
- Lubián, L.M., 1989. Concentrating cultured marine microalgae with chitosan. *Aquac. Eng.* 8, 257–265. [https://doi.org/10.1016/0144-8609\(89\)90013-7](https://doi.org/10.1016/0144-8609(89)90013-7)
- Madeira, M.S., Cardoso, C., Lopes, P.A., Coelho, D., Afonso, C., Bandarra, N.M., Prates, J.A.M., 2017. Microalgae as feed ingredients for livestock production and meat quality: A review. *Livest. Sci.* 205, 111–121. <https://doi.org/10.1016/j.livsci.2017.09.020>
- Markou, G., Nerantzis, E., 2013. Microalgae for high-value compounds and biofuels production: A review with focus on cultivation under stress conditions. *Biotechnol. Adv.* 31, 1532–1542. <https://doi.org/10.1016/j.biotechadv.2013.07.011>
- Matilde S.Chauton, Kjell Inge Reitan, Niels Henrik Norsker, Ragnar Tveterås, Hans T.Kleivdal, 2015. A techno-economic analysis of industrial production of marine microalgae as a source of EPA and DHA-rich raw material for aquafeed: Research challenges and possibilities. *Aquaculture* 436, 95–103. <https://doi.org/10.1016/j.aquaculture.2014.10.038>
- Matsuda, Y., Hara, T., Colman, B., 2001. Regulation of the induction of bicarbonate uptake by dissolved CO₂ in the marine diatom, *Phaeodactylum tricornutum*. *Plant, Cell Environ.* 24,

- 611–620. <https://doi.org/10.1046/j.1365-3040.2001.00702.x>
- Matsui, H., Hopkinson, B.M., Nakajima, K., Matsuda, Y., 2018. Plasma membrane-type aquaporins from marine diatoms function as CO₂/NH₃ channels and provide photoprotection. *Plant Physiol.* 178, pp.00453.2018. <https://doi.org/10.1104/pp.18.00453>
- Matsumoto, M., Nojima, D., Nonoyama, T., Ikeda, K., Maeda, Y., Yoshino, T., Tanaka, T., 2017. Outdoor cultivation of marine diatoms for year-round production of biofuels. *Mar. Drugs* 15, 8–10. <https://doi.org/10.3390/md15040094>
- McClure, D.D., Luiz, A., Gerber, B., Barton, G.W., Kavanagh, J.M., 2018. An investigation into the effect of culture conditions on fucoxanthin production using the marine microalgae *Phaeodactylum tricornutum*. *Algal Res.* 29, 41–48. <https://doi.org/10.1016/J.ALGAL.2017.11.015>
- MechaTronix Horticulture Lighting, 2020a. More micromoles for less money [WWW Document].
- MechaTronix Horticulture Lighting, 2020b. CoolStack®: The next dimension in LED grow lights [WWW Document].
- Megía-Hervás, I., Sánchez-Bayo, A., Bautista, L.F., Morales, V., Witt-Sousa, F.G., Segura-Fornieles, M., Vicente, G., 2020. Scale-up cultivation of *Phaeodactylum tricornutum* to produce biocrude by hydrothermal liquefaction. *Processes* 8. <https://doi.org/10.3390/pr8091072>
- Meiser, A., Schmid-staiger, U., Tr, W., 2004. Optimization of eicosapentaenoic acid production by *Phaeodactylum tricornutum* in the flat panel airlift reactor_2004_J Appl Phycol 16_215-225.pdf. *J. Appl. Phycol.* 16, 215–225.
- Mirón, A.S., Cerón García, M.C., Gómez, A.C., Camacho, F.G., Grima, E.M., Chisti, Y., 2003. Shear stress tolerance and biochemical characterization of *Phaeodactylum tricornutum* in quasi steady-state continuous culture in outdoor photobioreactors. *Biochem. Eng. J.* 16, 287–297. [https://doi.org/10.1016/S1369-703X\(03\)00072-X](https://doi.org/10.1016/S1369-703X(03)00072-X)
- Moejes, F., Succurro, A., Popa, O., Maguire, J., Ebenhöf, O., 2017. Dynamics of the Bacterial Community Associated with *Phaeodactylum tricornutum* Cultures. *Processes* 5, 77. <https://doi.org/10.3390/pr5040077>
- Molina Grima, E., Belarbi, E.-H., Ación Fernández, F. G., Robles Medina, A., Chisti, Y., 2003. Recovery of microalgal biomass and metabolites: process options and economics. *Biotechnol. Adv.* 20, 491–515. [https://doi.org/10.1016/S0734-9750\(02\)00050-2](https://doi.org/10.1016/S0734-9750(02)00050-2)
- Moosburner, M.A., Gholami, P., McCarthy, J.K., Tan, M., Bielinski, V.A., Allen, A.E., 2020. Multiplexed Knockouts in the Model Diatom *Phaeodactylum* by Episomal Delivery of a Selectable Cas9. *Front. Microbiol.* 11, 1–13. <https://doi.org/10.3389/fmicb.2020.00005>
- Mus, F., Toussaint, J.-P.P., Cooksey, K.E., Fields, M.W., Gerlach, R., Peyton, B.M., Carlson, R.P., 2013. Physiological and molecular analysis of carbon source supplementation and pH stress-induced lipid accumulation in the marine diatom *Phaeodactylum tricornutum*. *Appl. Microbiol. Biotechnol.* 97, 3625–3642. <https://doi.org/10.1007/s00253-013-4747-7>
- Negoro, M., Shioji, N., Miyamoto, K., Micira, Y., 1991. Growth of Microalgae in High CO₂ Gas and Effects of SO_x and NO_x. *Appl. Biochem. Biotechnol.* 28–29, 877–886. <https://doi.org/10.1007/BF02922657>
- Norsker, N.H., Barbosa, M.J., Vermuë, M.H., Wijffels, R.H., 2011. Microalgal production - A close look at the economics. *Biotechnol. Adv.* 29, 24–27. <https://doi.org/10.1016/j.biotechadv.2010.08.005>
- Nunez, M., Quigg, A., 2016. Changes in growth and composition of the marine microalgae *phaeodactylum tricornutum* and *nannochloropsis salina* in response to changing sodium bicarbonate concentrations. *J. Appl. Phycol.* 28, 2123–2138. <https://doi.org/10.1007/s10811-015-0746-7>
- Nur, M.M.A., Muizelaar, W., Boelen, P., Buma, A.G.J., 2019. Environmental and nutrient

- conditions influence fucoxanthin productivity of the marine diatom *Phaeodactylum tricornutum* grown on palm oil mill effluent. *J. Appl. Phycol.* 31, 1–12. <https://doi.org/10.1007/s10811-018-1563-6>
- Nymark, M., Sharma, A.K., Sparstad, T., Bones, A.M., Winge, P., 2016a. A CRISPR/Cas9 system adapted for gene editing in marine algae. *Sci. Rep.* 6, 24951. <https://doi.org/10.1038/srep24951>
- Nymark, M., Sharma, A.K., Sparstad, T., Bones, A.M., Winge, P., Kumar Sharma, A., Sparstad, T., Bones, A.M., Winge, P., 2016b. A CRISPR/Cas9 system adapted for gene editing in marine algae. *Sci. Rep.* 6, 1–6. <https://doi.org/10.1038/srep24951>
- Nymark, M., Valle, K.C., Hancke, K., Winge, P., Andresen, K., Johnsen, G., Bones, A.M., Brembu, T., 2013. Molecular and Photosynthetic Responses to Prolonged Darkness and Subsequent Acclimation to Re-Illumination in the Diatom *Phaeodactylum tricornutum*. *PLoS One* 8. <https://doi.org/10.1371/journal.pone.0058722>
- Oeltjen, A., Krumbein, W.E., Rhiel, E., 2002. Investigations on transcript sizes, steady state mRNA concentrations and diurnal expression of genes encoding fucoxanthin chlorophyll a/c light harvesting polypeptides in the centric diatom *Cyclotella cryptica*. *Plant Biol.* 4, 250–257. <https://doi.org/10.1055/s-2002-25737>
- Oka, K., Ueno, Y., Yokono, M., Shen, J.R., Nagao, R., Akimoto, S., 2020. Adaptation of light-harvesting and energy-transfer processes of a diatom *Phaeodactylum tricornutum* to different light qualities. *Photosynth. Res.* 146, 227–234. <https://doi.org/10.1007/s11120-020-00714-1>
- Olaizola, M., Grewe, C., 2019. Commercial microalgal cultivation systems, in: *Grand Challenges in Algae Biotechnology*. pp. 3–34.
- Oostlander, P.C., van Houcke, J., Barbosa, M.J., Wijffels, R.H., 2020. Microalgae production cost in aquaculture hatcheries. *Aquaculture* 525, 735310. <https://doi.org/10.1016/j.aquaculture.2020.735310>
- Ovide, C., Bérard, C., Vergne, N., Lecroq, T., Plasson, C., Burel, C., Bernard, S., Driouich, A., Lerouge, P., Tournier, I., Dauchel, H., Bardor, M., 2018. Comparative in depth RNA sequencing of *P. tricornutum*'s morphotypes reveals specific features of the oval morphotype 1–19. <https://doi.org/10.1038/s41598-018-32519-7>
- Padmaperuma, G., 2017. Microalgal co-cultures for biomanufacturing applications .
- Pahl, S.L., Lee, A.K., Kalaitzidis, T., Ashman, P.J., Sathe, S., Lewis, D.M., 2013. Harvesting, thickening and dewatering microalgae biomass, in: *Algae for Biofuels and Energy*. Springer Netherlands, Dordrecht, pp. 165–185. https://doi.org/10.1007/978-94-007-5479-9_10
- Park, K.Y., Wi, S.J., 2016. Potential of plants to produce recombinant protein products. *J. Plant Biol.* 59, 559–568. <https://doi.org/10.1007/s12374-016-0482-9>
- Penhaul Smith, J.K., Hughes, A.D., McEvoy, L., Day, J.G., 2020. Tailoring of the biochemical profiles of microalgae by employing mixotrophic cultivation. *Bioresour. Technol. Reports* 9, 100321. <https://doi.org/10.1016/j.biteb.2019.100321>
- Pereira, H., Sardinha, M., Santos, T., Gouveia, L., Barreira, L., Dias, J., Varela, J., 2020. Incorporation of defatted microalgal biomass (*Tetraselmis* sp. CTP4) at the expense of soybean meal as a feed ingredient for juvenile gilthead seabream (*Sparus aurata*). *Algal Res.* 47, 101869. <https://doi.org/10.1016/j.algal.2020.101869>
- Pérez-López, P., González-García, S., Allewaert, C., Verween, A., Murray, P., Feijoo, G., Teresa Moreira, M., 2014. Environmental evaluation of eicosapentaenoic acid production by *Phaeodactylum tricornutum*. *Sci. Total Environ.* 466–467, 991–1002. <https://doi.org/10.1016/j.scitotenv.2013.07.105>
- Petroutsos, D., Finazzi, G., Villanova, V., Fortunato, A.E., Singh, D., Dal Bo, D., Conte, M., Obata, T., Jouhet, J., Fernie, A.R., Marechal, E., Falciatore, A., Pagliardini, J., Le

- Monnier, A., Poolman, M., Curien, G., Bo, D.D., Conte, M., Obata, T., Jouhet, J., Fernie, A.R., Marechal, E., Falciatore, A., Pagliardini, J., Monnier, A. Le, Poolman, M., Curien, G., Petroutsos, D., Finazzi, G., Finazzi, G., 2017. Investigating mixotrophic metabolism in the model diatom *Phaeodactylum tricornutum*. *Philos. Trans. R. Soc. B Biol. Sci.* 372, 1–14. <https://doi.org/10.1098/rstb.2016.0404>
- Piiparinen, J., Barth, D., Eriksen, N.T., Teir, S., Spilling, K., Wiebe, M.G., 2018. Microalgal CO₂ capture at extreme pH values. *Algal Res.* 32, 321–328. <https://doi.org/10.1016/j.algal.2018.04.021>
- Plotka-Wasyłka, J., de la Guardia, M., Andruch, V., Vilková, M., 2020. Deep eutectic solvents vs ionic liquids: Similarities and differences. *Microchem. J.* 159, 1–7. <https://doi.org/10.1016/j.microc.2020.105539>
- Podevin, N., Davies, H. V., Hartung, F., Nogué, F., Casacuberta, J.M., 2013. Site-directed nucleases: A paradigm shift in predictable, knowledge-based plant breeding. *Trends Biotechnol.* 31, 375–383. <https://doi.org/10.1016/j.tibtech.2013.03.004>
- Postma, P.R., Miron, T.L., Olivieri, G., Barbosa, M.J., Wijffels, R.H., Eppink, M.H.M., 2015. Mild disintegration of the green microalgae *Chlorella vulgaris* using bead milling. *Bioresour. Technol.* 184, 297–304. <https://doi.org/10.1016/j.biortech.2014.09.033>
- Praba, T., Ajan, C., Citarasu, T., Selvaraj, T., Dhas, A.S., Gopal, P., Babu, M.M., 2016. Growth and Oil Yield in Selected Marine. *J. Aquac. Trop.* 31, 165–177.
- Qiao, H., Cong, C., Sun, C., Li, B., Wang, J., Zhang, L., 2016. Effect of culture conditions on growth, fatty acid composition and DHA/EPA ratio of *Phaeodactylum tricornutum*. *Aquaculture* 452, 311–317. <https://doi.org/10.1016/j.aquaculture.2015.11.011>
- Ra, C.H., Sirisuk, P., Jung, J.-H.H., Jeong, G.-T.T., Kim, S.-K.K., 2018. Effects of light-emitting diode (LED) with a mixture of wavelengths on the growth and lipid content of microalgae. *Bioprocess Biosyst. Eng.* 41, 457–465. <https://doi.org/10.1007/s00449-017-1880-1>
- Ras, M., Steyer, J.P., Bernard, O., 2013. Temperature effect on microalgae: A crucial factor for outdoor production. *Rev. Environ. Sci. Biotechnol.* 12, 153–164. <https://doi.org/10.1007/s11157-013-9310-6>
- Rastogi, A., Maheswari, U., Dorrell, R.G., Vieira, F.R.J., Maumus, F., Kustka, A., McCarthy, J., Allen, A.E., Kersey, P., Bowler, C., Tirichine, L., 2018. Integrative analysis of large scale transcriptome data draws a comprehensive landscape of *Phaeodactylum tricornutum* genome and evolutionary origin of diatoms. *Sci. Rep.* 8, 1–14. <https://doi.org/10.1038/s41598-018-23106-x>
- Reboloso-Fuentes, M.M., Navarro-Pérez, A., Ramos-Miras, J.J., Guil-Guerrero, J.L., 2001. Biomass nutrient profiles of the microalga *Phaeodactylum tricornutum*. *J. Food Biochem.* 25, 57–76. <https://doi.org/10.1111/j.1745-4514.2001.tb00724.x>
- Reddy, H.K., Muppaneni, T., Patil, P.D., Ponnusamy, S., Cooke, P., Schaub, T., Deng, S., 2014. Direct conversion of wet algae to crude biodiesel under supercritical ethanol conditions. *Fuel* 115, 720–726. <https://doi.org/10.1016/j.fuel.2013.07.090>
- Rees, T.A. V., Cresswell, R.C., Syrett, P.J., 1980. Sodium-dependent uptake of nitrate and urea by a marine diatom. *BBA - Biomembr.* 596, 141–144. [https://doi.org/10.1016/0005-2736\(80\)90178-9](https://doi.org/10.1016/0005-2736(80)90178-9)
- Regmi, B., 2014. An experimental study on the effects of light irradiance and photoperiod on the growth rate and lipid content in microalgae *Phaeodactylum tricornutum*.
- Remmers, I.M., Martens, D.E., Wijffels, R.H., Lamers, P.P., 2017. Dynamics of triacylglycerol and EPA production in *Phaeodactylum tricornutum* under nitrogen starvation at different light intensities. *PLoS One* 12, e0175630. <https://doi.org/10.1371/journal.pone.0175630>
- Remmers, I.M., Wijffels, R.H., Barbosa, M.J., Lamers, P.P., 2018. Can We Approach Theoretical Lipid Yields in Microalgae? *Trends Biotechnol.* 36, 265–276.

- <https://doi.org/10.1016/j.tibtech.2017.10.020>
- Research, C., 2020. Credence Research market [WWW Document]. Algae Prod. Mark. By Type. URL <https://www.credenceresearch.com/report/algae-products-market> (accessed 3.22.21).
- Réveillon, D., Séchet, V., Hess, P., Amzil, Z., 2016. Production of BMAA and DAB by diatoms (*Phaeodactylum tricornutum*, *Chaetoceros* sp., *Chaetoceros calcitrans* and, *Thalassiosira pseudonana*) and bacteria isolated from a diatom culture. *Harmful Algae* 58, 45–50. <https://doi.org/10.1016/j.hal.2016.07.008>
- Richmond, A., 2013. Biological Principles of Mass Cultivation of Photoautotrophic Microalgae, *Handbook of Microalgal Culture: Applied Phycology and Biotechnology: Second Edition*. <https://doi.org/10.1002/9781118567166.ch11>
- Rodolfi, L., Biondi, N., Guccione, A., Bassi, N.O., D'Ottavio, M., Arganaraz, G., Tredici, M.R., Ottavio, M.D., Arganaraz, G., Tredici, M.R., 2017. Oil and eicosapentaenoic acid production by the diatom *Phaeodactylum tricornutum* cultivated outdoors in Green Wall Panel (GWP®) reactors. *Biotechnol. Bioeng.* 114, 2204–2210. <https://doi.org/10.1002/bit.26353>
- Rodolfi, L., Zittelli, G.C., Bassi, N., Padovani, G., Biondi, N., Bonini, G., Tredici, M.R., 2009. Microalgae for Oil: Strain Selection, Induction of Lipid Synthesis and Outdoor Mass Cultivation in a. *Biotechnol. Bioeng* 102, 100–112. <https://doi.org/10.1002/bit.22033>
- Rogato, A., Richard, H., Sarazin, A., Voss, B., Cheminant Navarro, S., Champeimont, R., Navarro, L., Carbone, A., Hess, W.R., Falciatore, A., 2014. The diversity of small non-coding RNAs in the diatom *Phaeodactylum tricornutum*. *BMC Genomics* 15. <https://doi.org/10.1186/1471-2164-15-698>
- Rogers, J.N., Rosenberg, J.N., Guzman, B.J., Oh, V.H., Mimbela, L.E., Ghassemi, A., Betenbaugh, M.J., Oyler, G.A., Donohue, M.D., 2014. A critical analysis of paddlewheel-driven raceway ponds for algal biofuel production at commercial scales. *Algal Res.* 4, 76–88. <https://doi.org/10.1016/j.algal.2013.11.007>
- Roselet, F., Burkert, J., Abreu, P.C., 2016a. Flocculation of *Nannochloropsis oculata* using a tannin-based polymer: Bench scale optimization and pilot scale reproducibility. *Biomass and Bioenergy* 87, 55–60. <https://doi.org/10.1016/j.biombioe.2016.02.015>
- Roselet, F., Vandamme, D., Roselet, M., Muylaert, K., Abreu, P.C., 2016b. Effects of pH, Salinity, Biomass Concentration, and Algal Organic Matter on Flocculant Efficiency of Synthetic Versus Natural Polymers for Harvesting Microalgae Biomass. *Bioenergy Res.* 10, 427–437. <https://doi.org/10.1007/s12155-016-9806-3>
- Roselet, F., Vandamme, D., Roselet, M., Muylaert, K., Abreu, P.C., 2015. Screening of commercial natural and synthetic cationic polymers for flocculation of freshwater and marine microalgae and effects of molecular weight and charge density. *Algal Res.* 10, 183–188. <https://doi.org/10.1016/j.algal.2015.05.008>
- Ruiz, J., Olivieri, G., De Vree, J., Bosma, R., Willems, P., Reith, J.H., Eppink, M.H.M., Kleinegris, D.M.M., Wijffels, R.H., Barbosa, M.J., 2016. Towards industrial products from microalgae. *Energy Environ. Sci.* 9, 3036–3043. <https://doi.org/10.1039/c6ee01493c>
- Rwehumbiza, V.M., Harrison, R., Thomsen, L., 2012. Alum-induced flocculation of pre-concentrated *Nannochloropsis salina*: Residual aluminium in the biomass, FAMES and its effects on microalgae growth upon media recycling. *Chem. Eng. J.* 200–202, 168–175. <https://doi.org/10.1016/j.cej.2012.06.008>
- Ryckebosch, E., Muylaert, K., Foubert, I., 2012. Optimization of an analytical procedure for extraction of lipids from microalgae. *JAOCS, J. Am. Oil Chem. Soc.* 89, 189–198. <https://doi.org/10.1007/s11746-011-1903-z>
- Samo, T.J., Kimbrel, J.A., Nilson, D.J., Pett-Ridge, J., Weber, P.K., Mayali, X., 2018. Attachment between heterotrophic bacteria and microalgae influences symbiotic

- microscale interactions. *Environ. Microbiol.* 20, 4385–4400. <https://doi.org/10.1111/1462-2920.14357>
- Sánchez-Martín, J., González-Velasco, M., Beltrán-Heredia, J., 2009. Acacia mearnsii de Wild tannin-based flocculant in surface water treatment. *J. Wood Chem. Technol.* 29, 119–135. <https://doi.org/10.1080/02773810902796146>
- Sánchez-Porro, C., Kaur, B., Mann, H., Ventosa, A., 2010. Halomonas titanicae sp. nov., a halophilic bacterium isolated from the RMS Titanic. *Int. J. Syst. Evol. Microbiol.* 60, 2768–2774. <https://doi.org/10.1099/ijs.0.020628-0>
- Sapana, M.M., Sonal, C.G., D, R.P., 2012. Use of Moringa Oleifera (Drumstick) seed as Natural Absorbent and an Antimicrobial agent for Ground water Treatment. *Res. J. Recent Sci. Res. J. Recent Sci* 1, 31–40.
- Schlesinger, A., Eisenstadt, D., Bar-Gil, A., Carmely, H., Einbinder, S., Gressel, J., 2012. Inexpensive non-toxic flocculation of microalgae contradicts theories; overcoming a major hurdle to bulk algal production. *Biotechnol. Adv.* 30, 1023–1030. <https://doi.org/10.1016/j.biotechadv.2012.01.011>
- Schulze, P.S.C.C., Pereira, H.G.C.C., Santos, T.F.C.C., Schueler, L., Guerra, R., Barreira, L.A., Perales, J.A., Varela, J.C.S.S., 2016. Effect of light quality supplied by light emitting diodes (LEDs) on growth and biochemical profiles of Nannochloropsis oculata and Tetraselmis chuii. *Algal Res.* 16, 387–398. <https://doi.org/10.1016/j.algal.2016.03.034>
- Schulze, P.S.C.S., Barreira, L.A., Pereira, H.G.C.G., Perales, J.A., Varela, J.C.C.S., 2014. Light emitting diodes (LEDs) applied to microalgal production. *Trends Biotechnol.* 32, 422–430. <https://doi.org/10.1016/j.tibtech.2014.06.001>
- Scott, S.A., Davey, M.P., Dennis, J.S., Horst, I., Howe, C.J., Lea-Smith, D.J., Smith, A.G., 2010. Biodiesel from algae: Challenges and prospects. *Curr. Opin. Biotechnol.* 21, 277–286. <https://doi.org/10.1016/j.copbio.2010.03.005>
- Selesu, N.F.H., de Oliveira, T. V., Corrêa, D.O., Miyawaki, B., Mariano, A.B., Vargas, J.V.C., Vieira, R.B., 2016. Maximum microalgae biomass harvesting via flocculation in large scale photobioreactor cultivation. *Can. J. Chem. Eng.* 94, 304–309. <https://doi.org/10.1002/cjce.22391>
- Seo, S., Jeon, H., Chang, K.S., Jin, E.S., 2018. Enhanced biomass production by Phaeodactylum tricornutum overexpressing phosphoenolpyruvate carboxylase. *Algal Res.* 31, 489–496. <https://doi.org/10.1016/j.algal.2017.08.017>
- Seo, S., Jeon, H., Hwang, S., Jin, E., Chang, K.S., 2015. Development of a new constitutive expression system for the transformation of the diatom Phaeodactylum tricornutum. *Algal Res.* 11, 50–54. <https://doi.org/10.1016/j.algal.2015.05.012>
- Serif, M., Dubois, G., Finoux, A.L., Teste, M.A., Jallet, D., Daboussi, F., 2018. One-step generation of multiple gene knock-outs in the diatom Phaeodactylum tricornutum by DNA-free genome editing. *Nat. Commun.* 9, 1–10. <https://doi.org/10.1038/s41467-018-06378-9>
- Serif, M., Lepetit, B., Weißert, K., Kroth, P.G., Rio Bartulos, C., 2017. A fast and reliable strategy to generate TALEN-mediated gene knockouts in the diatom Phaeodactylum tricornutum. *Algal Res.* 23, 186–195. <https://doi.org/10.1016/j.algal.2017.02.005>
- Sethi, D., Butler, T.O., Shuhaili, F., Vaidyanathan, S., 2020. Diatoms for carbon sequestration and bio-based manufacturing. *Biology (Basel)*. 9, 1–29. <https://doi.org/10.3390/biology9080217>
- Severes, A., Hegde, Shashank, D'Souza, L., Hegde, Smitha, 2017. Use of light emitting diodes (LEDs) for enhanced lipid production in micro-algae based biofuels. *J. Photochem. Photobiol. B Biol.* 170, 235–240. <https://doi.org/10.1016/j.jphotobiol.2017.04.023>
- Shah, M.R., Lutz, G.A., Alam, A., Sarker, P., Kabir Chowdhury, M.A., Parsaemehr, A., Liang, Y., Daroch, M., 2018. Microalgae in aquafeeds for a sustainable aquaculture

- industry. *J Appl Phycol* 30, 197–213. <https://doi.org/10.1007/s10811-017-1234-z>
- Shelef, G., Sukenik, A., Green, M., 1984. *Microalgae Harvesting and Processing: A Literature Review*.
- Shemesh, Z., Leu, S., Khozin-Goldberg, I., Didi-Cohen, S., Zarka, A., Boussiba, S., 2016. Inducible expression of Haematococcus oil globule protein in the diatom *Phaeodactylum tricorutum*: Association with lipid droplets and enhancement of TAG accumulation under nitrogen starvation. *Algal Res.* 18, 321–331. <https://doi.org/10.1016/j.algal.2016.07.002>
- Shi, F., Wei, X., Feng, J., Sun, Y., Zhu, L., 2018. Variation of bacterial community associated with *Phaeodactylum tricorutum* in response to different inorganic nitrogen concentrations. *Acta Oceanol. Sin.* 37, 118–128. <https://doi.org/10.1007/s13131-018-1272-7>
- Shimura, S., Fujita, Y., 1975. Changes in the activity of fucoxanthin-excited photosynthesis in the marine diatom *Phaeodactylum tricorutum* grown under different culture conditions. *Mar. Biol.* 33, 185–194. <https://doi.org/10.1007/BF00390922>
- Silva, A.M., Torzillo, G., Rica, C., Rica, C., Pedro, S., Jose, S., 2013. Productivity and biochemical composition of *Phaeodactylum tricorutum* (Bacillariophyceae) cultures grown outdoors in tubular photobioreactors and open ponds. *Biomass and Bioenergy* 4, 1–8. <https://doi.org/10.1016/j.biombioe.2013.03.016>
- Simonazzi, M., Pezzolesi, L., Guerrini, F., Vanucci, S., Samorì, C., Pistocchi, R., 2019. Use of waste carbon dioxide and pre-treated liquid digestate from biogas process for *Phaeodactylum tricorutum* cultivation in photobioreactors and open ponds. *Bioresour. Technol.* 292, 121921. <https://doi.org/10.1016/j.biortech.2019.121921>
- Singh, G., Patidar, S.K., 2018. Microalgae harvesting techniques: A review. *J. Environ. Manage.* 217, 499–508. <https://doi.org/10.1016/j.jenvman.2018.04.010>
- Şirin, S., Trobajo, R., Ibanez, C., Salvadó, J., 2012. Harvesting the microalgae *Phaeodactylum tricorutum* with polyaluminum chloride, aluminium sulphate, chitosan and alkalinity-induced flocculation. *J. Appl. Phycol.* 24, 1067–1080. <https://doi.org/10.1007/s10811-011-9736-6>
- Sirisuk, P., Ra, C.-H., Jeong, G.-T., Kim, S.-K., 2018. Effects of wavelength mixing ratio and photoperiod on microalgal biomass and lipid production in a two-phase culture system using LED illumination. *Bioresour. Technol.* 253, 175–181. <https://doi.org/10.1016/J.BIORTECH.2018.01.020>
- Siron, R., Giusti, G., Berland, B., 1989. Changes in the fatty acid composition of *Phaeodactylum tricorutum* and *Dunaliella tertiolecta* during growth and under phosphorus deficiency. *Mar. Ecol. Prog. Ser.* 55, 95–100. <https://doi.org/10.3354/meps055095>
- Slade, R., Bauen, A., 2013. Micro-algae cultivation for biofuels: Cost, energy balance, environmental impacts and future prospects. *Biomass and Bioenergy* 53, 29–38. <https://doi.org/10.1016/j.biombioe.2012.12.019>
- Slattery, S.S., Diamond, A., Wang, H., Therrien, J.A., Lant, J.T., Jazey, T., Lee, K., Klassen, Z., Desgagné, I., Penix, D., Karas, B.J., Edgell, D.R., Desgagné-Penix, I., Karas, B.J., Edgell, D.R., 2018. An Expanded Plasmid-Based Genetic Toolbox Enables Cas9 Genome Editing and Stable Maintenance of Synthetic Pathways in *Phaeodactylum tricorutum*. *ACS Synth. Biol.* 7, 328–338. <https://doi.org/10.1021/acssynbio.7b00191>
- Song, Z., Lye, G.J., Parker, B.M., 2020. Morphological and biochemical changes in *Phaeodactylum tricorutum* triggered by culture media: Implications for industrial exploitation. *Algal Res.* 47, 101822. <https://doi.org/10.1016/j.algal.2020.101822>
- Sørensen, M., Berge, G.M., Reitan, K.I., Ruyter, B., 2016. Microalga *Phaeodactylum tricorutum* in feed for Atlantic salmon (*Salmo salar*) -Effect on nutrient digestibility,

- growth and utilization of feed. *Aquaculture* 460, 116–123. <https://doi.org/10.1016/j.aquaculture.2016.04.010>
- Soto, K., Collantes, G., Zahr, M., Kuznar, J., 2005. Simultaneous enumeration of *Phaeodactylum tricornutum* (MLB292) and bacteria growing in mixed communities. *Investig. Mar.* 33, 143–149. <https://doi.org/10.4067/S0717-71782005000200002>
- Specht, E.A., Mayfield, S.P., 2014. Algae-based oral recombinant vaccines. *Front. Microbiol.* 5, 1–7. <https://doi.org/10.3389/fmicb.2014.00060>
- Spilling, K., Brynjólfssdóttir, Á., Enss, D., Rischer, H., Guðfinnur Svavarsson, H., Svavarsson, H.G., 2013. The effect of high pH on structural lipids in diatoms. *J. Appl. Phycol.* 25, 1435–1439. <https://doi.org/10.1007/s10811-012-9971-5>
- Spilling, K., Seppälä, J., Tamminen, T., 2011. Inducing autoflocculation in the diatom *Phaeodactylum tricornutum* through CO₂ regulation. *J. Appl. Phycol.* 23, 959–966. <https://doi.org/10.1007/s10811-010-9616-5>
- Steinrücken, P., Erga, S.R., Mjøs, S.A., Kleivdal, H., Prestegard, S.K., 2017. Bioprospecting North Atlantic microalgae with fast growth and high polyunsaturated fatty acid (PUFA) content for microalgae-based technologies. *Algal Res.* 26, 392–401. <https://doi.org/10.1016/J.ALGAL.2017.07.030>
- Steinrücken, P., Prestegard, S.K., de Vree, J.H., Storesund, J.E., Pree, B., Mjøs, S.A., Erga, S.R., 2018. Comparing EPA production and fatty acid profiles of three *Phaeodactylum tricornutum* strains under western Norwegian climate conditions. *Algal Res.* 30, 11–22. <https://doi.org/10.1016/J.ALGAL.2017.12.001>
- Strickland, J.D.H., Parsons, T., 1968. A practical handbook of seawater analysis. https://doi.org/10.1007/978-1-4615-5439-4_19
- Stukenberg, D., Zauner, S., Dell’Aquila, G., Maier, U.G., 2018. Optimizing CRISPR/Cas9 for the Diatom *Phaeodactylum tricornutum*. *Front. Plant Sci.* 9, 1–11. <https://doi.org/10.3389/fpls.2018.00740>
- Sukenik, A., Bilanovic, D., Shelef, G., 1988. Flocculation of microalgae in brackish and sea waters. *Biomass* 15, 187–199. [https://doi.org/10.1016/0144-4565\(88\)90084-4](https://doi.org/10.1016/0144-4565(88)90084-4)
- Suleiman, M., Zecher, K., Yücel, O., Jagmann, N., Philipp, B., 2016. Interkingdom cross-feeding of ammonium from marine methylamine-degrading bacteria to the diatom *Phaeodactylum tricornutum*. *Appl. Environ. Microbiol.* 82, 7113–7122. <https://doi.org/10.1128/AEM.01642-16>
- Taher, H., Al-Zuhair, S., Al-Marzouqi, A.H., Haik, Y., Farid, M., 2014. Effective extraction of microalgae lipids from wet biomass for biodiesel production. *Biomass and Bioenergy* 66, 159–167. <https://doi.org/10.1016/j.biombioe.2014.02.034>
- Timmermans, N.B., 2017. Fucoxanthin: A promising bioproduct to be derived from algae? *Rijksuniversiteit Groningen*.
- Tirichine, L., Rastogi, A., Bowler, C., 2017. Recent progress in diatom genomics and epigenomics. *Curr. Opin. Plant Biol.* 36, 46–55. <https://doi.org/10.1016/j.pbi.2017.02.001>
- Tocquin, P., Fratamico, A., Franck, F., 2012. Screening for a low-cost *Haematococcus pluvialis* medium reveals an unexpected impact of a low N/P ratio on vegetative growth. *J. Appl. Phycol.* 24, 365–373. <https://doi.org/10.1007/s10811-011-9771-3>
- Tommasi, E., Cravotto, G., Galletti, P., Grillo, G., Mazzotti, M., Sacchetti, G., Samorì, C., Tabasso, S., Tacchini, M., Tagliavini, E., Samor, C., Tabasso, S., Tacchini, M., Tagliavini, E., 2017. Enhanced and Selective Lipid Extraction from the Microalga *P. tricornutum* by Dimethyl Carbonate and Supercritical CO₂ Using Deep Eutectic Solvents and Microwaves as Pretreatment. *ACS Sustain. Chem. Eng.* 5, 8316–8322. <https://doi.org/10.1021/acssuschemeng.7b02074>
- Tredici, M.R., Bassi, N., Prussi, M., Biondi, N., Rodolfi, L., Zittelli, G.C., Sampietro, G., 2015. Energy balance of algal biomass production in a 1-ha “Green Wall Panel” plant: How

- to produce algal biomass in a closed reactor achieving a high Net Energy Ratio q . *Appl. Energy* 154, 1103–1111. <https://doi.org/10.1016/j.apenergy.2015.01.086>
- Tripathi, A.D., Mishra, R., Maurya, K.K., Singh, R.B., Wilson, D.W., 2018. Estimates for world population and global food availability for global health, The Role of Functional Food Security in Global Health. Elsevier Inc. <https://doi.org/10.1016/B978-0-12-813148-0.00001-3>
- Uduman, N., Qi, Y., Danquah, M.K., Forde, G.M., Hoadley, A., 2010. Dewatering of microalgal cultures: A major bottleneck to algae-based fuels. *J. Renew. Sustain. Energy* 2, 12701–23104. <https://doi.org/10.1063/1.3571565>
- Valdez-Flores, M.A., Fe, J. V., German-Báez, L.J., Valdez-Flores, M.A., Félix-Medina, J. V., Norzagaray-Valenzuela, C.D., Santos-Ballardo, D.U., Reyes-Moreno, C., Shelton, L.M., Valdez-Ortiz, A., 2017. Chemical composition and physicochemical properties of *Phaeodactylum tricornutum* microalgal residual biomass. *Food Sci. Technol. Int.* 23, 681–689. <https://doi.org/10.1177/1082013217717611>
- Van Haver, L., Nayar, S., 2017. Polyelectrolyte flocculants in harvesting microalgal biomass for food and feed applications. *Algal Res.* 24, 167–180. <https://doi.org/10.1016/j.algal.2017.03.022>
- van Tol, H.M., 2019. Computational and Experimental Models of Diatom-Bacteria Interaction. Thesis 161.
- Vandamme, D., Beuckels, A., Markou, G., Foubert, I., Muylaert, K., 2015a. Reversible Flocculation of Microalgae using Magnesium Hydroxide. *Bioenergy Res.* 8, 716–725. <https://doi.org/10.1007/s12155-014-9554-1>
- Vandamme, D., Foubert, I., Meesschaert, B., Muylaert, K., 2010. Flocculation of microalgae using cationic starch. *J. Appl. Phycol.* 22, 525–530. <https://doi.org/10.1007/s10811-009-9488-8>
- Vandamme, D., Foubert, I., Muylaert, K., 2013. Flocculation as a low-cost method for harvesting microalgae for bulk biomass production. *Trends Biotechnol.* 31, 233–239. <https://doi.org/10.1016/j.tibtech.2012.12.005>
- Vandamme, D., Gheysen, L., Muylaert, K., Foubert, I., 2018. Impact of harvesting method on total lipid content and extraction efficiency for *Phaeodactylum tricornutum*. *Sep. Purif. Technol.* 194, 362–367. <https://doi.org/10.1016/J.SEPPUR.2017.10.035>
- Vandamme, D., Pohl, P.I., Beuckels, A., Foubert, I., Brady, P. V., Hewson, J.C., Muylaert, K., 2015b. Alkaline flocculation of *Phaeodactylum tricornutum* induced by brucite and calcite. *Bioresour. Technol.* 196, 656–661. <https://doi.org/10.1016/j.biortech.2015.08.042>
- Velmurugan, N., Deka, D., 2018. Transformation techniques for metabolic engineering of diatoms and haptophytes: current state and prospects. *Appl. Microbiol. Biotechnol.* 102, 4255–4267. <https://doi.org/10.1007/s00253-018-8925-5>
- Veluchamy, A., Rastogi, A., Lin, X., Lombard, B., Murik, O., Thomas, Y., Dingli, F., Rivarola, M., Ott, S., Liu, X., Sun, Y., Rabinowicz, P.D., McCarthy, J., Allen, A.E., Loew, D., Bowler, C., Tirichine, L., 2015. An integrative analysis of post-translational histone modifications in the marine diatom *Phaeodactylum tricornutum*. *Genome Biol.* 16, 1–18. <https://doi.org/10.1186/s13059-015-0671-8>
- Veuger, B., Middelburg, J.J., Boschker, H.T.S., Houtekamer, M., 2005. Analysis of ¹⁵N incorporation into D-alanine: A new method for tracing nitrogen uptake by bacteria. *Limnol. Oceanogr. Methods* 3, 230–240. <https://doi.org/10.4319/lom.2005.3.230>
- Villanova, V., Fortunato, A.E., Singh, D., Bo, D.D., Conte, M., Obata, T., Jouhet, J., Fernie, A.R., Marechal, E., Falciatore, A., Pagliardini, J., Le Monnier, A., Poolman, M., Curien, G., Petroustos, D., Finazzi, G., 2017. Investigating mixotrophic metabolism in the model diatom *Phaeodactylum tricornutum*. *Philos. Trans. R. Soc. B Biol. Sci.* 372, 20160404. <https://doi.org/10.1098/rstb.2016.0404>

- Vuong, T.T., Kwon, B.R., Eom, J.I., Shin, B.K., Kim, S.M., 2019. Interaction between marine bacterium *Stappia* sp. K01 and diatom *Phaeodactylum tricorutum* through extracellular fatty acids. *J. Appl. Phycol.* 71–82. <https://doi.org/10.1007/s10811-019-01931-5>
- Wagner, H., Jakob, T., Lavaud, J., Wilhelm, C., 2016. Photosystem II cycle activity and alternative electron transport in the diatom *Phaeodactylum tricorutum* under dynamic light conditions and nitrogen limitation. *Photosynth. Res.* 128, 151–161. <https://doi.org/10.1007/s11120-015-0209-7>
- Wang, H., Zhang, Y., Chen, L., Cheng, W., Liu, T., 2018. Combined production of fucoxanthin and EPA from two diatom strains *Phaeodactylum tricorutum* and *Cylindrotheca fusiformis* cultures. *Bioprocess Biosyst. Eng.* 41, 1061–1071. <https://doi.org/10.1007/s00449-018-1935-y>
- Wang, L.-J., Fan, Y., Parsons, R., Hu, G.-R., Zhang, P.-Y., Li, F.-L., 2018. A Rapid Method for the Determination of Fucoxanthin in Diatom. *Mar. Drugs* 16, 33. <https://doi.org/10.3390/md16010033>
- Wang, L., Liang, W., Yu, J., Liang, Z., Ruan, L., Zhang, Y., 2013. Flocculation of *Microcystis aeruginosa* using modified larch tannin. *Environ. Sci. Technol.* 47, 5771–5777. <https://doi.org/10.1021/es400793x>
- Wang, S., Said, I.H., Thorstenson, C., Thomsen, C., Ullrich, M.S., Kuhnert, N., Thomsen, L., 2018a. Pilot-scale production of antibacterial substances by the marine diatom *Phaeodactylum tricorutum* Bohlin. *Algal Res.* 32, 113–120. <https://doi.org/10.1016/j.algal.2018.03.014>
- Wang, S., Verma, S.K., Hakeem Said, I., Thomsen, L., Ullrich, M.S., Kuhnert, N., 2018b. Changes in the fucoxanthin production and protein profiles in *Cylindrotheca closterium* in response to blue light-emitting diode light. *Microb. Cell Fact.* 17, 1–13. <https://doi.org/10.1186/s12934-018-0957-0>
- Wang, W., Yu, L.J., Xu, C., Tomizaki, T., Zhao, S., Umena, Y., Chen, X., Qin, X., Xin, Y., Suga, M., Han, G., Kuang, T., Shen, J.R., 2019. Structural basis for blue-green light harvesting and energy dissipation in diatoms. *Science* (80-.). 363. <https://doi.org/10.1126/science.aav0365>
- Wang, X., Liu, Y.H., Wei, W., Zhou, X., Yuan, W., Balamurugan, S., Hao, T. Bin, Yang, W.D., Liu, J.S., Li, H.Y., 2017. Enrichment of Long-Chain Polyunsaturated Fatty Acids by Coordinated Expression of Multiple Metabolic Nodes in the Oleaginous Microalga *Phaeodactylum tricorutum*. *J. Agric. Food Chem.* 65, 7713–7720. <https://doi.org/10.1021/acs.jafc.7b02397>
- Wen, X., Wang, Z., Ding, Y., Geng, Y., Li, Y., 2020. Enhancing the production of astaxanthin by mixotrophic cultivation of *Haematococcus pluvialis* in open raceway ponds. *Aquac. Int.* 28, 625–638. <https://doi.org/10.1007/s10499-019-00483-2>
- Weyman, P.D., Beerli, K., Lefebvre, S.C., Rivera, J., McCarthy, J.K., Heuberger, A.L., Peers, G., Allen, A.E., Dupont, C.L., 2015. Inactivation of *Phaeodactylum tricorutum* urease gene using transcription activator-like effector nuclease-based targeted mutagenesis. *Plant Biotechnol. J.* 13, 460–470. <https://doi.org/10.1111/pbi.12254>
- Whitton, R., Santinelli, M., Pidou, M., Ometto, F., Henderson, R., Roddick, F., Jarvis, P., Villa, R., Jefferson, B., 2018. Tertiary nutrient removal from wastewater by immobilised microalgae: impact of wastewater nutrient characteristics and hydraulic retention time (HRT). *H2Open J.* 1, 12–25. <https://doi.org/10.2166/h2oj.2018.008>
- Willis, A., Chiovitti, A., Dugdale, T.M., Wetherbee, R., 2013. Characterization of the extracellular matrix of *Phaeodactylum tricorutum* (Bacillariophyceae): structure, composition, and adhesive characteristics. *J. Appl. Phycol.* 49, 937–949. <https://doi.org/10.1111/jpy.12103>
- Wu, H., Li, T., Wang, G., Dai, S., He, H., Xiang, W., Hualian, W., Li, T., Guanghua, W., Dai,

- S., He, H., Xiang, W., 2016. A comparative analysis of fatty acid composition and fucoxanthin content in six *Phaeodactylum tricornutum* strains from different origins*. *Chinese J. Oceanol. Limnol.* 34, 391–398. <https://doi.org/10.1007/s00343-015-4325-1>
- Wu, S., Xie, X., Huan, L., Zheng, Z., Zhao, P., Kuang, J., Liu, X., Wang, G., 2016. Selection of optimal flocculant for effective harvesting of the fucoxanthin-rich marine microalga *Isochrysis galbana*. *J. Appl. Phycol.* 28, 1579–1588. <https://doi.org/10.1007/s10811-015-0716-0>
- Xie, W.H., Zhu, C.C., Zhang, N.S., Li, D.W., Yang, W.D., Liu, J.S., Sathishkumar, R., Li, H.Y., 2014. Construction of Novel Chloroplast Expression Vector and Development of an Efficient Transformation System for the Diatom *Phaeodactylum tricornutum*. *Mar. Biotechnol.* 16, 538–546. <https://doi.org/10.1007/s10126-014-9570-3>
- Xiong, J.Q., Kurade, M.B., Jeon, B.H., 2018. Can Microalgae Remove Pharmaceutical Contaminants from Water? *Trends Biotechnol.* 36, 30–44. <https://doi.org/10.1016/j.tibtech.2017.09.003>
- Yacob, M.R., Kabir, I., Radam, A., Abed, K.A., El Morsi, A.K., Sayed, M.M., Shaib, A.A.E., Gad, M.S., Carlo, A., Carolina, L., Ejikeme, P.M., Anyaogu, I.D., Ejikeme, C.L., Nwafor, N.P., Egbuonu, C.A.C., Ukogu, K., Ibemesi, J.A., Chemistry, I., Polytechnic, F., Schuchardt, U., Sercheli, R., Matheus, R., 1998. Catalysis in Biodiesel Production by Transesterification Processes-An Insight. *Egypt. J. Pet.* 9, 332–337.
- Yan, N., Fan, C., Chen, Y., Hu, Z., 2016. The potential for microalgae as bioreactors to produce pharmaceuticals. *Int. J. Mol. Sci.* 17, 1–24. <https://doi.org/10.3390/ijms17060962>
- Yang, J., Pan, Y., Bowler, C., Zhang, L., Hu, H., 2016. Knockdown of phosphoenolpyruvate carboxykinase increases carbon flux to lipid synthesis in *Phaeodactylum tricornutum*. *Algal Res.* 15, 50–58. <https://doi.org/10.1016/j.algal.2016.02.004>
- Yang, R., Wei, D., 2020. Improving Fucoxanthin Production in Mixotrophic Culture of Marine Diatom *Phaeodactylum tricornutum* by LED Light Shift and Nitrogen Supplementation. *Front. Bioeng. Biotechnol.* 8. <https://doi.org/10.3389/fbioe.2020.00820>
- Yang, R., Wei, D., Xie, J., 2020. Diatoms as cell factories for high-value products: chrysolaminarin, eicosapentaenoic acid, and fucoxanthin. *Crit. Rev. Biotechnol.* 40, 993–1009. <https://doi.org/10.1080/07388551.2020.1805402>
- Yao, S., Lyu, S., An, Y., Lu, J., Gjermansen, C., Schramm, A., 2019. Microalgae–bacteria symbiosis in microalgal growth and biofuel production: a review. *J. Appl. Microbiol.* 126, 359–368. <https://doi.org/10.1111/jam.14095>
- Yi, Z., Xu, M., Magnúsdóttir, M., Zhang, Y., Brynjólfsson, S., Fu, W., Martin-Jézéquel, V., 2015. Photo-oxidative stress-driven mutagenesis and adaptive evolution on the marine diatom *Phaeodactylum tricornutum* for enhanced carotenoid accumulation. *Mar. Drugs* 13, 6138–6151. <https://doi.org/10.3390/md13106138>
- Yodsuwan, N., Sawayama, S., Sirisansaneeyakul, S., 2017. Effect of nitrogen concentration on growth, lipid production and fatty acid profiles of the marine diatom *Phaeodactylum tricornutum*. *Agric. Nat. Resour.* 51, 190–197. <https://doi.org/10.1016/j.anres.2017.02.004>
- Yongmanitchai, W., Ward, O.P., 1993. Positional distribution of fatty acids, and molecular species of polar lipids, in the diatom *Phaeodactylum tricornutum*. *J. Gen. Microbiol.* 139, 465–472.
- Yongmanitchai, W., Ward, P., 1991. Growth of and Omega-3 Fatty Acid Production by *Phaeodactylum tricornutum* under Different Culture Conditions. *Appl. Environ. Microbiol.* 419–425.
- Young, J.N., Hopkinson, B.M., 2017. The potential for co-evolution of CO₂-concentrating mechanisms and Rubisco in diatoms. *J. Exp. Bot.* 68, 3751–3762. <https://doi.org/10.1093/jxb/erx130>

- Zhang, D., Wen, S., Wu, X., Cong, W., 2018. Effect of culture condition on the growth, biochemical composition and EPA production of alkaliphilic *Nitzschia plea* isolated in the Southeast of China. *Bioprocess Biosyst. Eng.* <https://doi.org/10.1007/s00449-018-1917-0>
- Zhang, W., Wang, F., Gao, B., Huang, L., Zhang, C., 2018. An integrated biorefinery process: Stepwise extraction of fucoxanthin, eicosapentaenoic acid and chrysolaminarin from the same *Phaeodactylum tricornutum* biomass. *Algal Res.* 32, 193–200. <https://doi.org/10.1016/j.algal.2018.04.002>
- Zhao, P., Gu, W., Wu, S., Huang, A., He, L., Xie, X., Gao, S., Zhang, B., Niu, J., Peng Lin, A., Wang, G., Lin, A.P., Wang, G., 2014. Silicon enhances the growth of *Phaeodactylum tricornutum* Bohlin under green light and low temperature. *Sci. Rep.* 4, 3958–3967. <https://doi.org/10.1038/srep03958>
- Zheng, H., Gao, Z., Yin, J., Tang, X., Ji, X., Huang, H., 2012. Harvesting of microalgae by flocculation with poly ($\hat{\text{T}}^3$ -glutamic acid). <https://doi.org/10.1016/j.biortech.2012.02.086>
- Zhu, B.-H., Zhang, R.-H., Lv, N.-N., Yang, G.-P., Wang, Y.-S., Pan, K.-H., 2018. The Role of Malic Enzyme on Promoting Total Lipid and Fatty Acid Production in *Phaeodactylum tricornutum*. *Front. Plant Sci.* 9, 1–8. <https://doi.org/10.3389/fpls.2018.00826>
- Zhu, B.H., Shi, H.P., Yang, G.P., Lv, N.N., Yang, M., Pan, K.H., 2016. Silencing UDP-glucose pyrophosphorylase gene in *Phaeodactylum tricornutum* affects carbon allocation. *N. Biotechnol.* 33, 237–244. <https://doi.org/10.1016/j.nbt.2015.06.003>

About the author



Thomas Butler conducted his Bachelor's degree in Marine Biology where he obtained a First-Class Honours at Newcastle University and in 2014 transitioned to Algal Biotechnology where he was the first student in the UK to obtain a Masters by Research in Algal Biotechnology conducted at the Scottish Association for Marine Science (SAMS), accredited by Aberdeen University. He was working on astaxanthin production from *Haematococcus* using an alternative life-cycle stage termed the 'red motile macrozooid' and has several publications in this area.

In 2016, Thomas Butler commenced his PhD in Microalgal Cell Factories at The University of Sheffield developing *Phaeodactylum tricornutum* as a biorefinery platform for the high-value product fucoxanthin with the remainder for aquaculture feed rich in eicosapentaenoic acid and protein. He explored a series of biobased flocculants and found that a tannic acid-based derivative was optimal which was suitable for wet extraction for the products of interest. In 2019 Thomas Butler undertook a 3-month Guest PhD at Wageningen University to conduct a pilot scale study on *P. tricornutum* in flat panel PBRs.

Thomas Butler currently works at Lgem/Synalgae situated in The Netherlands and he works as a Senior Research Scientist. Lgem/Synalgae is a biotech scale-up merger between Lgem, with greater than 15 years' experience in building photobioreactor systems/growing algae, and Synalgae, a high-TECH conglomerate specialised in process technology. Together Lem/Synalgae provide a high-end alga driven assortment of fully integrated growth systems but also ingredients. Thomas Butler is involved in various R & D projects including *Nannochloropsis* for the omega-3 fatty acid eicosapentaenoic acid (EPA), *Arthrospira* (Spirulina) / *Rhodomonas* as functional foods, marine microalgae for aquaculture, and *Galdieria* for phycocyanin.

His research interests are in the development of new technologies for cost-effective commercial microalgae production, creating a sustainable biobased manufacturing process aided with carbon capture, renewable energy, and the recycling of media.

List of publications

1. **Butler, T.O.** and Guimarães, B., 2021. Industrial perspective on downstream processing of *Haematococcus pluvialis*. In *Global Perspectives on Astaxanthin* (pp. 283-311). Academic Press.
2. **Butler, T.O.**, Acurio, K., Mukherjee, J., Dangasuk, M.M., Corona, O. and Vaidyanathan, S., 2020. The transition away from chemical flocculants: commercially viable harvesting of *Phaeodactylum tricornutum*. *Separation and Purification Technology*, p.117733.
3. Sethi, D., **Butler, T.O.**, Shuhaili, F. and Vaidyanathan, S., 2020. Diatoms for Carbon Sequestration and Bio-Based Manufacturing. *Biology*, 9(8), p.217.
4. **Butler, T.**, Kapoore, R., and Vaidyanathan, R (2020) *Phaeodactylum tricornutum*: A Diatom Cell Factory, *Trends in Biotechnology*, p.17.
5. Rocuzzo S, Couto N, Karunakaran E, Kapoore RV, **Butler T**, Mukherjee J, Hansson EM, Beckerman AP and Pandhal J (2020) Metabolic Insights Into Infochemicals Induced Colony Formation and Flocculation in *Scenedesmus subspicatus* Unraveled by Quantitative Proteomics. *Front. Microbiol.* 11:792.doi: 10.3389/fmicb.2020.00792.
6. Padmaperuma, G., **Butler, T.O.**, Shuhaili, F.A.A., Almalki, W.J. and Vaidyanathan, S., 2020. Microbial consortia: Concept and application in fruit crop management. In *Fruit Crops* (pp. 353-366). Elsevier.
7. **Butler T.**, Golan Y. (2020) Astaxanthin Production from Microalgae. In: Alam M., Xu JL., Wang Z. (eds) *Microalgae Biotechnology for Food, Health and High Value Products*. Springer, Singapore.
8. Kapoore, R.V.; **Butler, T.O.**; Pandhal, J.; Vaidyanathan, S. 2018. Microwave-Assisted Extraction for Microalgae: From Biofuels to Biorefinery, *Biology*, 7, 18.
9. **Butler, T.O.**, McDougall, G.J., Campbell, R., Stanley, M.S. and Day, J.G., 2017. Media Screening for Obtaining *Haematococcus pluvialis* Red Motile Macrozooids Rich in Astaxanthin and Fatty Acids. *Biology*, 7(1), p.2.